To the Graduate Council:

I am submitting herewith a dissertation written by Anita M. Katti entitled "Preparative Liquid Chromatography: A Study of the Elution and Displacement Modes." I have examined the final copy of this dissertation for form and content and recommend that it be accepted in partial fulfillment of the requirements for the degree of Doctor of Philosophy, with a major in Chemical Engineering.

Georges A. Guiochon,
Major Professor

We have read this dissertation
and recommend its acceptance:

Accepted for the Council:

Vice Provost
and Dean of The Graduate School

Preparative Liquid Chromatography:

A Study of the Elution and Displacement Modes

A Dissertation

Presented for the

Doctor of Philosophy

Degree

The University of Tennessee, Knoxville

Anita M. Katti

May 1990

ACKNOWLEDGMENTS

I wish to express my sincere gratitude to Professor Georges Guiochon for his patience and guidance during my graduate studies. His demeanor and intellectualism I will always remember.

I thank Professor Csaba Horvath for introducing me to chromatography and all its potential. Special thanks to Martin Czok who was always available for discussions and to Din Golshan-Shirazi, Yih-Fen Maa and Ann Lee for their encouragement. Many thanks to Zidu Ma, Rose Ramsey, J-X. Huang and Michel Righezza who have contributed to this thesis and to Jie Zhu who has been wonderful to work with. Many people made the lab a great place to work, learn and grow: Samir Ghodbane, Connie Knauer, Jenner Gutierrez, Corinne Curvale, Jennifer Van Horn Schudel, Lu Lin Hua, Prof. Lin, Teresa Finchum, Mark Aubel, Claude Guillemin, Riccardo Bonfichi, Alain Jaulmes, Wanda Reyes, Claire Vidal-Madjar, Eric Dose, Jeff Roles, Steve Jacobson, Shula Levin and Zoubair El Fallah.

I would like to thank Professors George Frazier, Pete Counce and Paul Bienkowski for serving on my committee. I thank the Department of Chemistry and the Department of Chemical Engineering for supporting the joint program permitting my doctoral degree.

My mother, father, brother and sister-in-law have been with me to suffer through my trials. I appreciate their support.

The University of Tennessee computer center has made this work possible. Special acknowledgement to Sue Smith. Also I thank Gilson Medical Electronics for the loan of the 232/401 automatic sample processor.

This work has been supported by the National Science Foundation and by the cooperative agreement between the University of Tennessee and Oak Ridge National Laboratory.

ABSTRACT

Binary separations have been investigated experimentally and theoretically in overloaded elution, frontal and displacement modes of chromatography using phenyl-ethanol and phenyl-propanol as model compounds. The Rouchon-Golshan-Shirazi implementation of the semi-ideal model of chromatography was used to predict the individual component band profiles in these three modes. A competitive Langmuir isotherm with parameters determined from single component data gives fair prediction of the experimental data. The displacement effect is confirmed with accuracy and the tag-along effect is demonstrated for the first time. However, improved predictions can be obtained by measuring the binary isotherm directly by the method of hodograph transform.

The effect of the sample size on the production rate for a binary mixture in overloaded elution chromatography was studied. The optimum sample size for component one is much larger than for component 2. The chromatogram obtained at the optimum sample size which maximizes the production rate for component two at constant column length, particle size and flow rate is such that the band of component one interferes just enough with that of component two to reach the purity requirements (i.e. 99 % yield).

TABLE OF CONTENTS

Chapter			Page
1.	Introduction		1
	1.1	Applications of Chromatography	1
	1.2	Objective	3
	1.3	Modes of Chromatography	6
	1.4	Instrumentation	7
		Traditional Packing Technology	8
		Dry Packing	8
		Slurry Packing	10
		Compression Technology	12
		Radial Compression	12
		Axial Compression	12
		Annular Expansion	14
		Sample Injection and Distribution	15
		Detection	16
2.	Theory		18
	2.1	One Component Problem	19
		Elution Mode	22
		Frontal Mode	27
		Application to Isotherm Determination	28
	2.2	Two and Multicomponent Problem	29
		Elution Mode	30
		Frontal Mode	37
		Displacement Mode	38
	2.3	The Semi-ideal Model	41
3.	One-Component Problem Comparison of Theory and Experiment		47
	3.1	Single Component Elution of Small Molecules	48
		Experimental	50
		Equipment	50
		Materials	50
		Experimental Procedure	52
		Isotherm Measurement and Detector Calibration	53
		Results and Discussion	55
	3.2	Single Component Overloaded Elution of Proteins	67
		Experimental	67
		Equipment	67
		Materials	69
		Experimental Procedure	69
		Isotherm Measurement and Detector Calibration	70
		Results and Discussion	72

4. Two-Component Problem..... 80
4.1. Overloaded Elution Chromatography..... 80
Evaluation of Fraction Collector..... 81
Determination of Concentration Time Profiles for Binary Mixtures..... 91
4.2. The Large Volume Injection..... 116
The Hodograph Transform..... 122
The 1/1 Rectangular Injection 127
The 1/1 Non-Rectangular Injection..... 133
The 1/3 Rectangular Injection..... 144
The 3/1 Rectangular Injection..... 151
Kinetic Models..... 159
4.3. Reevaluation of Overloaded Elution Data: Best Fit Langmuir Parameters..... 171
Semi-ideal..... 179
Craig..... 179
Control Diffusion..... 188
4.4 Quantitative Comparison of the Different Models for Predicting Overloaded Elution Profiles..... 188

5. Trace Enrichment of an Impurity..... 208
5.1. By Overloaded Elution Chromatography..... 209
Theoretical..... 210
Validity of Model..... 211
Effect of Sample Size..... 216
Enrichment by Recycling..... 219
5.2. By Displacement Chromatography.....
Calculation Parameters..... 226
Results and Discussion..... 226

6. Optimization of the Separation in Overloaded Elution Chromatography..... 234
6.1. Effect of Loading Factor and Sample Volume... 234
Definitions..... 235
Influence of the Separation Factor..... 237
Influence of the Composition of the Binary Mixture..... 243
Elution Profiles under Optimum Conditions... 246
6.2. Comparison with Knox and Pyper..... 252
6.3. The Tradeoff between Yield and Production Rate 254

7. Optimization of the Separation in Displacement Chromatography..... 261
7.1. Effect of Displacer Concentration..... 264
7.2. Effect of Column Length..... 272
7.3. Effect of Volume..... 278
7.4. Comparison with Results from the Literature.... 278

8. Summary and Conclusions..... 286
8.1. Comparison of Overloaded Elution and Displacement Chromatography 287
8.2. Recommendations..... 288

List of References..... 290
Appendices..... 300
Appendix A Programs for the Gilson 232-401..... 301
Appendix B Listing of Experimental Data..... 308
Appendix C The Analogy Between HTU in Adsorption and HETP in Chromatography..... 329
Vita..... 334

LIST OF TABLES

3.1	Summary of Isotherm Data for Phenyl-ethanol and Phenyl-propanol.....	49
3.2	Summary of Isotherm Data for 3,6 Dimethyl-phenol...	66
3.3	Summary of Protein Isotherm Data.....	73
4.1	Summary of Experimental Overloaded Elution Data....	91
4.2	Summary of Large Volume Injection Parameters.....	128
4.3	Quantitative Evaluation of the 1/1 Mixture in Overloaded Elution Chromatography.....	202
4.4	Quantitative Evaluation of the 1/3 Mixture in Overloaded Elution Chromatography.....	203
4.5	Quantitative Evaluation of the 3/1 Mixture in Overloaded Elution Chromatography.....	204
4.6	Quantitative Evaluation of the 9/1 Mixture in Overloaded Elution Chromatography.....	205
5.1	Enrichment by Recycling.....	222
6.1	Summary of Conditions for Optimum Production Rate..	236
6.2	Comparison Between Throughput by Semi-Ideal model and Knox and Pyper.....	253

LIST OF FIGURES

2.1 Summary of the Mass Balance Equations..... 20

2.2 Equilibrium and Non-equilibrium Expressions..... 21

3.1 Comparison of Isotherms of Phenyl-ethanol & Phenyl-propanol on 2 Analytical Columns Packed with the same Stationary Phase..... 49

3.2 Calibration Curve of Phenyl-ethanol and Phenyl-propanol by Direct Injection..... 54

3.3 Comparison of Theory and Experiment, Column #1 - Phenyl-ethanol..... 57

3.4 Comparison of Theory and Experiment, Column #1 - Phenyl-propanol..... 58

3.5 Adsorption Isotherm of Phenyl-ethanol by ECP..... 59

3.6 Adsorption Isotherm of Phenyl-propanol by ECP..... 60

3.7 Adsorption Isotherm of Dimethylphenol by ECP..... 61

3.8 Comparison of Theory and Experiment, Column #2 - Phenyl-ethanol..... 62

3.9 Comparison of Theory and Experiment, Column #2 - Phenyl-propanol..... 64

3.10 Comparison of Theory and Experiment, Column #2 - Dimethylphenol..... 65

3.11 Comparison of Theory and Experiment on Microbore Column for Dimethylphenol..... 68

3.12 Experimental Protein Adsorption Isotherms fit to Langmuir Equation..... 71

3.13 Experimental Protein Adsorption Isotherms fit to BiLangmuir Equation..... 74

3.14 Comparison of Theoretical and Experimental Band Profiles for Chicken Albumin, pH 8.6..... 76

3.15 Comparison of Theoretical and Experimental Band Profiles for Chicken Albumin, pH 9.6..... 77

3.16 Comparison of Theoretical and Experimental Band Profiles for Conalbumin, pH 9.6..... 79

4.1 Detector Response to 30 mg Injection of Phenyl-Ethanol..... 83

4.2 Detector Calibration Curve for Phenyl-ethanol..... 84

4.3 Evaluation of Fraction Collector..... 85

4.4 Experimental Response and Concentration Profiles . 86

4.5 Comparison of Experimental and Predicted Profiles using Single Component Isotherm Parameters & Rectangular Injection..... 93

4.6 Comparison of Non-Interacting Profile with Experimental Data for the 1/3 mixture..... 98

4.7 Comparison of Non-Interacting and Interacting Model. 99

4.8 Theoretical Profile assuming no interaction, 3/1... 102

4.9 Effect of Volume on the Band Profile..... 104

4.10 Comparison of Experimental and Predicted Profiles for 0.5 ml Rectangular Injection..... 108

4.11 Injection Profile..... 113

4.12 Comparison of Experimental and Predicted Profiles with Gaussian Injection..... 117

4.13 Schematic of Injector for Large Volume Experiments. 121

4.14 The Hodograph Transform..... 124

4.15 Algebraic Relationshiops for Calculating Isotherm.. 126

4.16 Measured Injection Profile for 3.5 min Plug..... 129

4.17 Detector Response Curve to a 1/1 Binary Mixture.... 130

4.18 Elution Profile after Fraction Collection, 1/1 Mixture..... 131

4.19 Comparison of Experimental and Predicted Elution Profiles, 1/1, using Single Component Isotherm Data. 132

4.20 Hodograph Transform of Experimental Data and Theoretical Predictions from Single Component Isotherm Data..... 134

4.21 Best Fit Lines in the Hodograph Space to Experimental Data..... 135

4.22 Comparison of Experimental and Predicted Elution Profiles, 1/1, using Best Fit Langmuir Parameters.. 136

4.23 Response Profile for Non-Rectangular Injection..... 138

4.24 Detector Response Curve to a 1/1 Binary Mixture.... 141

4.25 Elution Profile after Fraction Collection, 1/1 Mixture..... 142

4.26 Comparison of Experimental and Predicted Elution Profiles, 1/1, using Single Component Isotherm Data. 143

4.27 Hodograph Transform of Experimental Data and Theoretical Predictions from Single Component Isotherm Data..... 145

4.28 Best Fit Lines in Hodograph Space to Experimental Data..... 146

4.29 Comparison of Experimental and Predicted Elution Profiles, 1/1, using Best Fit Langmuir Parameters.. 147

4.30 Detector Response Curve to a 1/3 Binary Mixture.... 149

4.31 Elution Profile after Fraction Collection, 1/3 Mixture..... 150

4.32 Comparison of Experimental and Predicted Elution Profiles, 1/3, using Single Component Isotherm Data. 152

4.33 Hodograph Transform of Experimental Data and Theoretical Predictions from Single Component Isotherm Data..... 153

4.34 Best Fit Lines to Experimental Data in Hodograph Space..... 154

4.35 Comparison of Experimental and Predicted Elution Profiles, 1/3, using Best Fit Langmuir Parameters.. 155

4.36 Detector Response Curve to a 3/1 Binary Mixture.... 156

4.37 Elution Profile after Fraction Collection, 3/1 Mixture..... 157

4.38 Comparison of Experimental and Predicted Elution Profiles, 3/1, using Single Component Isotherm Data. 158

4.39 Hodograph Transform of Experimental Data and Theoretical Predictions from Single Component Isotherm Data..... 160

4.40 Best Fit Lines to Experimental Data in Hodograph Space..... 161

4.41 Comparison of Experimental and Predicted Elution Profiles, 3/1, using Best Fit Langmuir Parameters.. 162

4.42 Comparison of Experimental and Predicted Elution Profiles using Average Hodograph Parameters..... 163

4.43 Hodograph Transform of Experimental Data and Theoretical Predictions from Average Hodograph Parameters..... 167

4.44 Comparison of Experimental and Theoretical Elution Profiles using Dispersion and Kinetic Model, 1/1, Rectangular Injection..... 172

4.45 Comparison of Experimental and Theoretical Elution Profiles using Dispersion and Kinetic Model, 1/1, Non-rectangular Injection..... 173

4.46 Comparison of Experimental and Theoretical Elution Profiles using Dispersion and Kinetic Model, 1/3, Rectangular Injection..... 174

4.47 Comparison of Experimental and Theoretical Elution Profiles using Kinetic Model, 1/1, Rectangular Injection..... 175

4.48 Comparison of Experimental and Theoretical Elution Profiles using Kinetic Model, 1/1, Non-rectangular Injection..... 176

4.49 Comparison of Experimental and Theoretical Elution Profiles using Kinetic Model, 1/3, Rectangular Injection..... 177

4.50 Comparison of Experimental and Theoretical Elution Profiles using Kinetic Model, 3/1, Rectangular Injection..... 178

4.51 Comparison of Experimental and Predicted Profiles with Gaussian Injection using Best Fit Langmuir Parameters from Hodograph Transform..... 180

4.52 Comparison of Rectangular and Gaussian Injection Profiles..... 184

4.53 Comparison of Experimental and Predicted Profiles using the Craig model with Half-Gaussian Injection. 189

4.54 Comparison of Experimental and Predicted Profiles using the Control Diffusion model with Half-Gaussian Injection function..... 193

4.55 Comparison of Craig and Control Diffusion models... 197

4.56 Ideal Model Representation of Binary Overloaded Elution Profiles Marking the Characteristic Parameters..... 201

5.1 Linear Elution Chromatogram of Thymine Dimer and Monomer..... 212

5.2 Equilibrium Adsorption Isotherm of Thymine by ECP.. 213

5.3 Experimental and Predicted Band Profiles of Thymine. 214

5.4 Theoretical Profile of Dimer and Monomer in 1:1405 Ratio..... 215

5.5 Experimental Profile of Dimer and Monomer in same Ratio..... 217

5.6 Profile of Dimer and Monomer in Presence of Increase Amounts of Monomer..... 218

5.7 Theoretical Profile of a 1/24000 Mixture of Dimer/Monomer..... 220

5.8 Shaving of First Component and Reinjection..... 221

5.9 Experimental Profile of Monomer at 300 nm..... 224

5.10 Experimental Profile After First Recycle..... 225

5.11 Equilibrium Isotherms for Displacement Calculations. 227

5.12 Displacement Train of 2 Major Components and Profile of Impurity on 50 cm Column..... 228

5.13 Displacement Train of 2 Major Components and Profile of Impurity on 25 cm Column..... 230

5.14 Displacement Train with 1 Major Component and Profile of coeluting Impurities on 25 cm Column..... 231

5.15 Overloaded Elution Chromatogram and Profile of Impurity on 50 cm Column..... 232

6.1 Figure 6.1 Plot of the Production Rate vs the Loading Factor, 1/3, Selectivity 1.09..... 238

6.2 Influence of the Sample Volume on the Band Profile, $L_f 2$ %..... 240

6.3 Plot of the Production Rate vs the Loading Factor, 1/3, α 1.7..... 242

6.4 Plot of the Production Rate vs the Loading Factor, 3/1, Selectivity 1.7..... 244

6.5 Calculated Chromatograms Corresponding to the Optimum Production Rate for each Component, 1/3, Selectivity 1.09 and 1.25..... 247

6.6 Calculated Chromatograms Corresponding to the Optimum Production Rate for each Component, 1/3, 3/1, Selectivity 1.7..... 250

6.7 Calculated Chromatograms Corresponding to the Optimum Production Rate for each Component, 1/9, 9/1, Selectivity 1.7..... 251

6.8 Plot of the Yield as a Function of the Loading Factor for Binary Mixtures of Different Composition, Selectivity 1.7..... 256

6.9 Plot of the Yield of Component 1 as a Function of the Loading Factor for Samples of Different Volume, 1/3, selectivity 1.7..... 257

6.10 Plot of the Yield as a Function of the Loading Factor for Samples of Different Volume, 1/3, Selectivity 1.09..... 259

7.1 The Single Component Adsorption Isotherms for each Component and the Displacer..... 263

7.2 The Effect of the Concentration of the Displacer on the Displacement Profile at 25 cm..... 265

7.3 The Effect of the Displacer Concentration on the Displacement Profile at 25 cm..... 266

7.4 The Effect of the Displacer Concentration on the Yield at 99% Purity, 25 cm Column..... 270

7.5 The Effect of the Displacer Concentration on Yield at 95% Purity, 25 cm Column..... 271

7.6 The Effect of the Displacer Concentration on the Production at 98% Purity, 25 cm Column..... 273

7.7 Displacement Profiles as a Function of Column Length at Maximum Production for [D] 3M..... 274

7.8. The Effect of Column Length on the Yield at Constant Displacer Concentration and 99% Purity..... 276

7.9 The Effect of Column Length on Production at Constant Displacer Concentration and 99% Purity..... 277

7.10 Displacement Profiles as a Function of Column Length for a 5 ml Injection Volume..... 279

7.11 The Effect of Sample Concentration on the Peak Shape, Comparison with Experimental Data in the Literature. 283

7.12 The Effect of Column Length on the Peak Shape, Comparison with Experimental Data in the Literature. 284

LIST OF SYMBOLS

a Langmuir Parameter, k'/F, (ml/ml)

A1 BiLangmuir Parameter, (ml/ml)

A2 BiLangmuir Parameter, (ml/ml)

b Langmuir Parameter, (ml/mg)

A_+ Positive Slope of Line in Hodograph Plot

A_- Negative Slope of Line in Hodograph Plot

B1 BiLangmuir Parameter, (ml/mg)

B2 BiLangmuir Parameter, (ml/mg)

C Concentration in the mobile phase (mg/ml)

C_o Concentration of Sample (mg/ml)

csc Column Saturation Capacity (mg or mole)

D Molecular Diffusion Coefficient (cm2/sec)

D_{ap} Apparent Dispersion Coefficient (cm2/sec)

[D] Concentration of Displacer (mg/ml or M)

D_c Critical Displacer Concentration

dt_i time difference

$f_{i,comp}$ Ratio of amount of Component 1 to 2 in mixture

F Phase Ratio, V_{sp}/V_{mp}, (ml/ml stat. phase)

F_v Volumetric Flow rate (ml/min)

G^* Displacer concentration

h Height Parameter

H Height Equivalent to a Theoretical Plate (cm,um)

H^* Displacer Concentration

HETP Height Equivalent to a Theoretical Plate

H_{kin} Kinetic Contribution to the HETP (cm)

H_{th} Thermodynamic Contribution to the HETP (cm)

K Kinetic Rate Constant

k' Capacity Factor, t_R-t_o/t_o

L Column Length, cm

L_f Loading Factor, sample amount/csc_i

MW Molecular Weight

n Sample size (mole)

n_{sat} Saturation amount (mole)

Pr Production Rate (umol/ml s)

R number of dt units injection takes place

q Instantaneous Concentration in the Stationary Phase (mg/ml)

Q Equilibrium Concentration in the Stationary Phase (mg/ml)

Qs Saturation Concentration

t time (sec or min)

t_a Retention parameter

t_{cycle} Cycle time (sec,min)

t_o Dead Time (sec)

t_R Retention time of solute (sec)

u_o Linear Velocity (cm/sec)

uz Linear Velocity of the Peak Maximum (cm/sec)

uzo Linear Velocity of Gaussian Peak (cm/sec)

V Detector response (volts)

V_D Column Dead Volume (ml)

V_F Breakthrough Front Volume (ml)

V_{mp} Volume of Mobile Phase (ml)

V_{sp} Volume of Stationary Phase (ml)

Y Yield

z Column length (cm)

Greek

α Separation Factor

ϵ Porosity

σ Standard Deviation of a Gaussian Peak

ξ_+ y-intercept value corresponding to A_+

ξ_- y-intercept value corresponding to A_-

Subscript

i Component indicator

s Single Component parameter

h Parameter from Hodograph transform

Chapter 1

Introduction

The need to study preparative liquid chromatography has been spurred by purification problems in the pharmaceutical and biotechnological industries. Intermediates prepared by organic synthesis or products from fermentation processes often cannot be purified by traditional separation processes such as distillation, extraction or recrystallization either because they are nonvolatile, they are sensitive to strong organic solvents or they form products with very similar structure which do not lend themselves to these techniques. It has often been said that preparative chromatography is simply an extension of analytical chromatography. This is not true, however. Analytical chromatography is employed to collect information regarding the composition of organic reaction products or products from a fermentation bath. The goal in preparative chromatography is to produce significant amounts of pure compound. Thus, issues in analytical chromatography are analysis time, detection limits and resolution while in preparative chromatography they are production rate, purity and yield.

1.1 Applications of Chromatography

The applications of chromatographic separations can be divided into 4 categories.

Category #1: In classical analytical chromatography, information is extracted regarding the composition of the mixture. Once the components are separated the separated products are considered waste. The cost of the separation is measured in terms of the price per unit of information gathered. The information is the detector signal and the issue is maximizing the signal to noise ratio, increasing the limits of detection, reducing the size of the detector cell for less dispersion and reducing the time constants for signal measurement.

Category #2: In a number of applications in analytical or preparative chromatography there is further interest in the product after it is separated and it elutes from the column. Post column reactors are employed for example in amino acid analysis to increase the sensitivity of detection. Upon eluting from the chromatographic column a reactant is added continuously using a low dead volume mixer, given time to react and then passed through the detector for monitoring. Other examples are where the output is coupled via an interface to a mass spectrometer or NMR or Fourier Transform Infrared Spectrometer to gather very specific information about the products being separated.

Category #3: Outside of analytical separations there are separations where information is needed about the physical, chemical or biological properties of the purified material. For example, the separation of small amounts of product for toxicity studies, drug design, or for characterization of the compound. Preparative chromatography is often used here at the bench or semi-preparative

scale. The issue of primary importance is how does one quickly purify a sample in quantities of a few milligrams. Little time is spent after developing an analytical separation. Once the analytical method is developed the separation is extended to the preparative mode by injecting larger samples. Other times the same experimental conditions are employed with a larger sample size on a larger diameter column. In most cases, no time is spent on optimization of the preparative separation.

Category #4: The last category is where preparative chromatography is employed to purify products for sale. The primary issue is maximization of the production rate of the product(s) of interest. The experimental conditions are very different from those employed in analytical separations. For example, in contrast with analytical separations, it is important to have a large separation factor to increase the production rate. In industrial separations at the pilot plant or plant scale the economics of the separation must be considered in conjunction with the optimum conditions for separation.

This thesis will cover the issues in this last category, along with studies which aid in the understanding of adsorption processes and phenomenon which take place during band migration.

1.2 Objective

The goal of this thesis is (1) to test the validity of the semi-ideal model for predicting single component elution bands (2) to validate the method of the Hodograph transform for the determination of binary competitive isotherms and employ this method to predict

binary overloaded elution profiles, (3) to investigate the use of overloaded elution and displacement modes to the enrichment of impurities in the presence of major components (4) to apply this model to optimization production rate in overloaded elution chromatography and displacement chromatography and (5) to investigate the three modes of chromatography (frontal, elution and displacement) and determine their impact in preparative liquid chromatography.

This was accomplished by measuring single component adsorption isotherms of phenyl-ethanol and phenyl-propanol and showing for a pure component that there is little difficulty in predicting band profiles at high concentration. Using the measured single component parameters in a competitive Langmuir model, a comparison of experimental data with the predicted profile showed good agreement of the individual component profiles of binary mixtures in overloaded elution and displacement chromatography. From the individual component profiles measured for a large volume injection, the adsorption isotherm was determined by the method of the Hodograph transform assuming a competitive Langmuir model. By comparing experimental and theoretical profiles improved prediction were observed.

Assuming parameters in a competitive isotherm model, chromatograms under a variety of conditions were calculated by solving the mass balance equation. A study of the enrichment of an impurity in overloaded elution and the displacement modes was undertaken. Similarly, under a variety of conditions, the production rate for many binary separations was calculated.

This thesis is presented in 8 chapters.

Chapter 1 provides a general introduction to the problem of preparative chromatography and a review of the instrumentation.

Chapter 2 presents the development of the theory of chromatography, the current state of knowledge and the semi-ideal model which is used in this work.

Chapter 3 presents experimental and theoretical results on the single component problem. The adsorption isotherm of a pure component can be accurately measured either by frontal analysis or from a single overloaded elution profile. Use of this thermodynamic data and other column properties in the semi-ideal model gives excellent agreement of band profiles in overloaded elution chromatography.

In Chapter 4, for a pulse and large volume injection, a competitive Langmuir isotherm with parameters from the pure component isotherm is used to predict the individual component profiles of binary mixtures. The agreement between experimental and predicted profiles is good with this model. Transformation of the large volume data into the Hodograph space allows determination of the competitive isotherm from binary data. From this method of measuring the adsorption isotherm, improved predictions of the overloaded elution profiles are obtained.

Chapter 5 presents a theoretical study on the use of overloaded elution and displacement chromatography to enrich the concentration of an impurity in a mixture.

Chapter 6 presents a study of the optimum sample size for several binary mixtures in order to maximize the production rate for the first and second component.

Chapter 7, experimental and theoretically, discusses displacement chromatography and the conditions for optimization of the separation.

Lastly, Chapter 8 concludes and compares the two modes of chromatography, elution and displacement, for use in preparative chromatography. The advantages and disadvantages are discussed.

1.3 Modes of Chromatography

Analytical Chromatography is carried out in the elution mode where a small amount of sample is injected as a pulse. However, preparative separations can be carried out in one of 3 modes of chromatography: elution, frontal or displacement [Tiselius (1943)]. The primary difference between these three modes is the injection function. Elution chromatography in the generic sense involves passing the eluent or carrier through the column until it reaches equilibrium, then introducing the sample at the top of the column as a pulse. Injection of a small amount of sample in a small volume is called elution or linear elution chromatography and injection of a large sample concentration is called overloaded elution chromatography. Sometimes the term volume overload is used and this is injection of a large volume of a dilute sample. When the mobile phase is maintained at a constant composition the column is said to be operated isocraticly. This is in contrast to when the elution composition increases or decreases in some fashion,usually linearly, which is gradient elution.

Frontal chromatography or frontal analysis, sometimes called breakthrough analysis, is where the sample is pumped through the column and at specified times, the concentration of sample is increased,

giving rise to steps. Frontal chromatography is primarily used to extract the first component of a mixture or used for determination of equilibrium adsorption isotherms.

Displacement chromatography is where the mobile phase or carrier is equilibrated with the column, then the sample is injected as a pulse or large volume. Then, a displacer, a solute dissolved in the carrier which is more strongly adsorbed to the stationary phase than any of the sample components, is pumped into the column. The name arises from the fact that each component is displaced (i.e. desorbed or kicked off) from the stationary phase forming bands which are rectangular in shape.

1.4 Instrumentation

The instrumentation required in process scale chromatography can uses equipment which is quite different from what is employed in an analytical chromatograph. Thusfar, advancements in instrumentation have centered around designing improved column technology with some emphasis on distribution of the sample uniformly over the top of the column, detection and automation. Dedicated instruments covering a wide range of throughputs are available from different manufactures. The differences in column technology will be discussed in the next section.

The column efficiency or the HETP is measured by injecting a small amount of sample and measuring the response at the column outlet. For a gaussian response, the column efficiency is defined as

$$N=(\frac{t_R}{\sigma})^2 \qquad (1.1)$$

and the HETP as

$$HETP = \frac{L}{N} \qquad (1.2)$$

For columns of different inner diameter, the technique for packing columns should give the same efficiency as long as the stationary phase is the same. The packing technique should also be reproducible and give a HETP proportional to the average particle size. This permits the engineer a choice in the final column performance by adjusting the particle size, the column length and the inlet pressure.

Packing Technology

There are two types of methods for packing chromatographic columns, dry and slurry methods. Dry packing is easy to implement, but slurry methods afford more efficient columns especially when small particles are required [Kuhn (1931a,1931b)].

Dry Packing

The first preparative columns were prepared by dry packing. In this technique, the column is vibrated, rotated, tapped on the wall or dropped repeatedly while packing material is poured slowly into the tube. The factors which influence the column efficiency are the average particle size, the column diameter and the rate at which the packing material is poured [Kaminiski]. The main advantage of dry packing is its simplicity. It does not require any sophisticated equipment nor highly skilled manpower. There are important drawbacks, however. The column efficiency is not reproducible and is often low. The reduced plate height often exceeds 10 um. Most importantly, the

method does not work for particles smaller than 30 micron. The best results are obtained when the column is vibrated and rotated around its axis, but this requires expensive, complex equipment which does not work with smaller particles where electrostatic interaction lead to agglomeration and poor packing [Verzele].

After a column has been dry packed, a steady stream of mobile phase is circulated through the column, typically for a few hours, at the largest flow rate allowed by the pump, tubing or packing material. This further packs the material. Thus, the last step is to refill the top of the column.

This method as applied to particle sizes between 30 and 60 um permits inexpensive preparation of low or medium pressure columns having a good reduced plate height. In order to obtain reasonable elution times and acceptable throughputs, the columns must be operated well above the flow velocity corresponding to the maximum efficiency on the Van Deemter curve. The method is used primarily in academic laboratories where low production costs are required and when time is not critical. It must also be considered that elution chromatography is also a dilution process and the extent of dilution increases with increasing retention time and with decreasing column efficiency. The cost of concentrating the purified fraction and recovering the products must be considered seriously in preparative LC.

The column efficiency may be improved by using packing materials with a smaller average particle size and a narrower size distribution. The width of the size distribution is more important in preparative chromatography than in analytical chromatography because the column

diameter is larger and size segregation is easier. If the permeability changes significantly across the column cross-section, this will cause a change in the local velocity. These radial velocity gradients will cause band broadening. Diffusion in the radial direction is too slow to relax the concentration gradient caused by the changes in velocity over the cross-section.

Particles having an average diameter less than 25-30 micron cannot be dry packed because the electrostatic interactions between particles with a high surface to mass ratio result in attraction forces which become large compared to their mechanical inertia. Under these conditions, stable agglomerates form. This results in a column having the flow resistance of small particles and an efficiency corresponding to agglomerated particles. In order to form an emulsion and disperse the particles, slurry methods are employed.

Slurry Packing

Slurry packing is used to pack fine particles, less than 20 um, reproducibly and with high efficiency. The presence of the solvent drastically reduces the interaction energy between the particles [Bristow]. Slurry packing involves using a high pressure pump to pound into an empty column the packing material which is suspended in a slurry and placed in a reservoir. The pump can be a constant pressure or constant flow pump. In a constant pressure system, the flow rate is adjusted upto the maximum value the pump can sustain to maintain the pressure. The flow rate decreases as the column is packed. These pumps are usually operated pneumatically by using a air compressor.

In the constant flow system, HPLC type high pressure piston pumps are employed. In both cases columns are packed at pressures between 7000 and 10000 psi. Preparation of a stable packing and the exact procedure for packing a column is considered an art. The goal in slurry packing is to prevent selective sedimentation of the stationary phase. Viscous solvents are used to slow particle sedimentation which causes size segregation. For the packing of reversed phase materials, pure methanol or 30 % glycerol/methanol or 50% isopropanol/methanol slurry solvents are used with methanol as the packed solvent. For silica the packing is often done in hexane. For novel packing materials, experience is required to obtain a good slurry solvent.

Slurry packing was first developed for analytical columns, but the technique can be applied for the preparation of high efficiency preparative columns. The same procedure is used. The maximum pressure which may be applied is limited by the mechanical resistance of the column wall and the column end fittings. For example compression fittings can hold a 10000 psi on a 0.5 " i.d. column, but only about 2000 psi for a 2" i.d. column [Colin]. For the larger inner diameter columns, flanged-end fittings are employed. They are either bolted or fastened with special collars that can withstand the high pressure required. The column tubing and flanges are thick and are made of high tensile strength alloys which are heavy and expensive. As the column diameter increases, it becomes more difficult and more expensive to find a pump capable of delivering a fluid at such high velocities.

Outstanding performance has been achieved with 6 " i.d. columns packed with 10 um material obtaining plate heights around 18 um (reduced plate heights below 2).

The packing of industrial scale columns larger than 6" in diameter requires new technology. Instead of applying pressure through the use of a pump, various compression technologies have been developed where a piston or other external force compresses the packing.

Compression Technology

In order to pack large diameter columns reproducibly and with high efficiency compression technology was developed. It has the advantage that voids in column can be eliminated without repacking the column. There are three types of compression technologies which are employed to pack preparative scale columns for sale on the market: Radial Compression, Axial Compression and Annular Expansion.

Radial Compression

Radial compression was developed by Little et al. in the mid seventies [Little]. Flexible wall cartridges (0.5x10 cm, 4.7x30 cm) filled with silica or other packing material for liquid chromatography are used as the column. The cartridge is designed to have a space between the inner wall and the cartridge. Nitrogen at 500 psi is pressurized causing the flexible wall to shrink around the prepacked bed forming a tightly packed bed having high efficiency. This process of packing takes 1 minute.

The advantage of this bed are that if a void develops at the top of the column due to dissolution of the silica in the mobile phase or rearrangement of the packing, the cartridge can be repressurized to repack the bed. The cartridge need not be thrown away. The disadvantage of this method is that any radial inhomogeneities will result in radial velocities gradient and thus greater band broadening and a lower efficiency column. The second disadvantage is that currently the cartridges must be purchased from the manufacturer and personalized packing of novel stationary phases is not possible. Moreover the cartridges are available with particles sizes between 40-60 um. Also the plastic lining which can withstand organic solvents has a short life time due to mechanical fatigue.

Axial Compression

Axial compression was developed in the mid-seventies [Godbille (1974)] at about the same time radial compression was developed by Waters. The column design consists of a cylinder and a sliding piston which fits inside the cylinder. The appropriate fitting are used and the tolerances are small such that it does not leak between the barrel and the column during packing. To prepare a column, a slurry is made and poured into the cylindrical column. The top of the column is fitted with a frit and then the piston is slowly raised forcing the excess solvent out of the column through the frit retaining the packing as a dense plug. The maximum pressure applied to the bed in order to obtain a high quality packed column is between 5 and 20 atm depending

on the size of the particles. When compression is complete, the piston is locked into position to prevent unpacking of the column.

It takes approximately 10 minutes to pack a column [Godbille (1976)]. Reduced plate heights from 2.3 to 4.0 are readily achievable. Voids formed by silica dissolution can be removed by unlocking the cylinder and repacking the column.

The advantage of this procedure is that the bed remains stable, excellent performance is achieved at low pressures. Axial compression appears to be more desirable than radial compression because cartridges need no be purchases. Bulk packing material from any source can be used. The column length is adjustable over a large range by using the appropriate amount of stationary phase. The column and piston are easy to clean. It is easy to unpack and pack the column. Lastly, density gradients resulting from the packing are have a smaller effect on the column performance in the axial compression than in radial compression. This technology is sold with columns having diameter from 5 cm to 45 cm and the maximum column length varies between 40 cm and 1 meter depending on the column diameter and packing material. Smaller columns are also available in 1/2-2" diameters with a manually adjustable piston.

Annular Expansion

In 1987, Separation Technology developed [Jennings] another procedure for packing columns. The design is such that a cylinder is fitted with a conical rod having a small angle and a average diameter

of 1/2" for a 1.5" inner diameter column. The rod is pushed into the column to allow both axial and radial compression effects.

This technique has all the advantages of using compression technology in that voids can be eliminated. The biggest difficulty is uniformly distributing the sample about the annulus of the column.

Sample Injection and Distribution

In preparative chromatography, the problem is to spread the injected band over the entire column cross-section. In analytical chromatography a point like band spreads radially as well as axially [Knox (1976)]. However, often with high efficiency packing materials, the radial distribution is slow. Injection of a sample can be accomplished two ways, with the use of a sample loop or using sample distributors.

Sample loop injection should be carried out when using analytical or semi-preparative size columns and when the sample volume is less than 3 ml. For volumes greater than 3 ml, the velocity profile due to the Poiseuille flow distribution in the loop gives a tailing injection profile [Atwood]. In order to reduce the effect of dispersion of the sample, the loop can be filled with glass bead to flatten the velocity profile. An alternative is pump injection which can give rectangular profiles by switching appropriately the mobile phase and feed stream. However, an auxiliary pump must be used.

Development of distributors to spread the sample evenly across the column cross-section is used for larger columns. One of the simplest distributors in placing a metal frit at the entrance of the

column which has a permeability lower than that of the column. Additionally, one could put a space between this metal frit and the frit of the column to enhance distribution [Coq (1981)]. There are many other types of designs for distribution of the sample [Godbille (1976), DeJong, Coq (1979)].

Detection

There are two types of detection problems in preparative liquid chromatography. The first problem os that the concentration of the solute are so large that the detector is saturated. The second problem is determination of concentration of the individual components in an mixed band.

In order to reduce the sensitivity of the detector, short path length cells are used [Joraczko]. Othertimes, one operates a detector at wavelengths where the absorption is weak [Dose (1989)].

When the bands interfere, the effluent must be monitored either by on-line analysis or fraction collect with subsequent reinjection. The advantage of on-line analysis is that knowledge of the relative composition of each species can be obtained soon after elution of the band. With correct methods of Fast Analysis using short columns packed with 2-3 micron nonporous stationary phase the analysis times have been reduced to the order of 20 seconds. The drawback of this method is that the number of points obtained in describing the interference band is limited by the analysis time. The advantage of fraction collect is that with modern fraction collector and the use of conical bottom vials, collection can be made as short as 3 seconds if needed. The

disadvantage is that one must wait until the elution is complete before analyzing all of the fraction. Both methods are easily automatable.

Instrumentation in preparative chromatography is fairly well developed. Design of the optimum conditions for a preparative separation is more difficult. This requires the use of modeling to determine band profiles under a wide variety of conditions and calculating the production rate under each condition to find the optimum, the topic of this thesis.

Chapter 2

Theory

The theory of chromatography should answer the question: What is the band profile in the column under various conditions? In some cases, it can address the issue of how to measure thermodynamic and kinetic parameters from experimental data. It is convenient to divide this problem into sections concerning the number of solutes in the studied system. Several assumptions have to be made regarding whether the system is ideal or non ideal, equilibrium or nonequilibrium and whether the isotherms are linear or nonlinear. More specifically, the sources of diffusion/dispersion, the rate of transport of molecules from the mobile to the stationary phase and the isotherm shape must be assumed or determined for the non-ideal, nonlinear equilibrium and kinetic models. In order to complete the statement of the problem, the initial and boundary conditions must be specified. Is the column initially filled with the reference solute (nonadsorbing component) or an adsorbing component and the boundary condition is specified by the mode of chromatography the operation takes place (i.e. frontal, elution or displacement). Due to the nature of chromatography, practically all implementations (i.e. GC, LSC, LLC, I-X, HIC) are accounted for by the same theory.

This chapter is divided into 3 sections. Sections 2.1 and 2.2 review the literature where issues concerning the theory of preparative

liquid chromatography. Prominent contributions to the field are described with emphasis on nonlinear chromatography. Figure 2.1 and 2.2 summarizes the Mass Balance equations which are referenced by name in the discussion. Section 2.3 presents the theoretical model used in this work. The various model simplifications presented in Figure 2.1 and 2.2 will be discussed in detail in this section.

2.1 One Component Problem

The solution of the one component problem does not contribute directly to the understanding of the separation mechanism in chromatography, however, the theoretical analysis provides the fundamental concepts in nonlinear chromatography. For the one component problem, boundary conditions permit only elution of a pulse by a pure or mixed solvent and frontal analysis. All other chromatographic procedures required 2 or more solutes.

The mathematical description of the single component problem in terms of a differential mass balance was first written by Wilson in 1940 assuming ideal chromatography where the column is assumed to have an infinite efficiency (i.e. no diffusion, HETP=0) and the two phases are always in equilibrium, Equations (2.7). The amount adsorbed in the stationary phase, Q, is a function of the concentration in the mobile phase given by the equilibrium isotherm, Equation (2.8).

In 1943, Devault made a more rigorous study on the properties of the system of partial differential equations of chromatography and the formation of concentration shocks (discontinuity) in the cases of a pulse and a step injection.

Figure 2.1 Summary of the Mass Balance Equations

General Form of the Mass Balance Equation:

$$\frac{\partial C}{\partial t}+F\frac{\partial q}{\partial t}+u_o\frac{\partial C}{\partial z}=D\frac{\partial^2 C}{\partial z^2} \qquad (2.1)$$

where D is the molecular diffusion coefficient. q and C are related in the case of equilibrium:

$$q=Q=f(C) \qquad (2.2)$$

and in the case of a finite rate of mass transfer:

$$\frac{\partial q}{\partial t}=f(C,Q,q) \qquad (2.3)$$

Semi-Ideal Model:

$$\frac{\partial C}{\partial t}+F\frac{\partial q}{\partial t}+u_o\frac{\partial C}{\partial z}=D_{ap}\frac{\partial^2 C}{\partial z^2} \qquad (2.4)$$

where D_{ap} is the apparent dispersion coefficient:

$$D_{ap}=\frac{HL}{2t_o} \qquad (2.5)$$

$$Q=f(C) \qquad (2.8)$$

Ideal Model:

$$\frac{\partial C}{\partial t}+F\frac{\partial q}{\partial t}+u_o\frac{\partial C}{\partial z}=0 \qquad (2.7)$$

$$Q=f(C) \qquad (2.8)$$

Figure 2.2 Equilibrium and Non-equilibrium Expressions

Langmuir Equilibrium Expression:

$$Q=\frac{aC}{1+bC} \tag{2.9}$$

Freundlich Equilibrium Expression:

$$aC=Q^{n} \tag{2.10}$$

Linear Rate Expression:

$$\frac{\partial q}{\partial t}=K(Q-q) \tag{2.11}$$

Second Order (Langmuir) Rate Expression:

$$\frac{\partial q}{\partial t}=K[C(Q_s-q)-Bq(C_o-C)] \tag{2.12}$$

Weiss then described the progressive change of the band profile during migration for a Langmuir, Eqn (2.9), and Freundlich isotherm Eqn (2.10).

The theory of chromatography then expanded rapidly. The plate theory [Martin (1941)] or the stage model [Craig] and solutions of the partial differential equations were developed in parallel. The evolution of the theory of chromatography for a single component is discussed in the next two sections.

Elution Mode

Glueckauff (1947a,1949b) was one of the early investigators who made experimental and theoretical contributions in all modes of chromatography. For the single component problem, he measured the single component isotherm and showed experimentally and theoretically the development of the band profile in a pure solvent when the isotherm is concave up, concave down and sigmoidal. For a concave up isotherm, the profiles have a sharp front and diffuse rear boundary while for a concave down isotherm, the bands have a diffuse front and sharp rear boundary. On the other hand, for a sigmoidal isotherm, the profile depends on the final concentration with respect to the inflection point.

Martin was the first to develop the plate theory; however, in the mid 1940's, Craig developed an apparatus and a method to describe the distribution of solute in linear chromatography based on a multiple step extraction process where each stage is considered as a an ideal mixer. Mobile phase is transferred from one vessel to the next as new

mobile phase is added to the first vessel. The Craig machine gives the binomial distribution as the response to a pulse injection in linear chromatography, the same result obtained by Martin. It should be noted that the Craig separation represents intermittent flow since fluid is transferred from one mixing vessel to the next. The continuous flow model, however, leads to a Poisson type distribution. For a large number of stages the poisson and binomial distribution may be approximated by a Gaussian distribution function. The difference between these models has been discussed by Klinkenberg et al. and Keulemans. Villermaux in his book also showed the equivalence between the plate and continuous model. Although the Craig distribution model was used primarily to study linear chromatography, it can easily be extended to use of a nonlinear isotherm, thus is mentioned in this review as a significant contribution.

Many other developments were made in linear elution chromatography, particularly in describing the contributions to band broadening [Van Deemter] and more recently by [Horvath et al.(1978) and Huber (1973)], and a detailed analysis [Giddings] is not given here. However, for the nonlinear case the contributions to the HETP have been studied [Poppe and Kraak, Knox (1986), Eble et al (1987a, 1987b) and Golshan-Shirazi [(1988a,1989a)] by lumping all the sources of band broadening, kinetic and thermodynamic, into the column efficiency. They assumed that kinetic and thermodynamic factors

$$HETP=H_{th}+H_k \qquad (2.13)$$

contribute to the total HETP and presented correlations between the efficiency and the sample size.

Not only is it important to understand the contributions to band broadening, but to derive analytical solutions taking into account the different mechanisms of band broadening. Using a second order rate expression (Eqn. 2.13), Goldstein (1953a) derived an analytical solution to the mass balance equation for ideal nonlinear chromatography for a pulse injection of any width. This was an extension of the Thomas model (i.e large volume injection) to injections of any width. Goldstein (1953b) went further to show that in the limit of fast kinetics the solution obtained is the same as with equilibrium theory.

Carr [Wade et al.] simplified the equations derived by Goldstein for calculation of single component overloaded band profiles for a second order rate expression assuming a Dirac injection. He also characterized the profiles by calculating the first and second moments and studied their effect on the amount injected. Kinetic parameters were obtained from experimental band profiles by fitting them to theoretical profiles [Wade et al., Lucy et al.].

In the case of a linear isotherm, the effect of dispersion (Peclet number) and the mass transfer coefficient in a linear rate expression on the band profile was investigated by Villermaux. The appearance of split peaks was shown [Villermaux (1970)] and methods to extract equilibrium and kinetic parameters from the profiles is proposed [Villermaux (1972)].

If the rate of mass transfer is slow and equilibrium cannot be assumed, the rate of adsorption and desorption can be modeled with a linear rate expression, Figure 2.1. Carta (1988a) derived an

infinite series solution for a pulse of any width; however, it assumes the concentrations are small enough for equilibrium adsorption behavior.

Houghton simplified the problem by assuming equilibrium and using a parabolic isotherm equation and solved a simplified Burgers equation derived from the mass balance equation by replacing the diffusion term with an apparent dispersion coefficient, Equation (2.4). The analytical solution derived is valid as long as the isotherm can be approximated as a parabola. Due to the approximations made, however, mass is not conserved. Haarhoff and Van der Linde have derived an approximate solution, which is rigorous for a parabolic isotherm and a semi-equilibrium model. Golshan-Shirazi (1990b) has compared the profiles obtained with the Houghton and Haarhoff solution under conditions of increasing mass loaded.

Recently Do et al. has summarized the theoretical forms of many standard models with two parameters.

In the case of ideal, nonlinear elution assuming an equilibrium Langmuir isotherm analytical expression describing the band profile as a function of the loading factor have been derived [Golshan-Shirazi (1988a)]. The ideal solution is one of the simplest models of chromatography and it works well for predicting experimental elution profiles [Golshan-Shirazi (1989a)] for chromatographic columns where the particle size is small (i.e the efficiency is >1000 plates) and the loading factor is greater than 3 %. Later a close form solution was derived for any isotherm [Golshan-Shirazi (1990a)].

With the advent of fast computers, numerical solutions have appeared. A numerical solution of the semi-ideal model was developed [Guiochon et al. (1988a)] and used to predict band profiles for different sample size having measured the HETP, flow rate, void volume, extra column volume, column length and adsorption isotherm. Excellent agreement is obtained with experimental data [Golshan-Shirazi et al. (1988b,1988c)]. By replacing the equilibrium isotherm with a linear rate expression, the effect of the sample size and the kinetic rate constant on the band shape in overloaded elution chromatography was studied [Lin et al. (1988,1989a)].

The above model was used to describe the profile of a single component in the presents of a binary eluent containing a strongly adsorbed additive [Golshan-Shirazi (1989f)]. The appearance of system peaks was observed and the band shapes are in agreement with experimental results [Golshan-Shirazi (1989g)]. An inversion of the band shape appeared in the presence of a strong solvent. In other words if the isotherm of the solute was Langmuirian, in the presence of a strongly adsorbing additive the band appears to have the shape of an overloaded band with a concave up isotherm.

Recently, Snyder [Eble et al. (1987a)] used the Craig model to calculate band profiles in isocratic elution and develop general correlations between the capacity factor and the efficiency versus the sample loading. Experimental data confirm the relationships obtained [Eble et al. (1987b)]. They [Snyder (1988)] also used the Craig model to determine band profiles of a single solute in gradient chromatography with qualitative agreement (i.e. except for a factor of

1.8 between experimental and theoretical profiles) with experimental data [Cox (1989b)].

Frontal Mode

A general analytical solution to the Reiman problem (step injection) for a nonlinear system was first solve by Thomas (1944) assuming second order kinetics, and no diffusion term. Hiester and Vermeulen derived numerical solutions for Thomas's analytical results. By nondimensionalizing the equations, the entire family of breakthrough curves can be represented with a single curve dependent only on the rate constant. They also showed that the solution calculated using second order kinetics can be obtained using a linear rate expression. To obtain an exact solution, the rate constant is concentration dependent, but may be approximated by an average constant value. Similarly, Lapidus and Amundson showed the equivalence between the kinetic model and a semi-equilibrium model for fast kinetics in the linear equilibrium case. Cooney and Lightfoot gave a mathematical proof of the constant pattern behavior for a Langmuir isotherm (i.e. after a certain column length, the breakthrough front does not change shape). In the early seventies, many analytical and numerical solutions were derived assuming various rate expressions, and either Langmuir, Freundlich or irreversible isotherms. Ruthven has summarized these analytical solutions in his book.

Application to Isotherm Determination

The primary use of single component measurements is determination of single component adsorption isotherms. Measurement of the single component overloaded elution profiles can be used to determine the adsorption isotherm by the method of Elution by Characteristic Point (ECP) [Cremer and Huber (1961), Glueckauf (1949a)]. The detector response signal is converted to concentration by calibration of the detector by direct injection of the sample at different concentrations. The amount adsorbed is calculated by integration of the area under the peak (using partial sums):

$$Q(C) = (1/V_{sp}) \int_{C_1}^{C_2} (V - V_o)\, dC' \qquad (2.14)$$

This method does not take into account band broadening due to diffusional and kinetic resistances, thus this technique is limited to the use of high efficiency columns.

The method of ECP points out the general inverse problem of determining isotherms from peak shapes. If the isotherm is Langmuirian, for example, the analytical solution of the ideal model can be inverted to give isotherm parameters from one large and one small volume injection [Golshan-Shirazi (1988a)]. Other novel approaches for isotherm determination have been developed by systematically guessing values of the parameters of an isotherm model and then minimizing the error between the calculated and the measured peak profile the best isotherm is determined [Dose et al. (1990) and Jonsson et al.]. However, with this method an equation is needed (i.e. an adsorption isotherm model) a priori. There are other methods (i.e.

frontal analysis) where the amount adsorbed per unit volume of stationary phase is obtained directly from the experimental data and the fit to a model can be made afterwards.

Frontal analysis can also be used to determine the adsorption isotherm [James and Phillips (1954) and Schay and Szekely (1954)] by making step changes of increasing concentration [Eltekov (1985,1986)]. This method has been applied to the determination of isotherms of peptides [Jacobson et al. (1984)] and proteins [Huang et al. (1987a,1987b)]. In contrast to the method of ECP, in frontal analysis detector calibration is unnecessary, but can be made concurrently from the plateaux of the step changes in concentration for other uses. Additionally, ECP does not take into account dispersive and kinetic effects while frontal analysis is independent of these effects. The area from the dead time to the breakthrough curve gives the amount adsorbed:

$$Q_{i+1}=Q_i+\frac{(C_{i+1}-C_i)\,(V_F-V_o)}{V_{sp}} \qquad (2.15)$$

It has been shown experimentally that ECP and frontal analysis give the same experimental isotherm [Jacobson et al. (1984), Golshan-Shirazi et al. (1988b)].

2.2 Two and Multi-Component Problem

Wilson and Devault both discussed briefly the theoretical statement of the two component problem, but it was Glueckauf who first gave a comprehensive analysis of the chromatographic separation process for 2 solutes following competitive Langmuir adsorption in the elution

[Coates (1947)] and the displacement modes [Gluckauf (1946)]. Analytical solutions can be derived in only a few specific cases. More generally numerical solutions are required. Two approaches have been taken in finding numerical solutions, one is using various finite difference schemes and the second is using finite element or collocation methods.

Elution Mode

The term preparative chromatography is primarily associated with nonlinear chromatography with a pulse injection (i.e. overloaded elution chromatography) and is used primarily by chromatographers and biochemists to produce pure products at the bench scale. However, recently its use is expanding into other fields such as chemical engineering and analytical chemistry.

Theoretically Glueckauf (1949b) calculated the two component band profile assuming ideal chromatography with equilibrium Langmuir isotherms and experimentally determined 2 component band profiles by collecting fraction with an "automatic device" [Coates]. Except for the severe tailing of the second component band, good agreement was obtained between experimental and theoretical profiles. He extended these results to two component separations with a competitive Freundlich isotherm [Glueckauf (1947c)].

Helfferich and Klein developed a theory of multi-component chromatography based on the ideal model of chromatography. Although primarily used displacement applications, it can be readily applied in the elution mode [Geldart, Golshan-Shirazi (1989k)]. Rhee, Aris and

Amundson discussed in 1970 the chromatographic cycle and the separation of components in the column from a pulse injection as well as the separation in the time distance space. The primary purpose of this paper is to explain the mathematics of one-dimensional, isothermal, ideal equilibrium models of chromatography and the theory of simple waves. The theory of simple waves applies to large volume injections where simplifications of the solution occur because there is a constant state (the plateau), which does not appear in overloaded elution chromatography since the injection volume is sufficiently small that the plateau has eroded.

Recently, an analytical solution to the problem of Langmuir equilibrium isotherm for a pulse injection has been solved assuming ideal behavior [Golshan-Shirazi (1989h)]. This solution is based on the coherence condition described by Helfferich and Klein. The primary assumption in this derivation is that the concentration of each of the two components in the mixed zone at a given time and location have the same velocity. (This also means that the velocity at two different times is not the same.) The ideal model was then used to study the effect of the sample size, separation factor, product purity, sample composition, limiting pressure drop and particle size on the production rate [Golshan-Shirazi (1989b,1989c)].

Knox and Pyper have developed expressions to calculate the maximum throughput at low loading assuming no interaction between solutes on a column having infinite efficiency, 100% yield and 100% purity. Although this is a simple model, the optimum throughput for the second component predicted is in close agreement with models which

taken into account competitive effects, assuming 99% purity and taking into account dispersion [Katti (1989c)].

The Craig distribution model as applied to binary mixtures with an isotherm calculated on a scheme based on a 9 term polynomial expansion has been used by Snyder [Eble et al. (1987c, 1987d)]. Snyder calculated cumulative distribution profiles under slightly overloaded conditions and derived general empirical relationships between the capacity factor and the resolution. These cumulative distribution profiles were also compared with single solute experimental profiles. He identified displacement effects which can enhance the separation of two components compared to the single solute case. He proposed a phenomenon called the "blockage effect which is a poor restatement of displacement effects. Since computation times on an IBM XT were long, an attempt to combine empirical results from the blockage model with the model of Knox and Pyper to predict the recovery of solutes at increasing sample size [Snyder et al. (1987,1989b)].

Recently, Snyder (1989a) studied heavily overloaded separations with the Craig model; however, the two component band profiles obtained are not in accordance with theoretical results obtained for a competitive Langmuir isotherm [Gluckauff (1946)]. Moreover, he uses a emperical correction factor of 1.8 in order to obtain agreement of the predicted profiles with experimental data. It is believe that the reason for these discrepancies is that approximate isotherm used is not equivalent to a competitive Langmuir isotherm and thus he obtains strange peak shapes [Snyder (1989a)].

The band profile of a two component mixture was calculated using finite difference techniques [Guiochon et al. (1988b)] in order to determine the effect of the individual parameters such as the sample size [Ghodbane (1988b)], separation factor [Ghodbane (1988c)], flow velocity [Ghodbane (1988d)] and composition [Ghodbane(1988a), Guiochon (1988c)] on the production rate [Ghodbane (1988e)]. Optimization of the production rate as a function of the sample size for two components show that one should overload the column until the amount of overlap meets the purity requirements [Katti (1989c)]. Qualitative experimental verification of the displacement and tag-along effects presented in the work of Ghodbane has been shown [Newburger]. From measured equilibrium isotherms, the predicted profiles of small molecules were in quantitative agreement with experimentally determined profiles [Katti (1989a,1990)]. Application of overloaded elution to trace enrichment of one component in a two component mixture was studied experimentally and theoretically by increasing the loading factor to maximize displacement effects [Katti (1989b)]. Further applications have been made to three component mixtures [Jacobson (1989)].

In an ideal two component system, the saturation capacity of both the components are equal; however, few systems are ideal. The effect of converging and diverging single component isotherms on the band profile [Cox (1989a)] and on the displacement and tag-along effects [Golshan-Shirazi (1990c)] have been applied using the Craig and the ideal model; respectively.

Comparison of the Craig model with models based on solution of the semi-ideal model equation Eqn. 2.1 by using various finite difference techniques showed that the two approaches are equivalent (Czok et al. and Karol (1988,1989) even though the Craig model is a mechanistic model and finite difference schemes are mathematical approximations.

Czok modified the semi-ideal model so that the amount of dispersion for each component can be controlled independently by adding a dispersion term and using a dispersion coefficient such that the sum of the dispersion term and the numerical errors due to the finite difference scheme give the total amount of desired band broadening.

Another implementation of the semi-ideal model was made by discritizing the dispersion term directly and using the Lax-Wendroff finite difference scheme to reduce the contribution of numerical errors to band broadening. But it is much more difficult to obtain a stable solution [Lin et al. (1989d,1989e)] using this method.

Another aspect of 2 components separations is when the mobile phase contains a strongly adsorbing additive, such as an ion-pairing agent. Band profiles in this domain are inverted compared to when a nonadsorbing additive is used [Golshan-Shirazi (1989i)]. These results were also verified experimentally [Golshan-Shirazi (1989j)]. A review of theoretical end experimental 1 results with the semi-ideal model of chromatography has been presented in by Guiochon et al. (1989).

Using a forward finite difference method to model Eqn. 2.1, replacing Eqn. 2.2 with a linear kinetic rate expression and allowing the numerical error equal the degree of axial dispersion, the effect

of the kinetic constant on two component overloaded elution separations was studied [Golshan-Shirazi et al. (1989e)]. The chromatograms calculated showed that significant mass transfer effects cause tailing and retention time shifts.

Yu et al. (1987,1989) have used orthogonal collocation with gradient directed moving finite elements in order to solve the mass balance equation including a linear rate expression and inter and intra particle diffusion terms. The advantage of this method is that the numerical errors are low compared finite difference schemes; however, computation times typically require 1-2 hours of CPU to determine the profile with on a Gould NPI computer. Computation times for equilibrium models take only a few minutes. The equilibrium and non-equilibrium models have been used to scan the values of the various dimensionless quantities to identify the local equilibrium regime and understanding the relative importance of film mass transfer, intraparticle diffusion and axial dispersion for a specific system [Lee C.K. et al.(1990)]. Experimental results on proteins such as Lysozyme, BSA and Myoglobin show that the equilibrium model fails in predicting accurately the band profiles in ion exchange and a kinetic model must be used. Kinetic parameters are determined from correlations available in the literature [Wilson and Geankoplis (1966)].

Preparative chromatographic can also be operated in gradient elution. Zone migration in gradient elution [Yamamoto et al. (1987)] is more complex especially when the isotherm is non-linear. Snyder has shown the effect of the sample size on the band width [Cox (1988b)] and the band profile [Snyder (1989c,1989d)] in gradient elution

chromatography. Moreover, he has compared overloaded gradient profiles with those obtained in isocratic elution [Cox (1988a)]. Using a rigorous model [Antia et al.] have shown the effect of the gradient steepness and sample size on the production rate in overloaded gradient chromatography. However, gradient operation appears complex and industrial application would require a simpler pumping mechanism. The use of step gradient techniques for eluting compounds of widely different capacity factors has been investigated for protein purifications [Lee et al. (1988), Velayudhan (1988), Carta (1989)]. By choosing the appropriate step size and step time, the production rate is optimized.

Preparative chromatography also need not be a batch operation. The continuous annular chromatograph [Martin (1949); Scott et al. (1976)] was developed by rotating an annular bed of sorbent past a stationary feed entry point. As the compounds elute along the column the components separate in along helical trajectories and elute at different points in the column. At the end of the column pure components can be collect along the periphery of the annulus. This technology has been applied to the separation of Sugars [Howard]. Elution profiles were predicted by solving the steady state 2-dimensional (length, angle) mass balance for 2 components with a linear rate expression. For this particular application, the isotherms were linear and agreement with experimental data was excellent. By applying an electric field across the annulus [Scott (1986)], this technology has been applied to the separation od large molecules and proteins.

Recently this approach has been used in the displacement mode (see displacement section).

Frontal Mode

The study of band profiles and the effect of dispersion on the profile shape has been studied theoretically [Claesson, Rhee and Amundsun] and experimentally [Coates et al., Saunders et al. (1988, 1989a,1989b), Horstmann]. It has a large impact in affinity chromatography where there is irreversible adsorption until the mobile phase is altered. However, another use of two component frontal analysis is determination of binary adsorption isotherms [Jacobson et al. (1987)]. Experimentally, isotherms are measured by keeping the composition constant and increasing the sample amount in a stepwise fashion. By sampling the concentration at specific points and knowing the sample concentration at each step, the isotherm along a line of constant composition is determined. The ratio of the composition is changed inorder to determine the entire isotherm surface. This method has been applied to the measurement of the competitive adsorption isotherms where an interchange of the elution order occurs at increasing sample size [Huang (1989), Lin et al. (1989b)].

An improved method is proposed by Ma et al. based on determining the profile of a two component mixture for several large volume injections. By transforming the chromatogram into Hodograph space, Langmuir parameters can be determined by a least square fit to the straight lines.

Frontal chromatography has also been applied in affinity chromatography applications [Arve et. al.] or to characterize new adsorbent materials [Rixey et.al].

Displacement Mode

The difference between elution and displacement chromatography were recognized by Tswett in the early 1900's. However it wasn't until Tiselius (1943,1949) clearly defined and discussed the various possible modes of chromatography (elution, frontal, displacement). Gluckauff (1946 and 1949b) in 1946 analyzed theoretically displacement development. He also showed the effect of the flow rate on displacement development [Glueckauf (1947b)]. In the last 40 years the enormous growth of linear elution chromatography for analytical separations has overshadowed the use of displacement chromatography, in spite of several important industrial applications. A comprehensive review of the history and development of displacement chromatography and its applications has been published by Frenz et al. (1988). The major advances and recent applications will be reviewed on this section.

On the theoretical front Helfferich presented a general theory that could be applied to multicomponent displacement separations by a transformation of variable called the h-transform. This theory assumes ideal chromatography with equilibrium competitive Langmuir isotherms, but can be extended to introduce column efficiency [Wang Sep. Sci, Frenz PhD. Thesis]. Rhee and Amundson (1982) applied the theory of multicomponent chromatography to elucidate the characteristics of

displacement systems for Langmuir isotherms. Later, numerical methods were developed to study displacement separations when the column has a finite efficiency [Katti (1988)]. The effect of kinetic parameters has been studied which in the least show the smoothening of the sharp front and rear boundaries and in the worse case shows that an isotachic train can not be observed if the rate of mass transfer is sufficiently slow [Golshan-Shirazi et al. (1989d)].

Basmadjian et. al. modeled displacement separations neglecting accumulation in the mobile phase and band dispersion. He reexamined some of the pioneering work of Glueckauf by using geometrical concepts to predict adsorption behavior, for example by illustrating the significance of the Watershed point. He investigated the displacement of a less adsorbed species with a more strongly adsorbed species and visa versa. Phillips et al. (1988) have used a kinetic and dispersive model to determine the independent effect of mobile phase velocity, feed volume and particle size on the throughput.

In the 1940's as a part of the Manhattan Project, rare earth oxides were separated in the displacement mode [Spedding (1949,1950)]. Displacement chromatography was employed in the mid 1940's at the American Petroleum Institute [Mair] to fractionate petroleum distillates in 52.4 ft x 3/4 " I.D. columns. In the late 1960's, Sorbex and several other similar processes were developed at UOP using various novel technologies to achieve what is essentially displacement chromatography on a moving bed column without physically moving the bed [Broughton]. This technology was recently reviewed by Wankat.

In the late 1970's Horvath [(1981,1983,1985), Frenz (1988)] and co-workers reintroduced this technique. They capitalized on various technological advances, high-efficiency columns and fast [Maa] high-performance liquid chromatography. Methods for separating small organic molecules [Horvath (1981)], polymyxin antibiotics [Frenz (1985)], oligomycin antibiotics [Valko], steroids [Kalasz (1981)], enantiomer on chiral columns [Vigh (1989a,1989b)] amino acids [Kalasz (1982)], short peptides [Horvath (1983), Cramer (1987,1988)], polypeptides [Viscomi et al. (1988,1989,1990)], insulin [Vigh (1987)], nucleotides [El Rassi et al.] and proteins [Liao et.al, Subramanian et al. (1988,1989)] were developed.

Carrier displacement chromatography has been employed for the displacement of proteins using carboxymethyldextrans as spacers as well as a displacer [Torres et. al (1985) and Peterson (1987)]. Other workers have investigated the separation of Lithium isotopes for either the enrichment or the isolation of pure isotopes [Jacques, Fujii, Fujine (1982,1983)] by ion-exchange displacement chromatography. The literature presented thusfar has utilized chromatography in the batch mode. The continuous annular chromatograph has been applied to displacement separations in addition to overloaded elution separation. A typical continuous annular chromatograph is 0.6 meters long has an annulus 12.7 mm wide and a diameter 279 mm and is packed with 50 um diameter particles. This process has been applied to the separation of heavy metals [Begovich], rare earth oxides [Taniguchi et.al] and amino acids [Carta (1988b), De Carli (1988,1989,1990)].

These studies demonstrate the utility of displacement chromatography for the separation of various mixtures and its capacity to achieve high yields and high purities.

2.3 The Semi-Ideal Model

In most application of preparative chromatography to industrial scale problems, conditions will be employed where chromatography is easy to operate and in a form which gives a high degree of reproducibly. Thus, many simplifying assumptions can be made. One of the simplest general forms of the mass balance equation for one component is:

$$\frac{\partial C}{\partial t}+F\frac{\partial q}{\partial t}+u_o\frac{\partial C}{\partial z}=D\frac{\partial^2 C}{\partial z^2} \qquad (2.16)$$

where D is the molecular diffusion coefficient. This equation assumes no change in viscosity or density of the mobile phase with composition of the solute, no sorption effect, no solute solute interaction, the mobile phase is incompressible, constant flow velocity, isothermal flow, the dispersion coefficient is independent of concentration. The functions C, the mobile phase concentration and Q, the stationary phase concentration are not independent and require a relationship. When equilibrium can be assumed then

$$q=Q=f(C) \qquad (2.17)$$

Otherwise the rate of mass transfer between the mobile and stationary phase must be defined. Two expressions are commonly used. The linear rate expression:

$$\frac{\partial q}{\partial t}=K(Q-q) \qquad (2.18)$$

and the second order rate expression:

$$\frac{\partial q}{\partial t}=K[C(Q_s-q)-Bq(C_o-C)] \qquad (2.19)$$

In order to solve Eqn. 2.16 with either Eqn 2.17, 2.18 or 2.19, an inlet boundary condition and initial condition specifying whether the bed is filled with solute or not must be defined. The nature of this boundary condition depends on the mode of chromatography and must be specified accordingly.

It has been shown by Giddings and Haarhoff et al. that if the kinetics is fast, but not infinitely fast, Eqn. (2.16) and (2.18) can be replaced by Eqn. (2.20) and (2.21). Thus the semi-ideal model of chromatography is:

$$\frac{\partial C}{\partial t}+F\frac{\partial q}{\partial t}+u_o\frac{\partial C}{\partial z}=D_{ap}\frac{\partial^2 C}{\partial z^2} \qquad (2.20)$$

$$D_{ap}=\frac{HL}{2t_o} \qquad (2.21)$$

where the molecular diffusion coefficient D, Eqn. (2.16), is replaced by an apparent dispersion coefficient, Dap. The apparent dispersion coefficient Da is related to the column variance according to the Einstein relationship:

$$\sigma^2=2Dt_o \qquad (2.22)$$

where to is the retention time of an unretained compound. In linear chromatography, the variance of the band profile is related to the column length and the HETP:

$$\sigma^2 = HL \qquad (2.23)$$

Combining equations (2.22) and (2.23) the apparent dispersion coefficient is related to classical parameters, column plate height, mobile phase velocity:

$$D_{ap} = \frac{HL}{2t_o} = \frac{Hu_o}{2} \qquad (2.24)$$

In the ideal model of chromatography, plug flow and radial homogeneity is assumed. Thus the column has an infinite column efficiency (i.e. no band broadening, HETP = 0) and the apparent dispersion coefficient is zero. The RHS of Eqn. (2.20) can be simplified to:

$$\frac{\partial C}{\partial t} + F\frac{\partial q}{\partial t} + u_o\frac{\partial C}{\partial z} = 0 \qquad (2.25)$$

Using a forward finite difference scheme, Eqn. (2.25) can be solved by numerical computation. The finite difference scheme employed in this work is as follows:

$$C_{z,t} = C_{z-1,t} - \frac{dz}{u_o dt}\left[C_{z-1,t} - C_{z-1,t-1} + F(Q_{z-1,t} - Q_{z-1,t-1})\right] \qquad (2.26)$$

Since the column is sliced into discrete segments and for each segment there is associated a concentration, the concentration is not distributed continuously throughout the column. The approximation has the consequence that mass is averaged over the segments and the final result is band broadening. In this manner, dispersion is reintroduced into the ideal model. Therefore, the advantage of the semi-ideal model is that the diffusion coefficient and the mass transfer coefficient

need not be measured. The only measurements required are the HETP, the adsorption isotherm, flow rate, void time and column length.

By adjusting appropriately dz and dt, the amount of band broadening can be adjusted to be equal the apparent dispersion coefficient, Dap. Assuming that the space increment is equal to the HETP,

$$dz=H \tag{2.27}$$

it can be shown [Rouchon] that in the linear case that the numerical dispersion is equivalent to Dap when the time increment equal to:

$$dt=\frac{2H}{u_{zo}} \tag{2.28}$$

where

$$u_z=\frac{u_o}{(1+F\frac{\partial Q}{\partial C})} \tag{2.29}$$

and

$$u_{zo}=\frac{L}{t_R} \tag{2.30}$$

A rigorous proof of this relationship is based on the replacement of each term in Eqn. (2.25) by a taylor series expansion [Lin (1989c)].

For the multicomponent system, Equation (2.20) is extended to:

$$\frac{\partial C_i}{\partial t}+F\frac{\partial q_i}{\partial t}+u_o\frac{\partial C_i}{\partial z}=D_{ap}\frac{\partial^2 C_i}{\partial z^2} \tag{2.31}$$

The competitive Langmuir isotherm is frequently used because of it simplicity and utility to relate the concentration of the solute in the stationary phase, Q, to the mobile phase concentration, C:

$$Q_i = \frac{a_i C_i}{(1+\Sigma b_i C_i)} \qquad (3.32)$$

The assumptions made in derivation of this isotherm are that the solution is ideal, the stationary phase is ideal, the solute gives monolayer coverage, their are no solute solute interactions and no solvent solute interactions.

In the case of a multicomponent mixture, uz, Eqn. (2.30) is not the same for each component. Assuming uzo was calculated from the average retention time at infinite dilution, for the two component case we obtain:

$$t_{r,avg} = T_{R1} + T_{R2} \qquad (2.33)$$

and

$$u_{zo} = \frac{L}{t_{r,avg}} \qquad (2.34)$$

This approximation implies that a peak having an retention time travg has an HETP equal to dz. However, the true HETP of each component is different and depends on the retention time of each component. It can be shown that this finite difference technique gives a capacity factor dependence on the HETP for a given dz and dt. If dz and dt is kept constant, as the retention time of the sample increases the HETP decreases. The limitation of this method is that the retention times much be sufficiently close that we approximate accurately the amount of dispersion. Moreover, this method cannot easily be extended to gradient elution because very large retention times would give a negative HETP. It should be mentioned that there are many finite

difference schemes and they propagate error in a different manner. That is the capacity factor dependence on the HETP at constant dz and dt is different [Czok et al.].

The primary objective in this thesis is to compare the predictions by this simple model with experimental data without empirical fitting of the model with the data. More sophisticated models could be solved, but at the sacrifice of larger computation times and difficult experimental measurements.

Chapter 3

One Component Problem: Comparison of Theory and Experiment

Prediction of band profiles in Preparative Chromatography requires minimally measurement of the equilibrium adsorption isotherm of each component, the dead time, the mobile phase linear velocity and the column HETP. Crosscheck of the data can give more accurate results if the retention time of each component at infinite dilution, the flow rate and the porosity are also measured. Predicting band profiles using this approach requires that the measured isotherm data is fitted to a model. The Freundlich, Langmuir, Bilangmuir and Fowler isotherms are the most commonly used. In this study, the Langmuir and BiLangmuir equations have been used to predict of single component bands in overloaded elution chromatography.

This chapter discusses the one component problem of chromatography. This involves measurement of the single component isotherms by frontal analysis and Elution by Characteristic Point (ECP) and prediction of the single component band profiles in overloaded elution chromatography as a function of the amount injected. Two applications are presented in this chapter. In the first, reversed-phase chromatography was employed using small organic molecules as the solute and in the second application, ion exchange was employed with protein solutes. The choice of the molecules was based on the following criteria: (1) solute-solute interactions could be neglected

(2) elute under isocratic conditions in reversed phase chromatography (3) could be used without further purification (4) absorbed in the UV. Phenyl-ethanol, phenyl-propanol and 2,6 dimethylphenol were used in these experiments. The two proteins studied where Chicken Albumin and Conalbumin.

3.1 Single Component Overloaded Elution of Small Molecules

This section will present measurement and prediction of single component elution profiles of phenyl-ethanol (PE) and phenyl-propanol (PP) in reversed-phase chromatography. The subsequent subsection will describe the experimental section.

In summary, two columns were packed with the same stationary phase. Table 3.1 compares the results of the isotherm measurements for 3-phenyl-ethanol and 2-phenyl-propanol. Comparison of the two columns shows that the retention time and capacity factor at infinite dilution give the same results for the two columns. However, the Langmuir 'b' parameters are significantly different. For the first column, the isotherm was measured for mobile phase phenyl-ethanol concentrations between 0 and 9 mg/ml and phenyl-propanol concentrations between 0 and 15 mg/ml. However, on the second column, the range of concentrations for the phenyl-ethanol was 0-16 mg/ml and only 0-5 mg/ml for the phenyl-propanol. The 'b' parameter for the phenyl-ethanol was larger on column # 2 indicating a larger degree of curvature due to the higher concentration range studied. The large differences in 'b' values for column #1 and #2 for phenyl-propanol, however, is not quite as clear. A plot of the isotherm for phenyl-ethanol and phenyl-

Table 3.1 Summary of Isotherm Data for Phenyl-ethanol and Phenyl-propanol

	Column # 1		Column # 2	
	PE	PP	PE	PP
t_R (sec)	310	416	300.5	426.1
k'	0.722	1.311	0.707	1.421
a (ml/ml)	1.9239	3.554	1.9369	3.4144
b (ml/mg)	0.01481	0.0255	0.02178	0.05920
b (ml/mmole)	1.8092	3.479	2.6612	8.0633
CSC (mg)	140	150	109	70
MW (g/mole)	122.17	136.2		
HETP (um)	0.0167		0.009	
t_0 (sec)	180		176	
porosity	0.755		0.706	
F	0.325		0.4165	
F_v (ml/min)	1.0		1.0	

propanol on these two columns is shown in Figure 3.1. This isotherm data provides parameters for the prediction of band profiles of binary mixtures which is discussed in Chapter 4.

Experimental

This section will describe the equipment used and the measurements required in order to compare experimental single component overloaded band profiles of two organic molecules with theoretical predictions.

Equipment

The modular liquid chromatograph used for the measurement of band profiles was assembled from two Model 510 Waters (Milford, MA) pumps, a Valco (Houston, TX) 6-port electrically actuated valve fitted with a 20 or 100 ul sample loop, a Kratos Spectroflow (Ramsey, NJ) variable wavelength detector operated at 272 nm. The pumps were controlled and the detector signal was monitored via a Waters System Interface Module (SIM) using the Waters Maxima 860 Dynamic Solutions (Ventura, CA) software installed on a NEC APCIV Powermate 2 computer. The electrical outputs of the valve and the detector were connected to the SIM box for automatic data acquisition.

Materials

Two 0.46x25 cm and one 0.1x100 mm adsorption column were packed in house at 9000 psi using standard procedures with 10um Vydac (Hesperia, CA) octadecyl-silica (ODS) stationary phases. The first

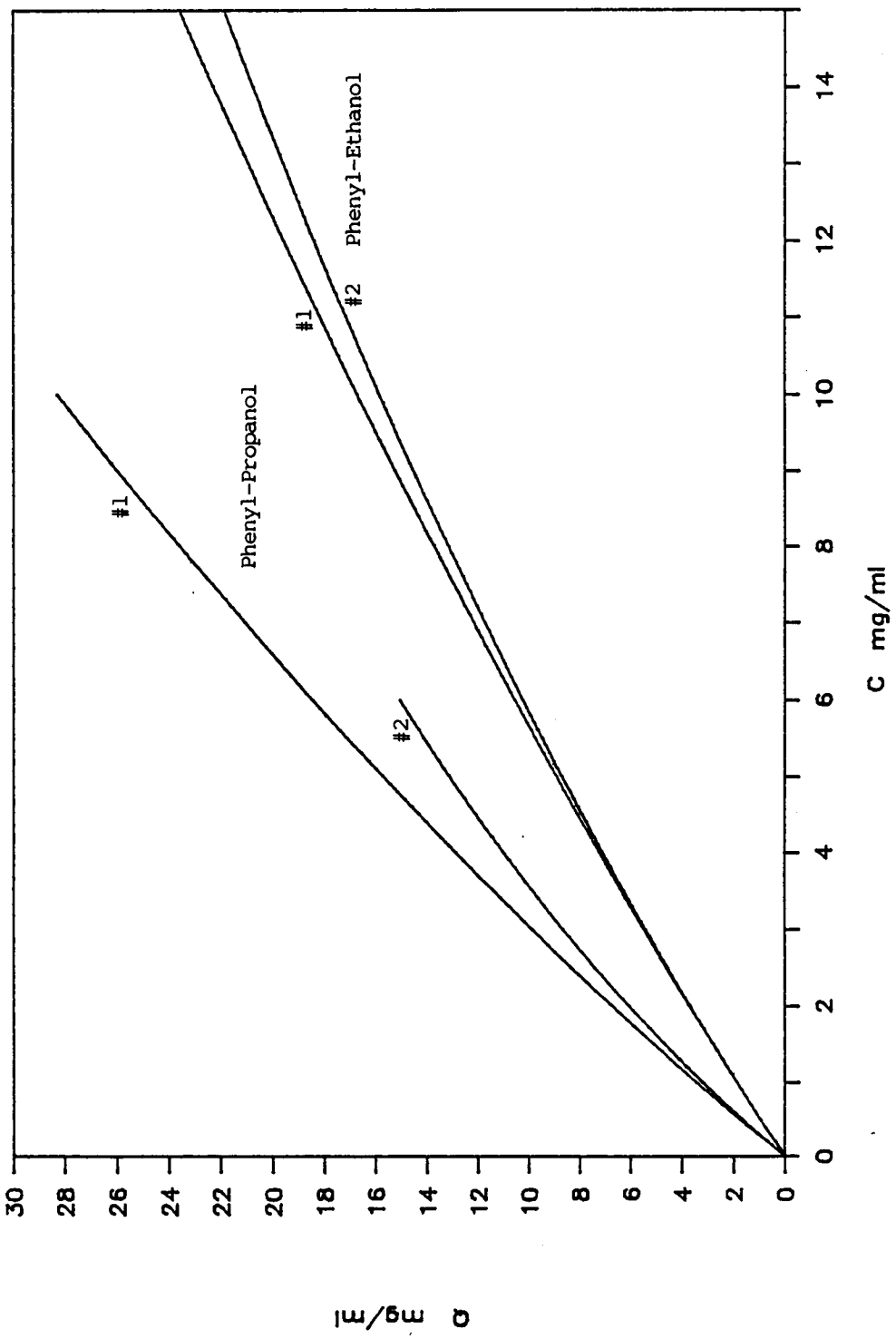


Figure 3.1 Comparison of Isotherms of Phenyl-ethanol and Phenyl-propanol on 2 Analytical Columns Packed with the same Stationary Phase

0.46x25 cm column packed is called column #1 and the second column #2.

The 3-phenyl-ethanol and 2-phenyl-propanol were purchased from Fluka (Ronkonkoma,NY) and used without further purification. 3,6 Dimethyl-phenol was purchased from Aldrich (Milwauke,WI). HPLC methanol and water (Burdick and Jackson, Muskegin,MI) were also used without further purification.

Experimental Procedure

The mobile phase was made by high pressure mixing of methanol and water degassed with Helium in a ratio of 1 to 1. The phenyl-ethanol and phenyl-propanol were made prior to the experiment by weighing the appropriate amount in a volumetric flask which was then filled with a hand mixed solution of 50% methanol/water. Small differences in the composition of the sample solvent and the eluent could be seen by the appearance of a small system peak in the elution experiments, but the differences was considered negligible.

The elution experiments were carried out by injecting the compound at a measured concentration in the 0.1 ml loop of the 6-port valve. Samples were injected twice and compared for reproducibility. By superposing the two chromatograms, it could be seen that the chromatograms obtained were identical. The flow rate was 1 ml/min, the data acquisition rate was 2 points/sec, and the elution time was set at 5 min. For each sample concentration, a file containing the elution curve was saved. After collecting the data, the files were translated to ASCII format, imported on the UTCC Vax computer, converted from

response to voltage using a calibration curve and saved for comparison with theoretical predictions.

Isotherm Measurement and Detector Calibration

Isotherms were measured using frontal analysis [James, Jacobson (1984), Golshan-Shirazi (1988b)] and by ECP. The apparatus used for the measurement of isotherms by frontal analysis was the same as described under the Equipment section except that the 6 port electrically actuated valve was replaced with a 10 port Valco Valve with two 5 ml sample loops [Lee A.(1990]. By injecting solutions of increasing concentration into the loop and switching the valve, step changes in the concentration were made. From the breakthrough curve, the amount adsorbed at each concentration step is determined by Equation (2.15). The Langmuir parameters are obtained by a nonlinear least square fit of the experimental data. From the plateaux concentration of each front in the isotherm measurement, the response for a known concentration was determined. The calibration curve was drawn and was fit to a polynomial. The degree of the polynomial was varied in order to fit the data well and avoid oscillations. Sometimes a polynomial having only odd powers was used. The experimental measurements were made between 0 and 80 mg/ml for the compounds studied. However, the curve fitting was done only in the range required for prediction of the band profiles. Figure 3.2 shows a typical example of the non-linear calibration curves for phenyl-ethanol and phenyl-propanol at 272 nm. Note that the phenyl-propanol absorbs more strongly than the phenyl-ethanol. This calibration curve has a

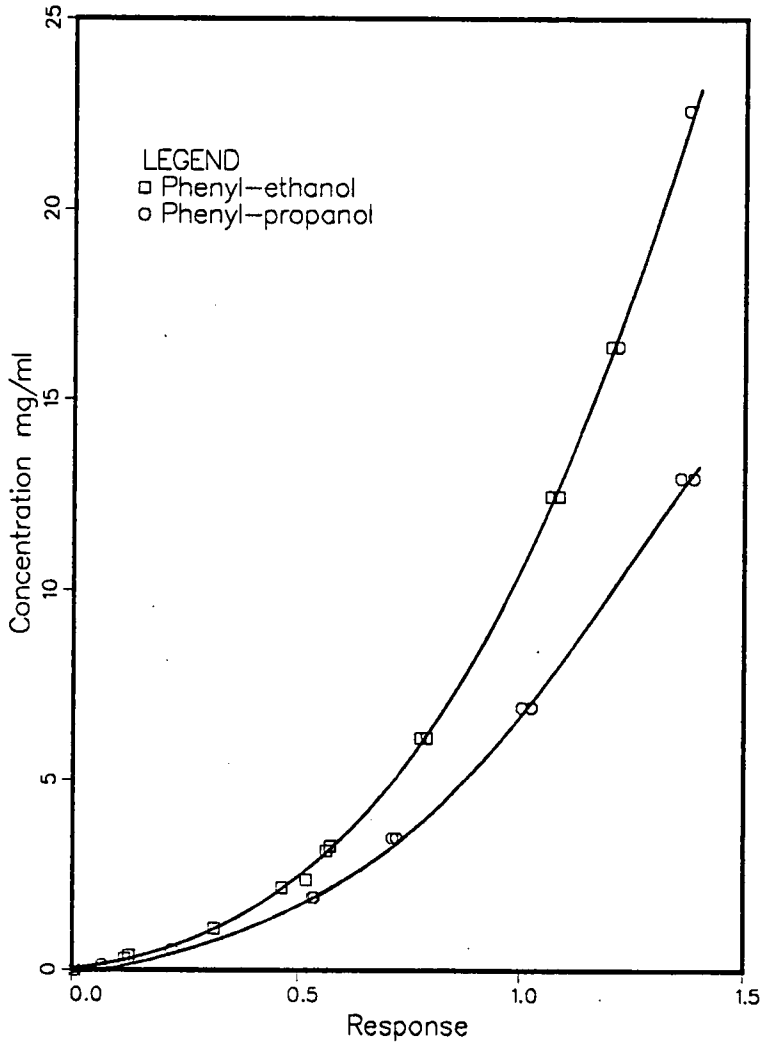


Figure 3.2 Calibration Curve of Phenyl-ethanol and Phenyl-propanol by Direct Injection

high degree of curvature due to the large concentration range investigated.

Isotherms by the method of ECP were determined from the concentration versus time chromatogram corresponding to the largest sample amount injected. The calibration curves to convert the response profiles to concentration were made by removing the column, putting it before the injector and injecting samples from a 5 ml loop directly into the detector.

Results and Discussion

On column # 1, the retention time at infinite dilution for 2-phenyl-ethanol and 3-phenyl-propanol were measured on the preparative column by injection of several samples at decreasing concentration. The dead time was measured from the solvent peak and was 3.08 minutes. The porosity was 0.75. The capacity factors were 0.72 and 1.3; respectively. The separation factor was 1.84. The measured column HETP was 0.01667 cm.

The single component Langmuir isotherm 'a' parameter used in the predictions was calculated from the capacity factor, k', and the phase ratio, F:

$$F = \frac{V_{sp}}{V_{mp}} \tag{3.1}$$

$$a = \frac{k'}{F} \tag{3.2}$$

The Langmuir b parameter was calculated from the least square fit of the Langmuir equation. The column saturation capacity for each component was calculated for each component:

$$csc_i = \frac{a_i}{b_i} V_{sp} \tag{3.3}$$

These values for these experimentally determined parameters are summarized in the Table 3.1.

Figure 3.3 shows a comparison of theory with experiment for phenyl-ethanol at a loading factor of 5%, 7.1 mg of sample introduced onto the column. Figure 3.4 shows a comparison of theory with experiment for a loading factor of 5% for phenyl-propanol which also corresponds to 7.1 mg of sample injected. The agreement between theory and experiment for these two compounds is good.

The isotherm measurements on column #2 were made by ECP. Figures 3.5, 3.6, and 3.7 show the best fit langmuir equation and the experimental data for phenyl-ethanol, phenyl-propanol and dimethyl-phenol; respectively. The experimental data is shown in squares and the fit is given by the line. Table 3.1 provides a summary of the isotherm parameters. Elution profiles were measured at different sample sizes. Figure 3.8 shows a comparison of theoretical and experimental band profiles for phenyl-ethanol when 0.20, 1.16 and 8.57

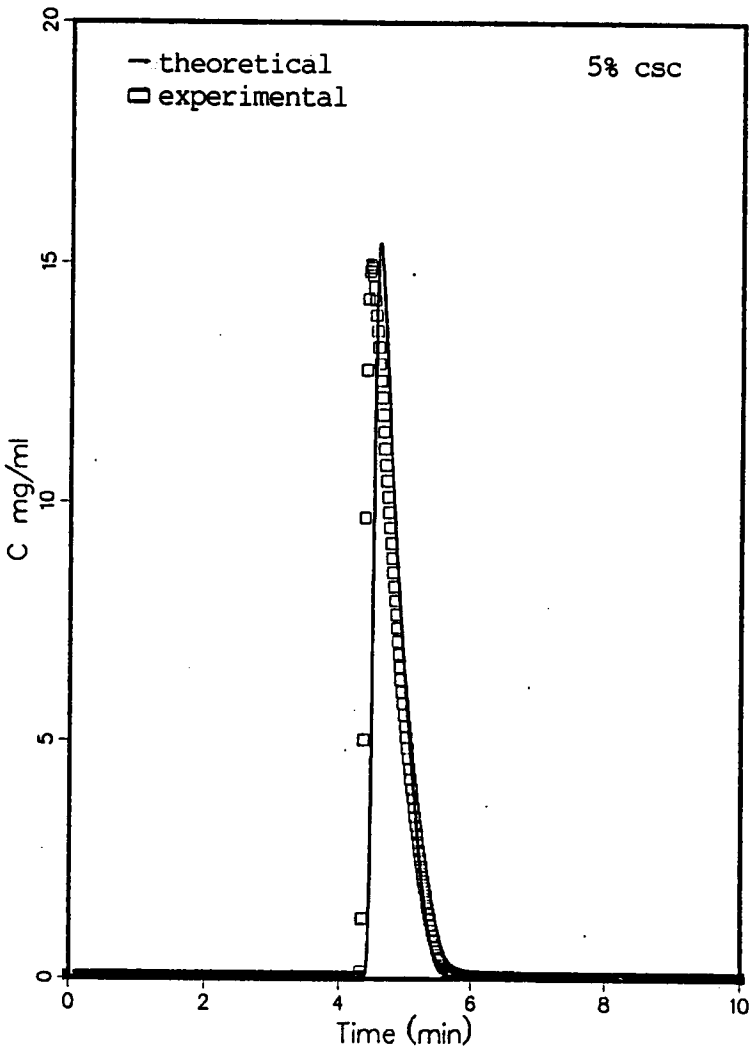


Figure 3.3 Comparison of Theory and Experiment, Column # 1 - Phenyl-ethanol

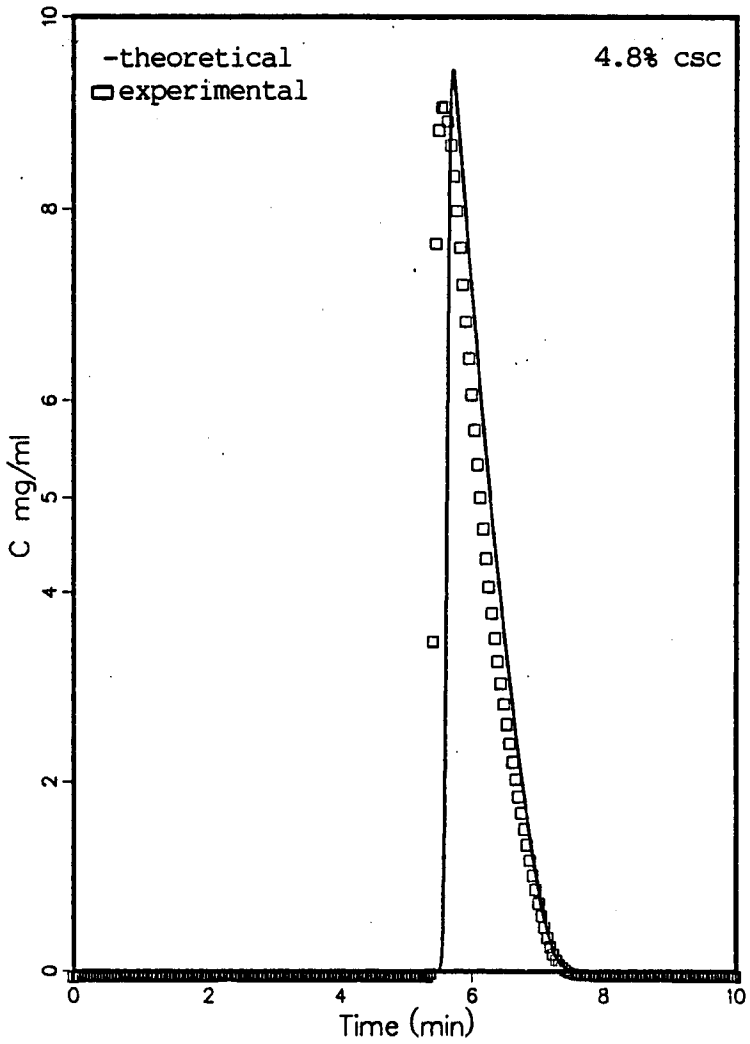


Figure 3.4 Comparison of Theory and Experiment, Column # 1 - Phenyl-propanol

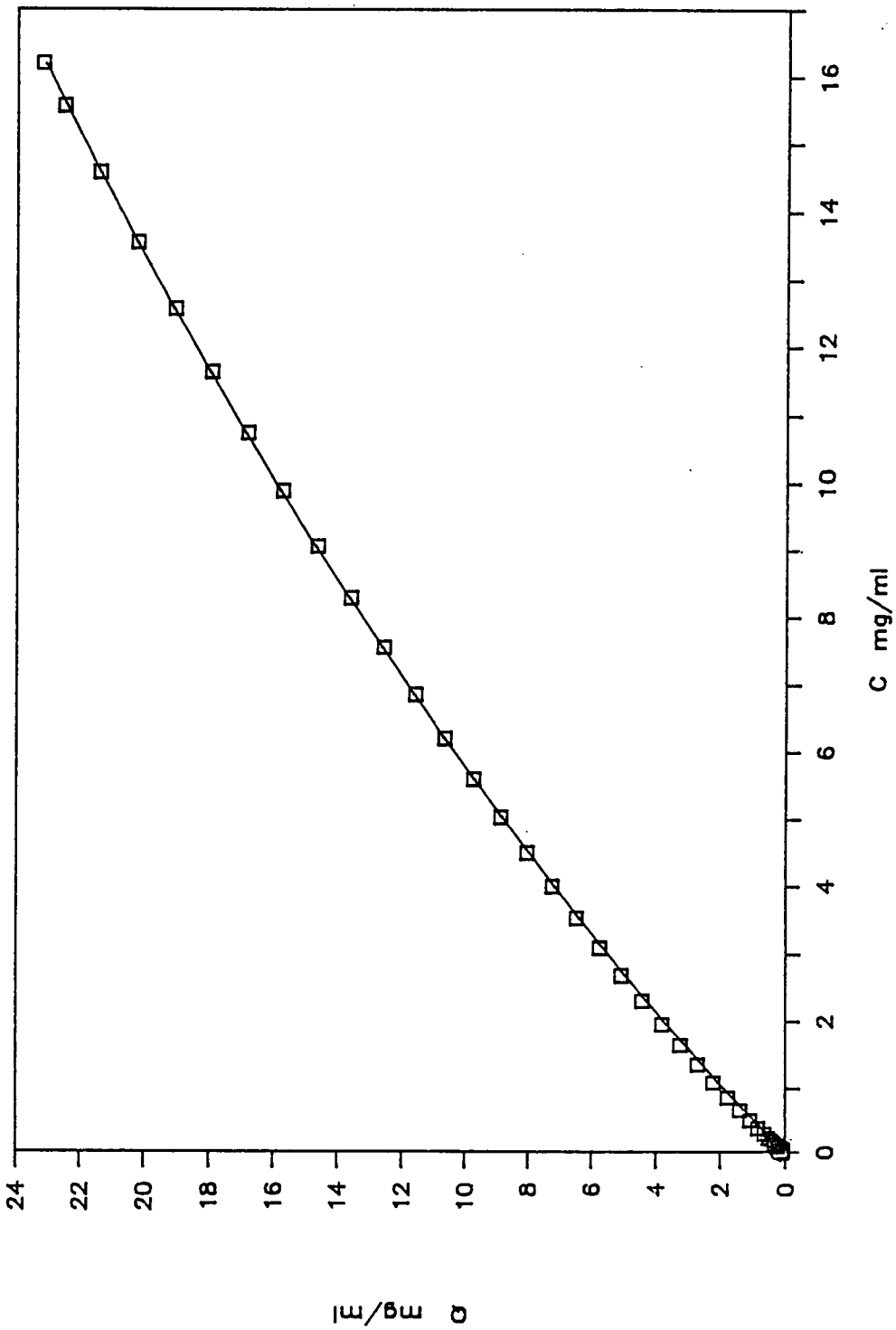


Figure 3.5 Adsorption Isotherm of Phenyl-ethanol by ECP

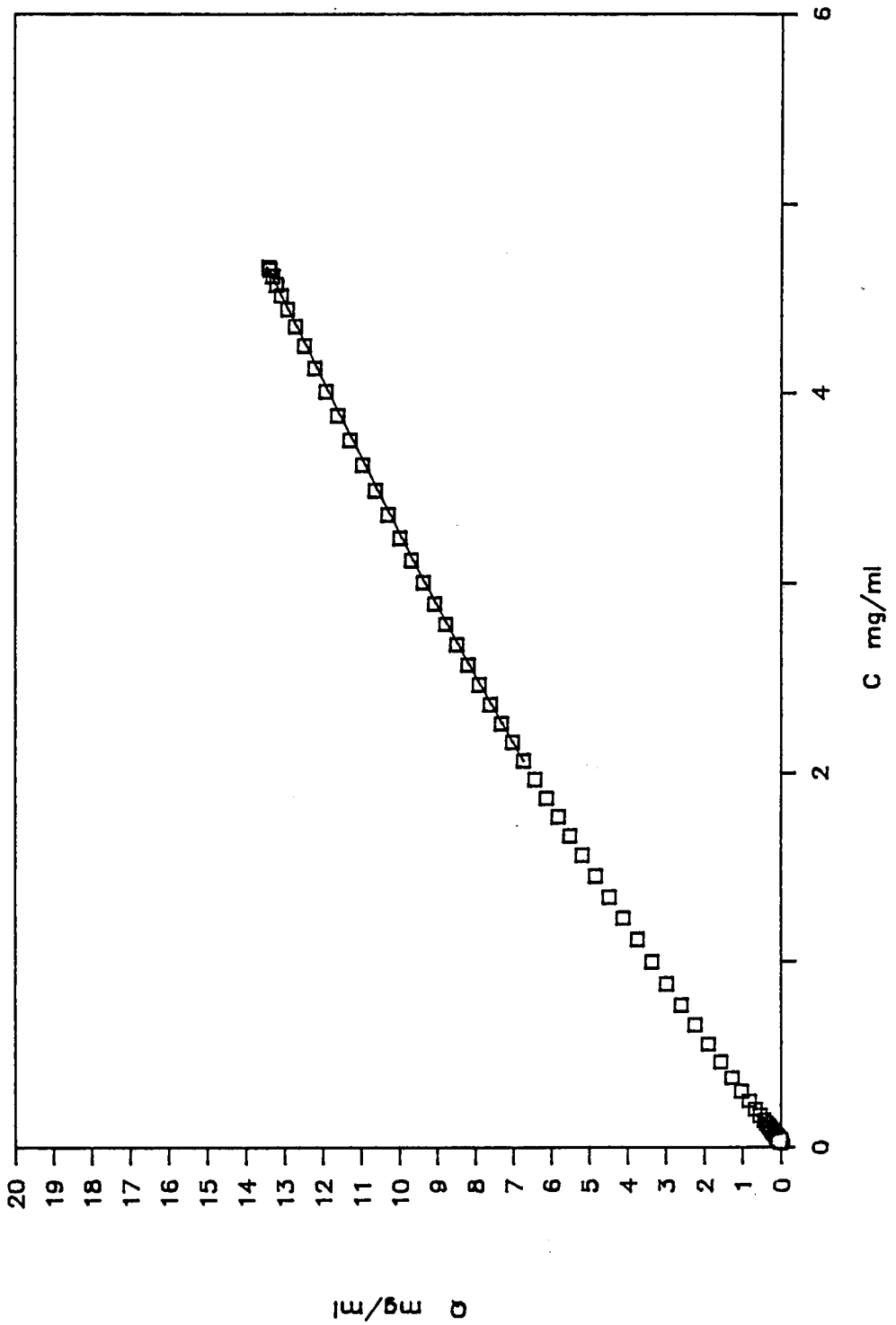


Figure 3.6 Adsorption Isotherm of Phenyl-propanol by ECP

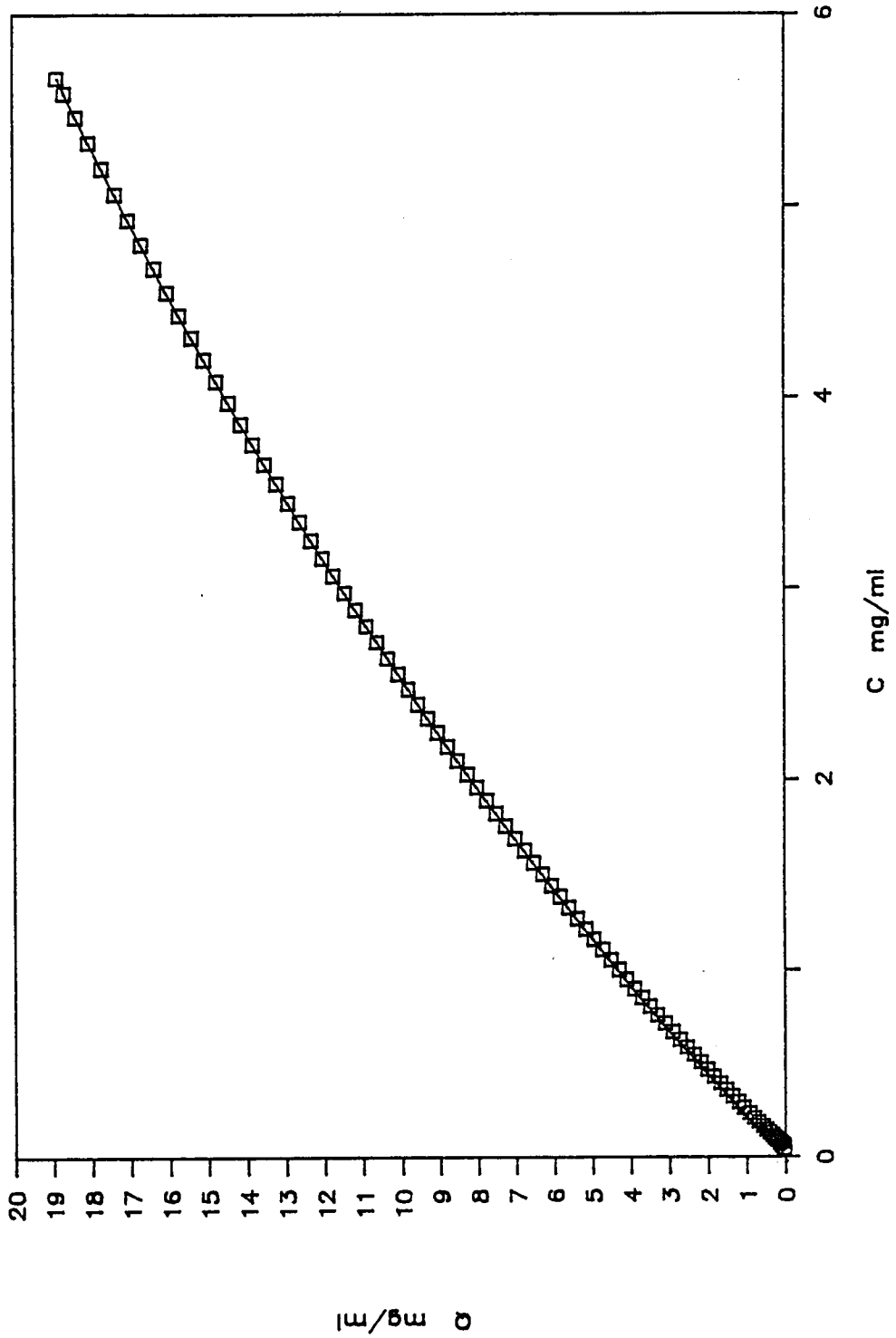


Figure 3.7 Adsorption Isotherm of Dimethylphenol by ECP

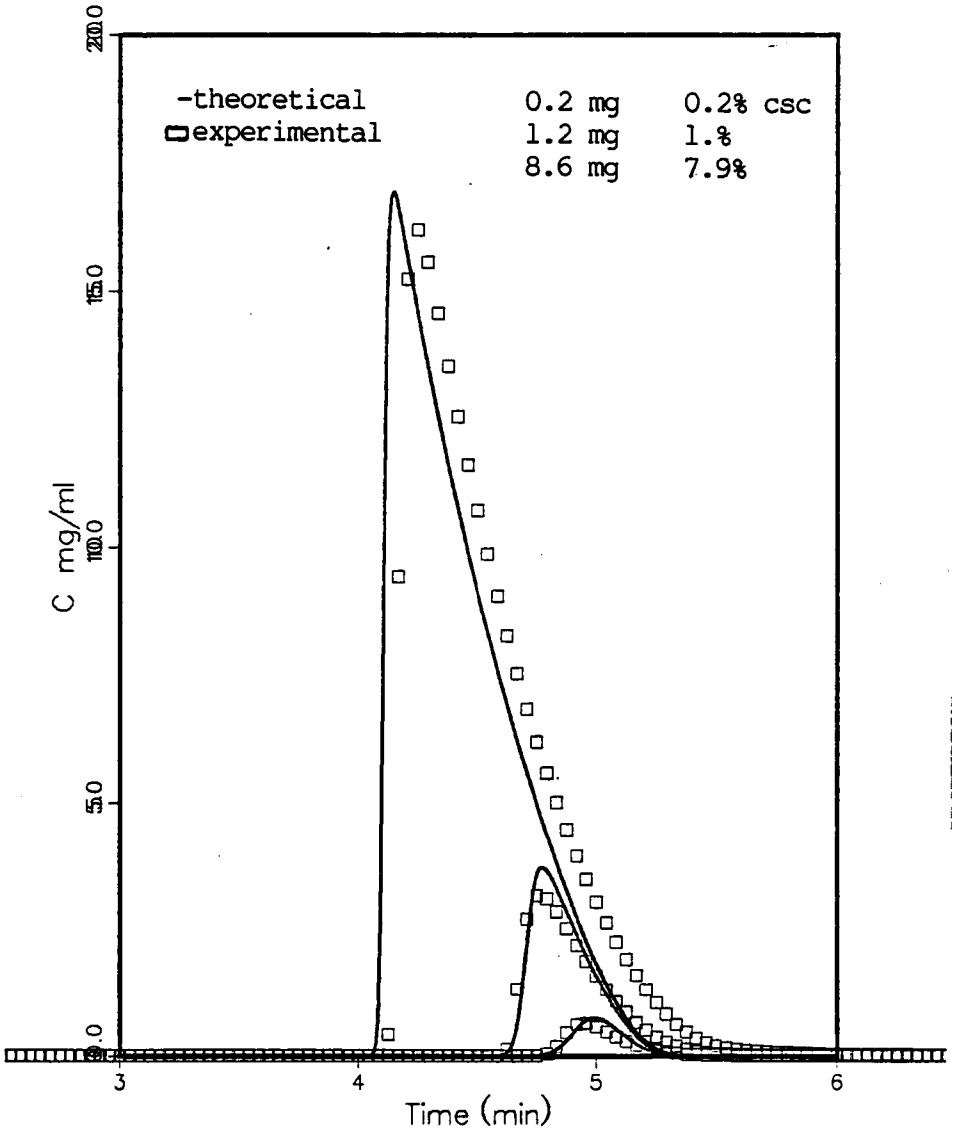


Figure 3.8 Comparison of Theory and Experiment, Column # 2 - Phenyl-ethanol

mg of sample was injected as a pure component. This corresponds to a loading factor of 0.19, 1.06, 7.89 per cent. The agreement for all the sample sizes is good.

Figure 3.9 shows a comparison of experimental and theoretical overloaded elution chromatograms for phenyl-propanol on column #2 with 0.908, 3.705, and 5.508 mg injected. This corresponds to a loading factor of 1.29, 5.26 and 7.82. Good agreement is found between the experimental and theoretical profiles. The bowing seen on the rear boundary of the experimental profiles is believed to be an artifact of the conversion from response to concentration. The high degree of curvature of the calibration curve often led to fits which were not smooth in all of their derivatives.

A third component, 2,6 dimethyl-phenol, was studied for later use as a potential displacer. Its retention time was higher than that of phenyl-propanol, thus its isotherm was measured by ECP to determine its suitability. A comparison of experimental and theoretical single component band profiles, Figure 3.10, was made with 0.077, 0.767, 3.88 and 7.767 mg of sample loaded; respectively. This corresponds to a loading factor of 0.097, 0.97, 4.88, and 9.7 per cent. Table 3.2 provides a summary of the isotherm parameters on column #2.

The isotherm of 3,6 dimethylphenol was also measured on a microbore column (0.1 x 100 mm) at a flow rate of 0.4 ml/min using a 20 ul sample loop. The column efficiency was low and extrapolation of the isotherm parameters to the analytical column proved to be insufficiently accurate, Table 3.2. This is probably due to the pumps delivering a slightly different mobile phase composition due to the

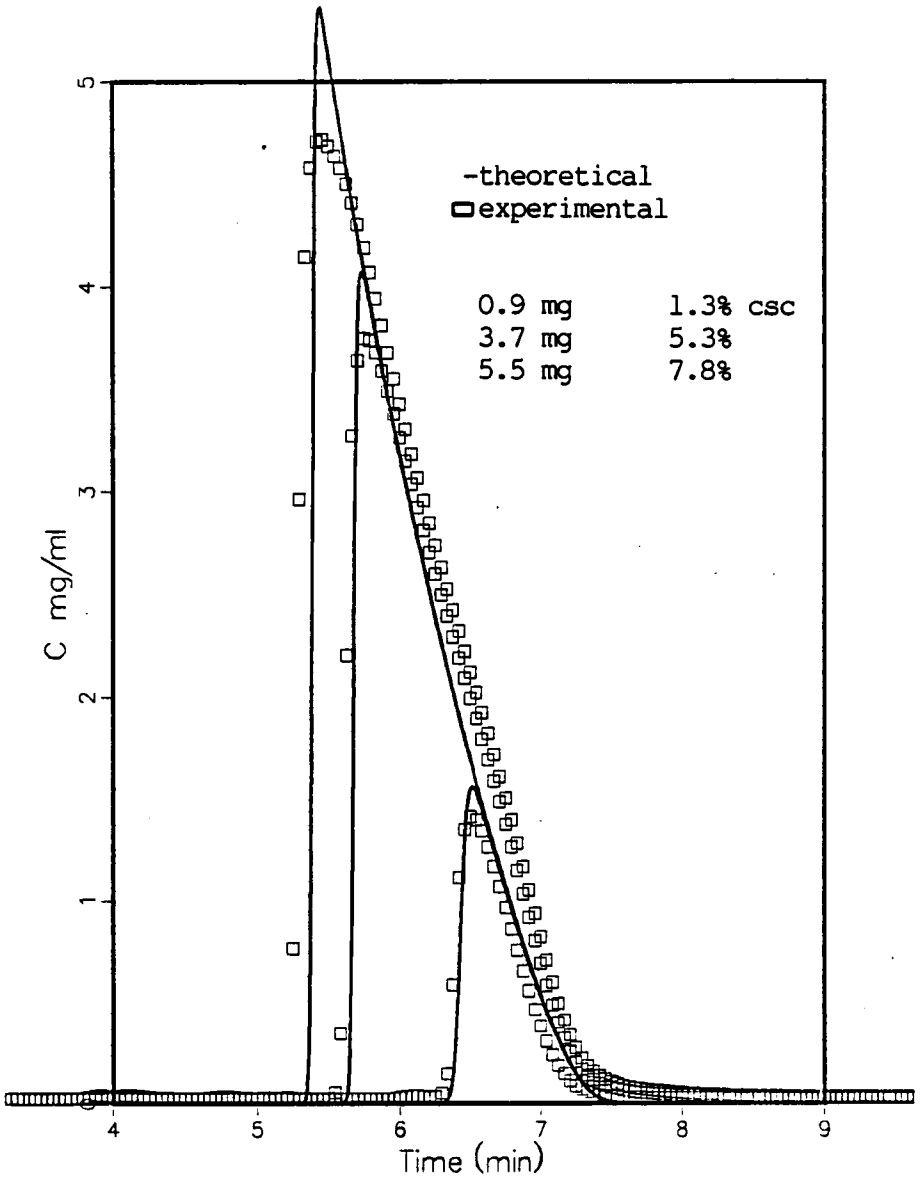


Figure 3.9 Comparison of Theory and Experiment, Column # 2 - Phenyl-propanol

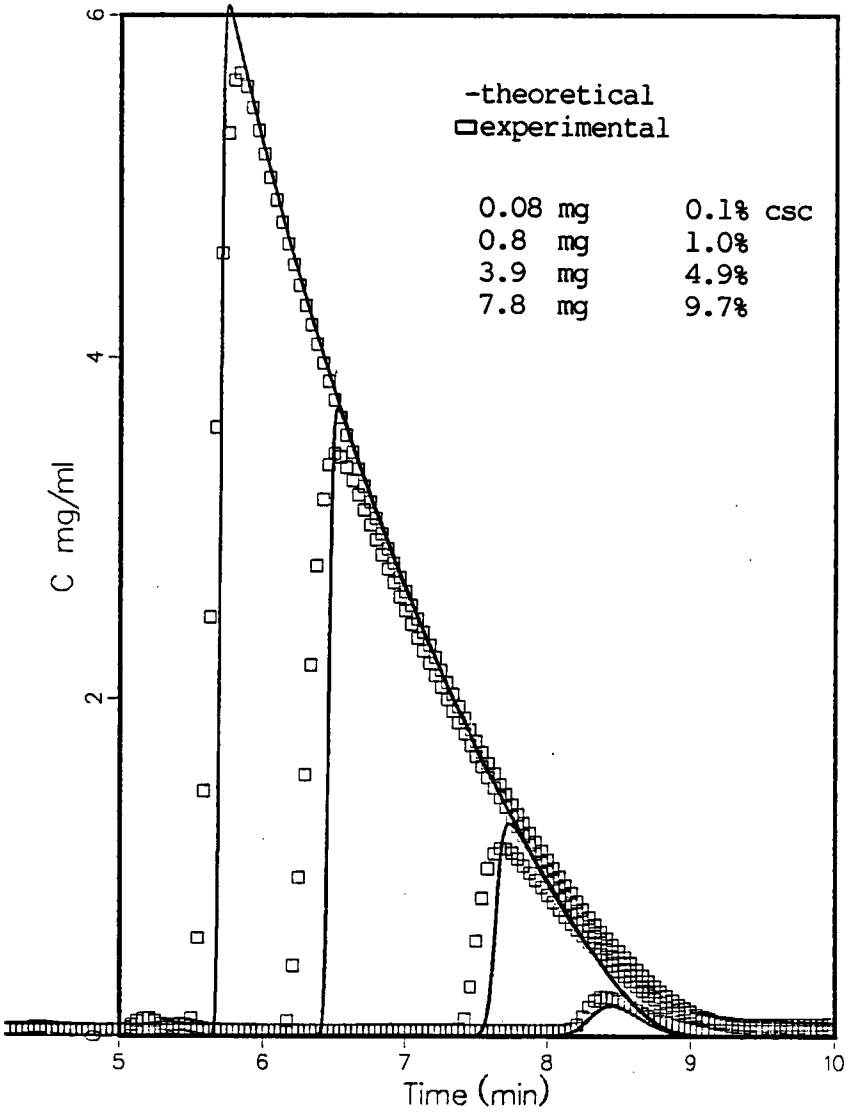


Figure 3.10 Comparison of Theory and Experiment, Column # 2 -Dimethylphenol

Table 3.2 Summary of Isotherm Data for 3,6 Dimethyl-phenol

	Column #2	Microbore Column
t_R (sec)	515.0	70.98
k'	1.926	9.04
a (ml/ml)	4.6897	13.3
b (ml/mg)	0.07213	0.0204
b (ml/mmole)	8.81172	2.487
CSC (mg)	79	20
MW (g/mole)	136.2	136.2
HETP (cm)	0.009	0.07
t_0 (sec)	176	7.07
porosity	0.706	0.6
F	0.4165	0.67
F_v (ml/min)	1.0	0.4

lower pressure drop and lower operating flow rate on the microbore column. Use of the isotherm parameters to predict profiles on the same column, however, was not a problem. Figure 3.11 shows a comparison of experimental and theoretical profiles on the microbore column with 0.09, 0.4 and 1.26 mg of dimethyl-phenol injected. This corresponds to a loading factor of 0.43, 1.95 and 6.13 per cent. The agreement is very good.

3.2 Single Component Overloaded Elution of Proteins

This section will discuss the measurement and prediction of band profiles of the proteins Chicken Albumin and Conalbumin under isocratic conditions in ion-exchange chromatography. Ion-exchange chromatography is usually carried out under gradient conditions due to the steep slope of the k' versus salt modifier concentration. However, the modeling of gradient elution chromatography is more difficult and thus one of the first steps in modeling protein adsorption was to consider the single component isocratic case.

Experimental

This section will describe the equipment used and the measurements made in order to compare experimental single component overloaded band profiles of two proteins with theoretical predictions.

Equipment

A modular liquid chromatographic used for the measurement of band profiles was assembled from a Gilson (Middleton, WI) Model 301 pump

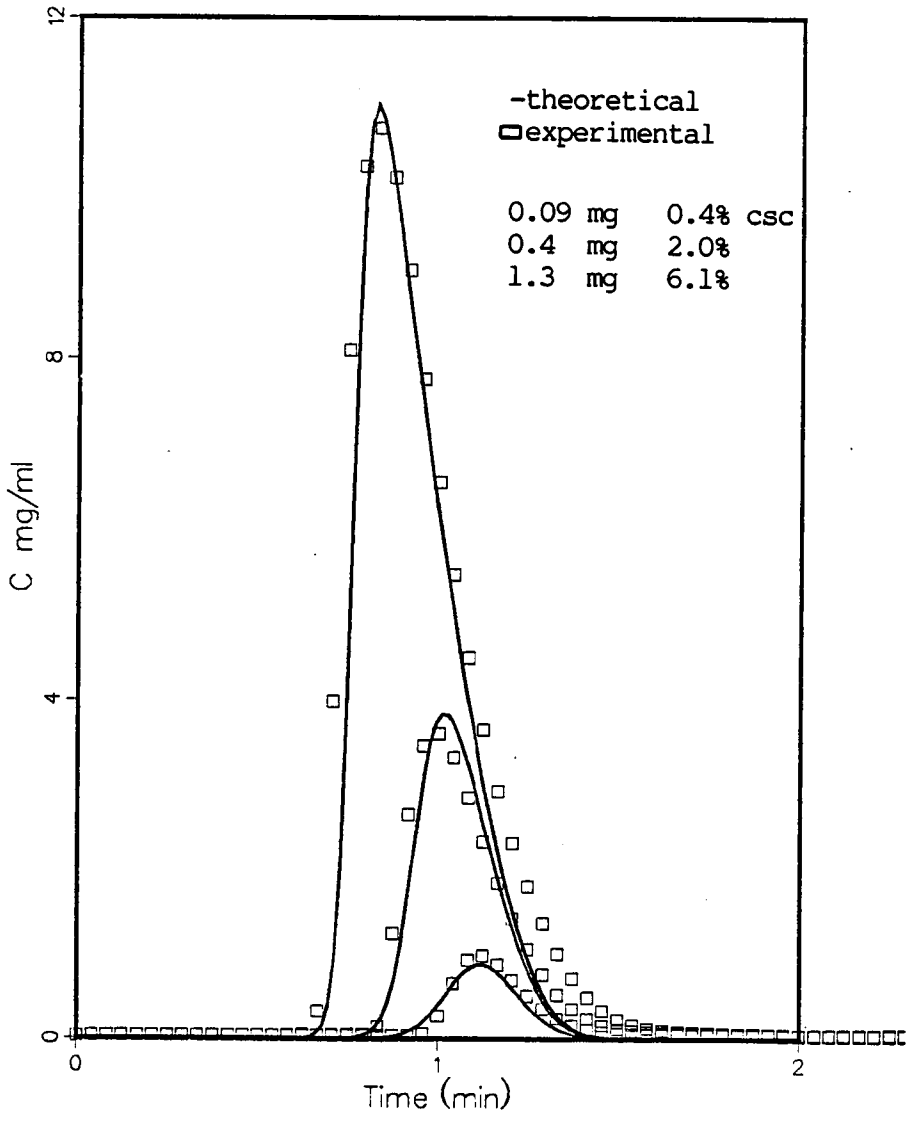


Figure 3.11 Comparison of Theory and Experiment on Microbore Column - Dimethylphenol

with a 5P pump head a Valco (Houston, TX) valve fitted with a 20 ul sample loop and a Kratos (Ramsey, NJ) Model 757 Spectorflow variable wavelength detector. One of the detector output analog signals was connected to a Kipp and Zonen (Delft,Holland) chart recorder and the other analog signal was connected to the SIM box for digitization of the detector response signal.

Materials

TSK-DEAE 5PW (TOSOH Corp.,Japan), 10 um average particle size, resin was used in these experiments. This is a polymeric based stationary phase with diethylaminoethyl groups covalently bound to the support by a spacer arm. This resin was packed in a 1x50 mm microbore column at 800 psi with water as the slurry solvent. The columns were packed with the Gilson Model 301 pump at low pressure to prevent compression of the particles [Huang (1990a,1990b)]. This 1x50 mm column was used for measurement of the isotherm and for the overloaded elution experiments.

Chicken Albumin and Conalbumin were purchased from Sigma Chemical Co. (St. Louis, MO). Tris Acetate was purchased from Mallinkrodt (Paris, KY) and bottled water from Burdick and Jackson (Muskegin, MI). All chemicals were used without further purification.

Experimental Procedure

The mobile phase was prepared by mixing the appropriate amount of Tris-acetate with water in a volumetric flask. The solution was

filtered through a 0.2 um Nylon 66 membrane filter (Gelman Sciences, Ann Arbor, MI). The stock mobile phase was stored covered in the refrigerator. Protein solutions were prepared daily just before performing the experiments.

The overloaded elution measurements were carried out by injecting the protein sequentially from high concentration to low concentration. Each concentration was injected in duplicate. Upon completion of all the injections, the column was washed with 8 M urea and as necessary with a 10 % NaOH solution to remove strongly adsorbed protein from the surface. This provided a clean adsorbent surface for further investigation . Otherwise the experiments gave inconsistent results. This procedure suggested that small amounts of protein are irreversibly bound to the surface.

Isotherm Measurement and Detector Calibration

Isotherms were measured using frontal analysis where a 10 port Valco (Houston, TX) valve was submerged in a Haake (Berlin, West Germany) water bath at 25 oC. The calibration curves were obtained from the plateau concentrations from each isotherm front. The calibration curve was regressed to a 5th degree polynomial.

The isotherm data was fit to the Langmuir model for each protein-mobile-phase studied. Figure 3.12 shows the isotherm data fit to a Langmuir equation. It is observed on this figure that the isotherms rise more steeply at low concentrations and saturate less fast than predicted by using the best fit parameters in the Langmuir equation. For this reason, a Langmuir equation can give only a poor fit of the

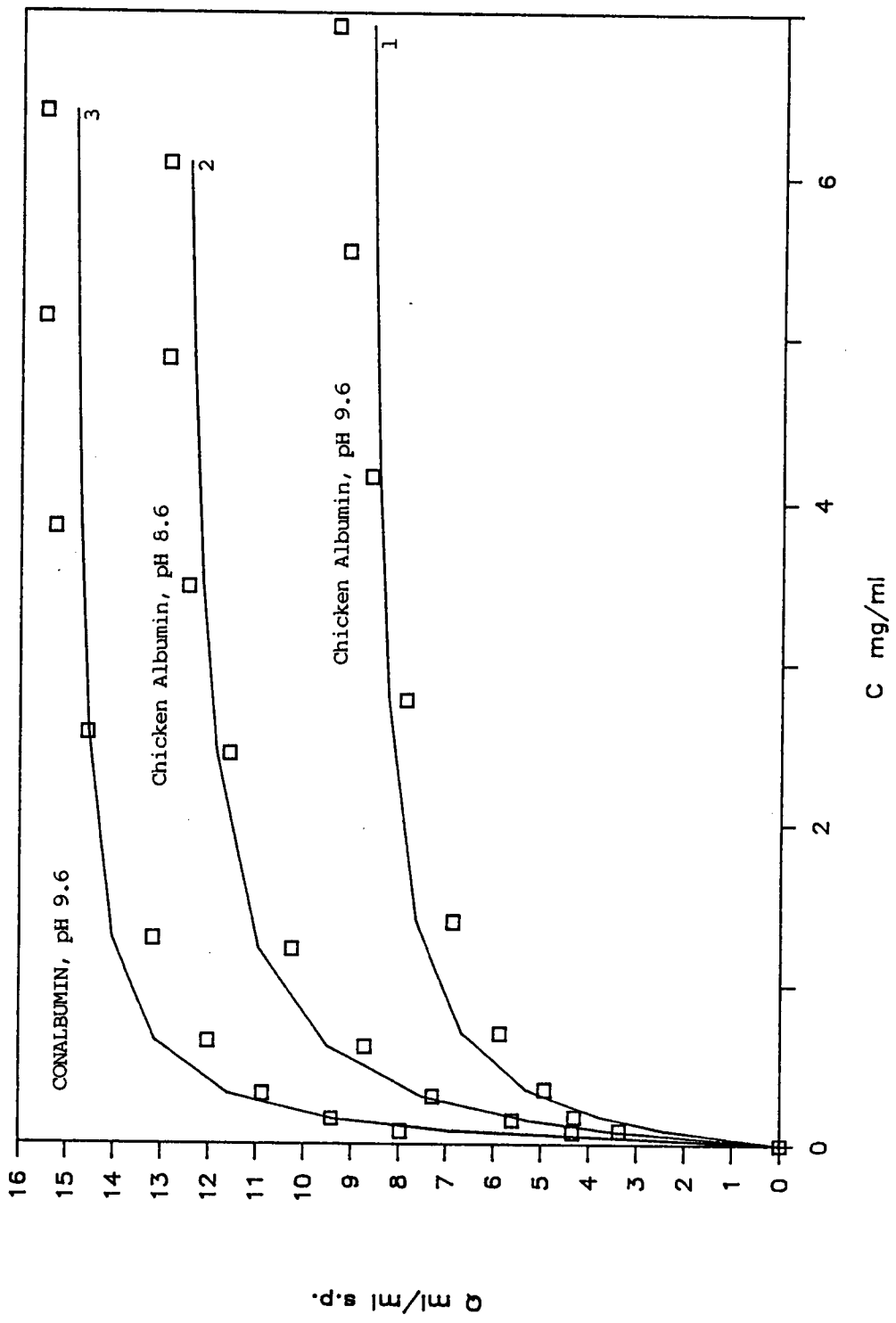


Figure 3.12 Experimental Protein Isotherm Data fit to Langmuir Equation

experimental data. The differences observed between the model and the experimental isotherm data are such that the band profiles predicted by the semi-ideal model of chromatography differ considerably from experimental chromatograms.

Various theoretical and empirical models of isotherms were tried without success. It was thought that the protein could be interacting in a nonLangmuirian fashion. A Scatchard plot [Andrade] of the data (a plot of Q/C versus C) shows a downward convex curve [Huang (1990a,1990b)], while for a Langmuir isotherm the Scatchard plot is linear. One of the simple models of an adsorption isotherm which accounts for the kind of results obtained assumes the existence of two types of non-cooperative, independent adsorption sites on the surface of the stationary phase. Thus, the data was fit to the bilangmuir equation:

$$q = \frac{A_1 C}{1+B_1 C} + \frac{A_2 C}{1+B_2 C} \qquad (3.4)$$

The best value of the four coefficients where obtained by taking the slope and intercept values of the two asymptotes of the Scatchard plot as the first guess and then use a Simplex program to calculate the best fit values of the coefficients [Dose (1987)].

Results and Discussion

Table 3.3 summarizes the coefficients obtained with a best fit to the Langmuir and BiLangmuir equations. Figure 3.13 shows the isotherm data using the best fit bilangmuir parameters to the isotherms of Chicken Albumin and Conalbumin proteins. An excellent fit is

Table 3.3 Summary of Protein Isotherm Data

	Experimental Conditions	Langmuir Parameters	BiLangmuir Parameters	CSC* mg
Chicken Albumin	50 mM Tris Ac+ 50 mM NaAc pH 8.6	a= 59.06 b= 4.56 csc=0.20	A1= 119.1 B1= 18.05 A2= 6.71 B2= 0.69	0.256
Chicken Albumin	50 mM Tris Ac+ 25mM NaAc pH 9.6	a=37.87 b= 4.22 csc=0.14	A1= 105 B1= 21.2 A2= 2.14 B2= 0.33	0.18
Conalbumin	50 mM Tris Ac+ 25 mM NaAc pH 9.6	a=156.48 b= 10.36 csc=0.24	A1= 353.2 B1= 34.0 A2= 4.93 B2= 0.77	0.264

*BiLangmuir Isotherm

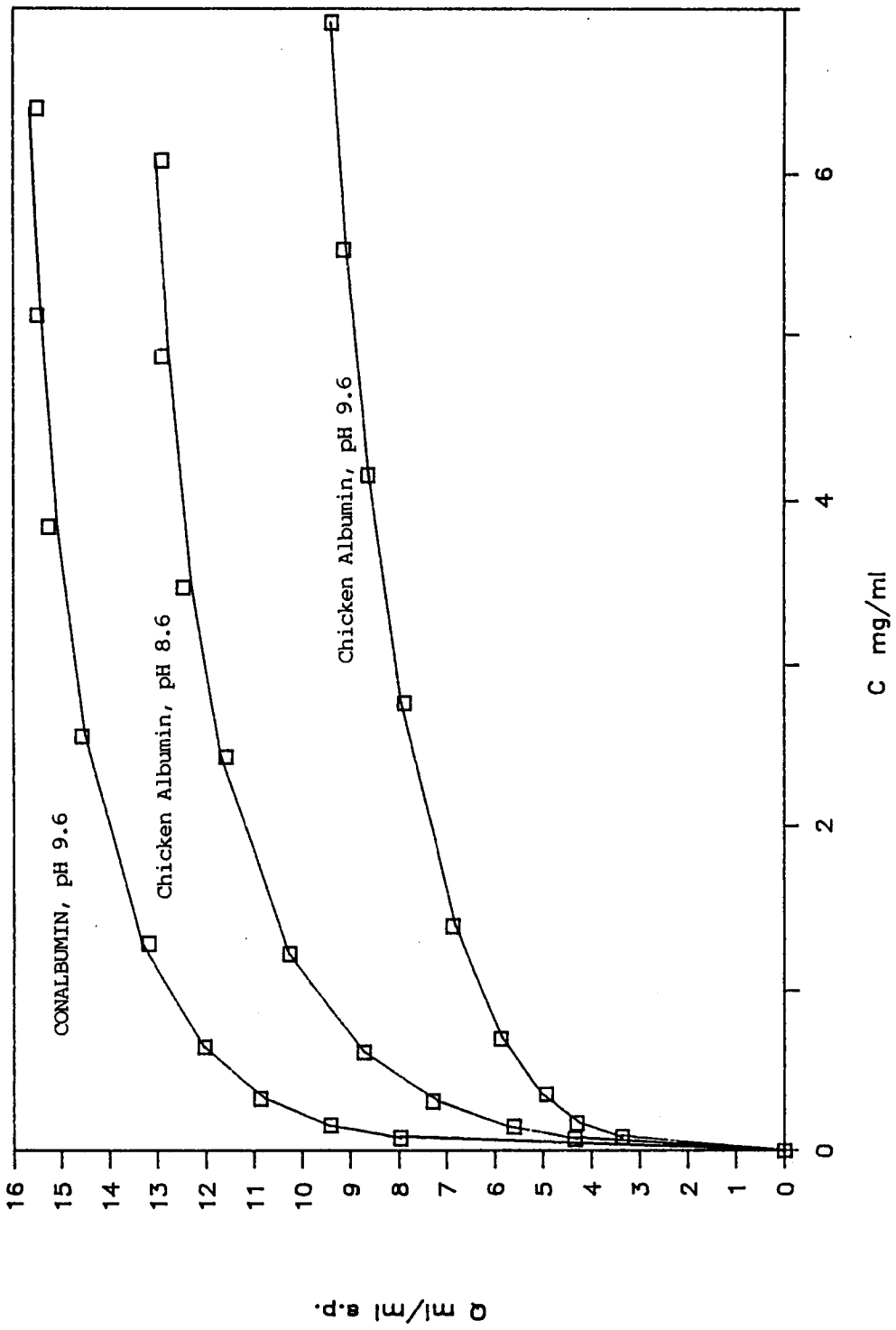


Figure 3.13 Protein Isotherm Data fit to BiLangmuir Equation

obtained for the Bilangmuir isotherm in contrast to the Langmuir equation (Figure 3.12).

In order to predict the overloaded elution chromatograms the dead time was measured and was 16.2 seconds. The HETP was assumed to be 0.01 cm based on other columns packed using the same procedure. The retention time was calculated from the a1 parameter of the bilangmuir isotherm.

Figure 3.14 shows in squares the experimental profiles and in solid line the predicted profile using the bilangmuir equilibrium isotherm equation. The 3 curves correspond to the injection of 0.1665 mg, 0.0985 mg and 0.07476 mg (i.e. 65 %, 38 % and 29.2 % of the column saturation capacity) of chicken albumin in an aqueous solution of 50 mM Tris Acetate and 50 mM Na Acetate, pH 8.6 with a mobile phase flow rate of 50 ul/min. The agreement between experimental and simulated chromatograms is good, although the variation of the band retention time with sample size is smaller for the experimental results than for the predicted profiles and the front of the experimental band for the largest sample is not as steep as predicted.

Figure 3.15 shows a comparison of experimental and predicted profiles for chicken albumin in 50 mM Tris-Acetate and 25 mM sodium acetate, pH 9.6 at a flow rate of 50 ul/min. Each curve corresponds to a sample size of 0.083, 0.067 and 0.048 mg of protein (i.e. loading factor of 46.2 %, 37.3 % and 26.7 %; respectively). The predicted profiles show a slight decrease in retention time with decreasing loading which is not seen experimentally. The peak maximum of the experimental profiles hardly move with decreasing sample size. However,

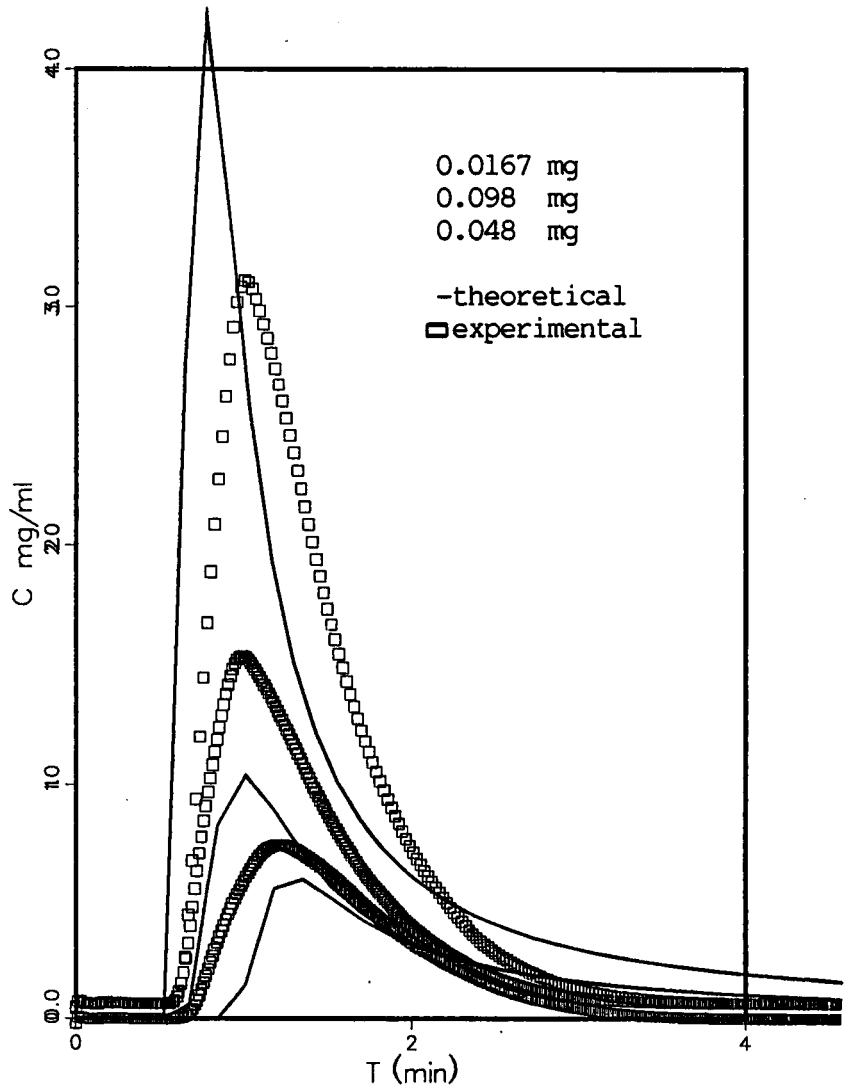


Figure 3.14 Comparison of Theoretical and Experimental Band Profiles for Chicken Albumin, pH 8.6

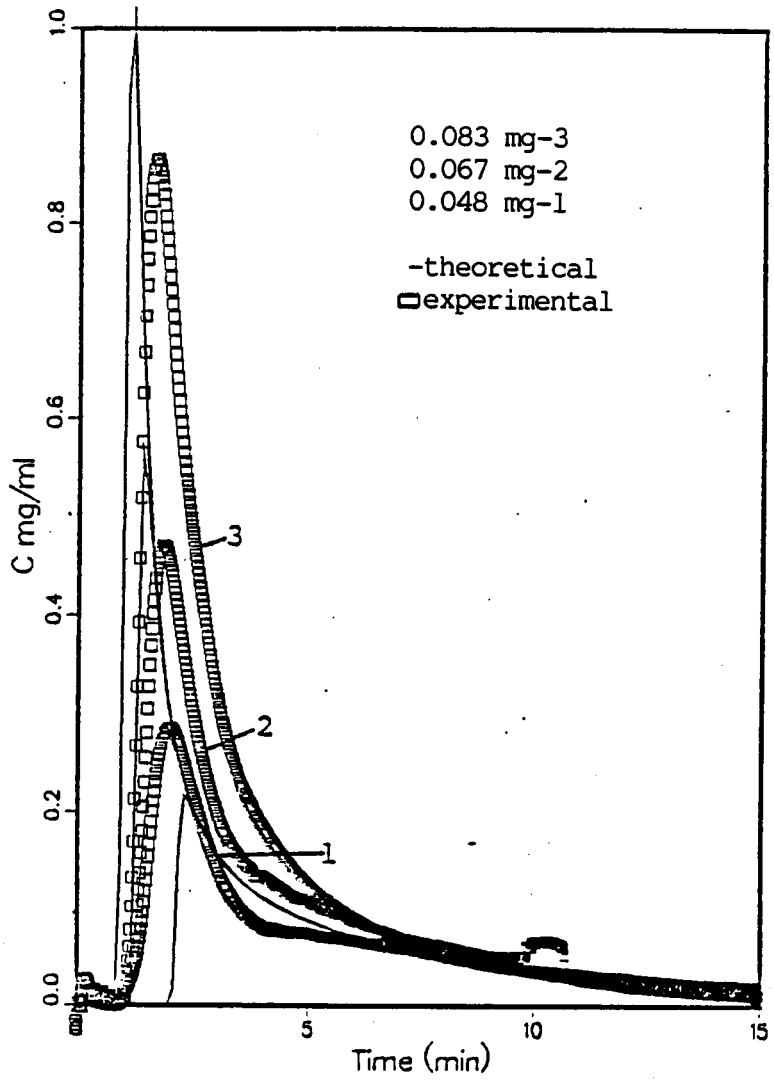


Figure 3.15 Comparison of Theoretical and Experimental Band Profiles for Chicken Albumin, pH 9.6

the general shape of the profiles predicted is good.

Figure 3.16 shows the band profile of conalbumin in 50 mM Tris Acetate and 25 mM sodium acetate, pH 9.6 at a flow rate of 50 ul/min. The sample size is 0.041 and 0.029 mg for each respective curve. This corresponds to a loading factor of 15 % and 11 %; respectively. Qualitative agreement between experimental and theoretical profiles is shown. Again, sample size dependence of the experimental retention time is lower than predicted and the front of the experimental bands is less steep than the front of the predicted bands.

The differences between experimental and experimental profiles may be due to the slow rate of adsorption and desorption on the surface of the stationary phase. For entropic reasons, the protein which interacts with the surface in several points has a rather low probability of dissociating all of the points at the same time. Furthermore, molecular diffusion of the protein in the solution is slow and its accommodation on the surface is low. For these reasons, a kinetic model of chromatography would probably give better results. The application of such a model would require an independent procedure for measurement of the rate constants.

Nonetheless it is remarkable that a semi-equilibrium model permits the satisfactory prediction of the band profiles of proteins under isocratic conditions.

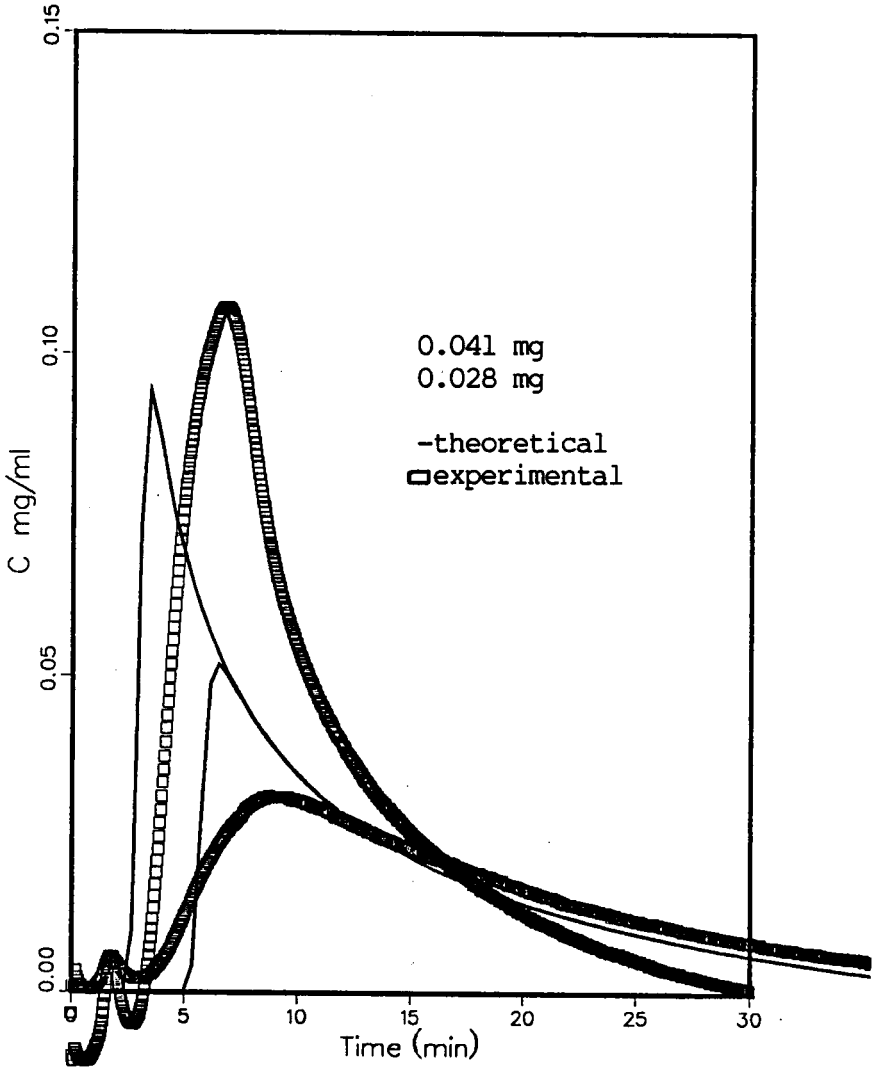


Figure 3.16 Comparison of Theoretical and Experimental Band Profiles for Conalbumin, pH 9.6

Chapter 4

Two-Component Problem

The purpose of chromatography is to separate components from a mixture. This chapter discusses the separation of binary mixtures by overloaded elution chromatography for small and large volume injections. Section 4.1 presents data taken when a sufficient amount of sample is loaded on the column such that the individual component profiles interfere and never completely separate. The semi-ideal model of chromatography as described in Chapter 2 is used to calculate the theoretical profiles using the single component Langmuir parameters in a competitive Langmuir isotherm. Section 4.2 will present data collected when the injection is sufficiently large that the profiles exhibit a plateau. The theory developed in Chapter 2 will be used to predict band profiles using a competitive Langmuir isotherm where the parameters are measured from single component data. Because the large volume injection leads to a constant state (the plateau), transformation of the concentration time profile to a plot of the concentration of the first component versus the concentration of the second results in the appearance of straight lines. By finding the Langmuir parameters which give the best fit straight line, an estimate of the adsorption isotherm can be made from mixture data. The best fit Langmuir parameters are determined for mixtures of different composition. Section 4.3 then uses these best fit Langmuir parameters

to predict the profile for binary overloaded elution data presented in section 4.1. Details concerning the composition dependence for nonlangmuirian systems is presented elsewhere [Ma et al.]

4.1 Overloaded Elution Chromatography

In chapter 3 experimental determination of the band profiles was made by measuring the detector response and converting the response to concentration by a calibration curve. The calibration curve is made by direct injection of the pure sample at different concentrations. However, for two component mixtures where the bands interfere and the calibration curve is nonlinear. Although it is possible to determine the individual component concentration profiles as a function of time by measuring the calibration curve surface, fitting the surface to a model and then deconvoluting the profile, the method of fraction collection was employed in this study. There are two methods of determining the individual component profiles by analysis of the individual components. One is by online analysis where the effluent of the preparative column is sampled and injected into an analytical chromatograph. The second method is by collecting fractions and reinjecting an aliquot into the column for analysis. The second method was chosen because it is possible to have a higher sampling rate and a completely automated system.

Evaluation of the Fraction Collector

The method of fraction collection was evaluated by comparing the band profile obtained from the detector response and a calibration

curve and that obtained by collecting fractions with reanalysis of a one component overloaded band. Figure 4.1 shows the chromatogram obtained at the detector outlet when 30 mg of phenyl-ethanol is injected using a 100 ul sample loop. A calibration curve, Figure 4.2, was determined and fit to a polynomial, Eqn. 4.1:

$$C=4.71V+6.62V^3+0.197V^5 \qquad (4.1)$$

where V is the response from the detector in volts and C is the concentration in mg/ml. The experimental data and the fitted polynomial are shown in Figure 4.2. This polynomial was used to convert the chromatogram, Figure 4.1, to a concentration time profile.

Figure 4.3 shows a comparison of data collected by fraction collection, reinjection and analysis (squares) with a concentration time profile determined from the detector response (solid line). There is essentially no difference between the two profiles. This exercise proves the accuracy of the method of fraction collection and the validity of the data.

Determination of Concentration-Time Profiles for Binary Mixtures

The individual band profiles of several binary mixtures was studied by comparing the detector response profile to the individual component profiles determined by fraction collection. Figures 4.4a-h, show the total profile given by the output of the detector and the corresponding individual concentration-time profile obtained by fraction collection for mixtures where the ratio of the amount of component 1 and component 2 is 1/1, 1/3, 3/1 and 9/1. The total amount of sample

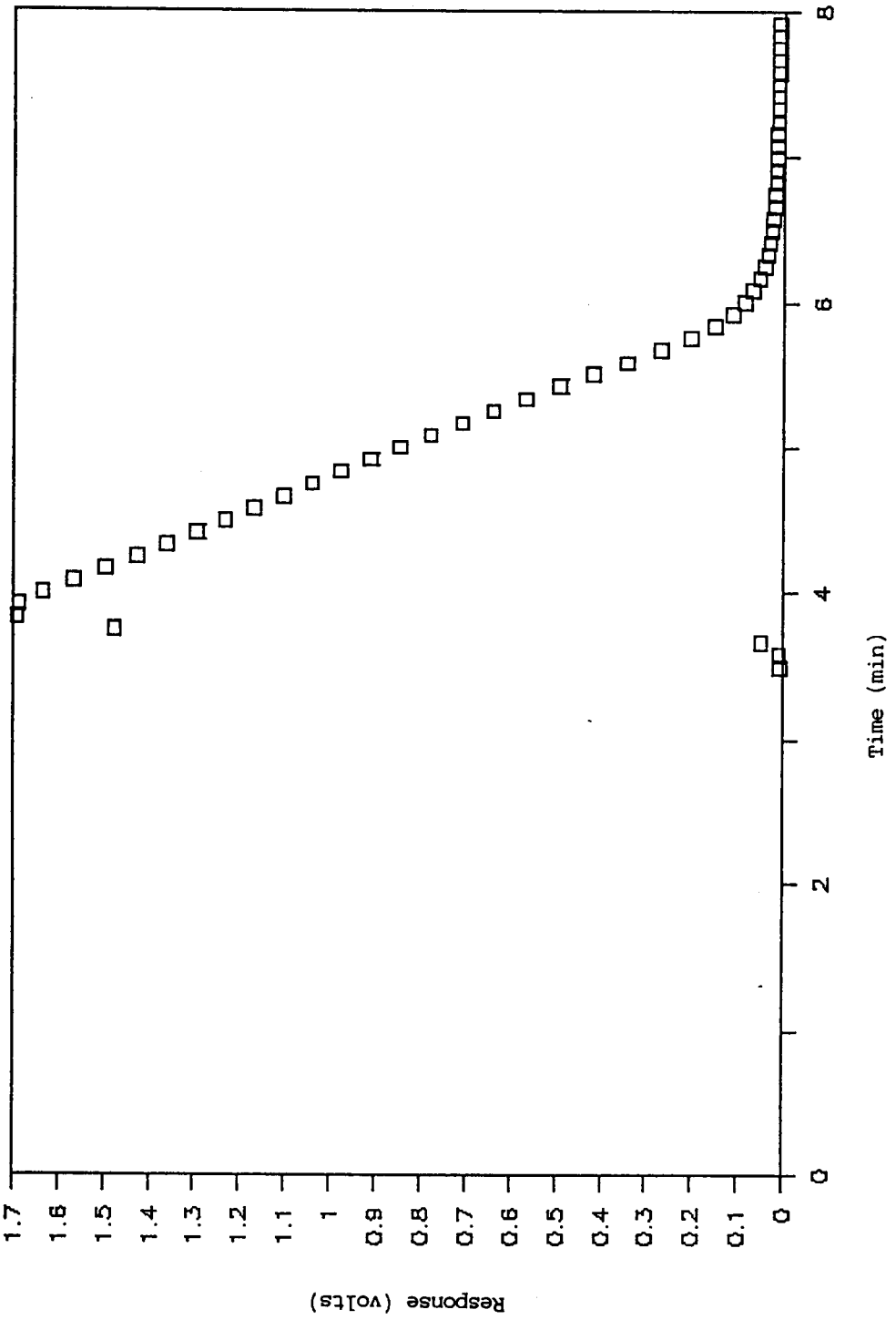


Figure 4.1 Detector Response to 30 mg Injection of Phenyl-ethanol

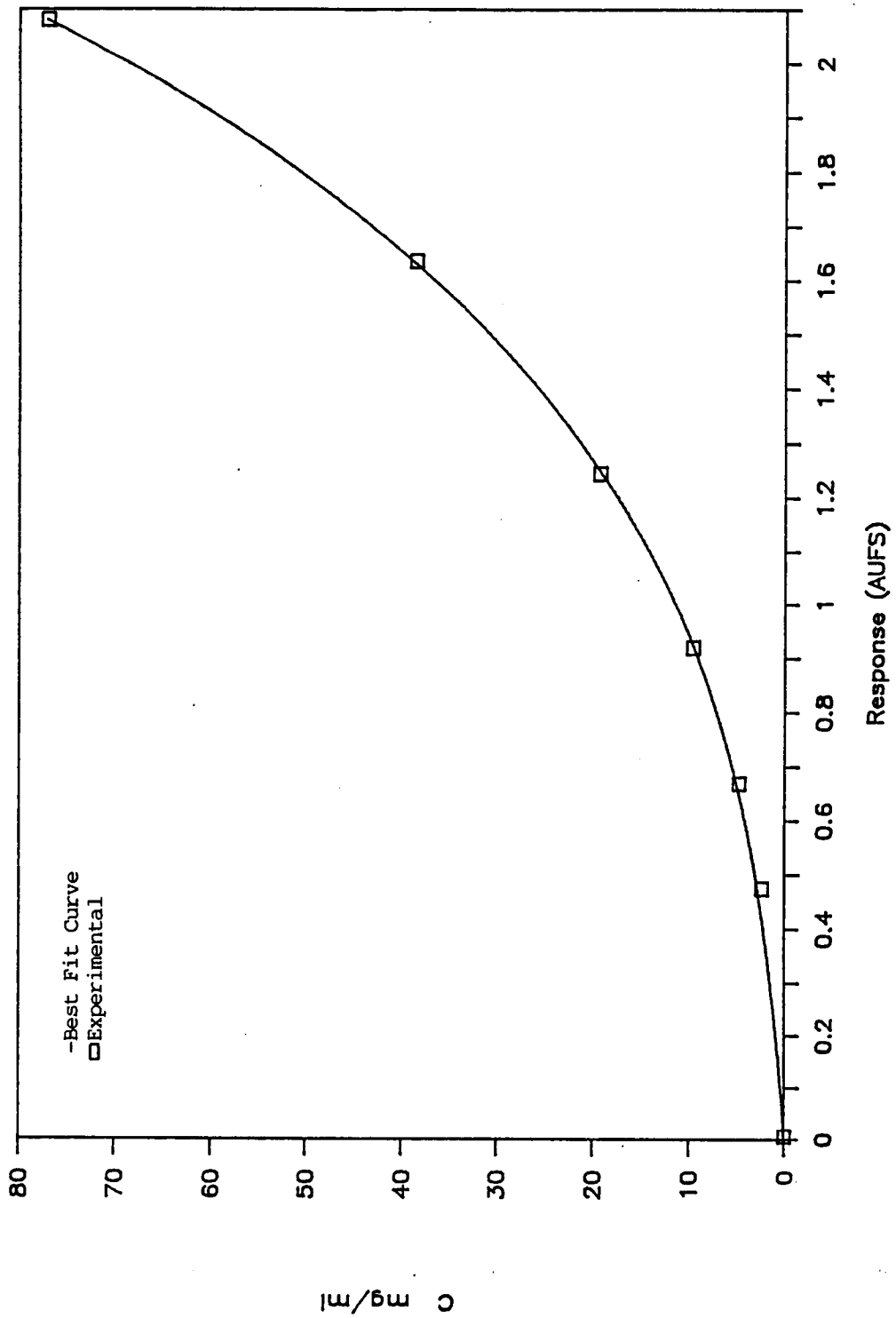


Figure 4.2 Detector Calibration Curve for Phenyl-ethanol

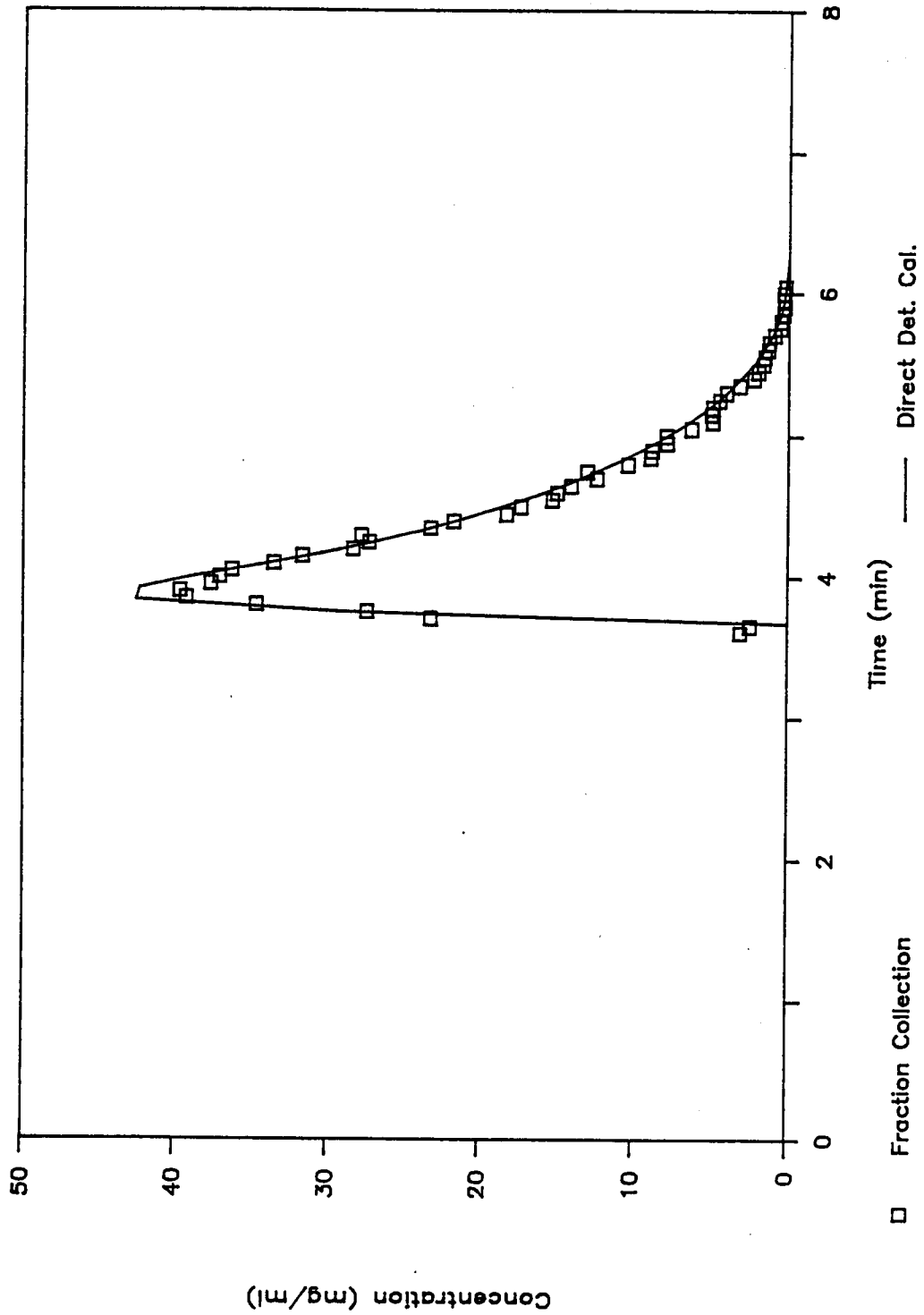
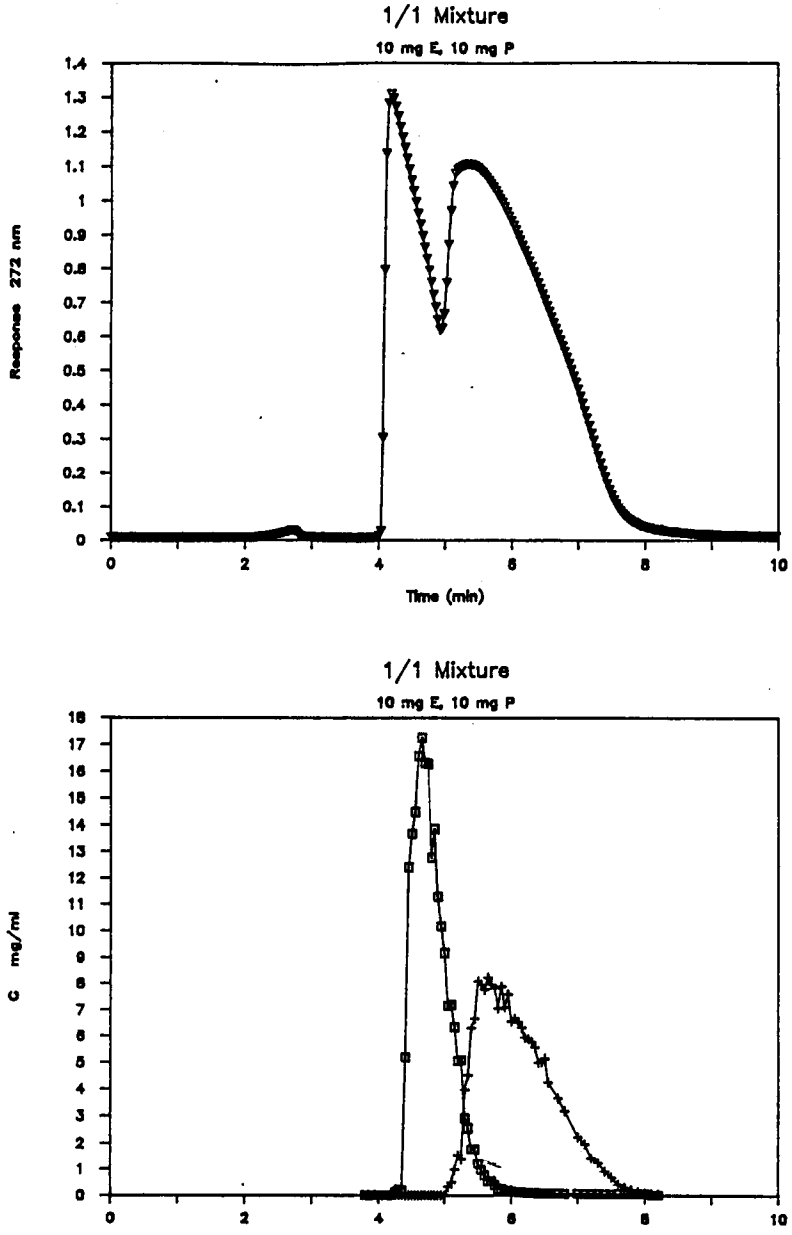
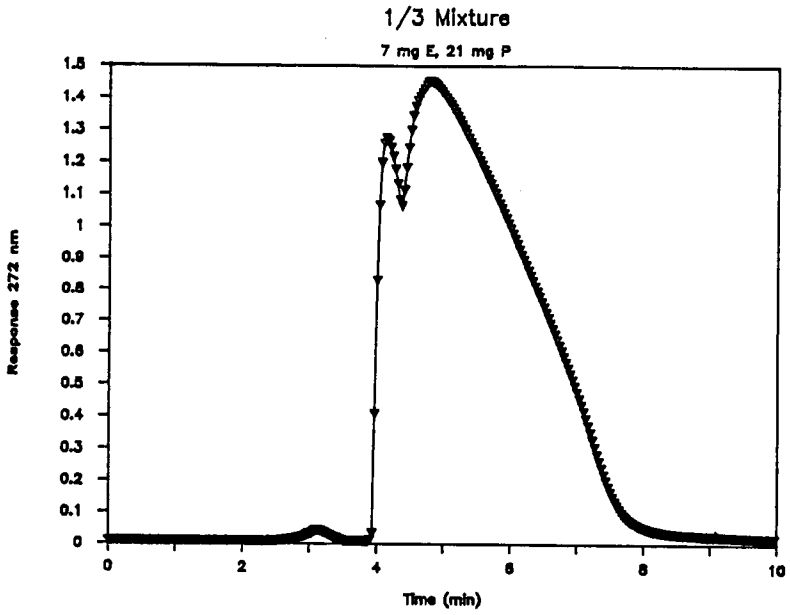


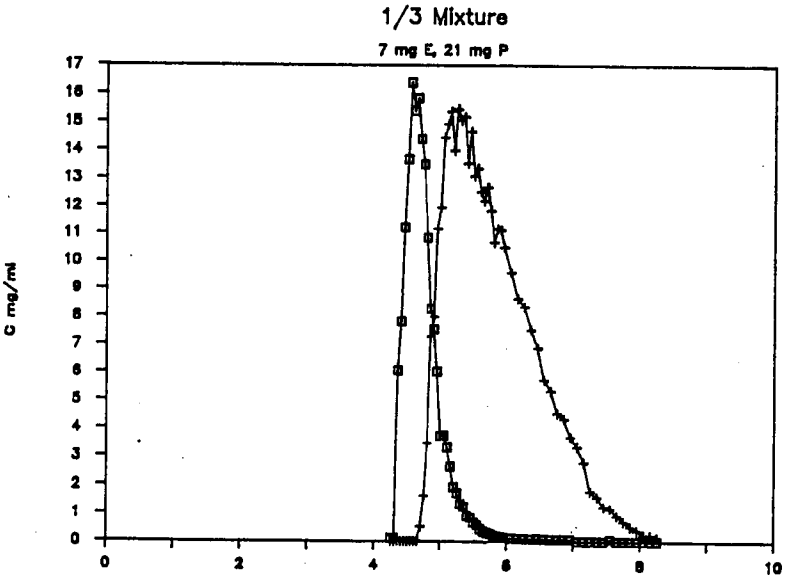
Figure 4.3 Evaluation of Fraction Collector



(a) Response Profile, ▽ Experimental
(b) Concentration Profile, □ Phenyl-ethanol,
+ Phenyl-propanol

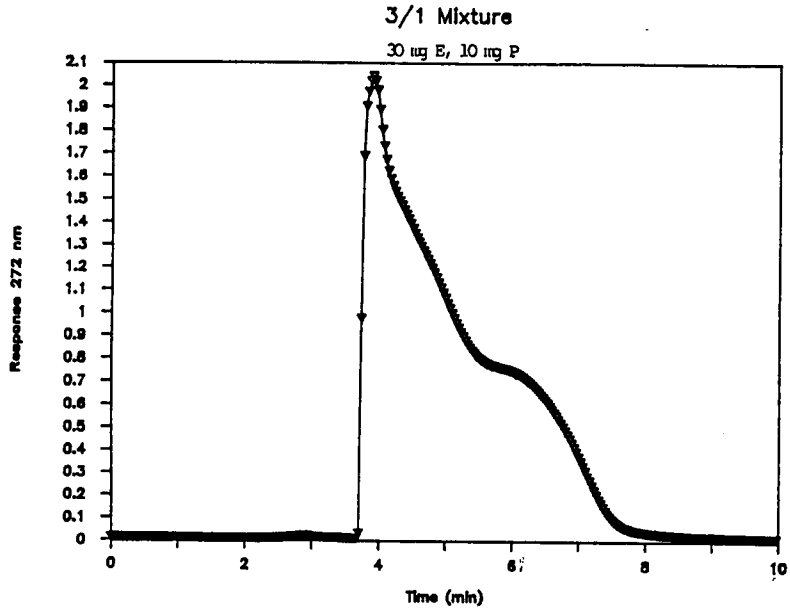
Figure 4.4 Experimental Response and Concentration Profiles

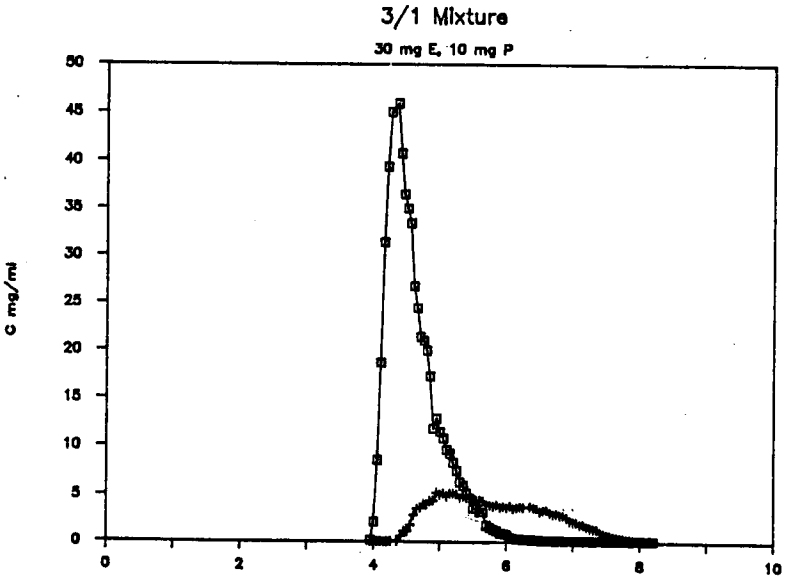




(c) Response Profile, v Experimental
(d) Concentration Profile, □ Phenyl-ethanol,
+ Phenyl-propanol

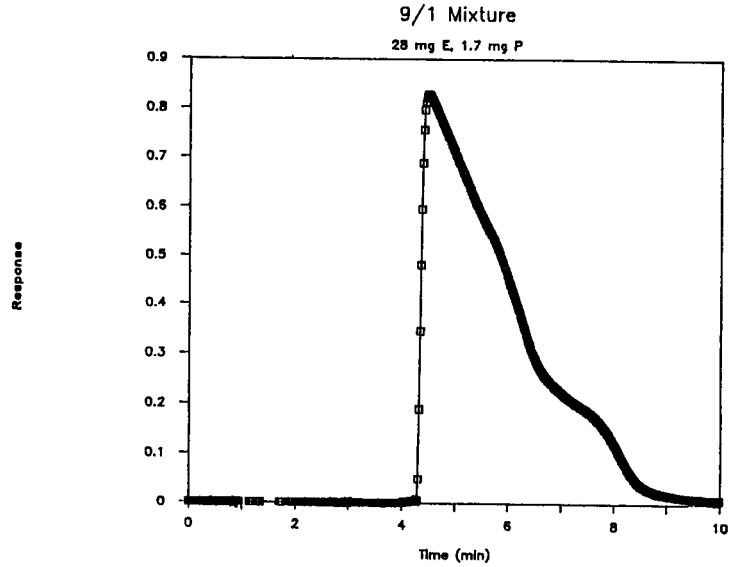
Figure 4.4 (continued)

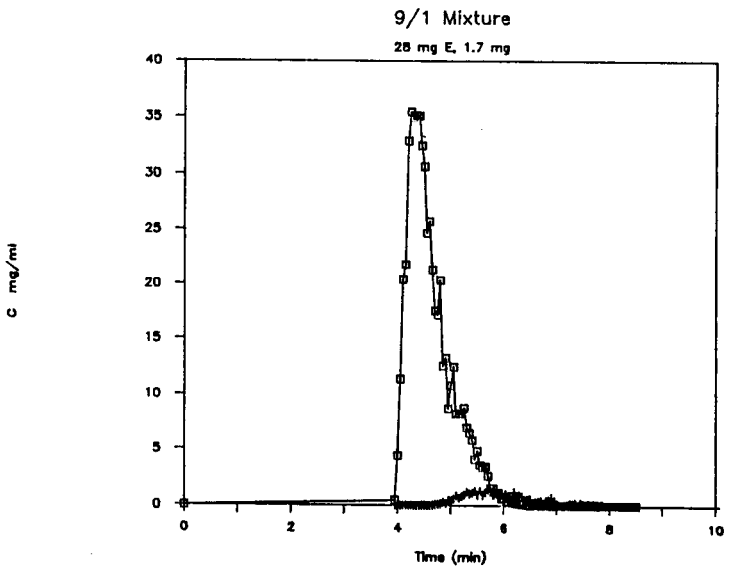




(e) Response Profile, ▽ Experimental
(f) Concentration Profile, □ Phenyl-ethanol,
+ Phenyl-propanol

Figure 4.4 (continued)





(g) Response Profile, □ Experimental
(h) Concentration Profile, □ Phenyl-ethanol, + Phenyl-propanol

Figure 4.4 (continued)

and component 2 is 1/1, 1/3, 3/1 and 9/1. The total amount of sample injected is 20 mg, 28 mg, 40 mg and 30 mg in Figure 4.4a-b, 4.4c-d, 4.4e-f and 4.4g-h; respectively. Table 4.1 summarizes the experimental sample sizes and loading factors for the different mixture compositions studied. This data was taken on column #1 where component 1 was Phenyl-ethanol and component 2 was phenyl-propanol. Since phenyl-ethanol has a lower UV response than phenyl-propanol at the same concentration, the detector response gives a distorted profile.

The response profiles for a 1/1 and a 1/3 mixture are shown in Figure 4.4a and 4.4c and the concentration profiles in Figure 4.4b and 4.4d. The shape of the individual component profiles are similar to those of the total profile. This is in part due to fact that the amount of interference is not extremely high. Figure 4.4e shows the response to a 3/1 mixture. The detector response seen at the top of the page gives the appearance that the second component might be gaussian in shape. Determination of the concentration-time chromatogram, on the bottom of the page, Figure 4.4f, shows the large amount of overlap and a long dilute band. Similarly, for a 9/1 mixture, Figure 4.4g-h shows the elongated rear profile of the second component.

Situations where there is strong interference, limited conclusions may be derived from the detector response and other methods of monitoring the preparative column effluent must be taken.

Table 4.1 Summary of Overloaded Elution Experimental Data

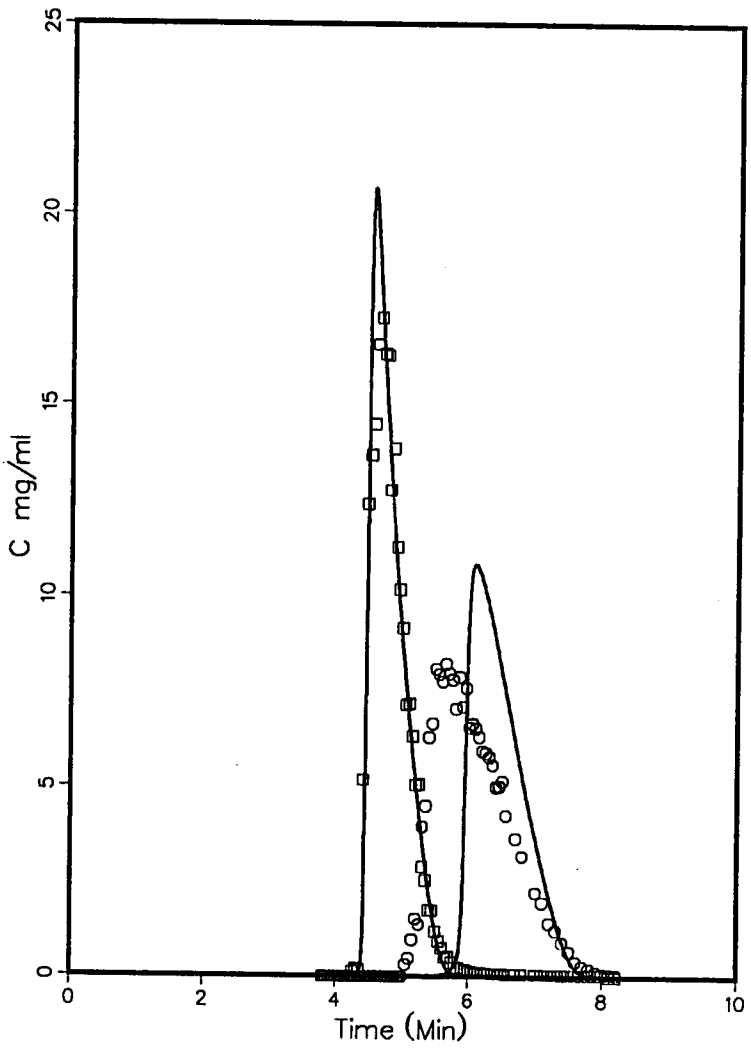
	total sample size (mg)	PE (mg)	PP (mg)	PE Lf(%)	PP Lf(%)
1/1	20	10	10	7	7
1/3	28	7	21	5	15
3/1	40	30	10	21	7
9/1	30	28	1.7	21	2.3

Loop Volume: 0.1 ml
Average column saturation capacity: 145 mg
Loading factors are based on single component isotherm data on Column #1, Table 3.1, in per cent CSC.
PE: Phenyl-ethanol, PP: Phenyl-propanol

Comparison of Experimental and Theoretical Profiles using Single-Component Langmuir Parameters in a Competitive Langmuir Model

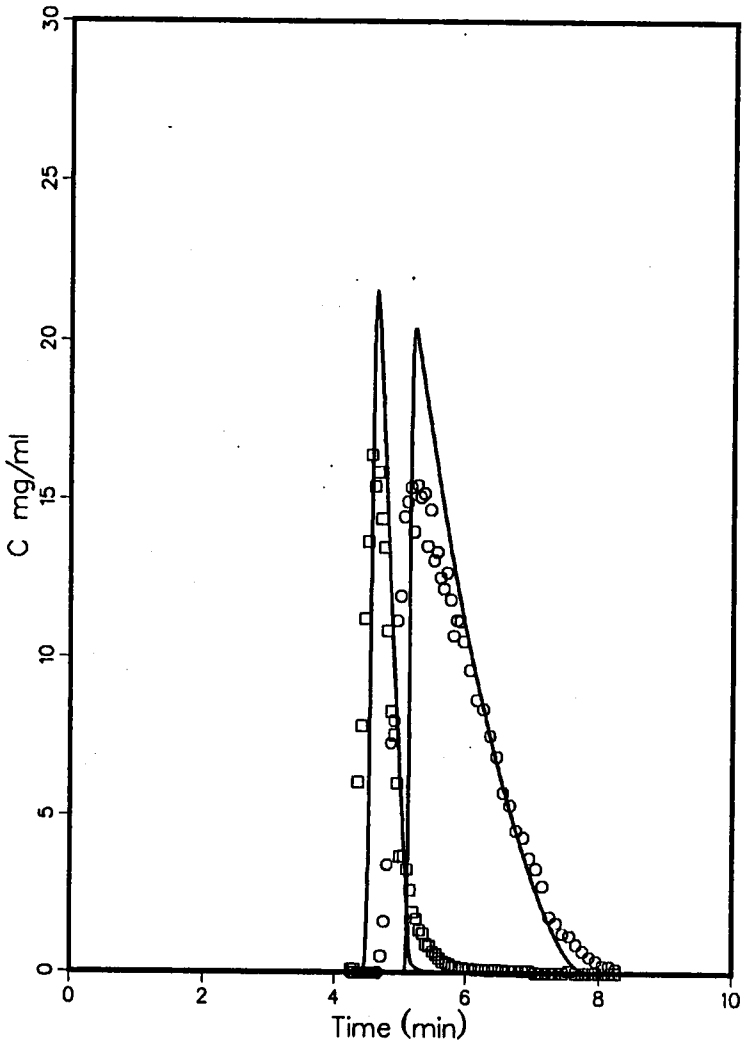
The semi-ideal model of chromatography, explained in detail in Chapter 2, was used to calculated the individual component profiles using the experimental conditions as parameters in the model. Table 3.1 summarizes the experimental parameters measured and used in the modeling. The competitive Langmuir adsorption isotherm equation uses single component adsorption parameters in this model. The injection function described in the boundary condition was assumed to be a rectangular plug having the same width as the sample loop, 0.1 ml, and an area equal to the amount injected.

Figure 4.5 shows a comparison between theoretical and experimental profiles under the 4 conditions experimental data was taken. Figure 5a, 5b, 5c and 5d illustrates the profiles when the ratio of the amount loaded is 1/1, 1/3, 3/1 and 9/1. The experimental profile of phenyl-ethanol is given in squares while the phenyl-propanol profile is shown in circles. In general, the front of the first component and the rear boundary of the second component are predicted virtually exactly by the model. However, the theoretical profiles (lines) show less interference compared to the experimental profiles (symbols). Although the rear boundary of the first eluting component compares very closely to the experimental values, the major difficulty appears in predicting the elution time of the front of the second eluting component. Another difference between the theoretical and experimental profiles is that consistently the theoretical profiles are

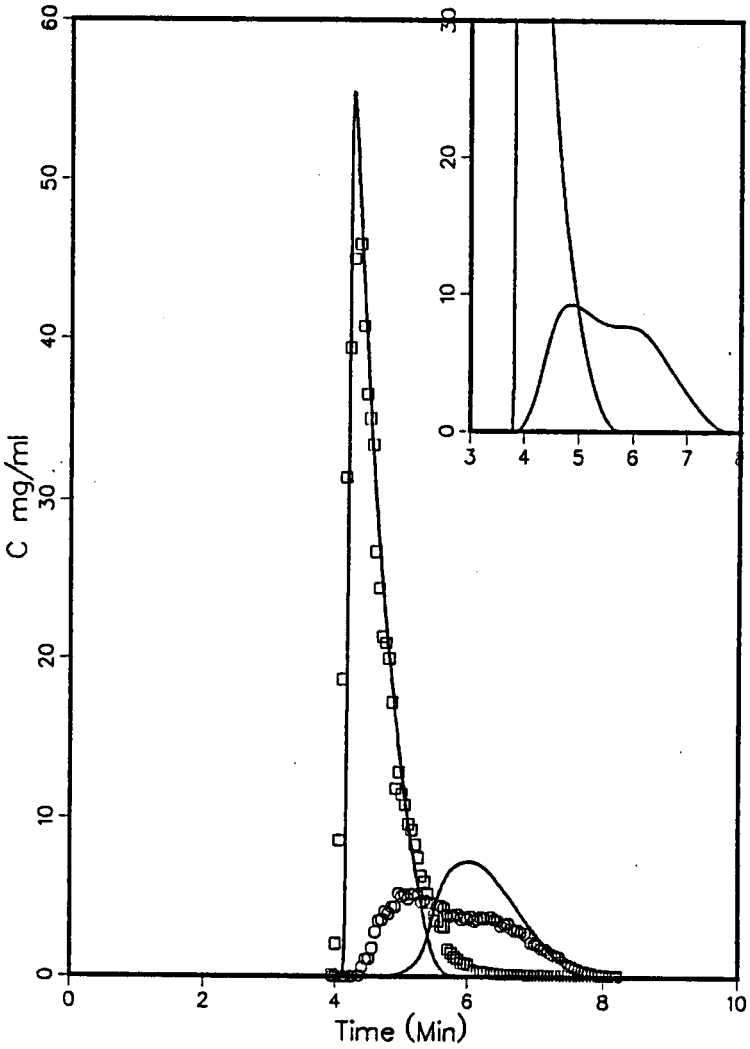


(a) 1/1 Mixture, □ Phenyl-ethanol, o Phenyl-propanol

Figure 4.5a Comparison of Experimental and Predicted Profiles using Single Component Isotherm Parameters and a Rectangular Injection Profile

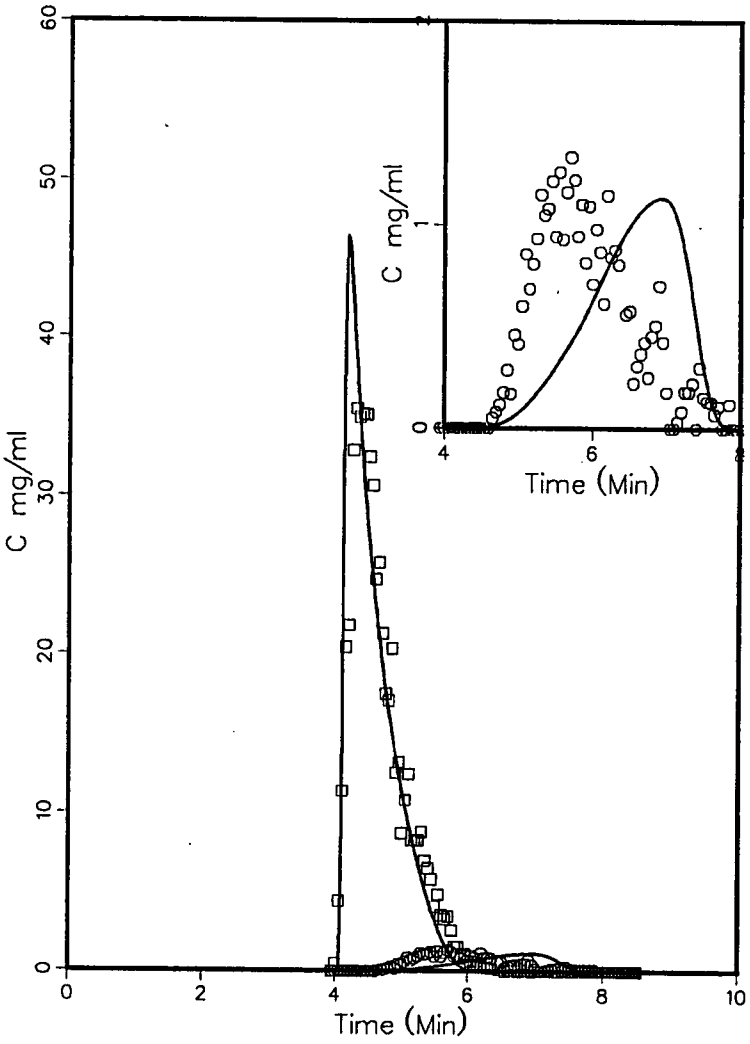


(b) 1/3 Mixture, □ Phenyl-ethanol, o Phenyl-propanol
Figure 4.5 (continued)



insert: chromatogram with twice the amount injected

(c) 3/1 Mixture, □ Phenyl-ethanol, o Phenyl-propanol
Figure 4.5 (continued)



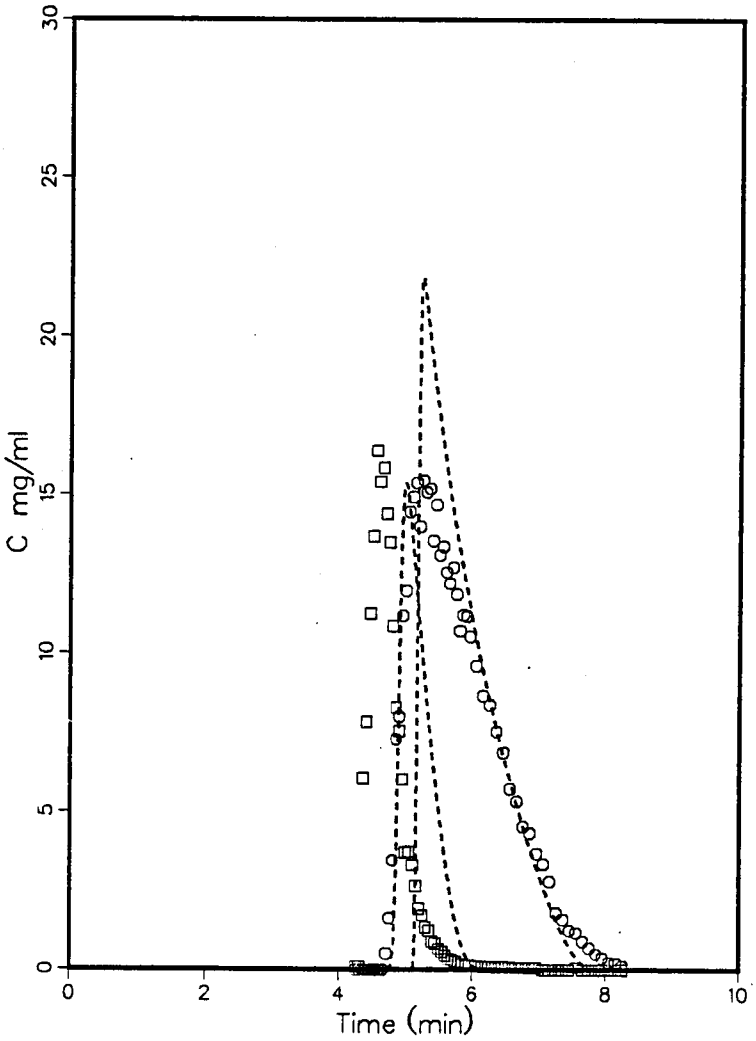
insert: expansion around second component

(d) 9/1 Mixture, □ Phenyl-ethanol, o Phenyl-propanol
Figure 4.5 (continued)

taller and narrower than the experimental profiles.

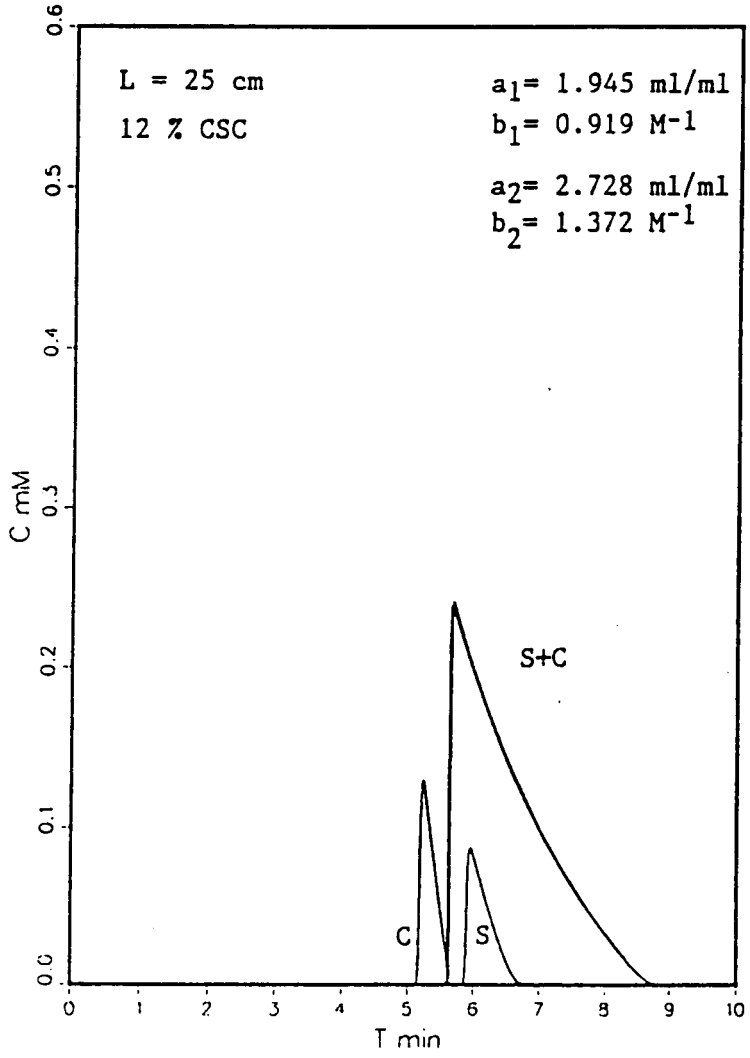
Regardless of the rather minor difference between the predicted and experimental band profiles, this two component data shows that the profiles obtained when the same amount of sample is injected alone is profoundly different from that obtained in a mixture. Figure 4.6 shows theoretical profiles obtained assuming no interaction between the components overlaid with the experimental data. The difference is striking. The non-interacting model shows a large degree of overlap between the first and the second component while the interacting model shows that the displacement effect "enhances" resolution. Moreover, the retention time of the front of the first and second components is not correctly predicted at all.

Figure 4.7 shows a comparison of a non-interacting model (i.e. using strictly single component adsorption isotherms) versus a competitive model (i.e. competitive Langmuir isotherm) for a 1/9 mixture and a 9/1 mixture. The a and b parameters for this particular figure are provided in the figure itself and is different from the other calculations. Figure 4.7a shows the comparison for a 1/9 mixture. The band profile of the second eluting component is the same whether a mixed isotherm or pure isotherm is used. This is true under the specific condition studied here, but at higher loadings significant differences can be seen. On the other hand, the band profile of the first component using a competitive isotherm elutes in front of the second component and partially overlays with the second component when injected alone. This phenomenon is caused by the second displacing the first component from the stationary phase. Since the second component



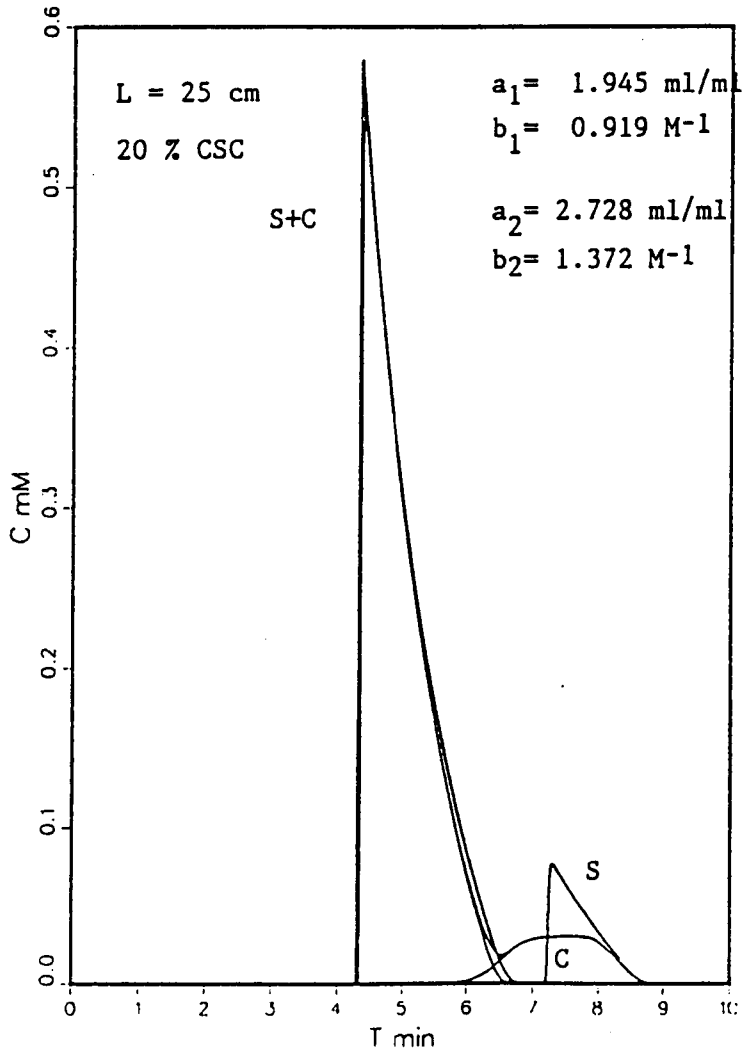
-- theoretical profile, □ Phenyl-ethanol, o Phenyl-propanol

Figure 4.6 Comparison of Non-Interacting Profile with Experimental Data for a 1/3 Mixture



(a) 1/9 Mixture, S - Profile with Single Component Isotherm
C - Profile with Competitive Isotherm

Figure 4.7 Comparison of Non-Interacting and Interacting Model



(b) 9/1 Mixture, S - Profile with Single Component Isotherm
C - Profile with Competitive Isotherm

Figure 4.7 (continued)

adsorbs more strongly to the stationary phase than the first component, the second component desorbs the first component from the column causing it to elute earlier in the presence of the second component. This effect is commonly called the displacement effect.

Conversely, if the first component is in larger amount compared to the second component a different effect occurs. Figure 4.7b compares interacting and noninteracting bands for a 9/1 mixture. The first eluting component exhibits roughly the same peak shape injected alone and in the mixture. At higher loading factors, this difference in profiles becomes more significant. However, the second component no longer exhibits the usual triangular shape profile for Langmuir shaped isotherms, but is pulled forward by the first component. This is called the tag-along-effect analogous to the younger brother taging-along with the older sister. Since the first component is major and occupies a large number of sites, the second component although strongly adsorbed is in smaller quantity and cannot effectively push the molecules of the first component from the stationary phase. Since there are not enough sites available on the surface for the second component to adsorb, a fraction of the second component molecules move faster through the column in the mixture than they would alone. This gives rise to long dilute profiles of the second component. Figure 4.8 shows the band profiles obtained for a 3/1 mixture under the same experimental conditions as shown in Figure 4.5c assuming no interaction. Comparing 4.8 and 4.5c, a strong tag-along effect is seen.

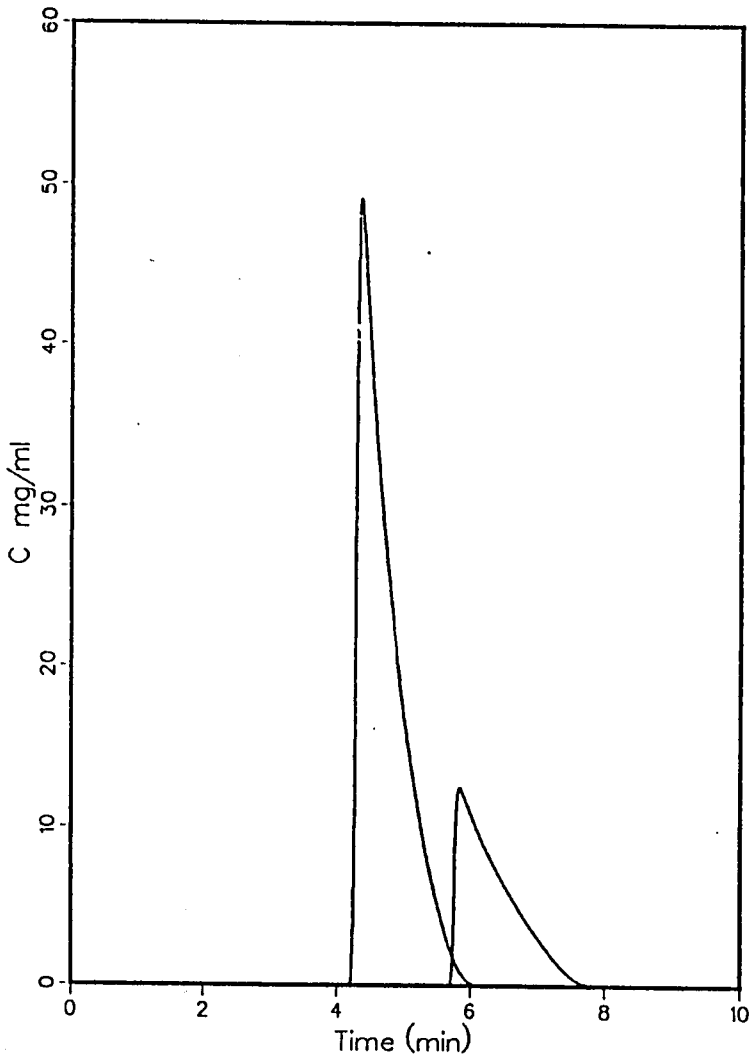


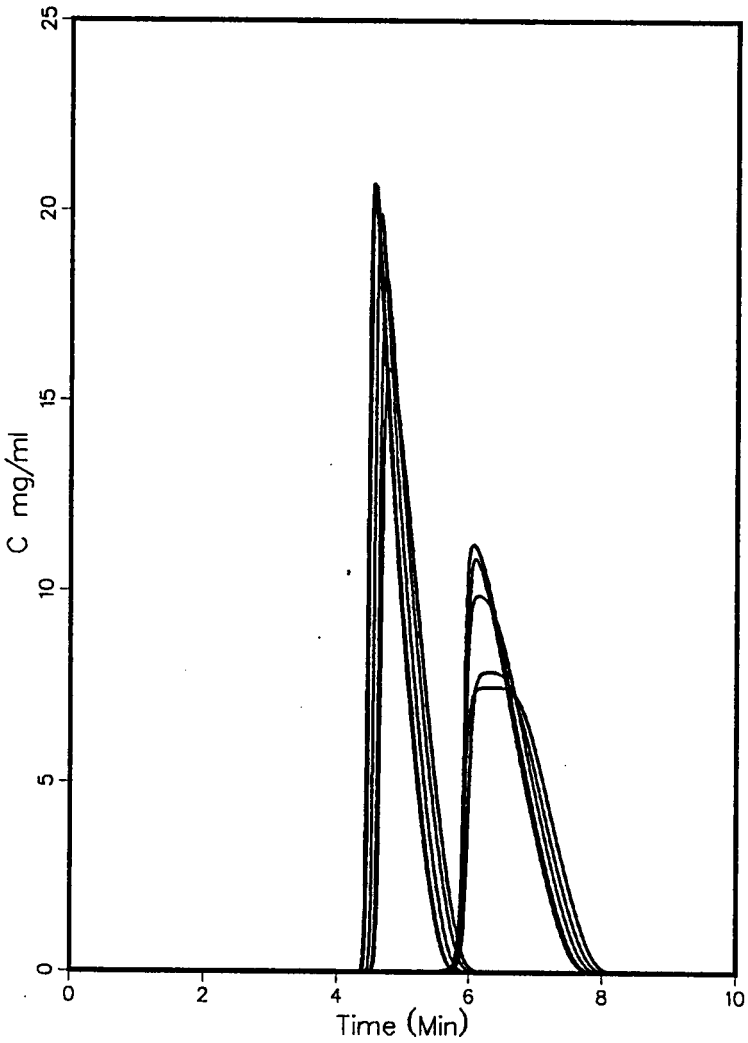
Figure 4.8 Theoretical Profile Assuming No Interaction, 3/1

In summary displacement effects occur when the second component is in larger quantity compared to the first while tag-along effects occur when the first component is in larger quantity than the second. There is good experimental agreement with the theoretical predictions.

Effect of Sample Loop Volume

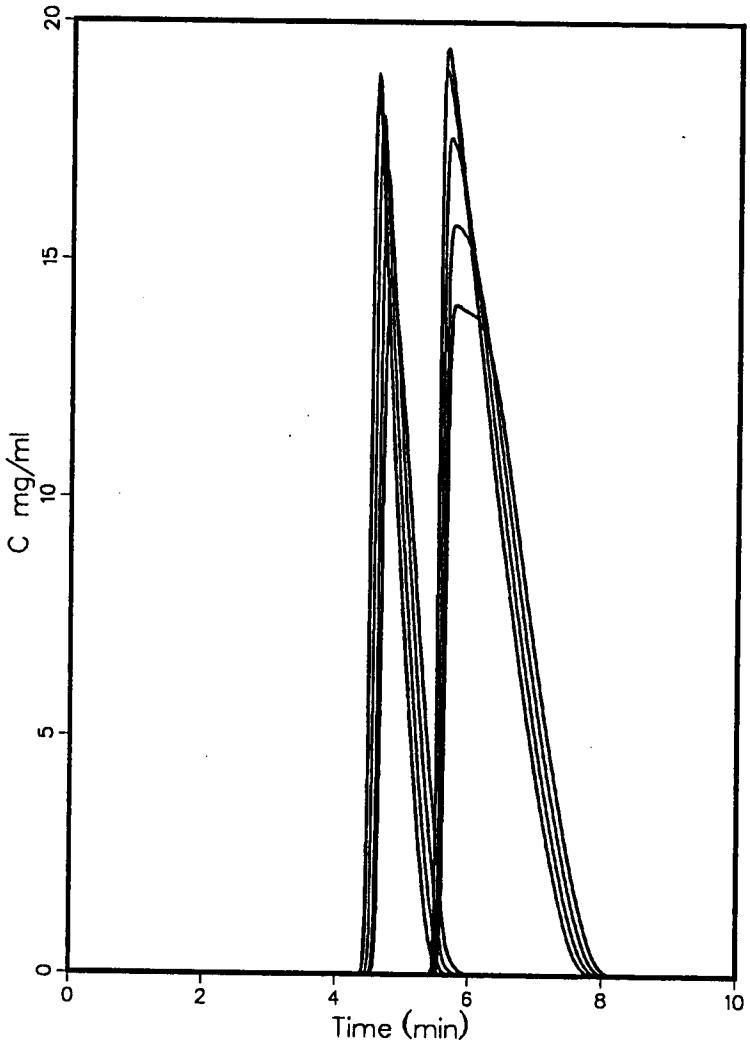
Thus far, it has been assumed that the injection profile is a plug having the same width as the injection loop. However, it is possible that there is dilution before adsorption on the column and that the sample upon entrance to the column deforms or broadens. In order to understand the importance of the injection volume on the band profile, band profiles with rectangular injections of increasing volume were calculated for all four mixtures. Figure 4.9 shows the calculated profiles having an injection time of 5.8, 11.6, 23.2, 34.8 and 46.5 seconds. This calculation is analogous to experimentally keeping the amount injected constant and increasing the same loop volume from 0.1, 0.2, 0.4, 0.58 to 0.77 ml and decreasing the concentration of the sample. These results show as the injection volume increases, the height of the first and second component decreases. For the 1/1, 1/3 and 9/1, Figure 4.9a, 4.9b and 4.9d, the top of the profiles become rounder and flatter; however, there is little change in the overall shape. But, for the 3/1 mixture the larger volume leads to more overlap and the shape conforms more closely to that seen experimentally.

Using a loop volume of 0.6 ml leads to the best agreement with experimental data. Figure 4.10 compares the experimental data with a



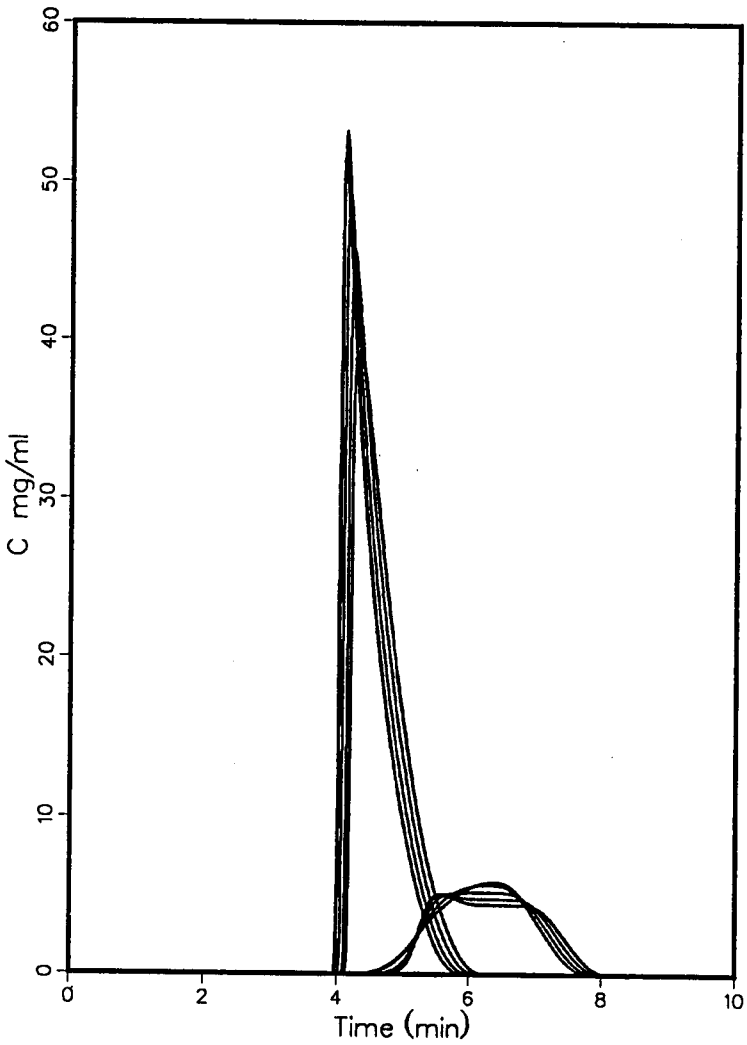
(a) 1/1 Mixture, 5.8, 11.6, 23.2, 34.8 and 46.5 seconds; respectively

Figure 4.9 Effect of Volume on the Band Profile



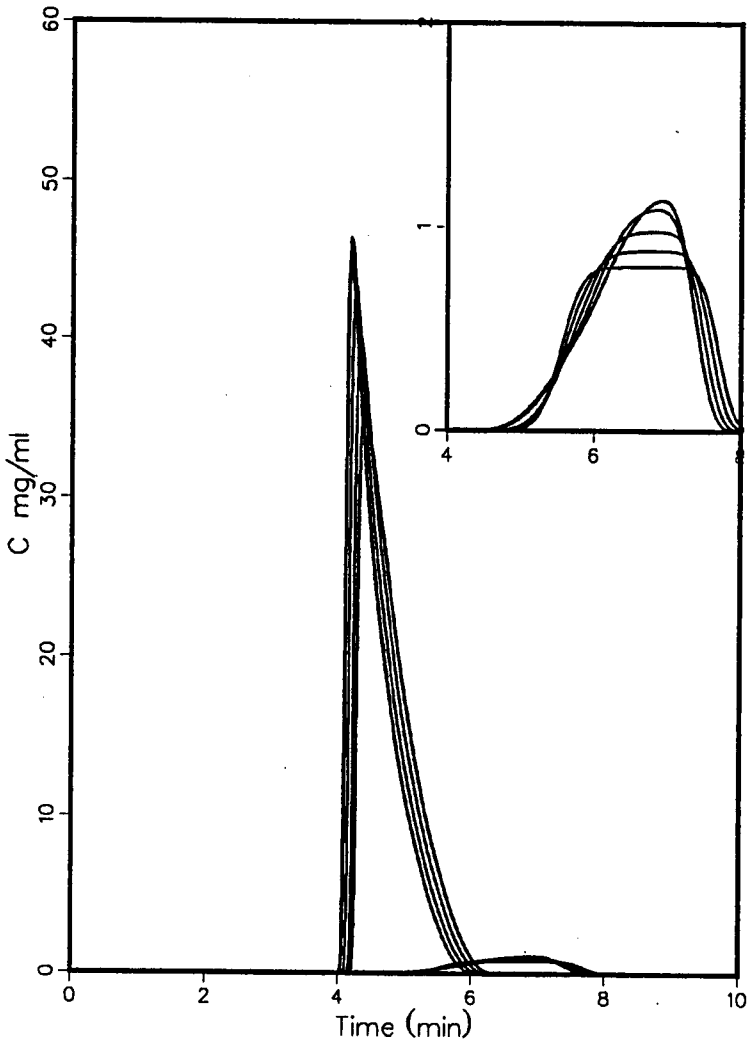
(b) 1/3 Mixture, 5.8, 11.6, 23.2, 34.8 and 46.5 seconds; respectively

Figure 4.9 (continued)



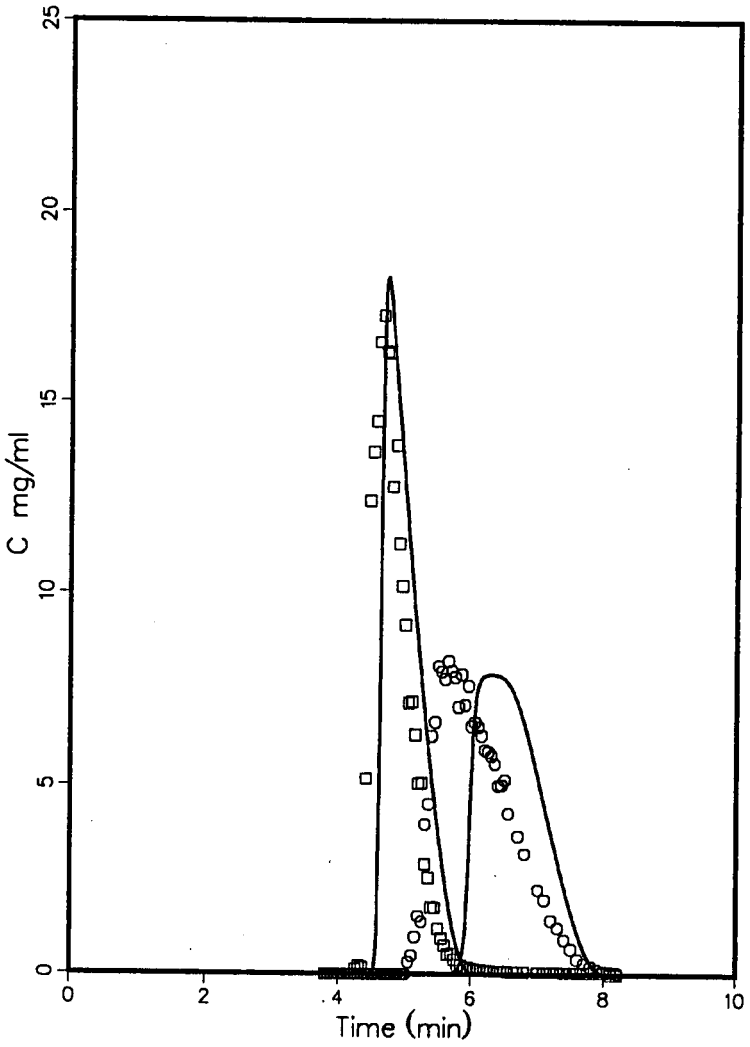
(c) 3/1 Mixture, 5.8, 11.6, 23.2, 34.8 and 46.5 seconds; respectively

Figure 4.9 (continued)



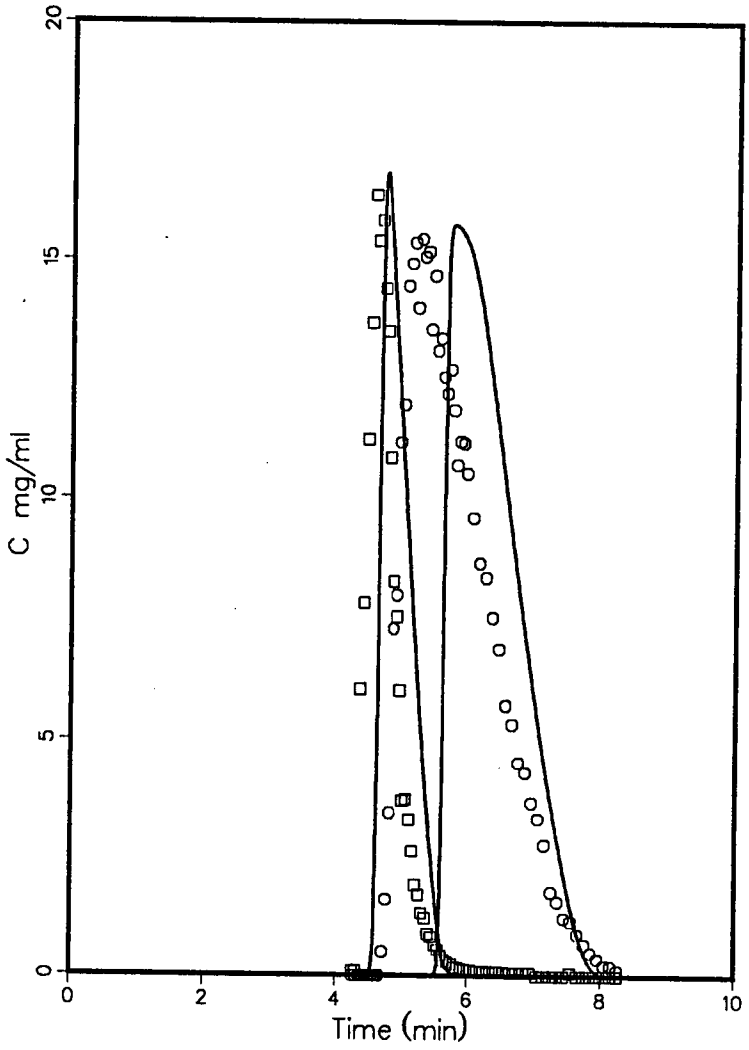
(d) 9/1 Mixture, 5.8, 11.6, 23.2, 34.8 and 46.5 seconds; respectively

Figure 4.9 (continued)



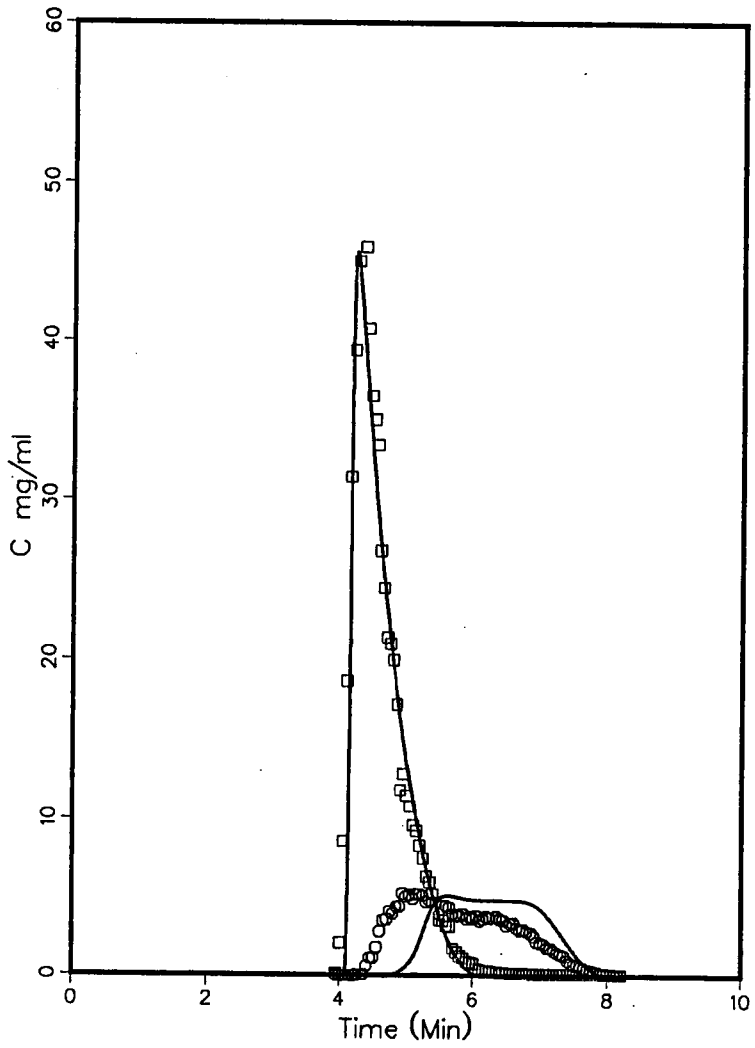
(a) 1/1 Mixture, □ Phenyl-ethanol, o Phenyl-propanol

Figure 4.10 Comparison of Experimental and Predicted Profiles for a 0.5 ml Rectangular Injection



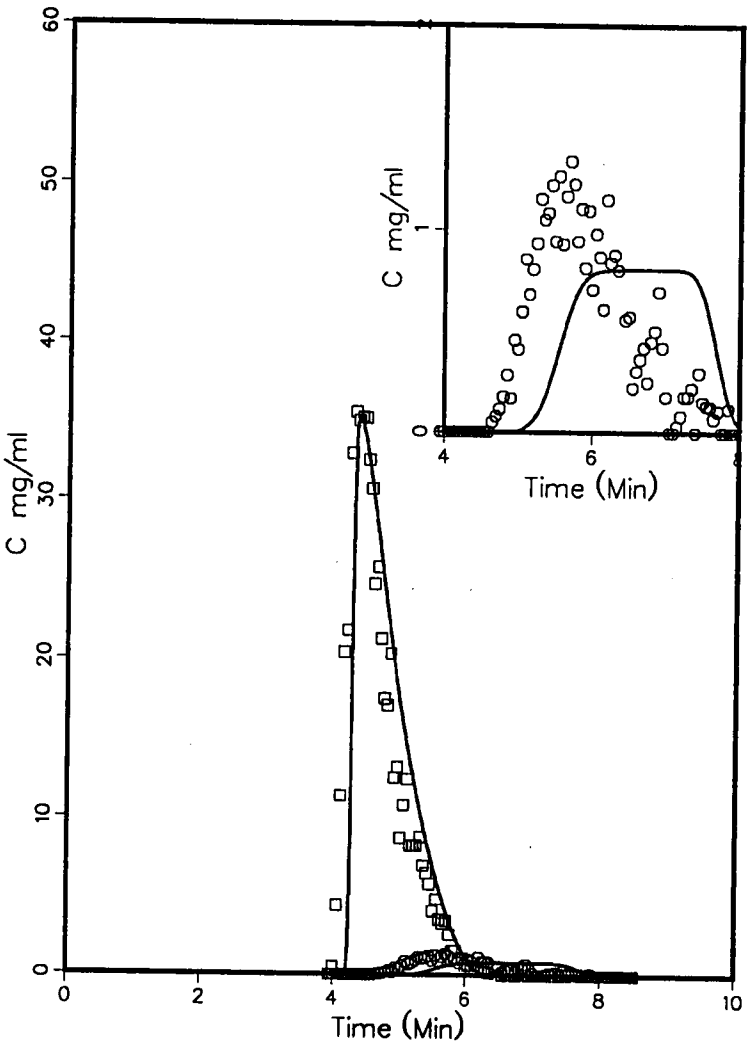
(b) 1/3 Mixture, □ Phenyl-ethanol, o Phenyl-propanol

Figure 4.10 (continued)



(c) 3/1 Mixture, □ Phenyl-ethanol, o Phenyl-propanol

Figure 4.10 (continued)

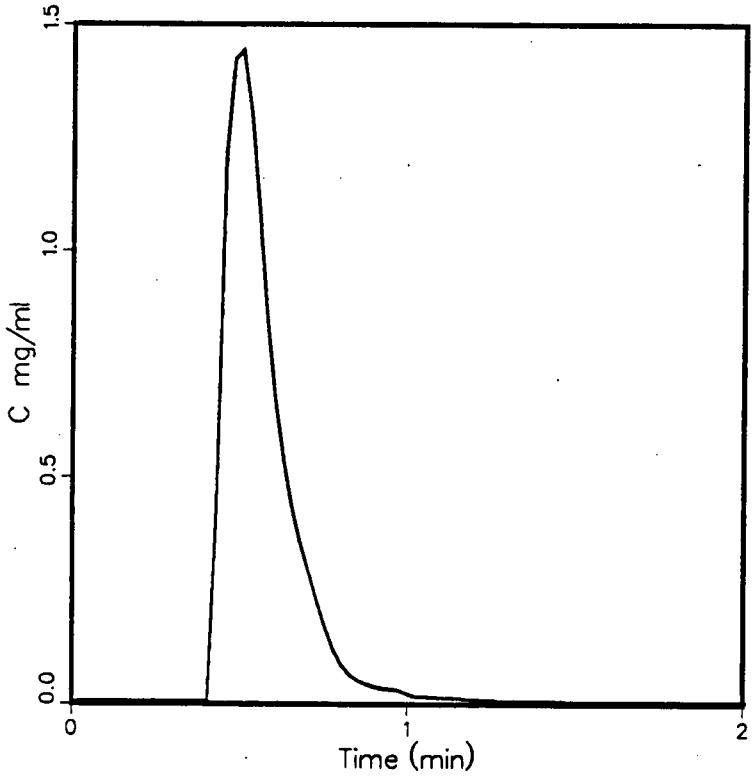


(d) 9/1 Mixture, □ Phenyl-ethanol, o Phenyl-propanol

Figure 4.10 (continued)

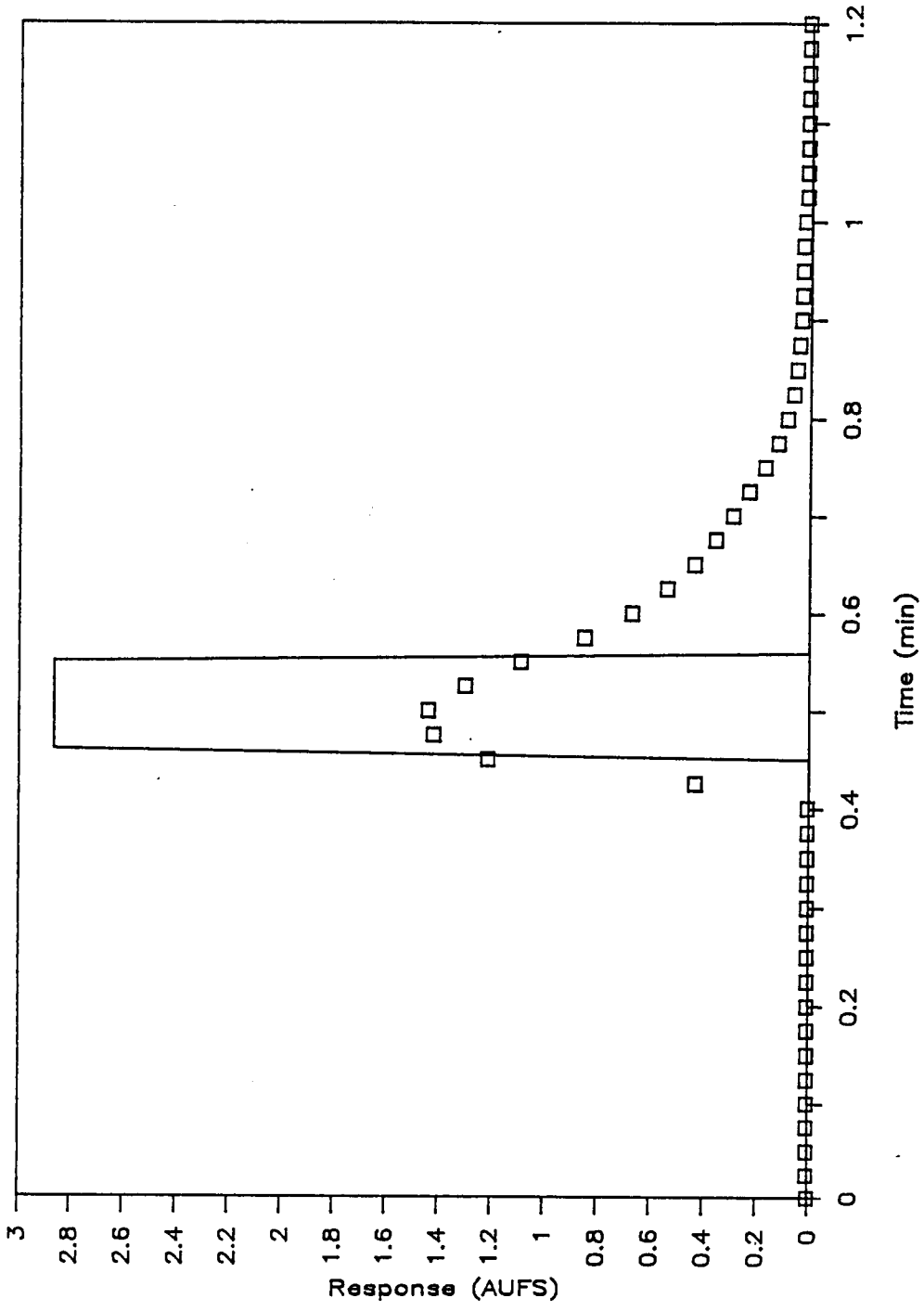
dilute injection corresponding to a 0.6 ml sample loop. Although the relative heights of the peak correspond almost exactly with the experimental data and there is significantly more agreement with the experimental data for the 1/3 mixture, there is a general discrepancy on the amount of interference.

This improvement in the agreement suggested measurement of the actual injection profile by removing the column and injecting the sample directly into the detector. Figure 4.11a shows the injection profile of a 1/3 mixture from a 0.1 ml sample loop in terms of response (volts) from the detector at 272 nm. This profile is not rectangular and looks like an exponentially modified gaussian. The extra column volume of the system is 0.417 min as seen by the offset from the origin. Comparison of the experimental profile (symbols) with a rectangular injection having the same width as the sample loop (0.1 ml), in Figure 4.11b, shows that there is significant dilution of the sample after the injector. The experimental curve was fit to half a gaussian where the area under the curve is equal to the amount injected and the standard deviation is twice the base width. Figure 4.11c shows a comparison between the experimental profile (symbols) and the fitted curve (line). The diffuse front of the profile is approximated by a vertical line and the rear boundary is slightly more diffuse than as modeled. It is this approximation to the experimental profile which is used in the rest of the studies to specify the gaussian (half-gaussian) injection function in the boundary conditions.



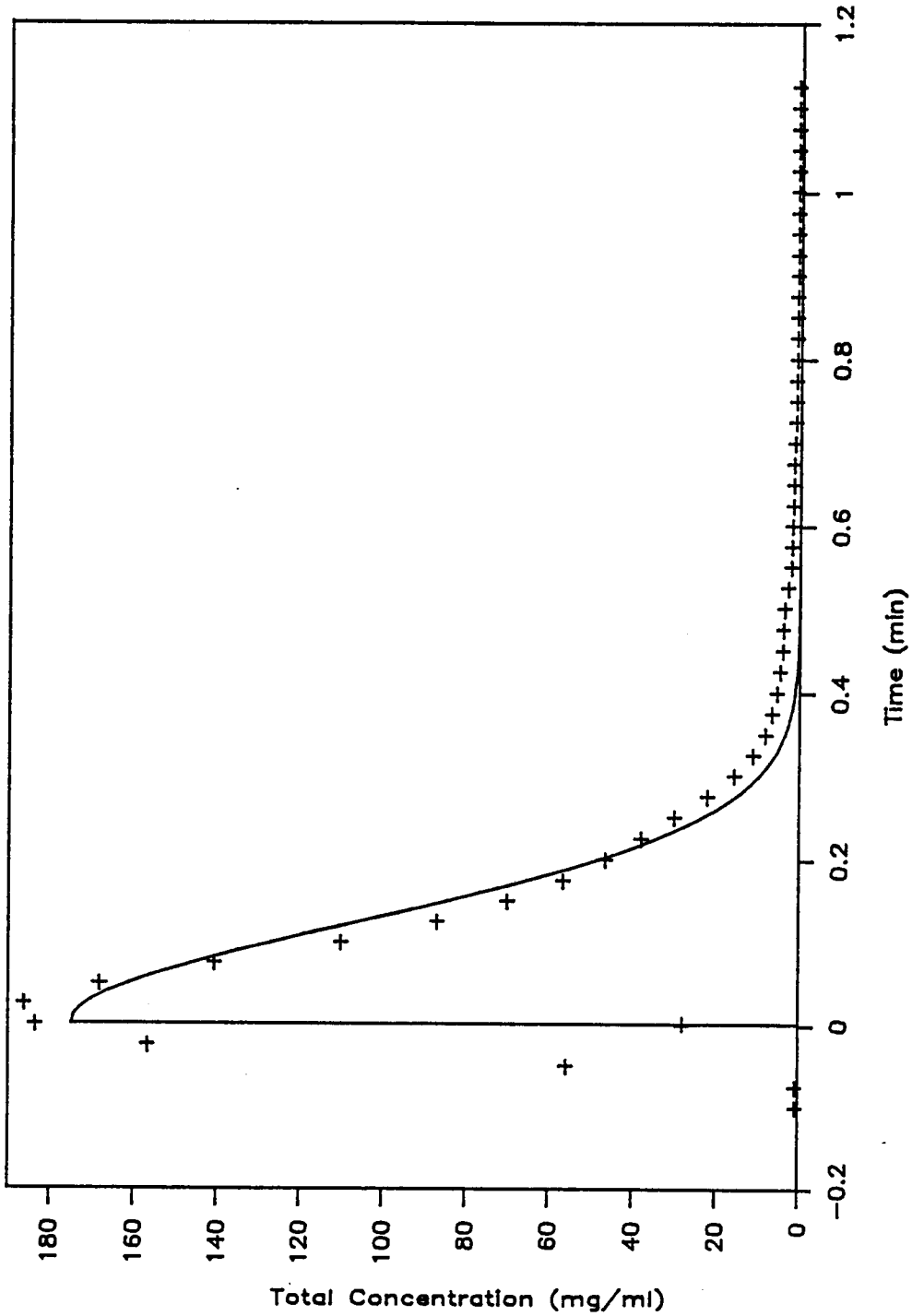
(a) Measured Profile with 0.1 ml Sample Loop

Figure 4.11 Injection Profile



(b) Comparison of 0.1 ml Ideal Rectangular Injection (-) with Measured Profile (□)

Figure 4.11 (continued)



(c) Comparison of Measured Profile (+) to Best Fit Half-Gaussian (-)

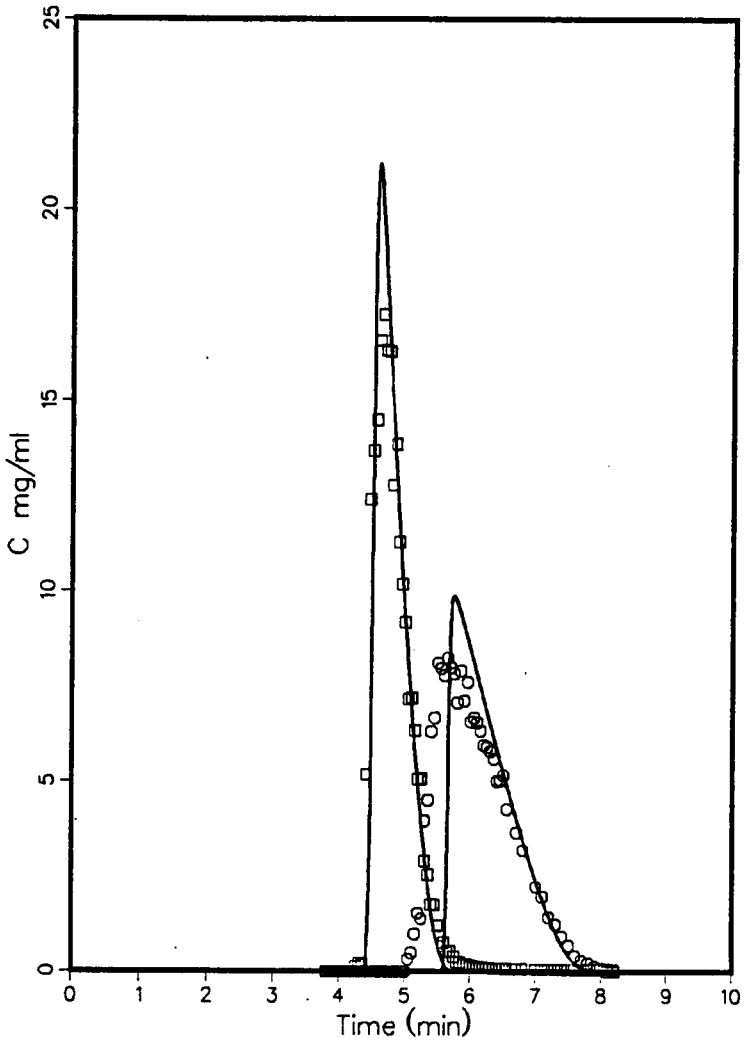
Figure 4.11 (continued)

Figure 4.12 shows a comparison of theory with experiment using the half-gaussian injection function. The flat top nature of the theoretical profiles is no longer seen giving profiles which are approximately the correct height, but still differ in the degree of interference.

From this work, we conclude that the one major assumption not yet addressed is that the competitive adsorption isotherm is obtained from single component data and not measured directly from mixture data. In order to collect data on the competitive isotherm, a method being developed in house was tested for the first time by collecting experimental data. The experimental data and the method are discussed in Section 4.3. Then in Section 4.4, the measured isotherm parameters based on mixtures are used to predict the band profiles of the binary mixtures. In this Section 4.4 we will return to the overloaded elution data presents here.

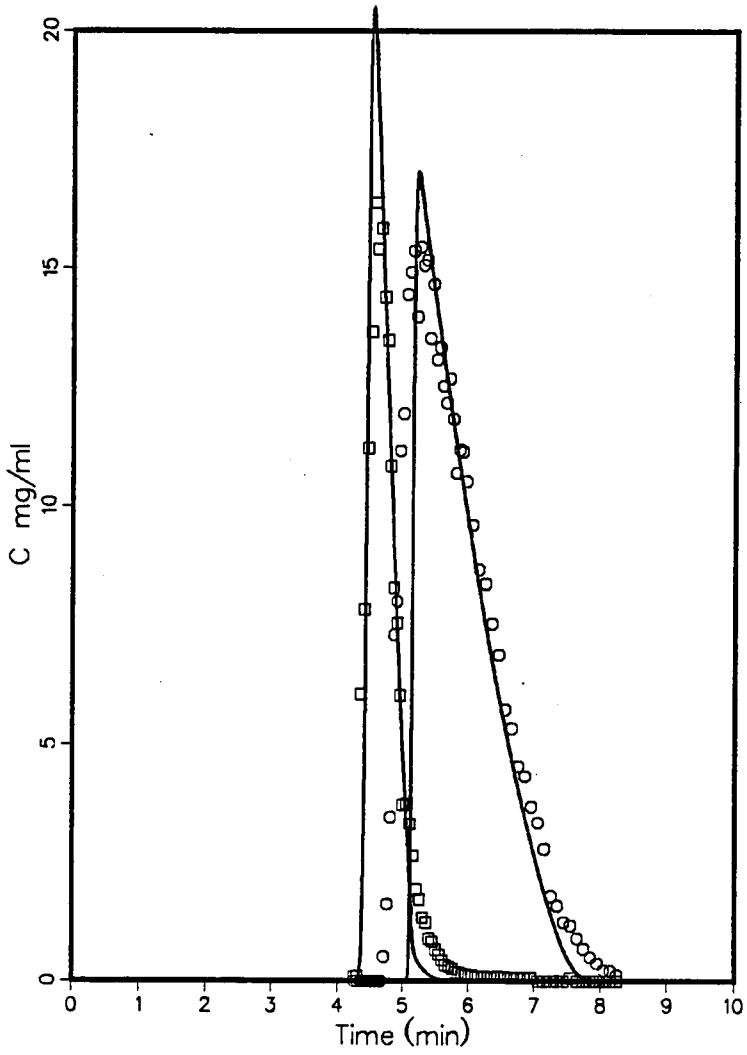
4.2 The Large Volume Injection

The experimental apparatus used for the large volume injection is almost the same as for the pulse injection. It is difficult to inject over a 3-5 minute period using a sample loop since diffusion in the tube leads to non-rectangular injection profiles. The injection valve was reconfigured so that one could switch from the mobile phase flowing to the sample solution dissolved in the mobile phase flowing into the column. Figure 4.13 illustrates the new configuration of the injection valve. The pressure restrictors used in this experiment were old columns to minimize the pressure drop upon switching. The second pump



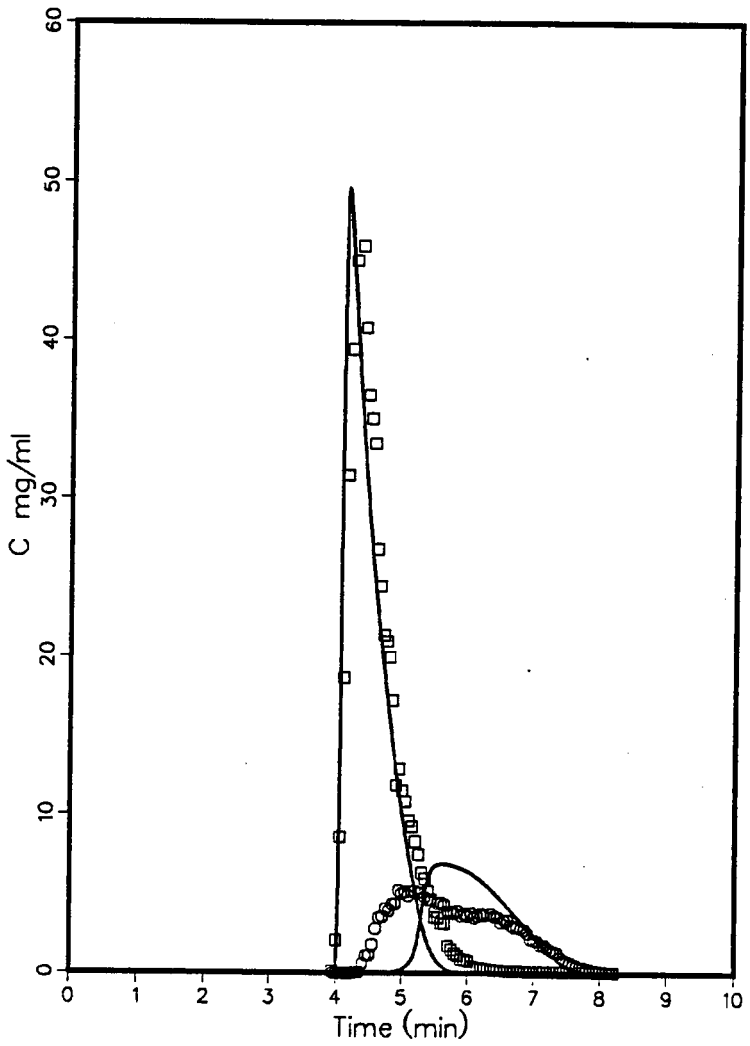
(a) 1/1 Mixture, - Theoretical Prediction, □ Phenyl-ethanol, o Phenyl-propanol

Figure 4.12 Comparison of Experimental and Predicted Profiles with Half-Gaussian Injection Profile



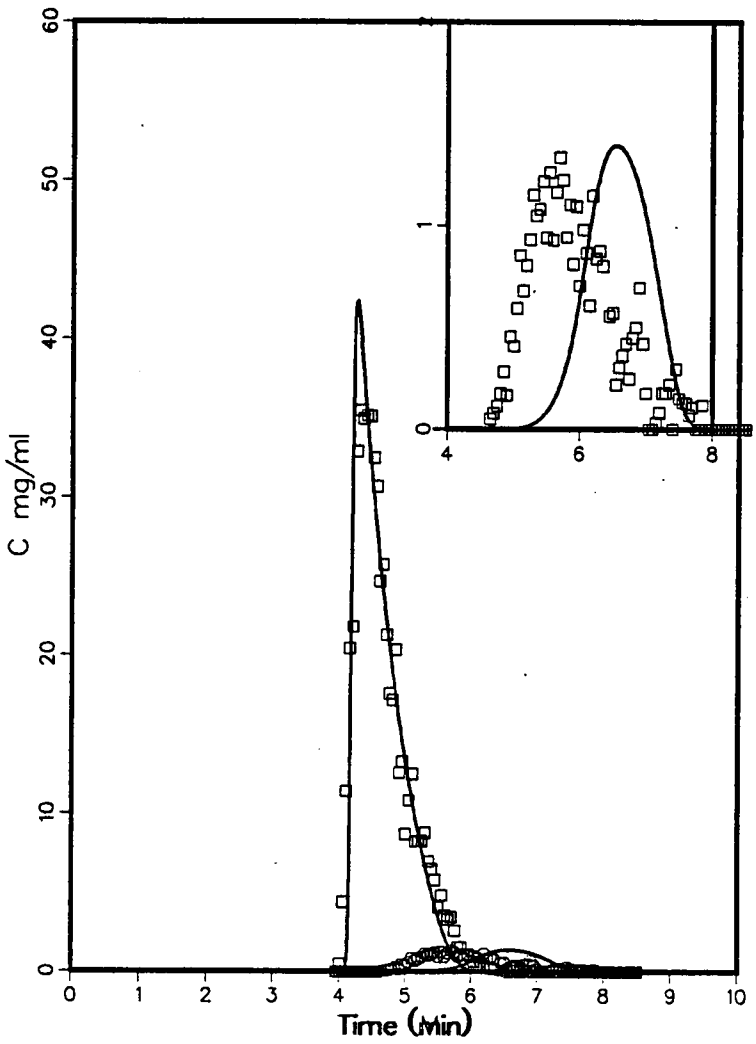
(b) 1/3 Mixture, - Theoretical prediction, □ Phenyl-ethanol, o Phenyl-propanol

Figure 4.12 (continued)



(c) 3/1 Mixture, - Theoretical prediction, □ Phenyl-ethanol, o Phenyl-propanol

Figure 4.12 (continued)



(d) 9/1 Mixture, - Theoretical prediction, □ Phenyl-ethanol, o Phenyl-propanol

Figure 4.12 (continued)

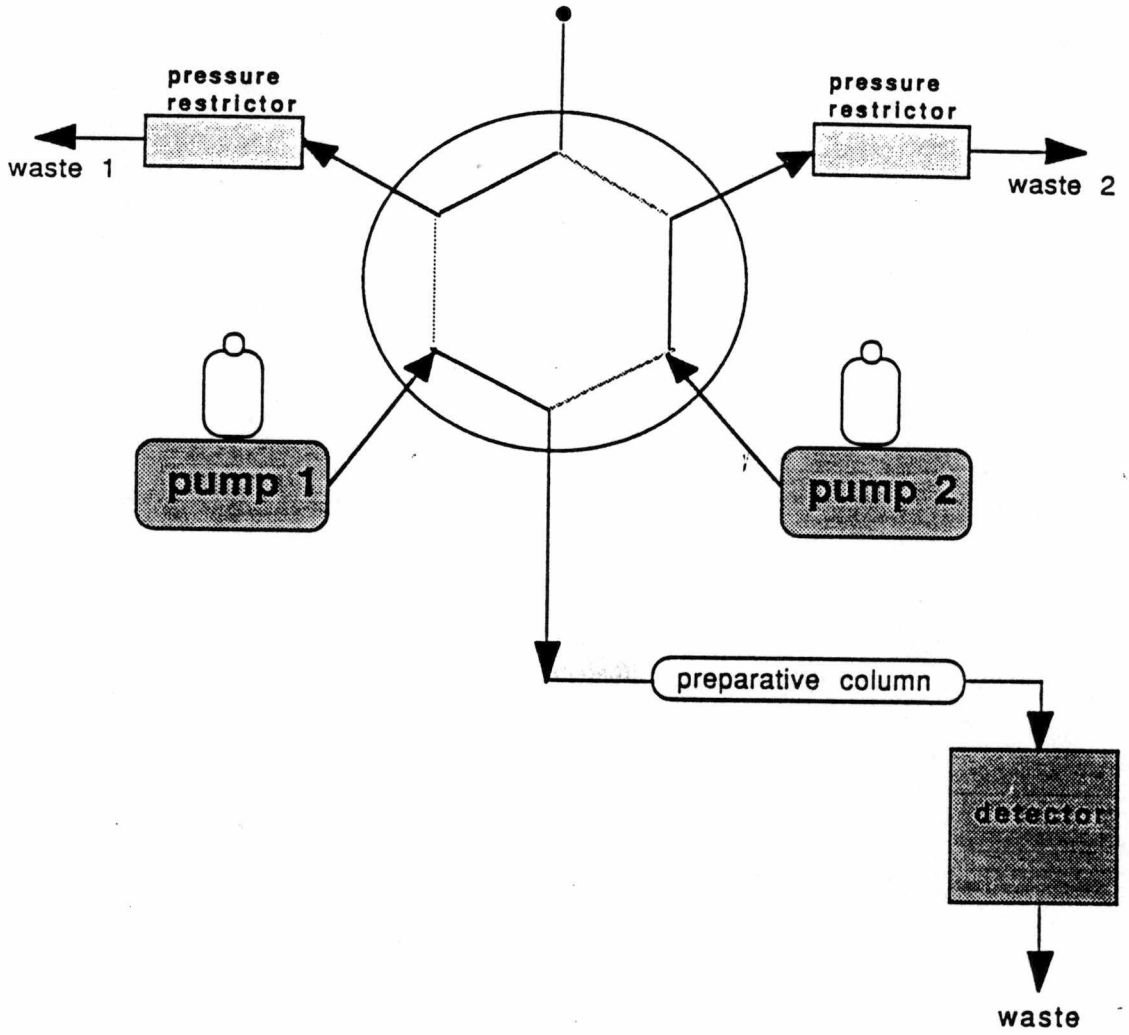


Figure 4.13 Schematic of Injector for Large Volume Experiments

used was a Gilson (Middleton, WI) model 301 pump fitted with a 5PW pump head, a flow through Pressure gauge and a SSI Pulse Damper (State College, Pa).

Similar to the overloaded elution experiments, the sample was loaded by switching the injector for a specific amount of time. The individual component profiles were obtained by fraction collection and reanalysis.

The Hodograph Transform

For a binary mixture, the concentration of each solute $C_1(x,t)$, $C_2(x,t)$ is a function of the column length x and time, t. Since measurement is made at the column outlet, the column length is constant and $C_1(t), C_2(t)$ are measured. The hodograph space is considered the inverse function where $t(C_1,C_2)$, $x(C_1,C_2)$. It has been shown [Aris] for the case of the Langmuir isotherm, the Hodograph transformation gives two straight lines for chromatographic profiles when the injection volume is large. The slope of these two straight lines are independent of the plateau concentration. Therefore, from an experimental data, these lines can be fit in order to determine the best parameters of the isotherm model.

When the Langmuir model does not account properly for the competitive interaction of the solutes, then the simple wave theory shows [Ma] that the slope of the straight lines are a function of the feed composition. Different isotherms predict different dependencies. For example, the modified Langmuir isotherm shows that the Langmuir b parameters are a function of concentration and thus could be determined

$$Q_1 = \frac{a_1 C_1 + a_{12} C_1 C_2}{1 + b_1 C_1 + b_2 C_2 + b_{12} C_1 C_2}$$
$$Q_2 = \frac{a_2 C_2 + a_{12} C_1 C_2}{1 + b_1 C_1 + b_2 C_2 + b_{12} C_1 C_2} \qquad (4.2)$$

from successive wide pulses of binary mixtures having different composition. Also the characteristic lines of the Hodograph transform are slightly curved.

Figure 4.14a illustrates a theoretical elution profile, having a competitive Langmuir isotherm, of a two component mixture when the injection volume is large enough that up elution, the chromatogram still exhibits a plateau. Figure 4.14b illustrates its hodograph transform. The conversion from an elution profile to a Hodograph plot occurs by plotting at each time the concentration of component 1 versus the concentration of component 2. Therefore, in the elution band, when the concentration of the first component rises a vertical line extends form the origin to point A ($C_{1,A}$,0) on the Hodograph plot. The intermediate plateau of the first component converts to a point (A) in the hodograph plot. The elution of the second component leads to a decrease in concentration of the first component and in the hodograph plot this transforms to a line extending from A ($C_{1,A}$,0) to B ($C_{10,A}$,$C_{20,B}$). The plateau concentration corresponding to the injection concentration, transforms into a single point (B). When the tail of the first component elutes from the column, the concentration of the second component decreases giving a straight line from point B ($C_{10,A}$,$C_{20,B}$) to C (0,$C_{20,B}$). After the first component has eluted, the second component is pure resulting in a line from point C to the origin.

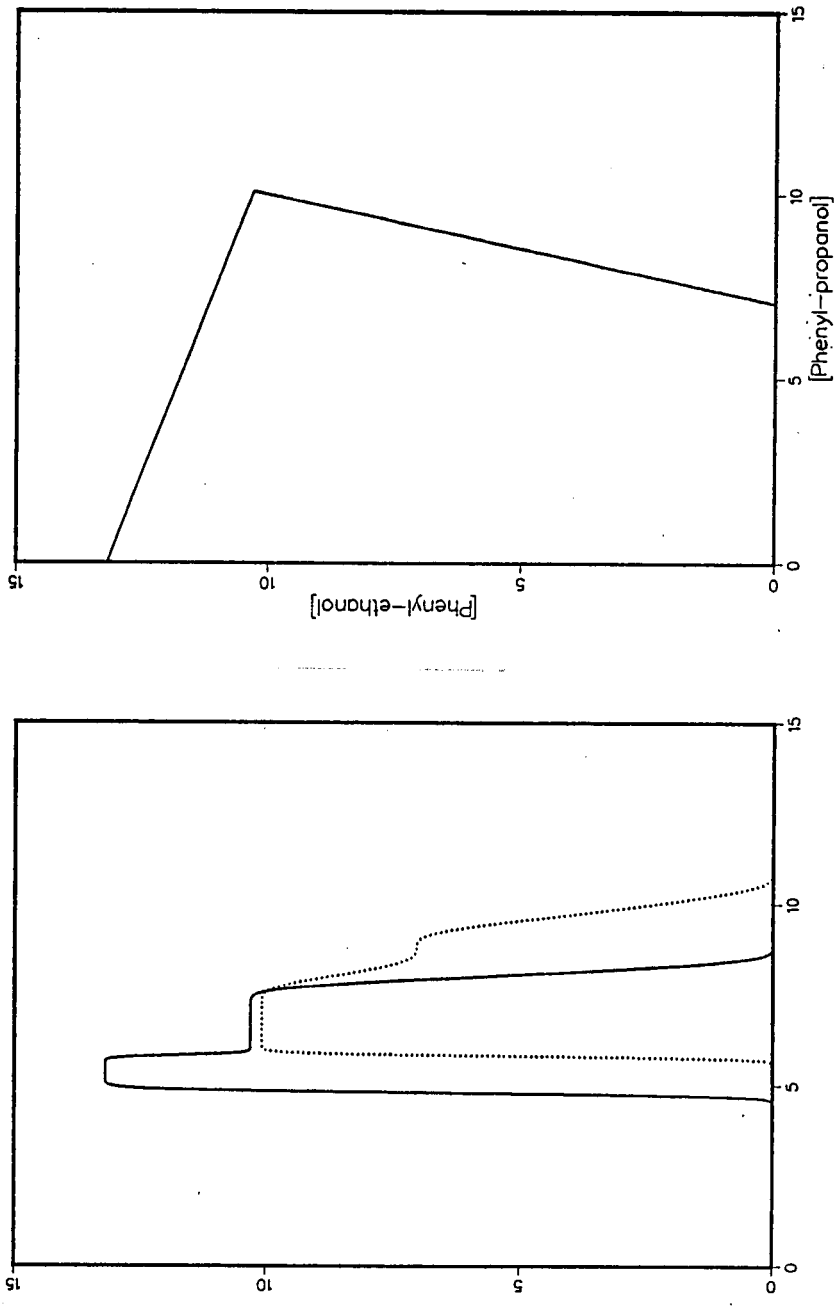


Figure 4.14 The Hodograph Transform

The key the value of the Hodograph transform is the mapping of the (z,t) plane on the (C1,C2) plane. The advantage of using the Hodograph Transform is that it is a universal plot and the lines obtained are independent of the column length, injection profile, mobile phase velocity and to a large extent kinetic effects. When the injection is wide enough to give a plateau it is possible to derive algebraic relationships between the separation factor, the slope and intercept values of the lines in the Hodograph plot and the b values of the competitive Langmuir adsorption isotherm. When the competitive isotherm deviates strongly from Langmuir behavior, then the Langmuir b values are a function of concentration. The concentration dependence must then be determined experimentally by systematically changing the plateaux concentration. Figure 4.15 summarizes the algebraic relationships used to calculate the b values from the best fit straight lines. These b values are called best fit Langmuir parameters. The a parameters are obtained as before from infinite dilution retention measurements and the phase ratio.

The next four sections will present data collected with a large volume, rectangular shaped injection profiles where the ratio of the amount injected is 1/1, 1/3 and 3/1 and one non-rectangular injection profile where the ratio is 1/1. For each mixture the injection profile, column output detector response and the concentration-time profile will be presented. Additionally, a comparison of theoretical and experimental elution profiles and Hodograph plots using a competitive Langmuir adsorption isotherm with single component Langmuir parameters will be presented. Lastly, comparisons with the best fit

$$b_1 = \frac{\alpha - 1}{A_+} - b_2 \frac{\alpha}{\xi_+}$$

$$b_2 = \left(\frac{\alpha - 1}{\alpha}\right) \frac{\frac{1}{A_+} - \frac{1}{A_-}}{\frac{1}{\xi_+} - \frac{1}{\xi_-}}$$

Figure 4.15 Algebraic Relationships for Calculating Isotherm

b parameters will be presented. Table 4.2 summarizes the experimental conditions and parameters derived from this study. For these experiments, the total concentration was kept constant, 20 mg/ml, but the ratio of the composition of the two components was varied.

The 1/1 Rectangular Injection

Figure 4.16 shows the measured injection profile for a rectangular injection using the configuration described in Figure 4.14. A sharp front and rear boundary is clearly obtained. Figure 4.17 shows the detector response monitored at 272 nm at the column outlet to a 1/1 mixture injected over 3.5 minutes. Figure 4.18 shows the chromatogram after analysis of the collected fractions. An attempt at making a correspondence between the concentration time profile in Figure 4.18 explains the detector response profile. The initial plateau is lower since phenyl-ethanol has a detector response about one-third of phenyl-propanol at 272 nm. The plateau corresponding to the inlet concentration is seen at 1.5 volts and does not saturate the detector, one advantage of working at 272 nm. The shoulder seen at 10 minutes occurs when the second component becomes pure. Figure 4.17 shows concentration of the first component at 5 minutes because of displacement effects from the second component. Errors occurring from reanalysis of the data are seen on the plateaux where slight scatter of the data is apparent.

A comparison of experimental and theoretical elution profiles for this mixture is shown in Figure 4.19. The theoretical profile is predicted using single component isotherm parameters in a competitive

Table 4.2 Summary of Large Volume Injection Parameters

	1/1 Rect.	3/1 Rect.	1/3 Rect.	1/1 Non-Rec.	Component Langmuir
b_E ml/mg:	0.02113	0.02661	0.02236	0.02955	0.0148
b_P ml/mg:	0.02557	0.02975	0.02947	0.02336	0.0255
b_E ml/mmol:	2.582	3.2517	2.732	3.611	1.809
b_P ml/mmol:	3.4826	4.052	4.041	3.691	3.479
csc E (mg):	98	78	93	70	140
csc P (mg):	150	129	130	164	150
avg. csc :	124	103	111	67	145
HETP:	0.0167	0.00847	0.00847	0.00847	--
uz cm/s:	0.06887	0.06920	0.069204	0.06920	--
u_o cm/s:	0.1355	0.13889	0.13889	0.13889	--
inj. time s:	210	300	216	270	
min:	3.5	5.0	3.6	4.5	
dt sec:	0.484	0.245	0.245	0.245	
number of dt:	434	1224	882	1102	
C_{Eo} mg/ml:	10.30225	15.1079	5.15355	10.3188	
C_{Po} mg/ml:	10.08625	5.0649	15.12175	9.2181	

b_1,avg = 3.044 ml/mmole standard deviation of 0.43
b_2,avg = 3.69 ml/mmole standard deviation of 0.27
csc E: 83.4 mg
csc P: 142 mg
avg csc: 113 mg
T_0: 184 seconds
T_{R1}: 308.5 seconds, k': 0.714, a_1: 1.924 ml/ml
T_{R2}: 414.0 seconds, k': 1.3, a_2: 3.554 ml/ml
L: 25 cm
porosity: 0.74
E: Phenyl-ethanol (1), P: Phenyl-propanol (2)

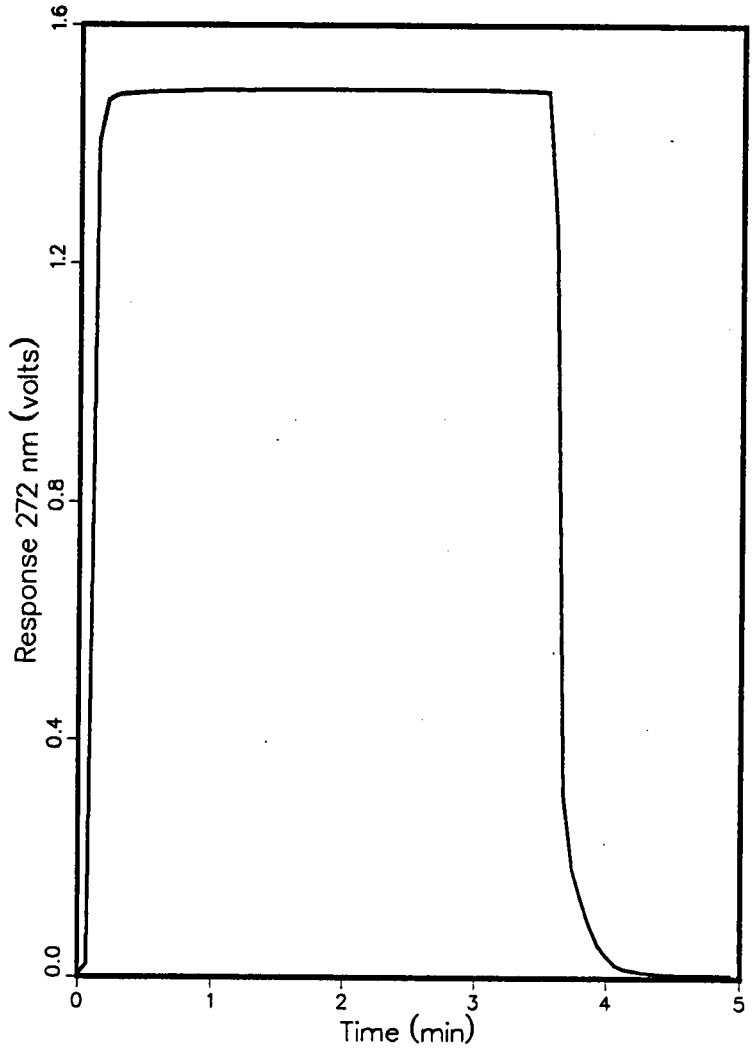


Figure 4.16 Measured Injection Profile for 3.5 min Plug

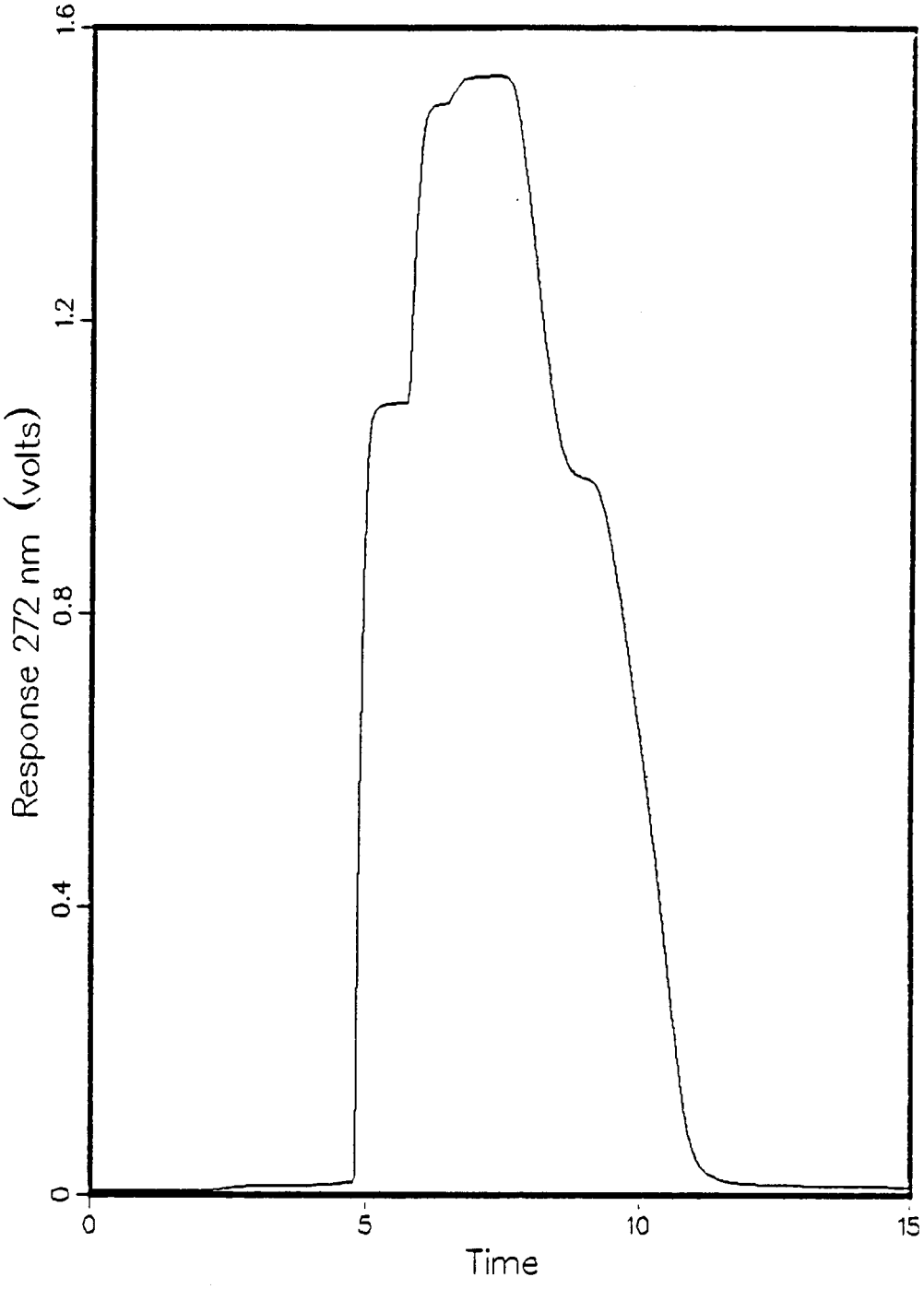
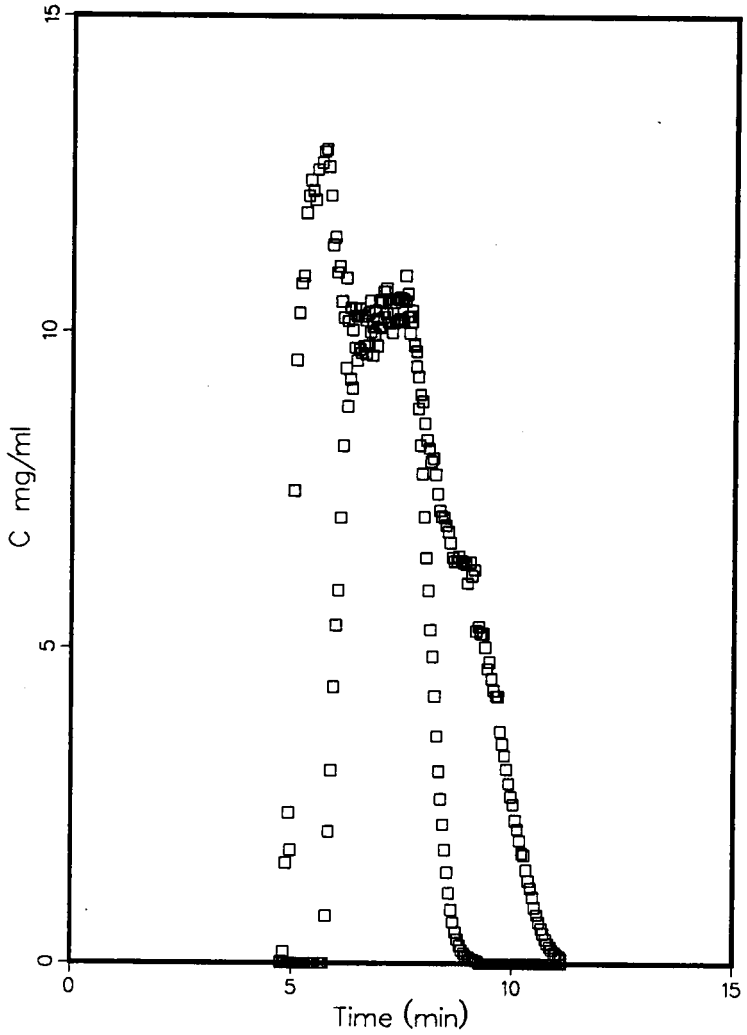
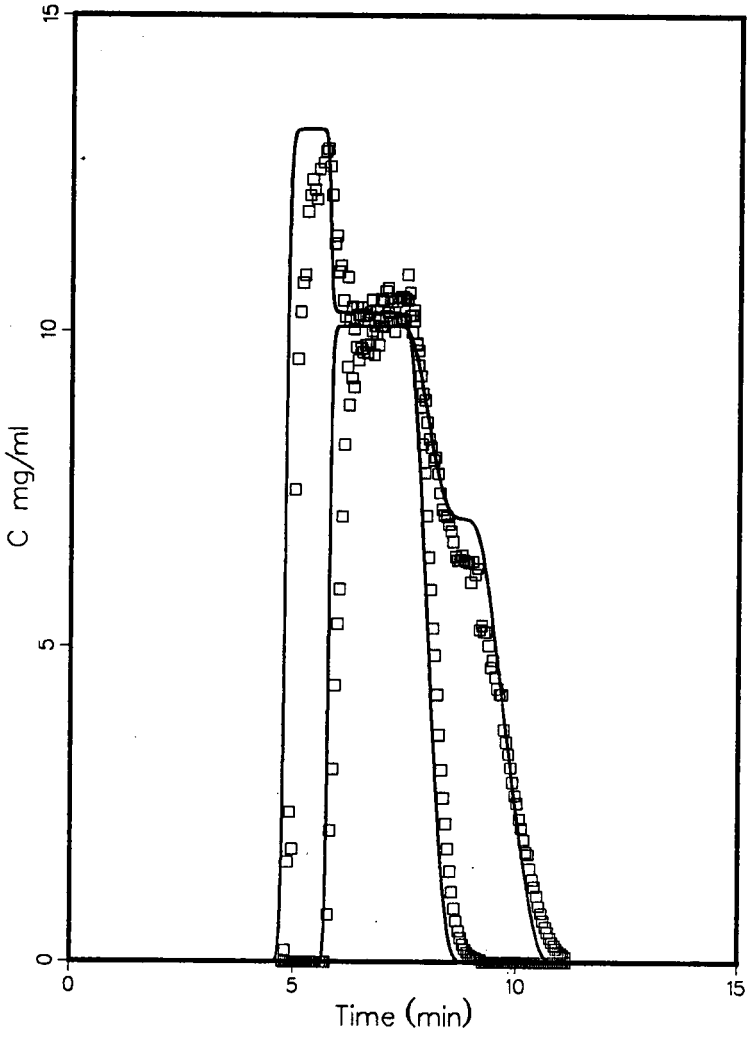


Figure 4.17 Detector Response Curve to a 1/1 Binary Mixture



□ Experimental

Figure 4.18 Elution Profile after Fraction Collection, 1/1 Mixture



- Theoretical, □ Experimental

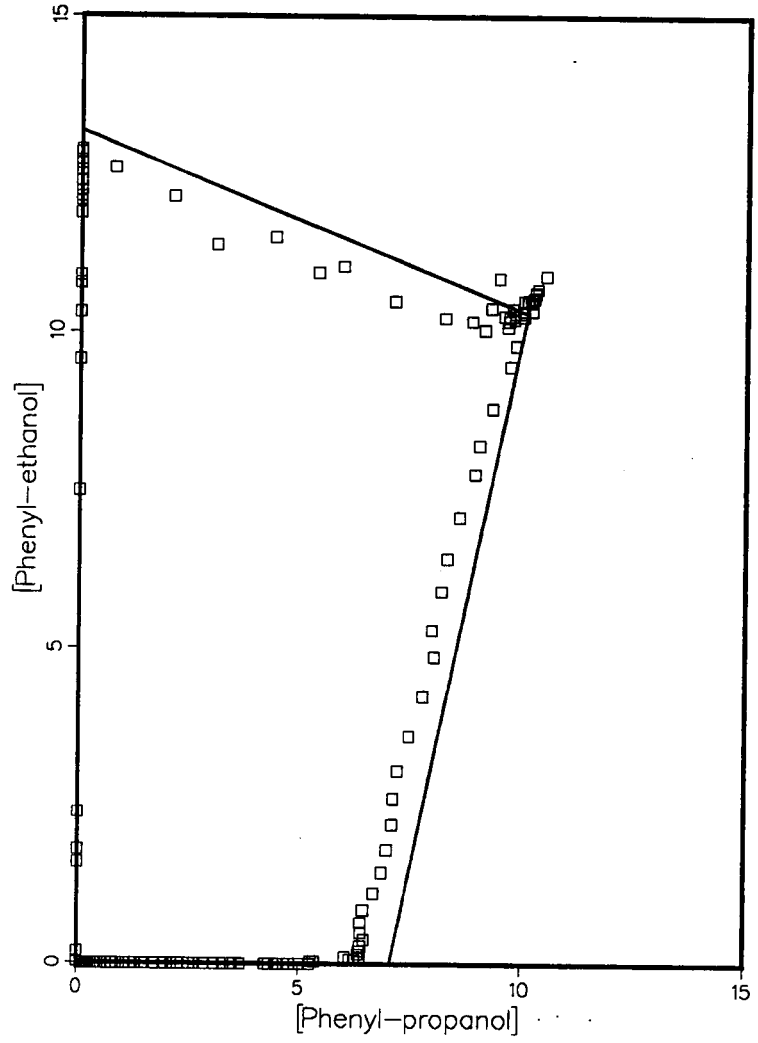
Figure 4.19 Comparison of Experimental and Predicted Elution Profiles, 1/1, using Single Component Isotherm Data

Langmuir model. In general, the front of the first and the second component are more diffuse than predicted. The major difference between theory and experiment is the prediction of the height of the plateau on the tail of the pure second component. Transformation to the Hodograph space, Figure 4.20, shows more clearly that there is a systematic difference between the experimental and theoretical profiles.

Using the experimental data and equations in Table 4.2, best fit Langmuir isotherm parameters are found in the Hodograph space, Figure 4.21. A least square fit of the experimental data gives good results. Using the semi-ideal model, the elution profile is predicted using the best fit Langmuir Parameters. Figure 4.22 shows a comparison of the theoretical profile and the experimental data. Although the front of the first and second components of the experimental profiles is more diffuse than predicted, the second component rear boundary is improved to give virtually an exact fit. The best fit b values are summarized in Table 4.2. The b parameter for both components increases from $b_{1,s}$= 1.809 ml/mmol and $b_{2,s}$= 3.479 ml/mmol in the single component case to $b_{1,h}$= 2.582 to $b_{2,h}$= 3.4826 from the Hodograph analysis. The increase in the b parameter means there is more interaction than predicted in the ideal case. The column saturation capacity in both cases is significantly lower.

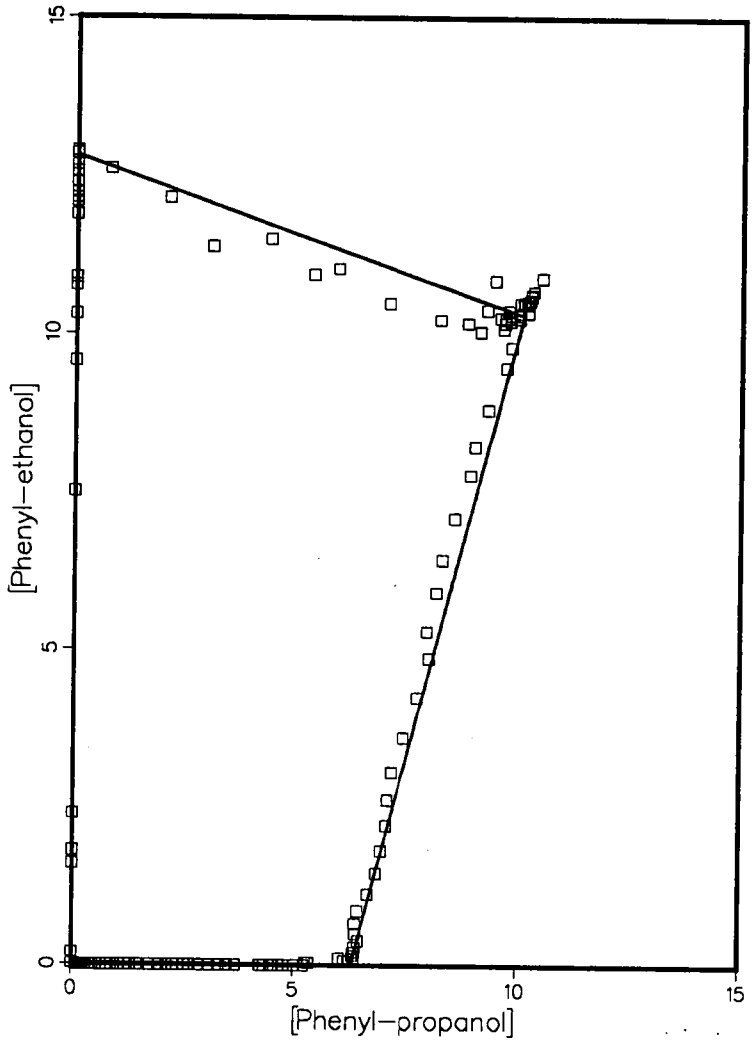
The 1/1 Non-rectangular Injection

In the next experiment, a non rectangular injection is considered. Experimentally this is accomplished by using a 5 ml sample loop and injecting over 5 min. However, during the elution, there is



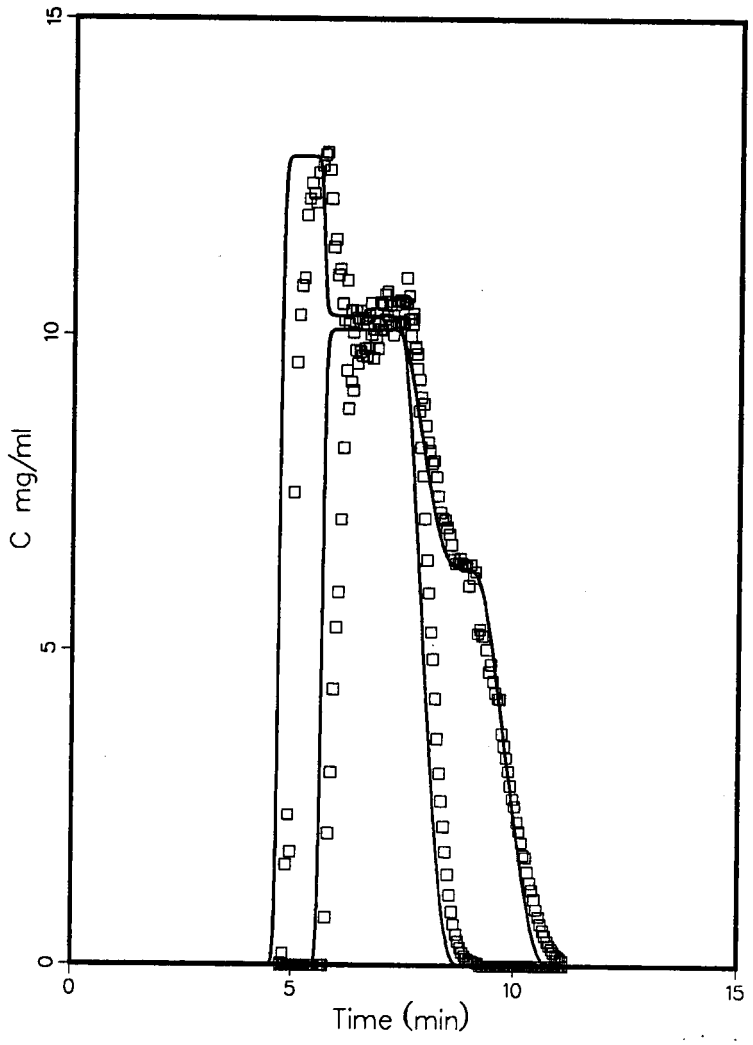
- Theoretical, □ Experimental

Figure 4.20 Hodograph Transform of Experimental Data and Theoretical Predictions from Single Component Isotherm Data



- Theoretical, □ Experimental

Figure 4.21 Best Fit Lines in the Hodograph Space to Experimental Data



- Theoretical, □ Experimental

Figure 4.22 Comparison of Experimental and Predicted Elution Profiles, using Best Fit Langmuir Parameters

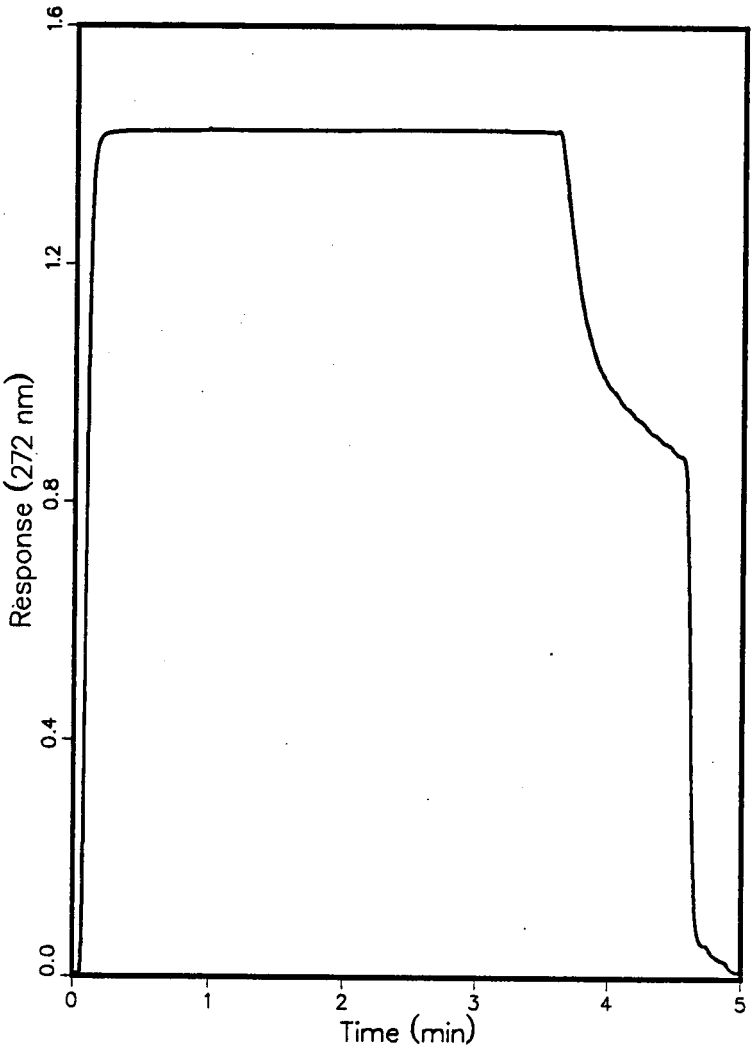
dispersion in the loop due to the poiseuille flow profile. Figure 4.23a shows the detector response to direct injection of pure phenyl-ethanol at high concentration into the detector without a column. Dispersion in the sample loop results in the appearance of a sharp drop in the concentration at 4 minutes. Using a calibration curve, the response curve for pure phenyl-ethanol was converted to Figure 4.23a shows the detector response to direct injection of pure concentration, Figure 4.23b. The true injection profile shows a almost linear decrease in concentration after 4 minutes. In order to predict exactly the elution profiles, this portion of the curve was fit to a curve. Figure 4.23c shows a comparison of the experimental injection profile (symbols) for both components compared to the fitted profile (line). The equation for the profile after 3.25 minutes for phenyl-ethanol and phenyl-propanol are:

$$R1 = -0.37257*t^2 - 0.85*t + 10.3188 \quad (4.3a)$$

$$R2 = -0.37257*t^2 - 0.7*t + 9.2181 \quad (4.3b)$$

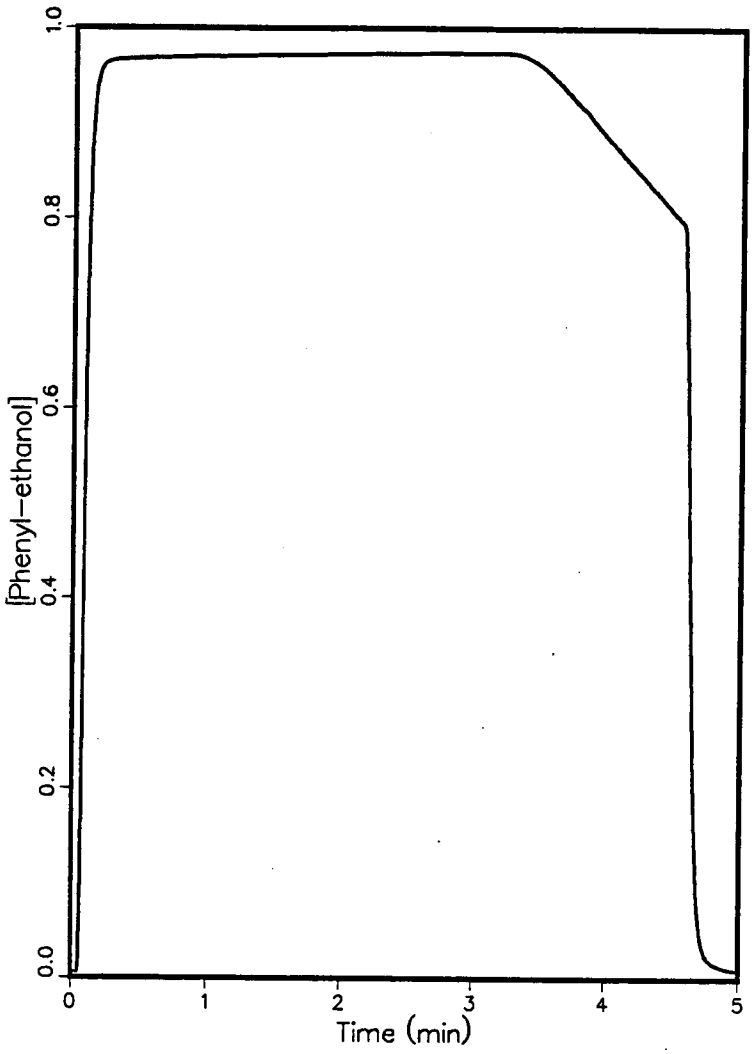
where t for these particular equations is in minutes.

The detector response at the column outlet to a 1/1 non-rectangular injection is shown in Figure 4.24. In contrast to the detector response for the rectangular profile, Figure 4.17, the plateau does not remain horizontal. Collecting and reanalyzing fractions gives the concentration-time chromatogram, Figure 4.25. Taking into account the injection profile, Figure 4.26 shows a comparison of theory with experiment using single component parameters in the competitive Langmuir isotherm model. The front is predicted well, though the shock



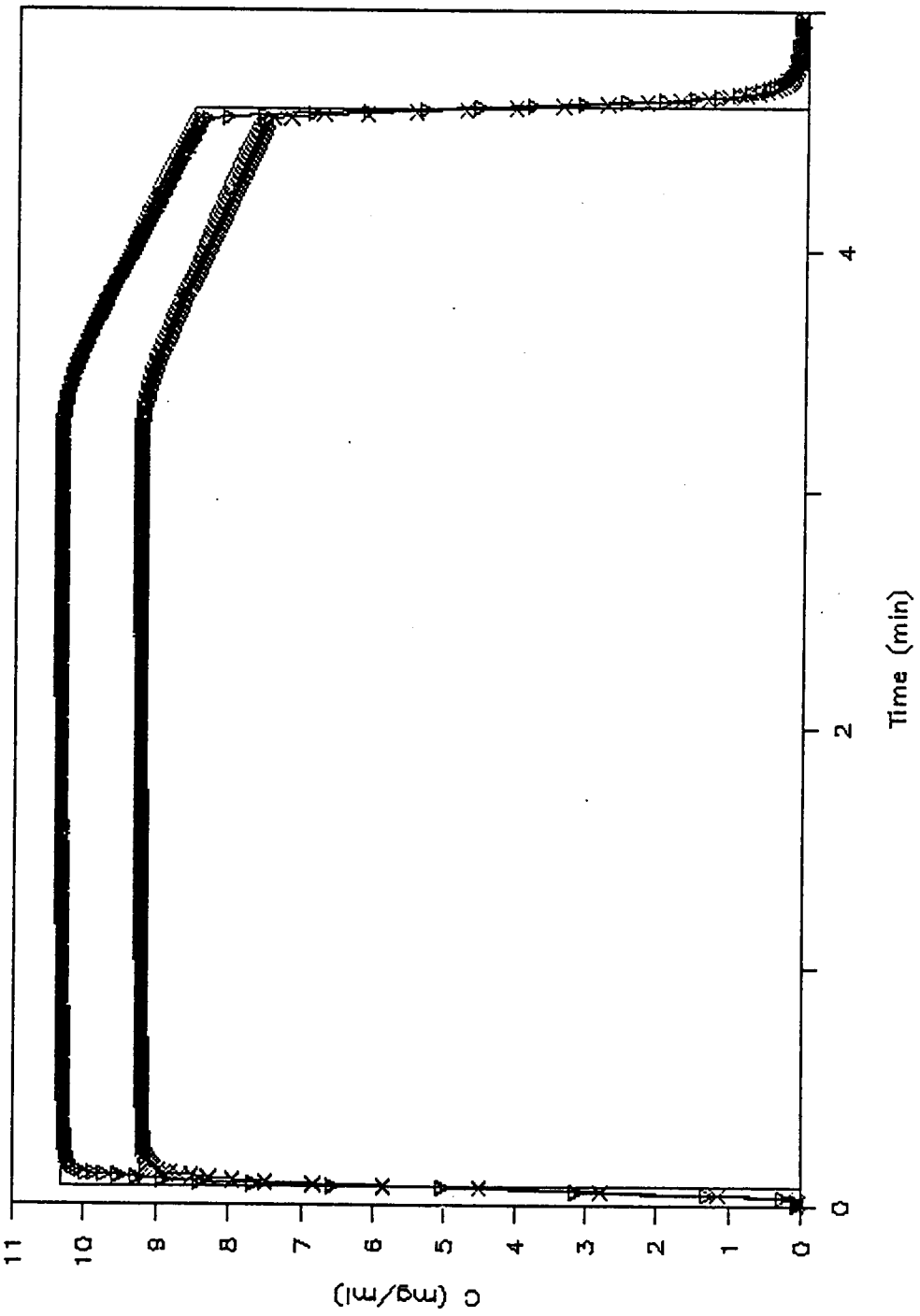
(a) Measured Detector Response

Figure 4.23 Non-Rectangular Injection



(b) Calibrated Response Profile for Non-Rectangular Injection

Figure 4.23 (continued)



(c) Comparison of Calibrated Response Profile and Best Fit Profile for Modeling Injection Function, ▽ Phenyl-ethanol, X Phenyl-propanol

Figure 4.23 (continued)

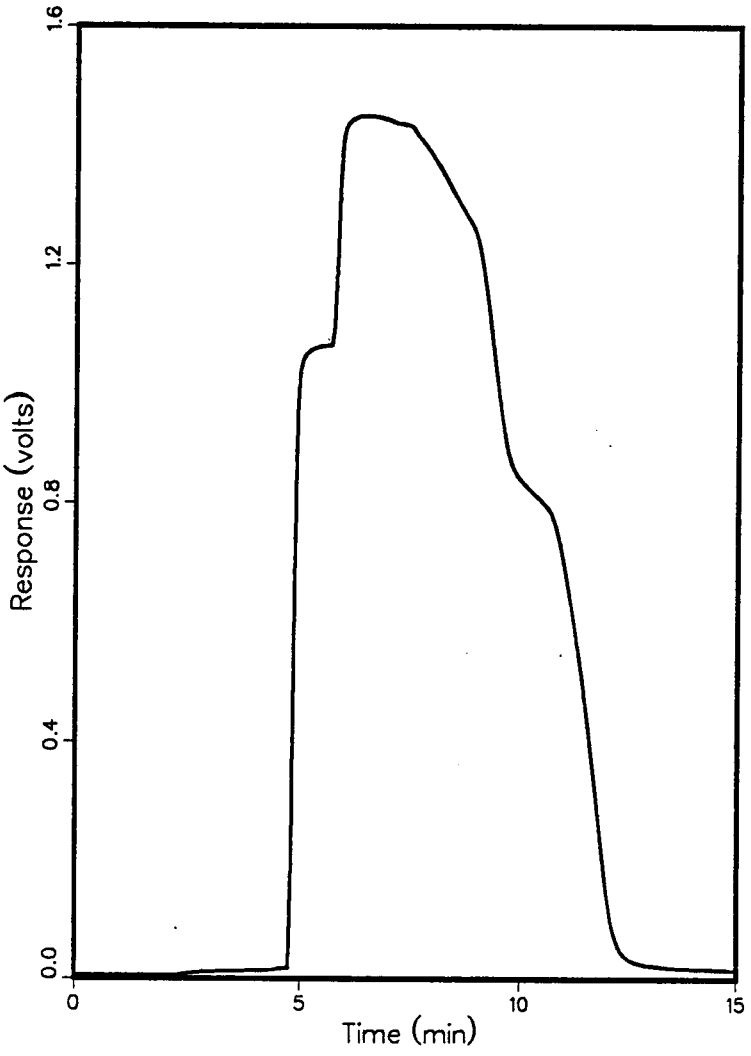
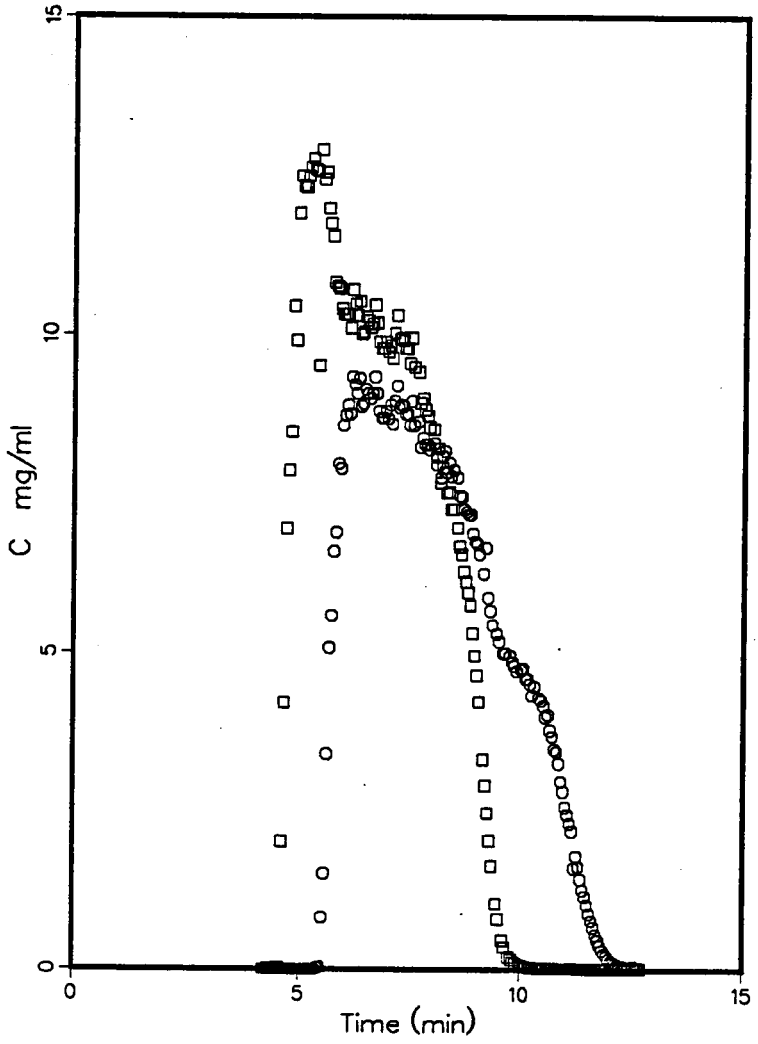
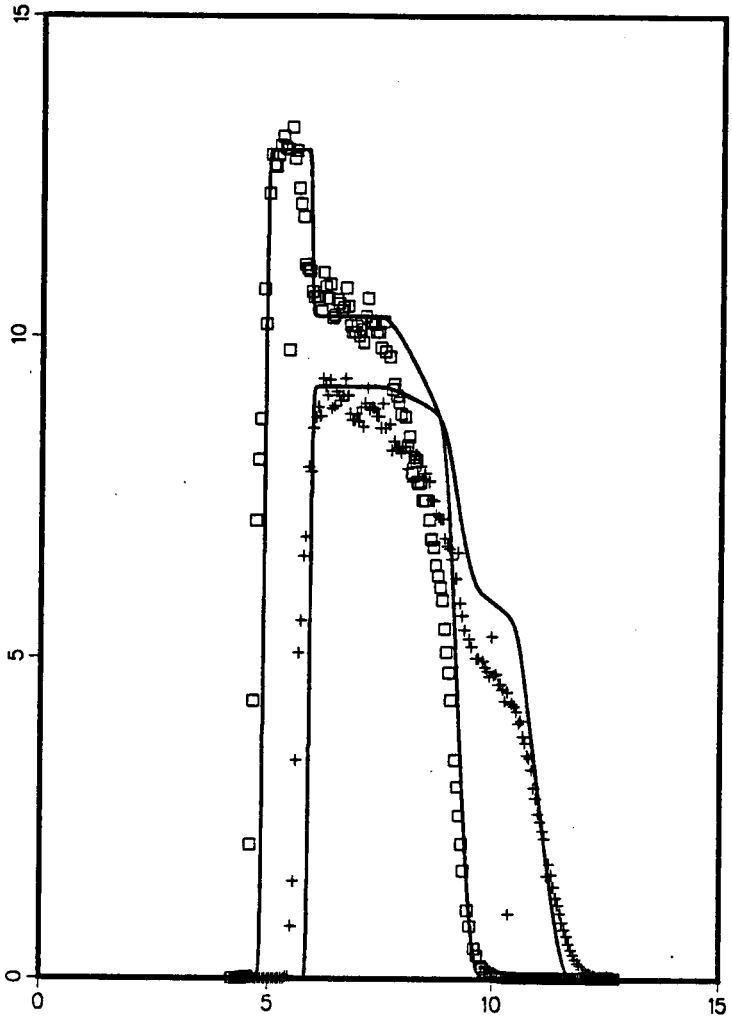


Figure 4.24 Detector Response to a 1/1 Binary Mixture



□ Phenyl-ethanol, o Phenyl-propanol

Figure 4.25 Elution Profile after Fraction Collection, 1/1 Mixture



□ Phenyl-ethanol, + Phenyl-propanol

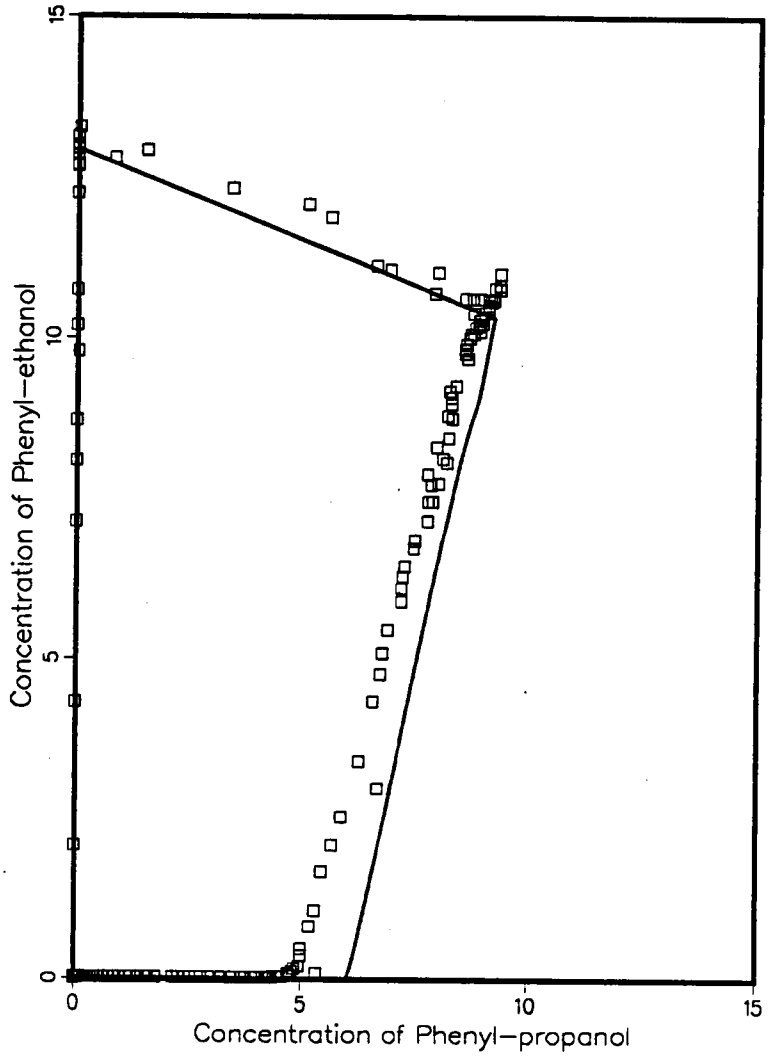
Figure 4.26 Comparison of Experimental and Predicted Elution Profiles, 1/1, using Single Component Data

at the start of the second component is a little more diffuse than predicted. The rear boundary however, is not very well predicted with this isotherm model. This is seen more clearly in the hodograph transform, Figure 4.27, where the line of negative slope fits the data well, however, the line of positive slope corresponding to the rear boundary is systematically deviating from the data. Using a least square fit, Figure 4.28 shows the lines with the best fit values of the Langmuir parameters. Figure 4.29a shows the predicted band profile. The best fit Langmuir parameters give better agreement with the experimental data. The injection profile must be taken into account, use of a rectangular injection of time 4.5 minutes gives significant deviation from the true profile, Figure 4.29b.

The best fit b parameters are $b_{1,h}$= 3.61 ml/mmol to $b_{2,h}$= 3.691 ml/mmol for the 1/1 diffuse injection. These parameters are larger than the single component b parameters and are even larger than for the rectangular 1/1 injection.

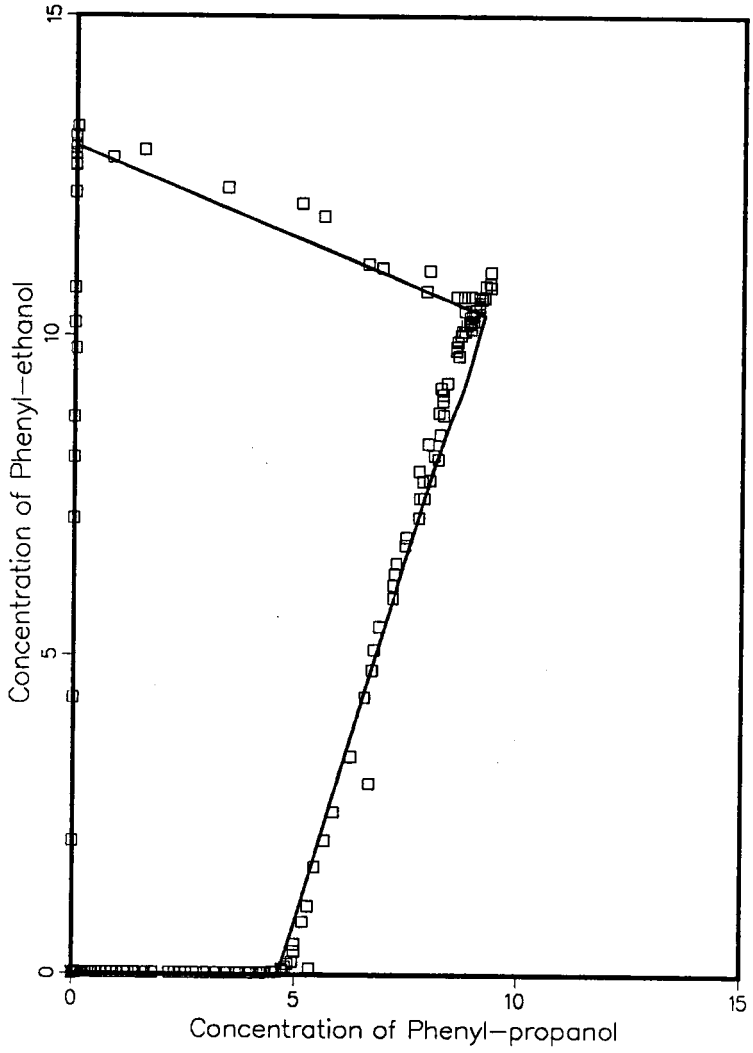
The 1/3 Rectangular Injection

In order to investigate the effect of the composition on the isotherm parameters a 1/3 and 3/1 mixture was studied using a rectangular injection profile. Figure 4.30 shows the detector response at the outlet of the column for two consecutive injections. Reproducibility of the chromatogram is excellent. Fraction collection and reanalysis gives the chromatogram in Figure 4.31. The plateaux is very clear and the errors on reanalysis are small.



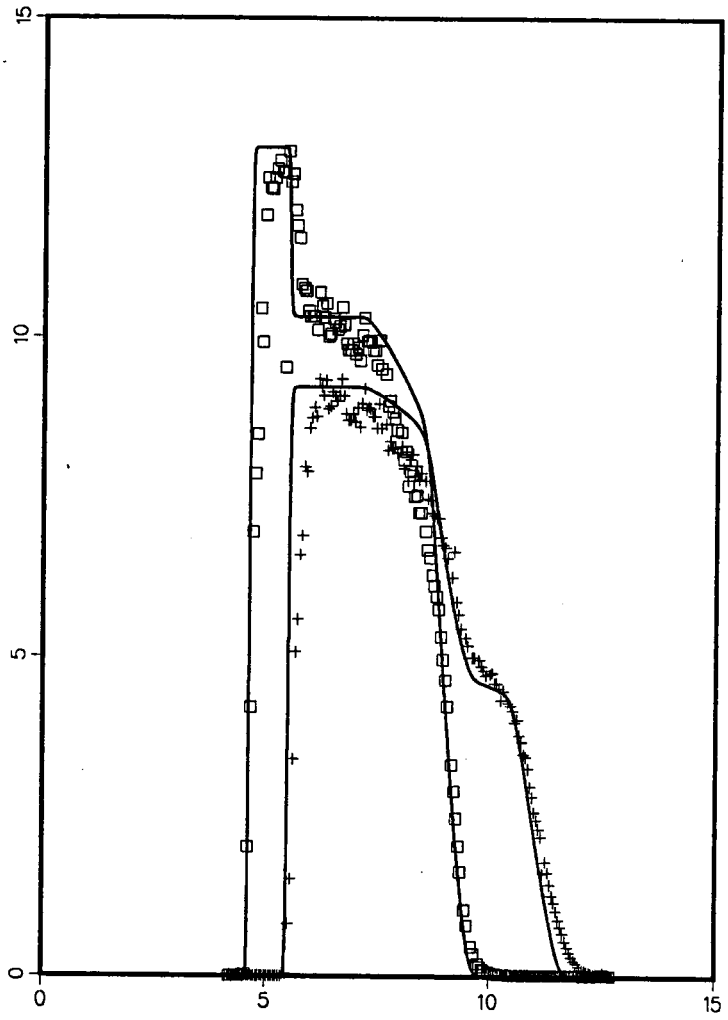
- Theoretical, □ Experimental

Figure 4.27 Hodograph Transform of Experimental Data and Theoretical Predictions from Single Component Isotherm Data



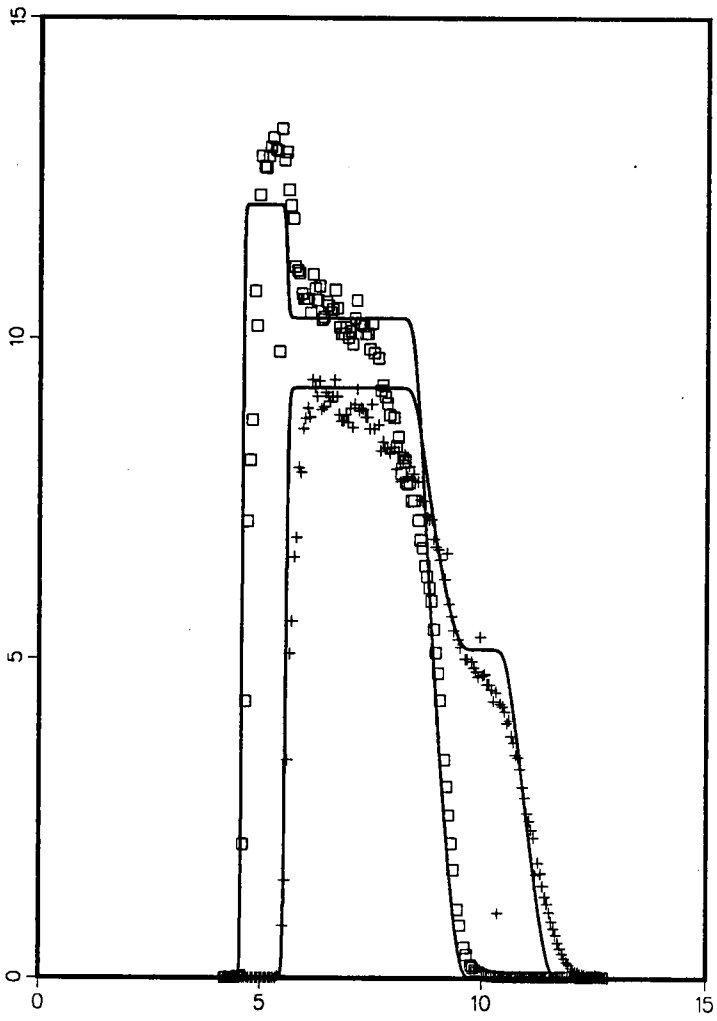
- Theoretical, □ Experimental

Figure 4.28 Best Fit Lines in Hodograph Space to Experimental Data



(a) Non-Rectangular Injection Profile, □ Phenyl-ethanol, + Phenyl-propanol

Figure 4.29 Comparison of Experimental and Predicted Elution Profiles, 1/1, using Best Fit Langmuir Parameters



(b) Rectangular Injection Profile, □ Phenyl-ethanol, + Phenyl-propanol

Figure 4.29 (continued)

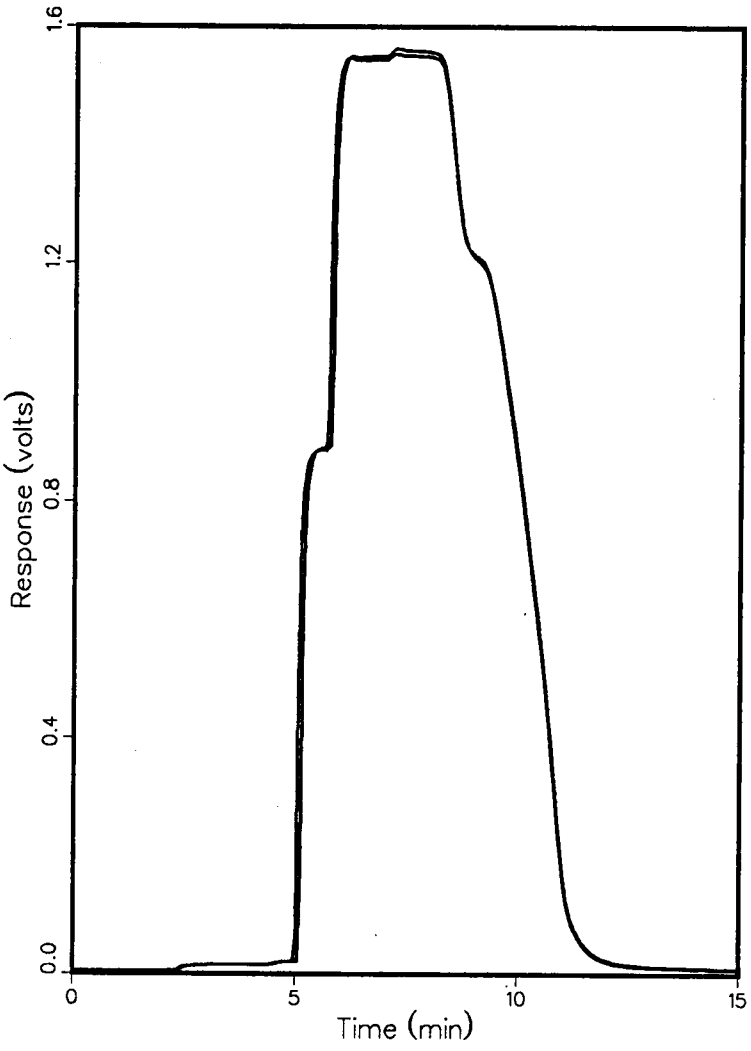
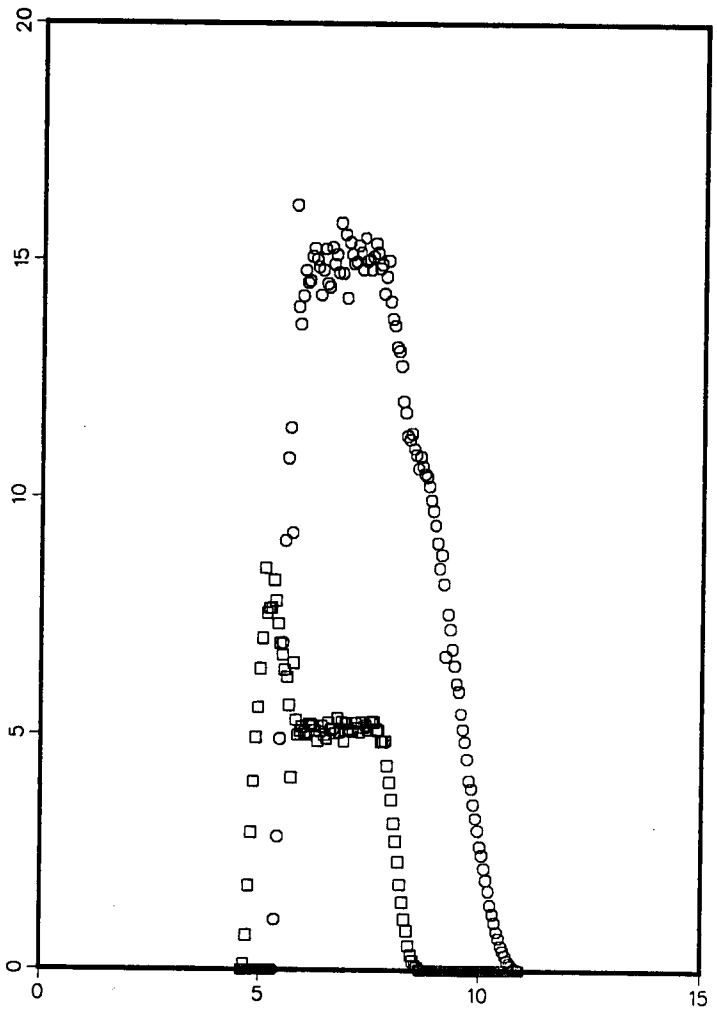


Figure 4.30 Detector Response Curve to a 1/3 Binary Mixture



□ Phenyl-ethanol, o Phenyl-propanol

Figure 4.31 Elution Profile after Fraction Collection, 1/3 Mixture

Figure 4.32 shows a comparison of theory and experiment using single component Langmuir parameters. In general, again, the experimental profile is slightly more diffuse than predicted. The small plateau on the rear boundary corresponding to pure phenylpropanol does not match exactly with the location of the experimental plateau. The Hodograph transform, Figure 4.33, shows systematic deviations on the rear boundary, while the front appears to match very well. Calculating the b parameters according the slope of best fit line in the Hodograph space, Figure 4.34 is obtained. The elution profile with these parameters gives an exact fit, Figure 4.35. The new b parameters are $b_{1,h}$= 2.732 to $b_{2,h}$= 4.041 ml/mmol.

The 3/1 Rectangular Injection

The last set of experiments were done with a 3/1 mixture. The detector response at the column outlet is given in Figure 4.36. This profile is characteristic of the two component large volume experiments. The differences in the profile with changing composition is the height of the pure first component plateau. At 10 minutes, the first component elutes from the column giving rise to a short plateaux for the second component. Clearly, this concentration is much lower for the 3/1 mixture in contrast to the 1/3 mixture. The elution profile after evaluation of the fractions is given in Figure 4.37. A comparison of theory and experiment using single component Langmuir parameters in the competitive Langmuir model is shown in Figure 4.38. Excellent agreement is obtained on the fronts of both components. The difficulty again comes in the prediction of the "plateau" on the rear

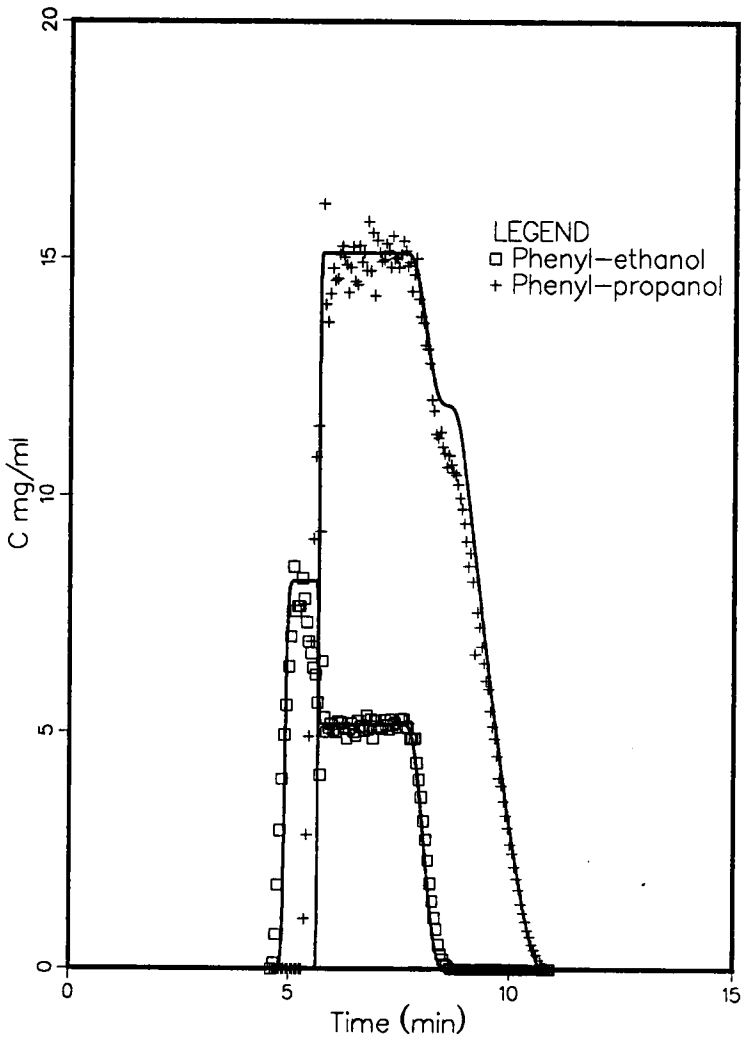
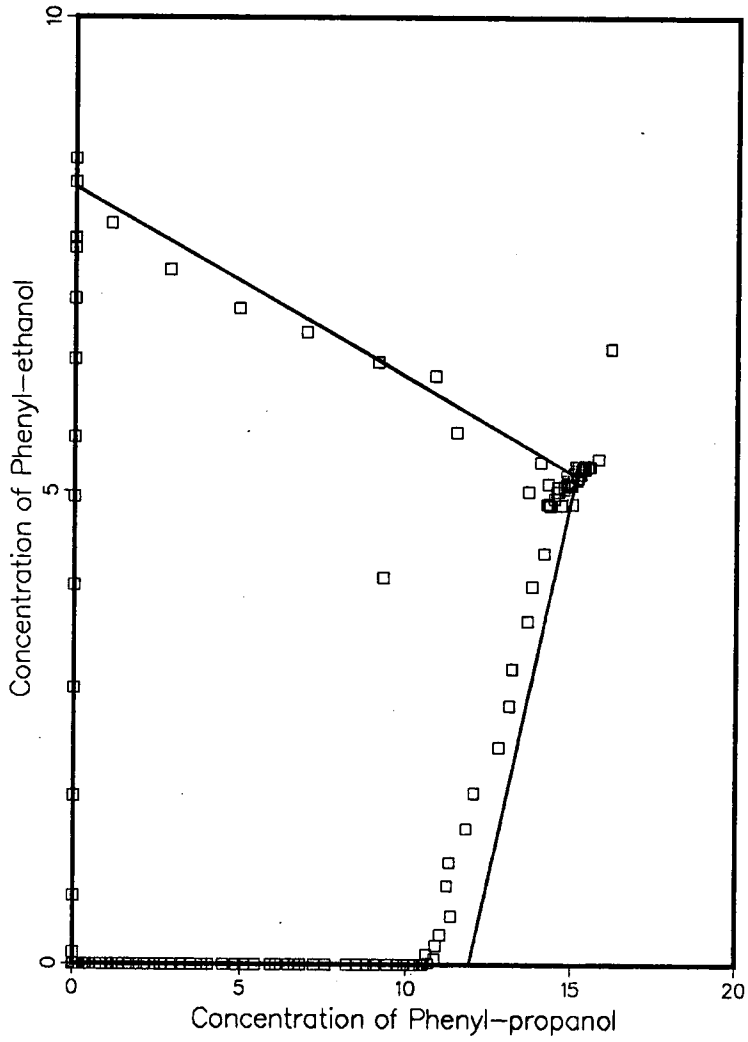
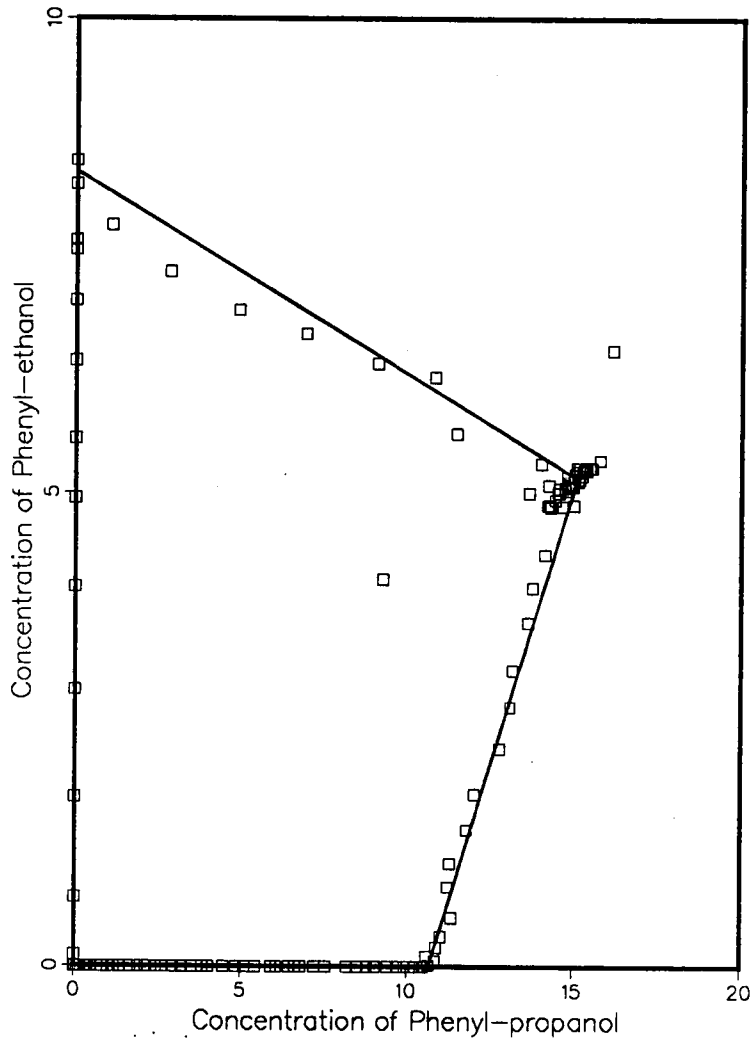


Figure 4.32 Comparison of Experimental and Predicted Elution Profiles, 1/3, using Single Component Isotherm Data



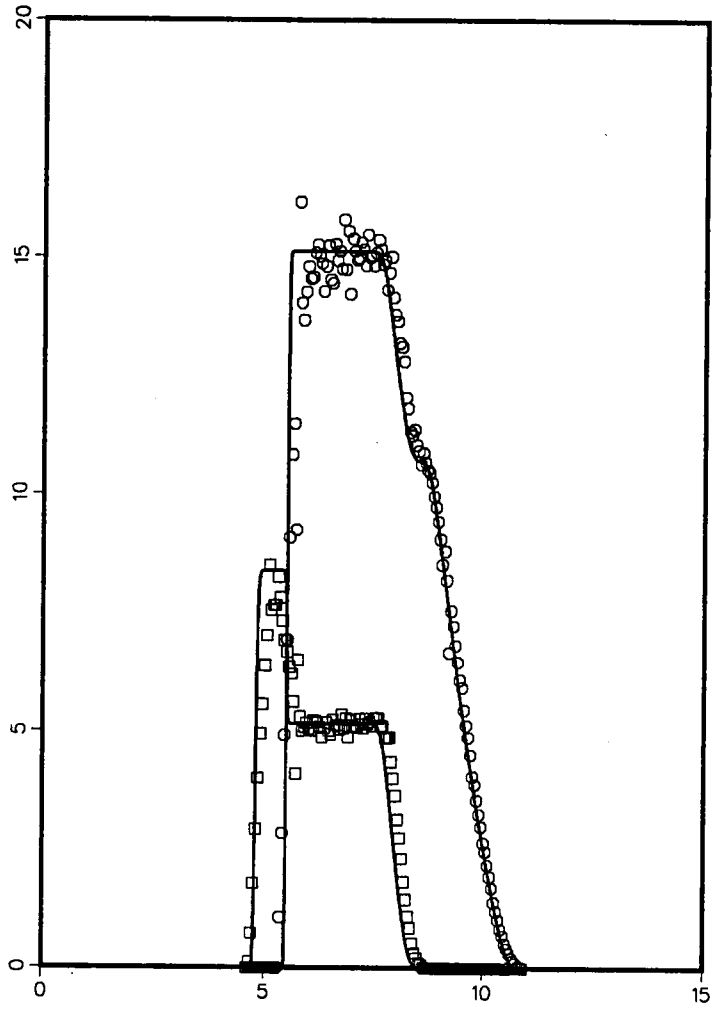
- Theoretical, □ Experimental

Figure 4.33 Hodograph Transform of Experimental data and Theoretical Predictions from Single Component Isotherm Data



- Theoretical, □ Experimental

Figure 4.34 Best Fit Lines to Experimental Data in Hodograph Space



□ Phenyl-ethanol, o Phenyl-propanol

Figure 4.35 Comparison of Experimental and Predicted Elution Profiles, 1/3, using Best Fit Langmuir Parameters

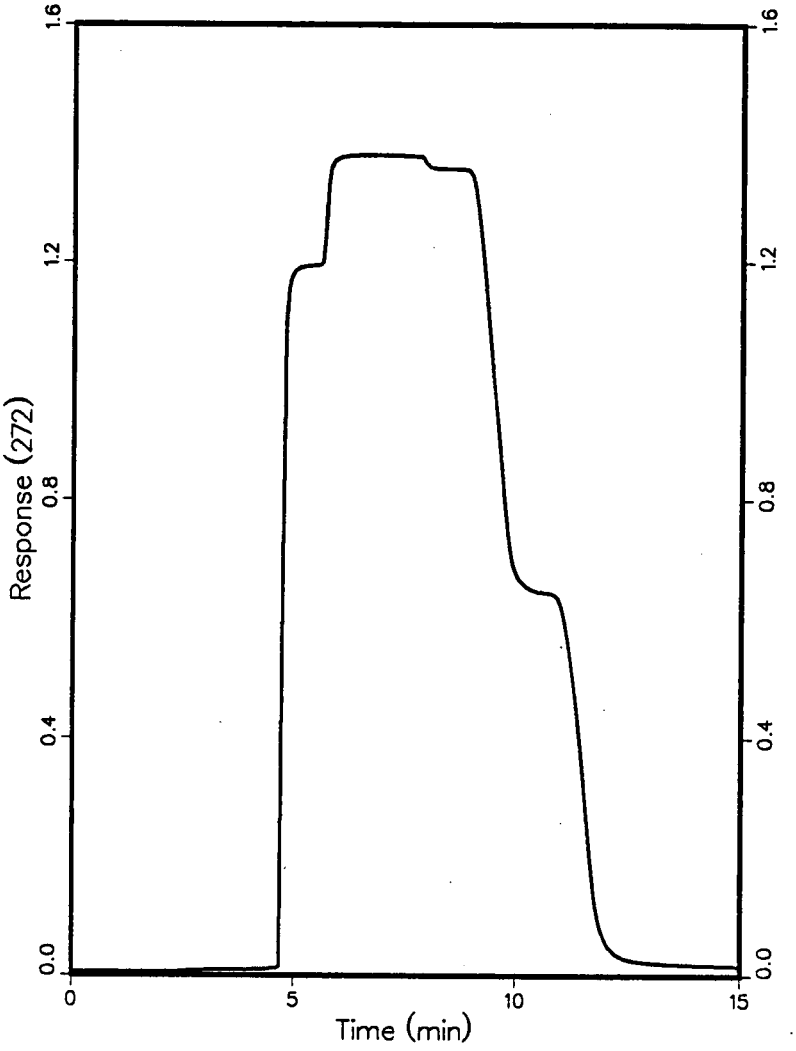


Figure 4.36 Detector Response Curve to a 3/1 Binary Mixture

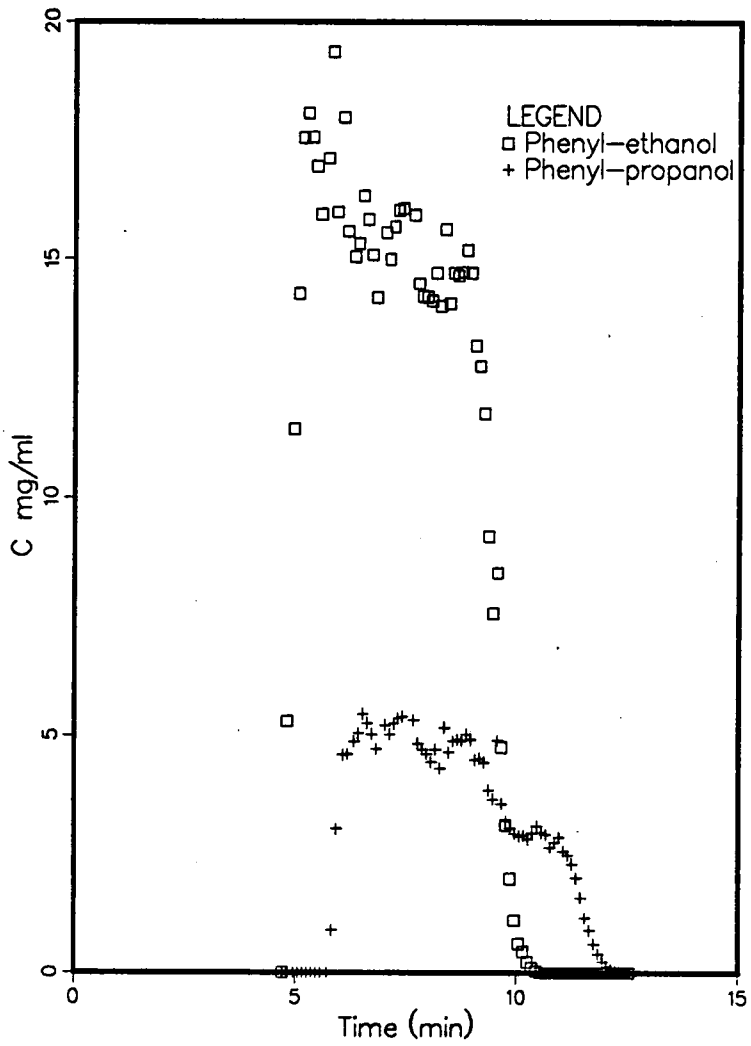


Figure 4.37 Elution Profile after Fraction Collection, 3/1 Mixture

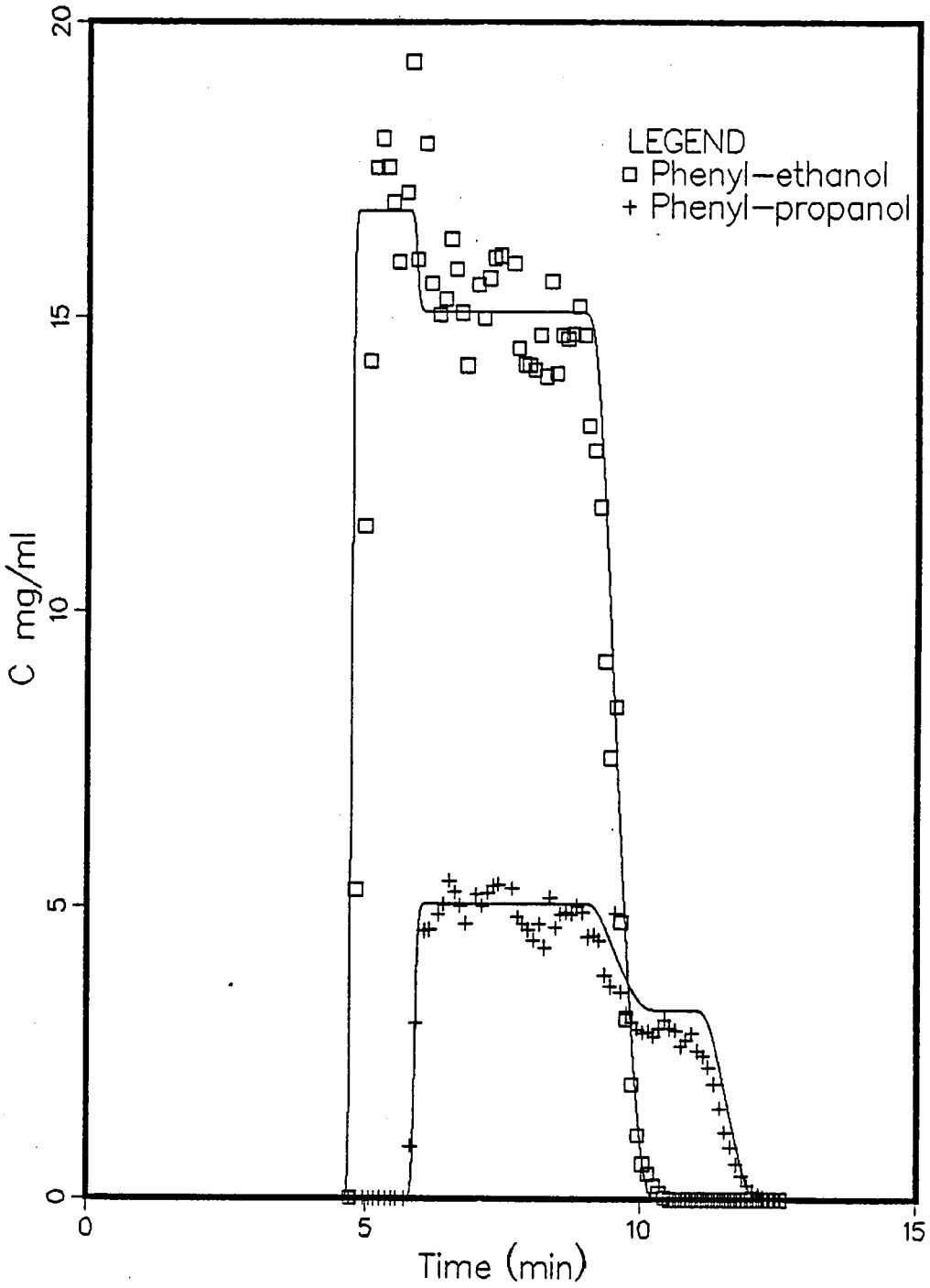


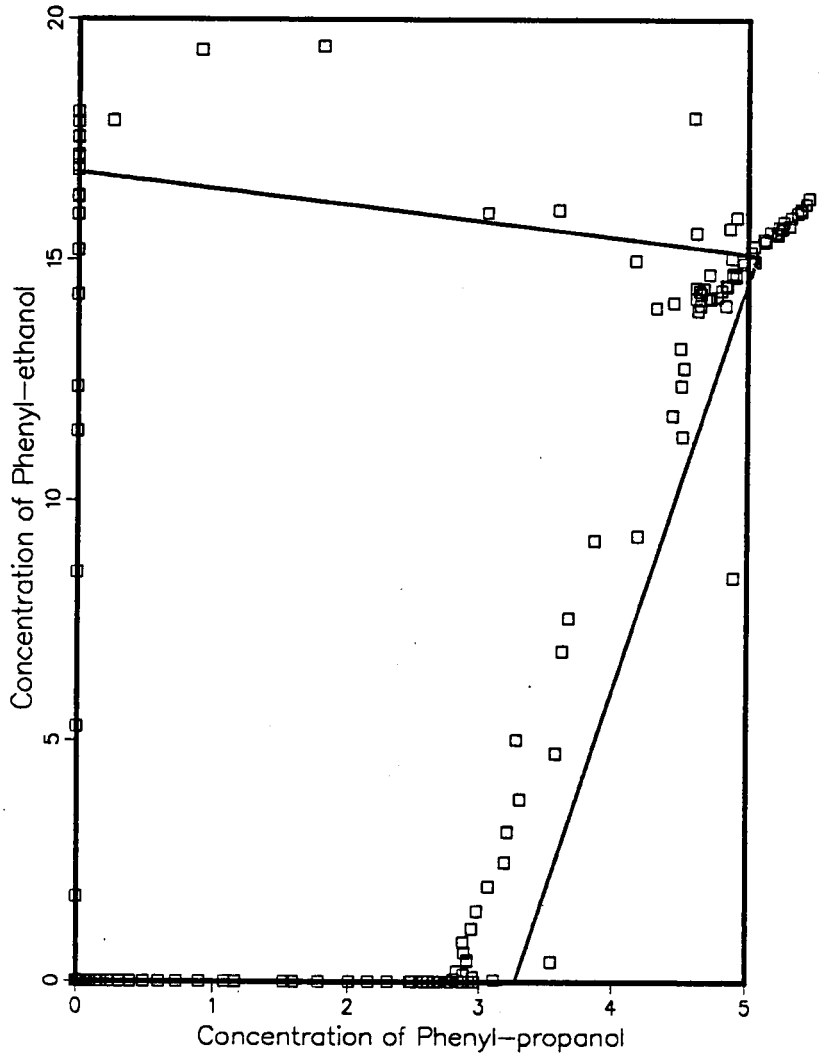
Figure 4.38 Comparison of Experimental and Predicted Elution Profiles, 3/1, using Single Component Isotherm Data

boundary when the first component concentration goes to zero. There is more scatter in this experimental data than the others. The hodograph transform gives an approximate, but does not exactly fit to the data, Figure 4.39. The best fit straight line are shown in Figure 4.40. The elution profile based on these new parameters is given in Figure 4.41. The b parameters obtained for this data $b_{1,h}$= 3.2517 and $b_{2,h}$= 4.052.

The average b value calculated from Table 4.2 was $b_{1,h}$= 3.044 +- 0.43 and $b_{2,h}$= 3.69 +- 0.27 ml/mmol. These average b values fit the experimental data under all the conditions well in both the elution, Figure 4.42a-d and Hodograph space, Figure 4.43a-d. These values will be used to reevaluate the overloaded elution data in Section 4.3. The next subsection is an aside on the use of other models to predict the large volume elution data.

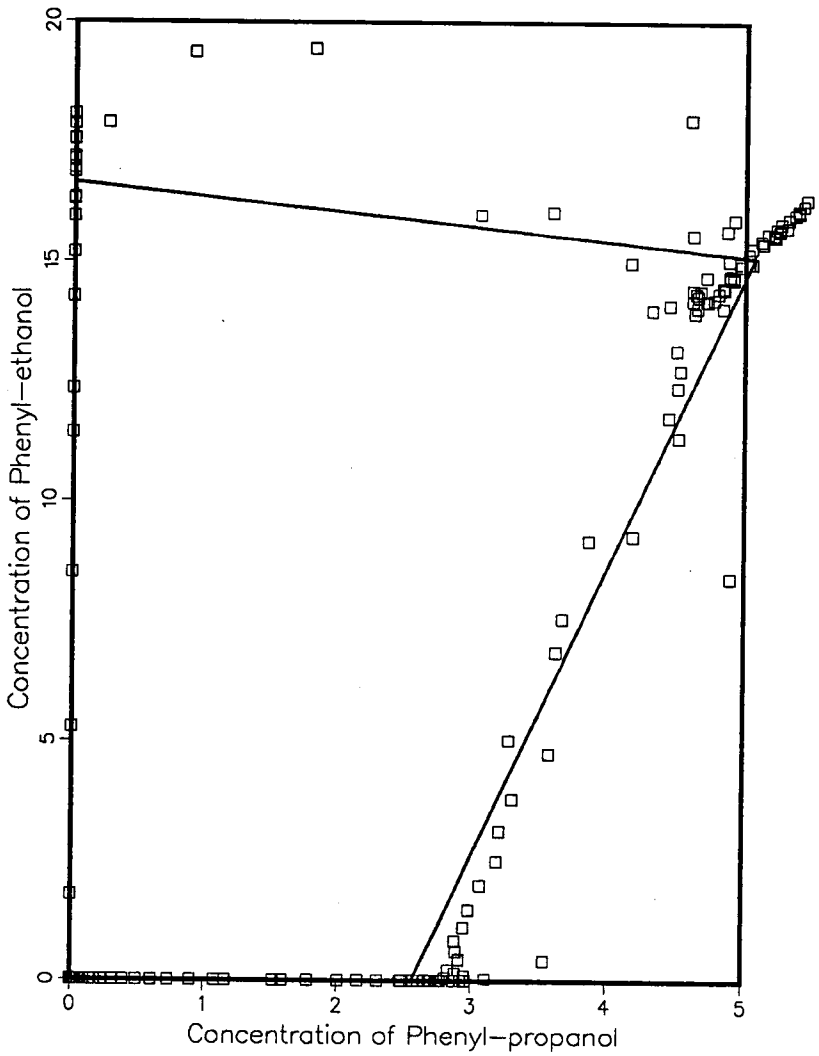
Kinetic Models

The theoretical analysis thus far used the semi-ideal model of chromatography. However, the scheme employed propagates errors according to the finite difference scheme. For comparison another finite difference scheme, Lax-Wendroff, was used with a kinetic and dispersive term. A large kinetic parameter was used so that equilibrium was assumed and the dispersion term was adjusted to give a 500 plate column. The best fit b parameters are used in the equilibrium isotherm. The advantage of this scheme is that errors are of the order dz squared. The band broadening due to the numerical scheme is small. The disadvantage of this scheme is that it is more



- Theoretical, □ Experimental

Figure 4.39 Hodograph Transform of Experimental Data and Theoretical Predictions from Single Component Isotherm Data



- Theoretical, □ Experimental

Figure 4.40 Best Fit Lines to Experimental Data in Hodograph Space

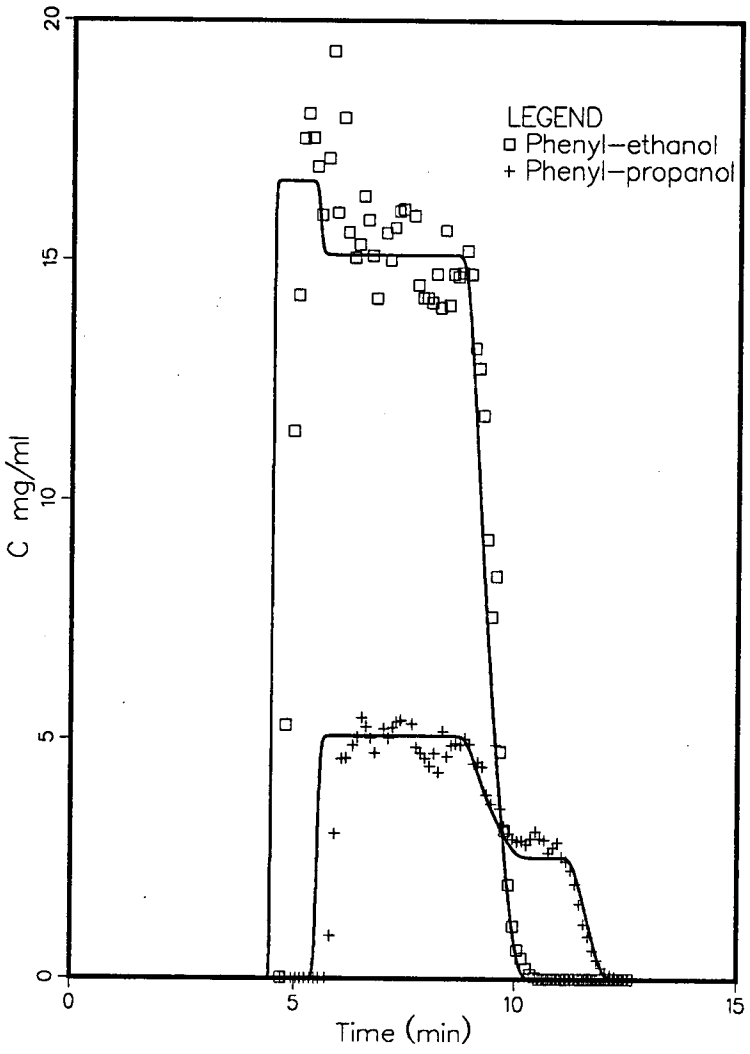
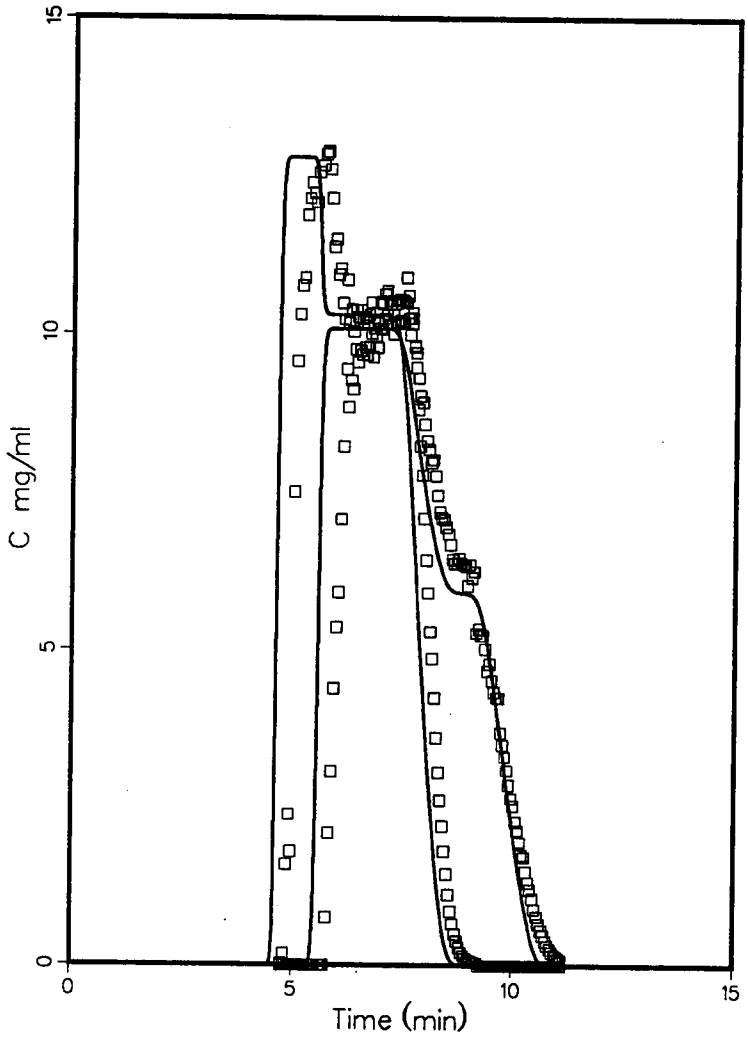
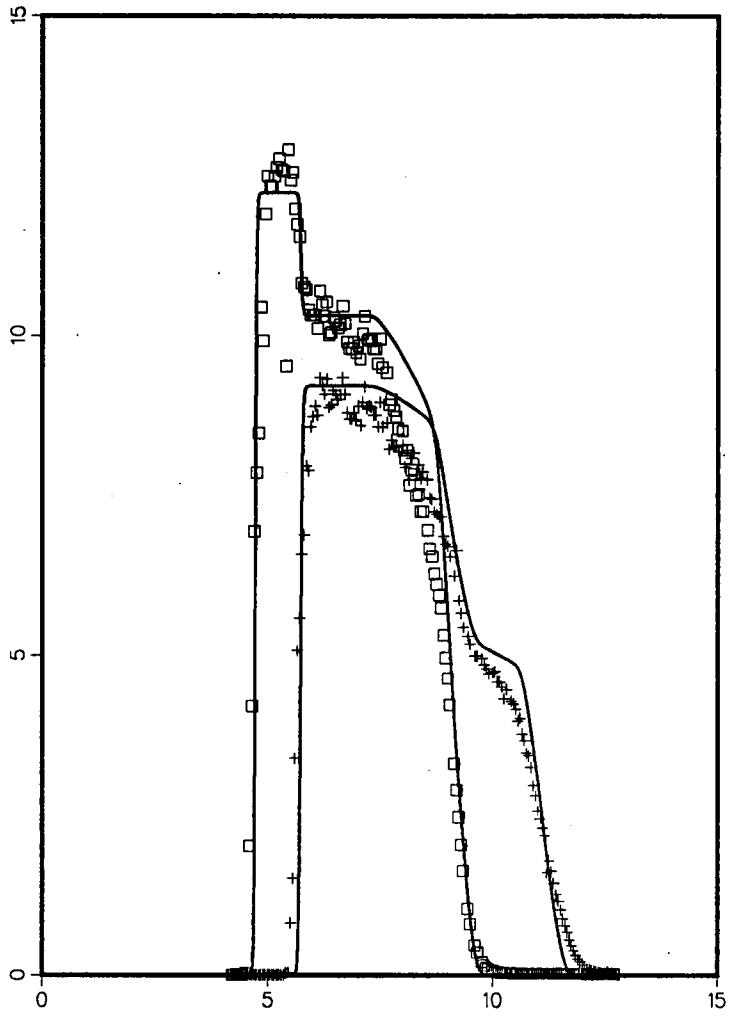


Figure 4.41 Comparison of Experimental and Predicted Theoretical Elution Profiles, 3/1, using Best Fit Langmuir Parameters



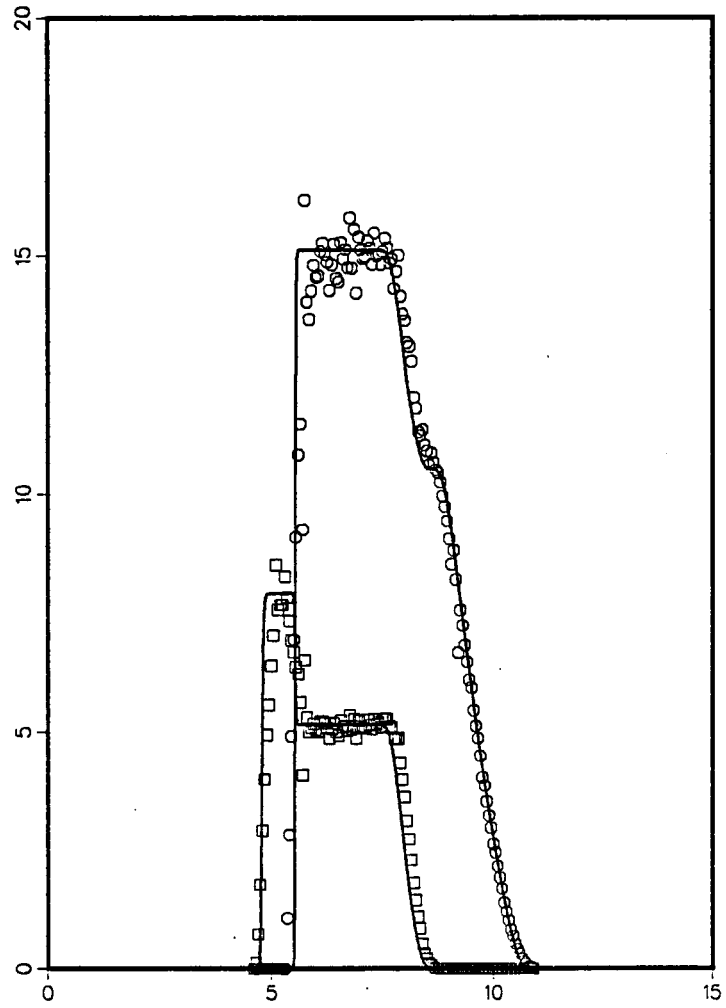
(a) 1/1 Rectangular Injection, - Theoretical, □ Experimental

Figure 4.42 Comparison of Experimental and Predicted Elution Profiles using Average Hodograph Parameters



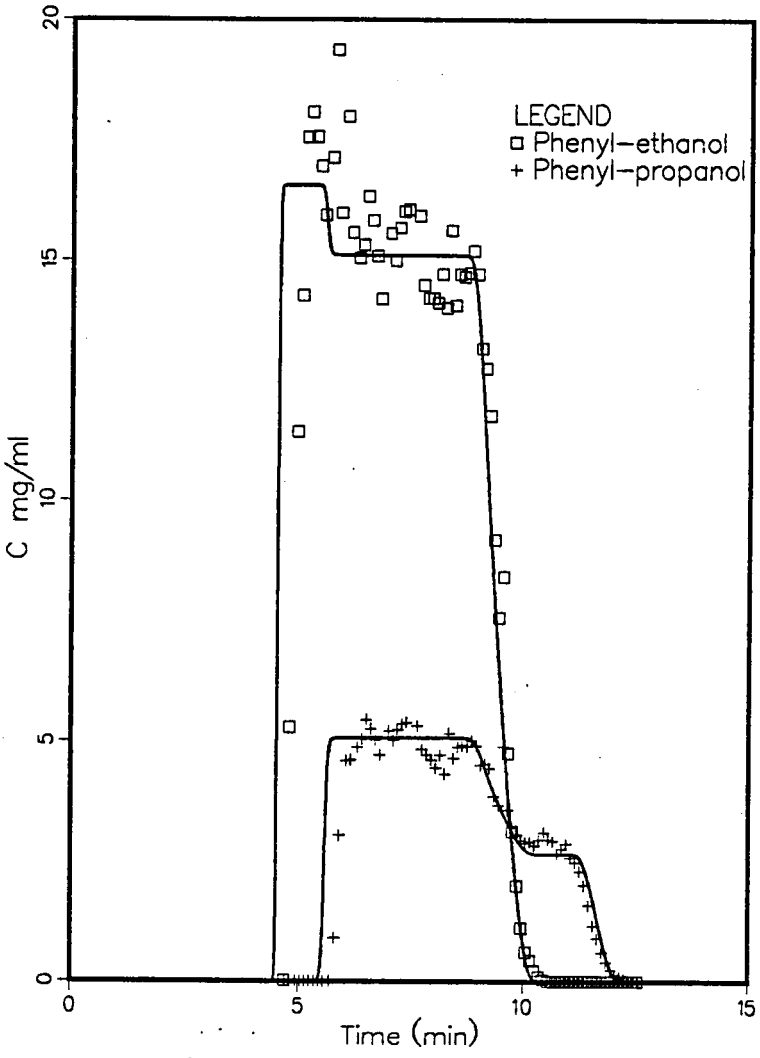
(b) 1/1 Diffuse Injection, - Theoretical, □ Phenyl-ethanol
+ Phenyl-propanol

Figure 4.42 (continued)



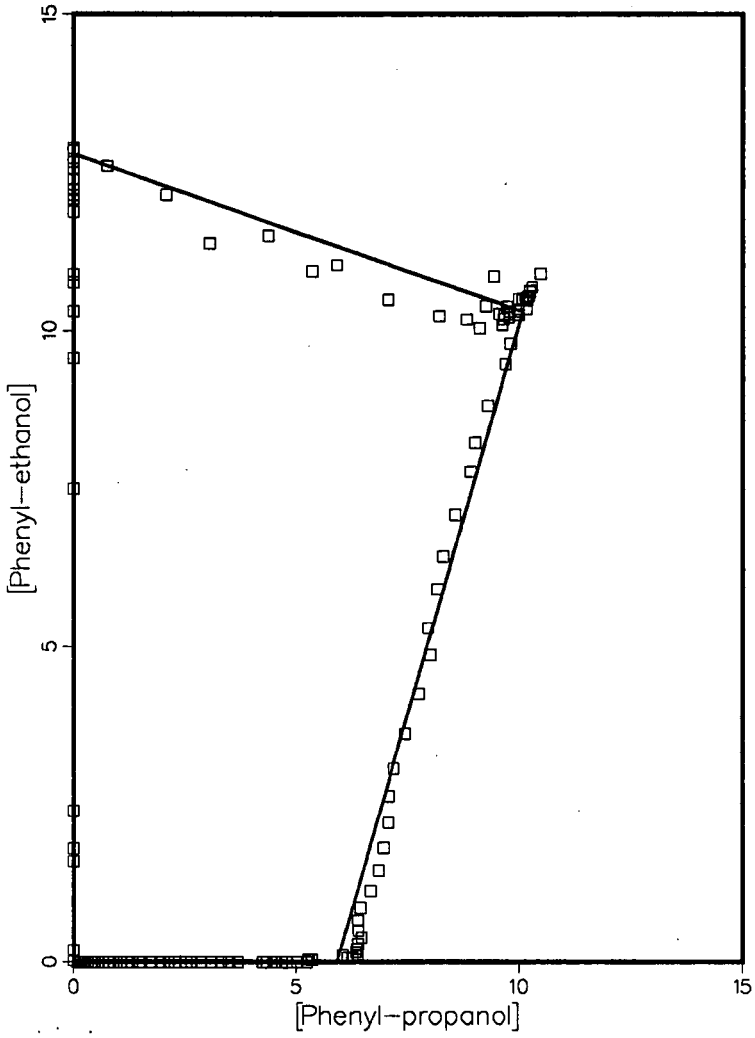
(c) 1/3 Mixture, - Theoretical, □ Phenyl-ethanol, o Phenyl-propanol

Figure 4.42 (continued)



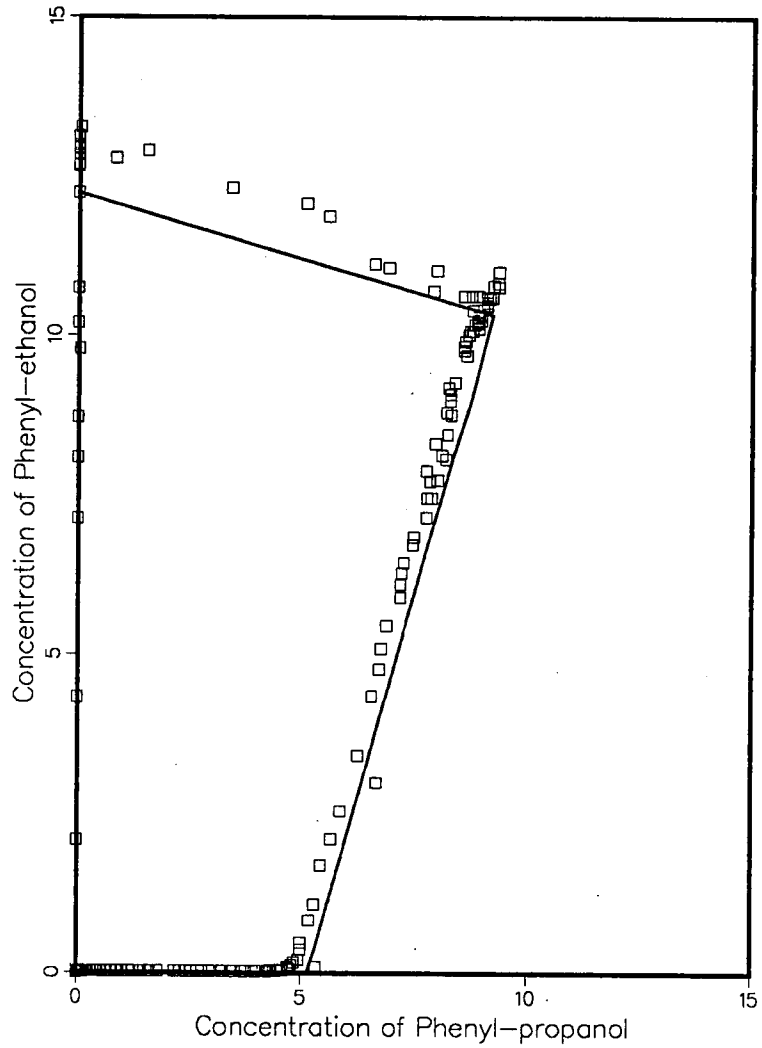
(d) 3/1 Mixture

Figure 4.42 (continued)



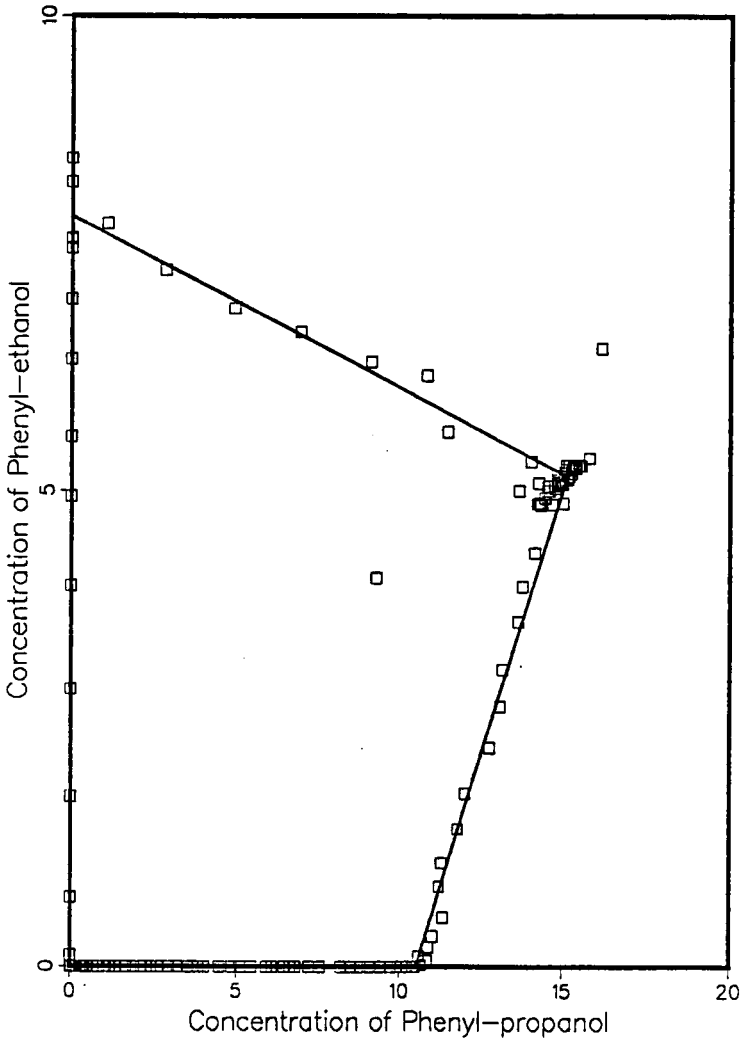
(a) 1/1 Rectangular Injection, - Theoretical, □ Experimental

Figure 4.43 Hodograph Transform of Experimental Data and Theoretical Predictions from Average Hodograph Parameters



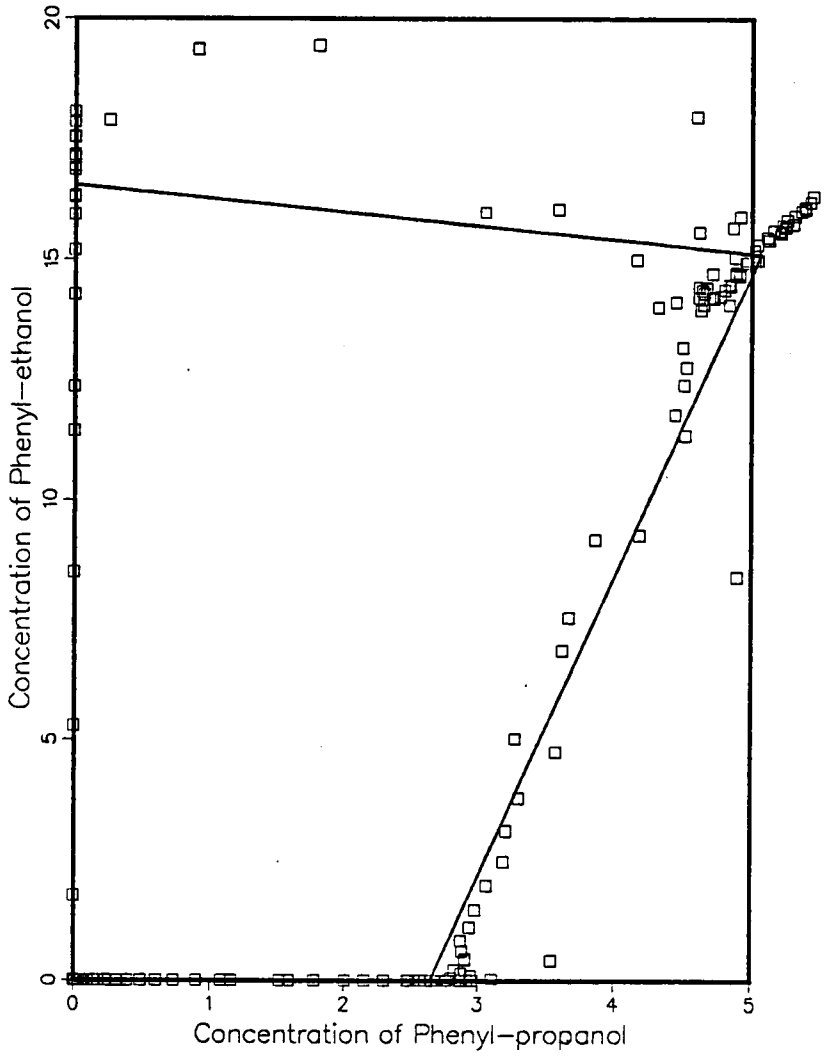
(b) 1/1 Diffuse Injection

Figure 4.43 (continued)



(c) 1/3 Mixture

Figure 4.43 (continued)



(d) 3/1 Mixture

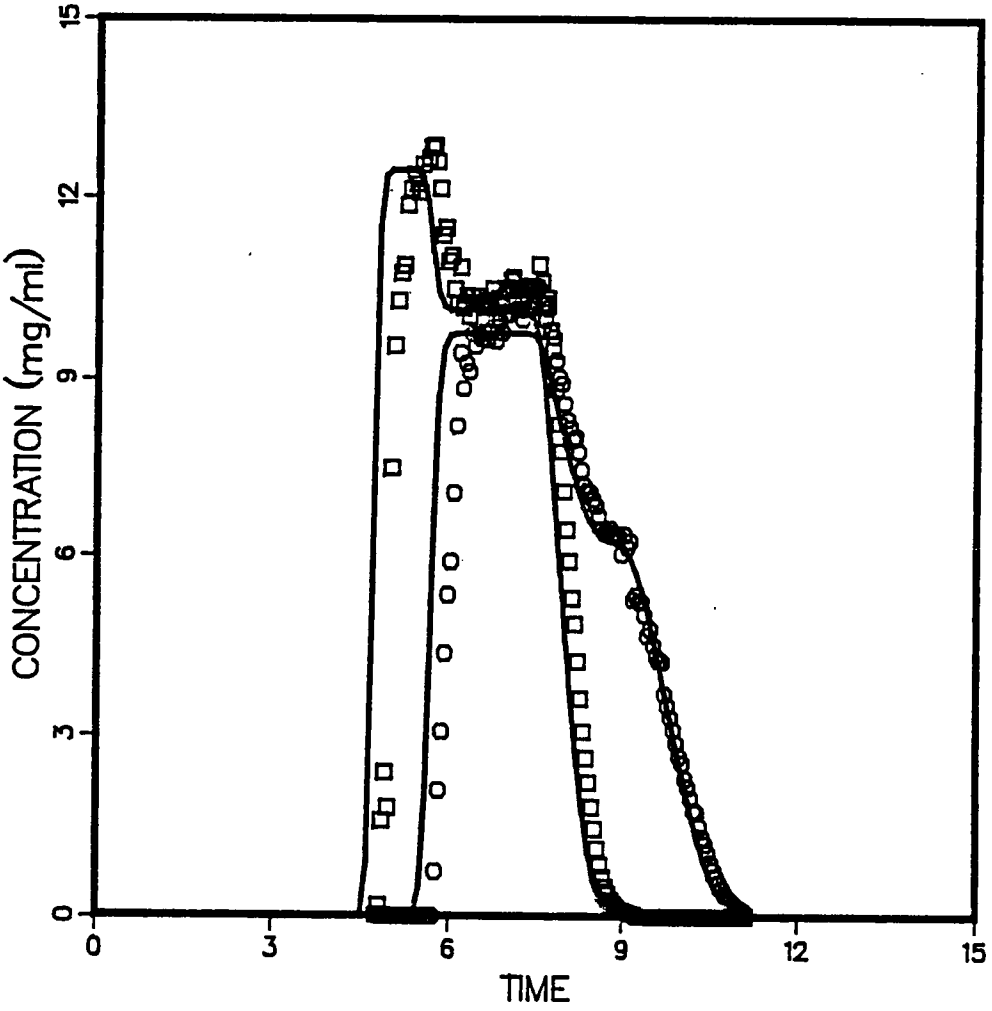
Figure 4.43 (continued)

difficult to get a stable solution and the computation time is larger than with the semi-ideal model. A comparison between theory and experimental data for the 1/1 rectangular injection is shown in Figure 4.44. The theoretical fronts are generally less sharp than that predicted by the semi-ideal model (Figure 4.22) and the shape of the rear boundary profile follows more exactly the true curvature. Similarly, the 1/1 non-rectangular injection, Figure 4.45, gives curved edges which conform to the data more closely; especially in the region where the first component is enhanced in concentration. The shape of the injection profile must be considered. Assuming a rectangular profile, Figure 4.46, the predicted curve deviates from the experimental results where the injection profile becomes non-rectangular. For a 1/3 mixture, Figure 4.47 the kinetic model gives an excellent fit in all regions of the curve.

Using only the kinetic model, no dispersion term, the kinetic parameter was adjusted to give an HETP of 0.01 cm (2500 plates) at infinite dilution for the 1/1 rectangular, Figure 4.48, 1/3, Figure 4.49 and 3/1, Figure 4.50 mixtures. Unlike the previous models, very sharp rectangular corners are predicted. Otherwise, the agreement is good. This model approaches closely the ideal model of chromatography.

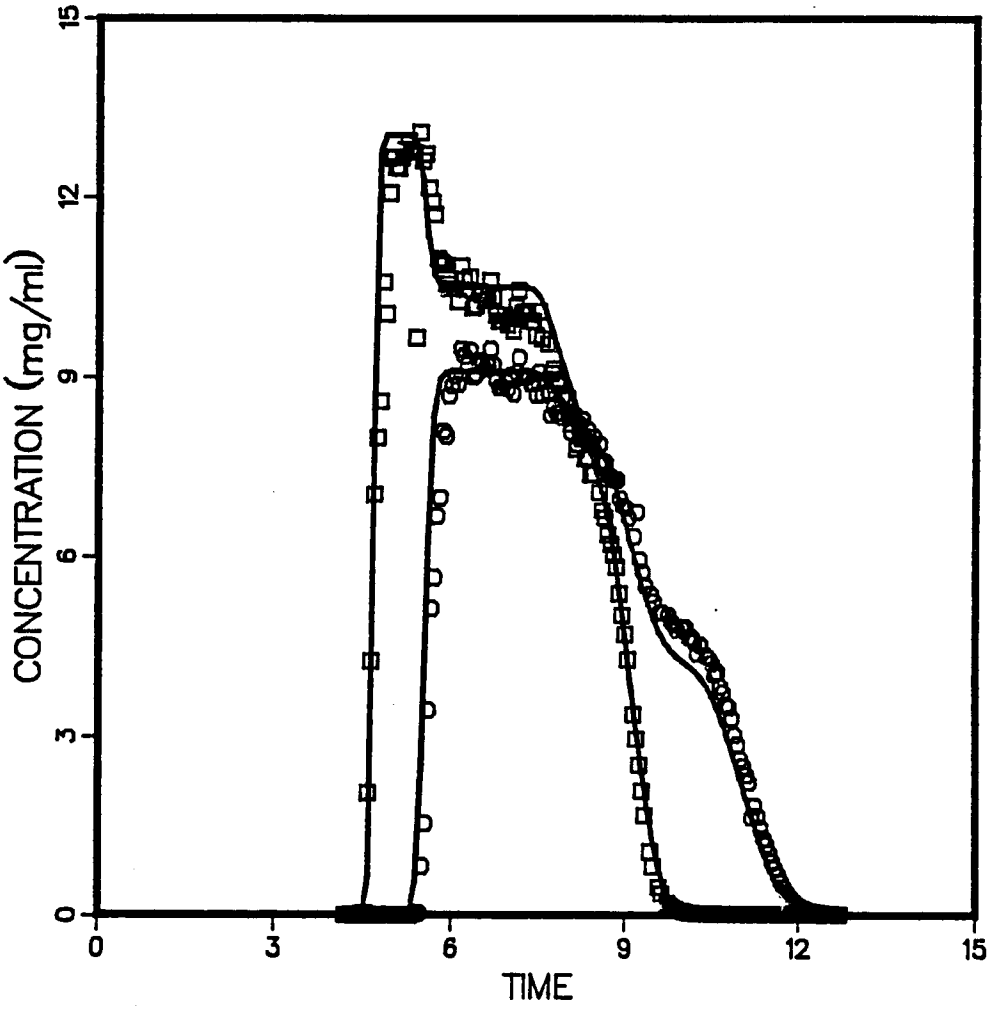
4.3 Reevaluation of Overloaded Elution Data: Best Fit Langmuir Parameters

The b parameter for all the compositions studied was averaged and used to reevaluate the overloaded elution data taken earlier.



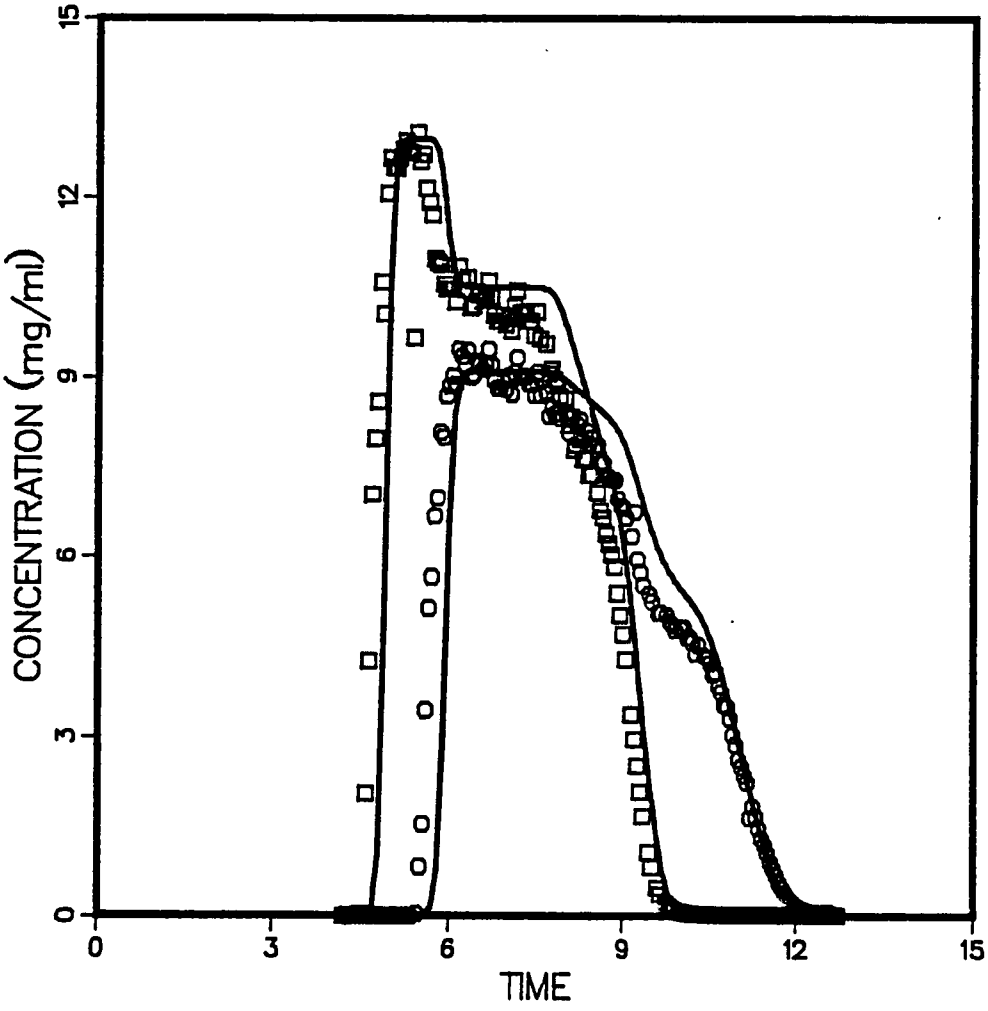
- Theoretical, □ Phenyl-ethanol, o Phenyl-propanol

Figure 4.44 Comparison of Experimental and Theoretical Elution Profiles using Dispersion and Kinetic Model, 1/1, Rectangular Injection



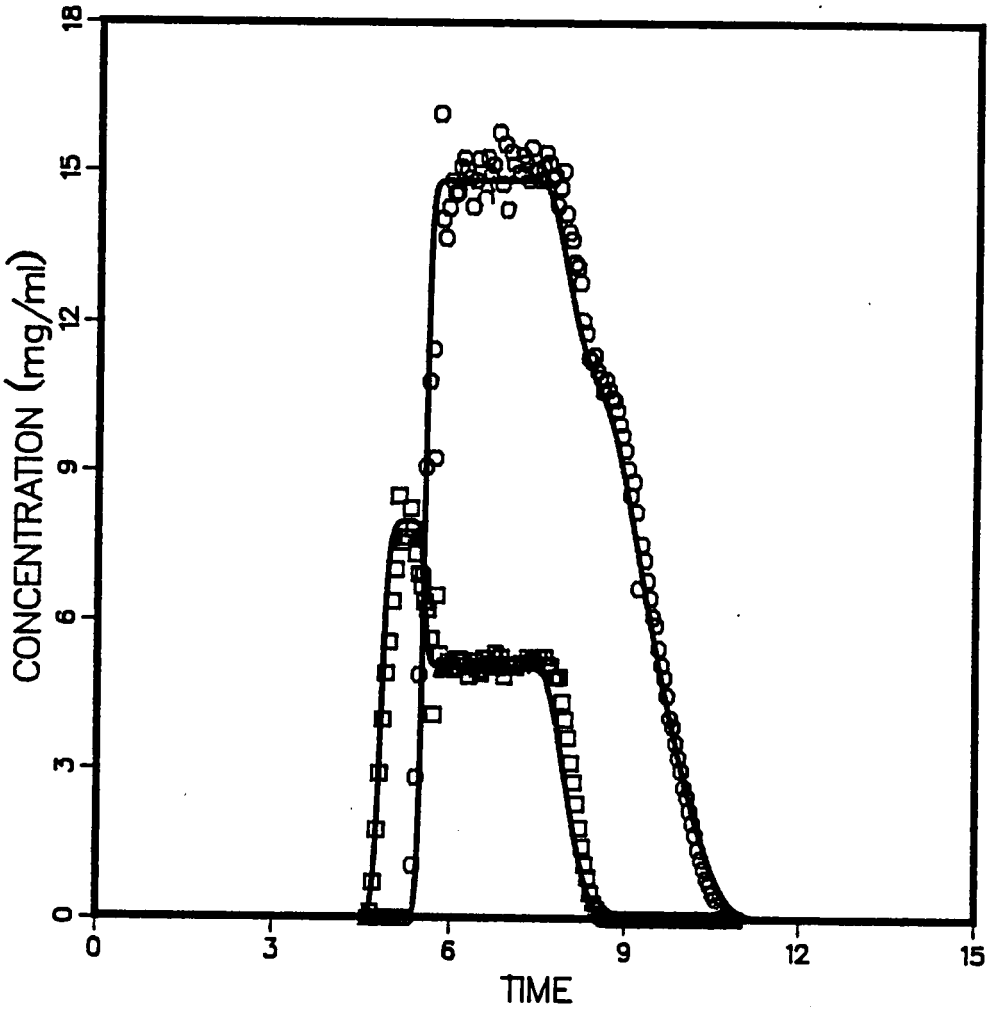
- Theoretical, □ Phenyl-ethanol, o Phenyl-propanol

Figure 4.45 Comparison of Experimental and Theoretical Elution Profiles using Dispersion and Kinetic Model, 1/1 Non-Rectangular Injection



- Theoretical, □ Phenyl-ethanol, o Phenyl-propanol

Figure 4.46 Comparison of Experimental and Theoretical Elution Profiles using Dispersion and Kinetic Model, 1/3, Rectangular Injection



- Theoretical, □ Phenyl-ethanol, o Phenyl-propanol

Figure 4.47 Comparison of Experimental and Theoretical Elution Profiles using Kinetic Model, 1/1, Rectangular Injection

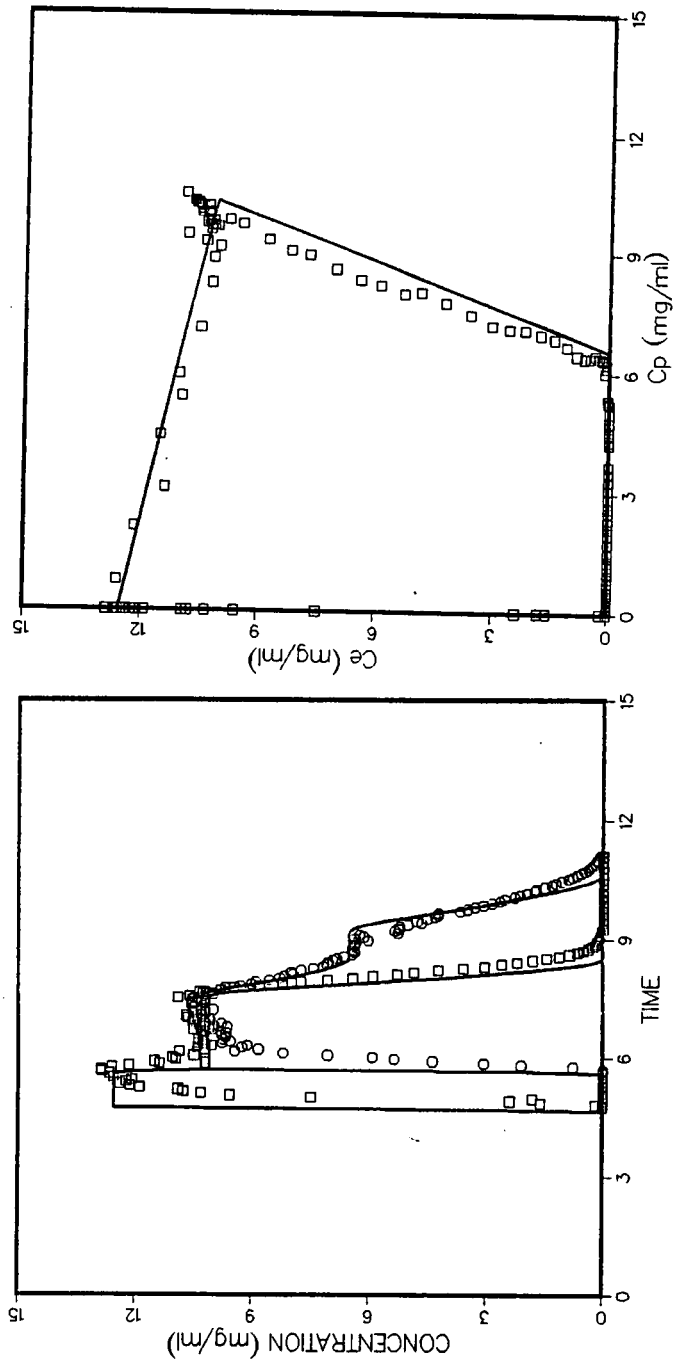
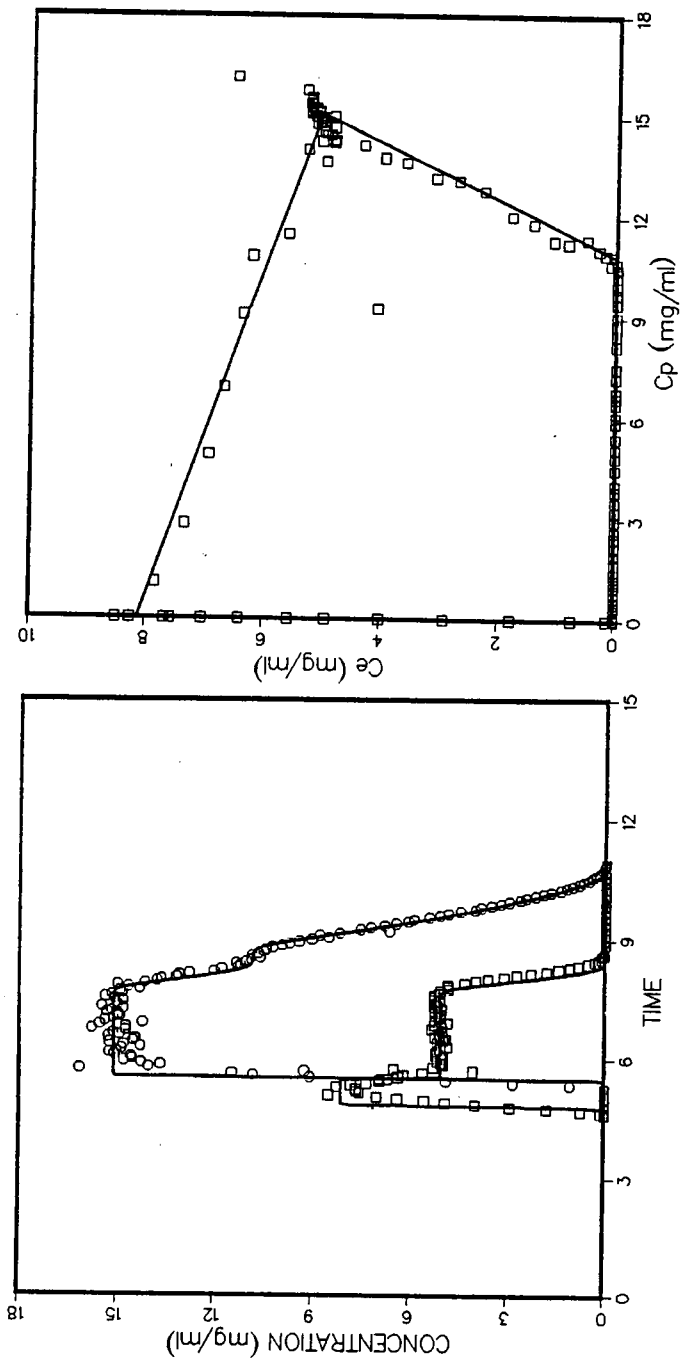
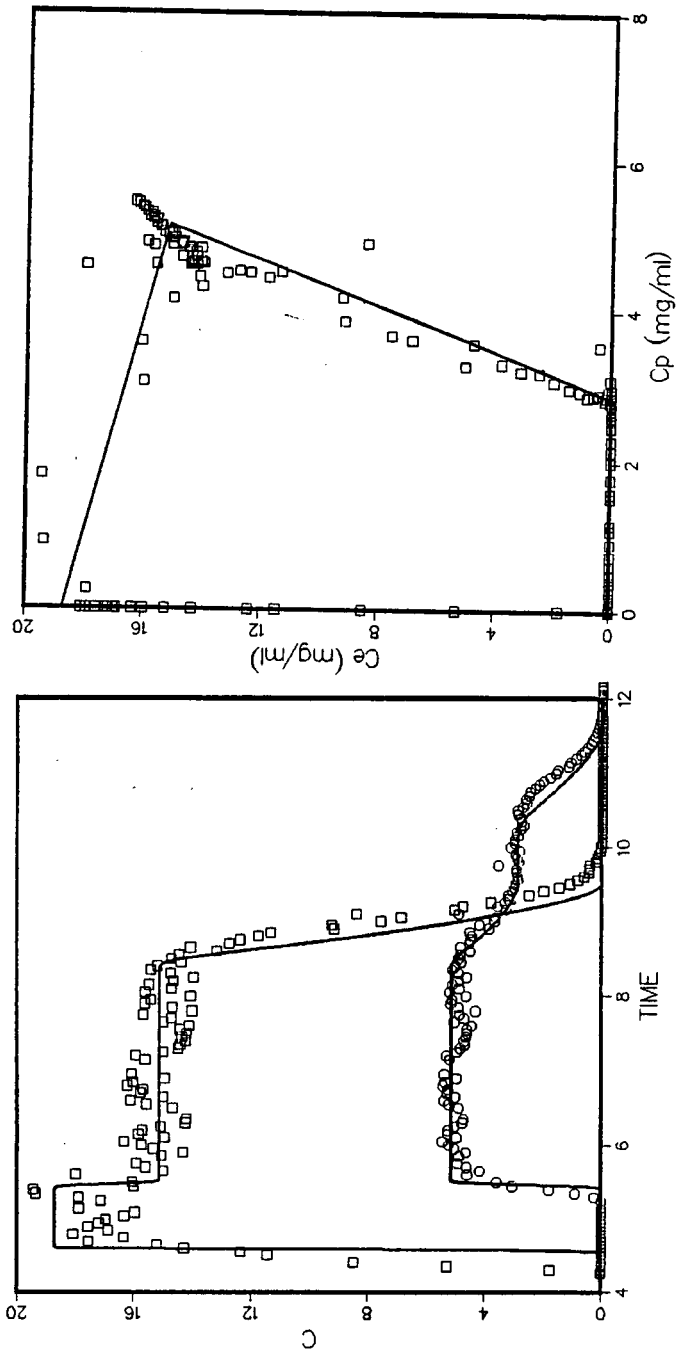


Figure 4.48 Comparison of Experimental and Theoretical Profiles using Kinetic Model, 1/1, Non-Rectangular Injection



- Theoretical, □ Phenyl-ethanol, o Phenyl-propanol

Figure 4.49 Comparison of Experimental and Theoretical Profiles using Kinetic Model, 1/3, Rectangular Injection



- Theoretical, □ Phenyl-ethanol, o Phenyl-propanol

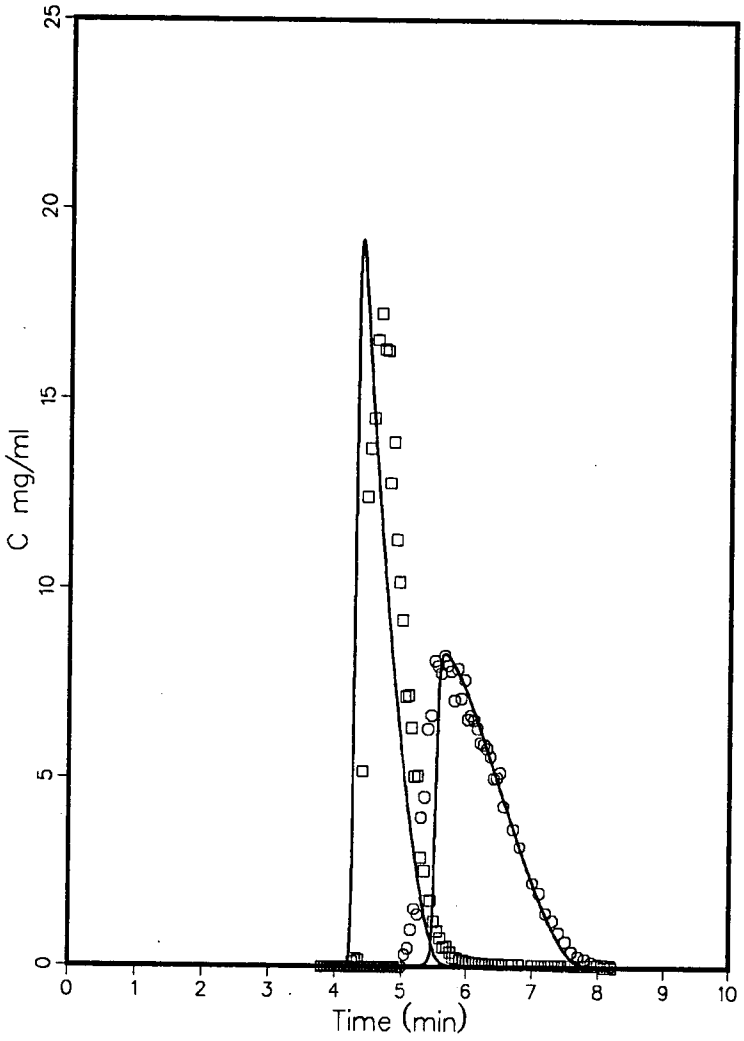
Figure 4.50 Comparison of Experimental and Theoretical Profiles using Kinetic Model, 3/1, Rectangular Injection

Semi-ideal Model

Figure 4.51a-d shows a comparison between theoretical and experimental data for the 1/1, 1/3, 3/1 and 9/1 mixtures taking into account the half-gaussian profile. All mixtures show very good agreement, and in general better agreement than using single component Langmuir parameters in a competitive Langmuir isotherm. Figure 4.51a shows the 1/1 mixture. The front of the first component does not agree exactly with the experimental data. However, the degree of interference and the profile of the second component follows very closely the data. For the 1/3 mixture, Figure 4.51b, the theoretical profile elutes 0.2 min earlier than found experimentally but the profiles otherwise match very well. The 3/1 mixture, Figure 4.51c, shows much better agreement with the average b parameter from the hodograph transform than using single component b parameters. The second component profile agrees exactly with the data. The first component is, however, shifted about 0.2 min. Similar results are seen for the 9/1 mixture, Figure 4.51d.

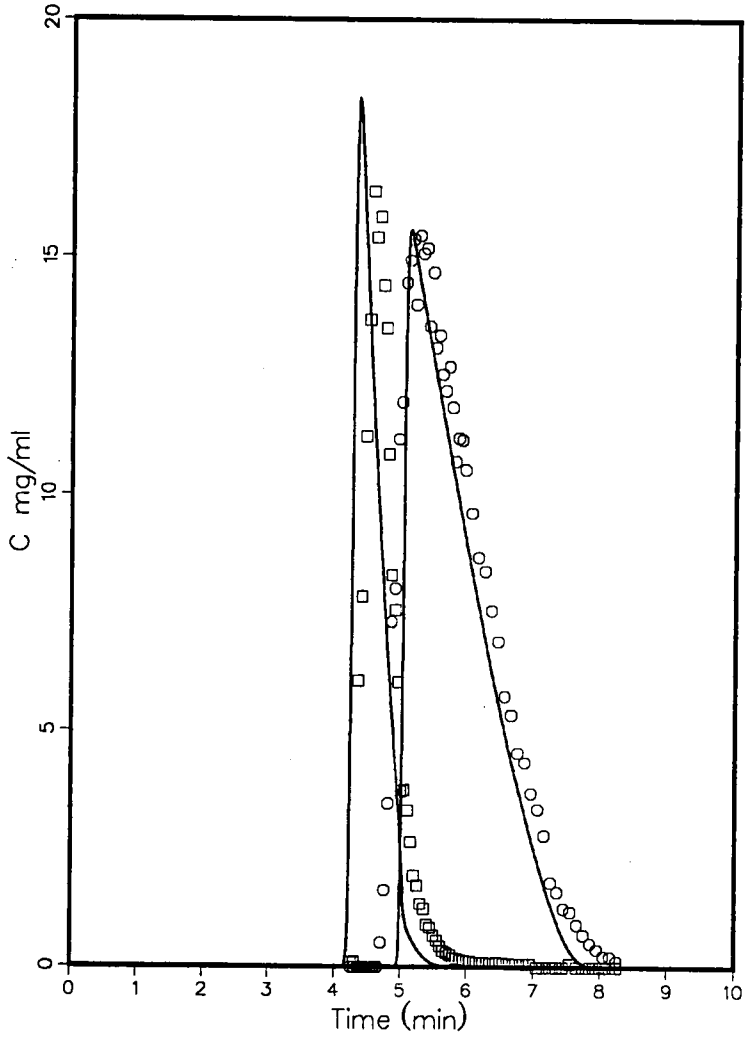
Comparison of theoretical profiles with a gaussian and rectangular injection show significant differences in the band profile, Figure 4.52a-d. In general, the rectangular profiles give rise to taller, narrower band profiles and consequently there is less interference than with the half-gaussian shaped injection profile. Thus, taking into account the shape of the profile results in better agreement with experimental data.

Craig Simulation



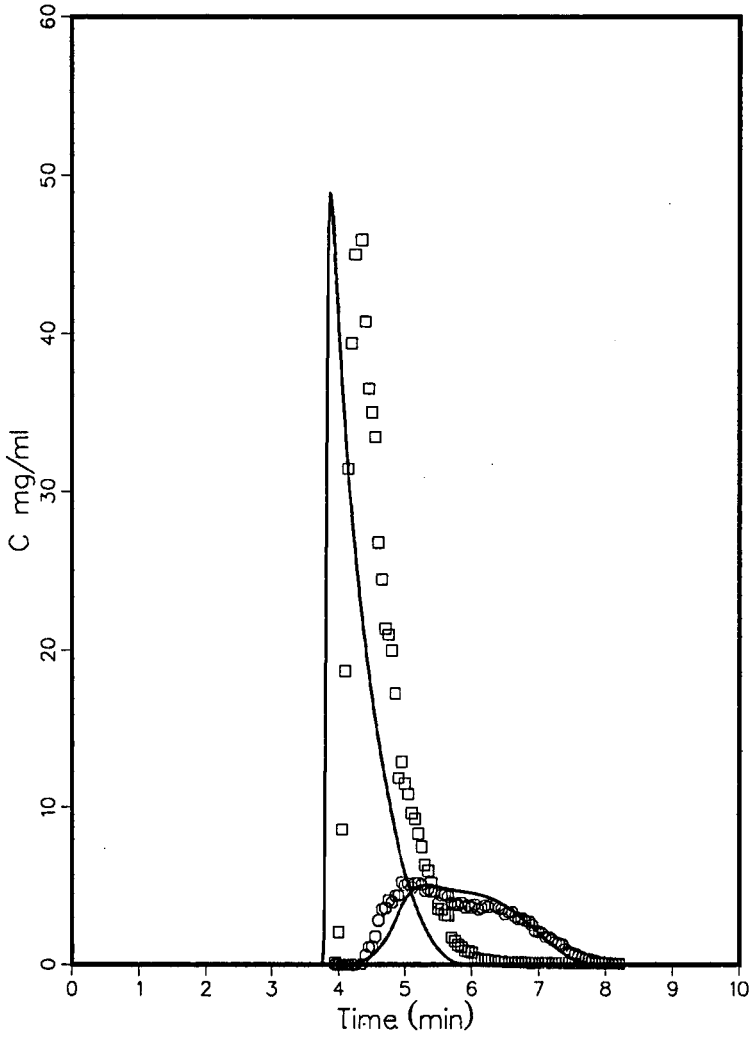
(a) 1/1 Mixture, - Theoretical, □ Phenyl-ethanol, o Phenyl-propanol

Figure 4.51 Comparison of Experimental and Predicted Profiles, Half-Gaussian Injection and Average Best Fit Hodograph Parameters



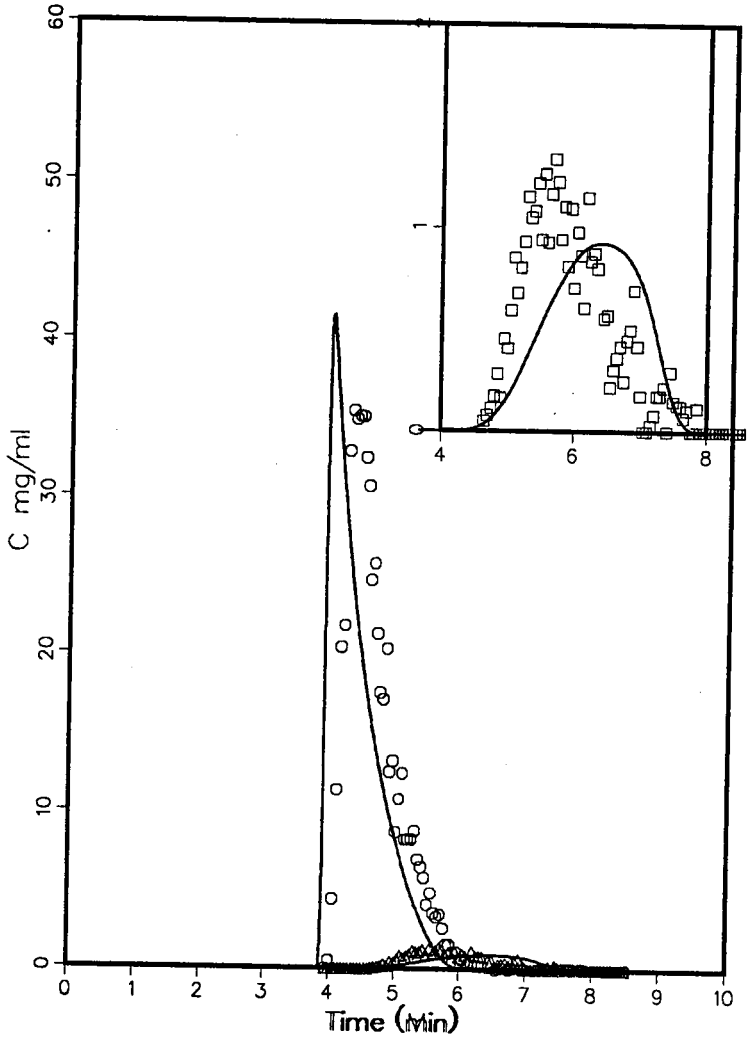
(b) 1/3 Mixture

Figure 4.51 (continued)



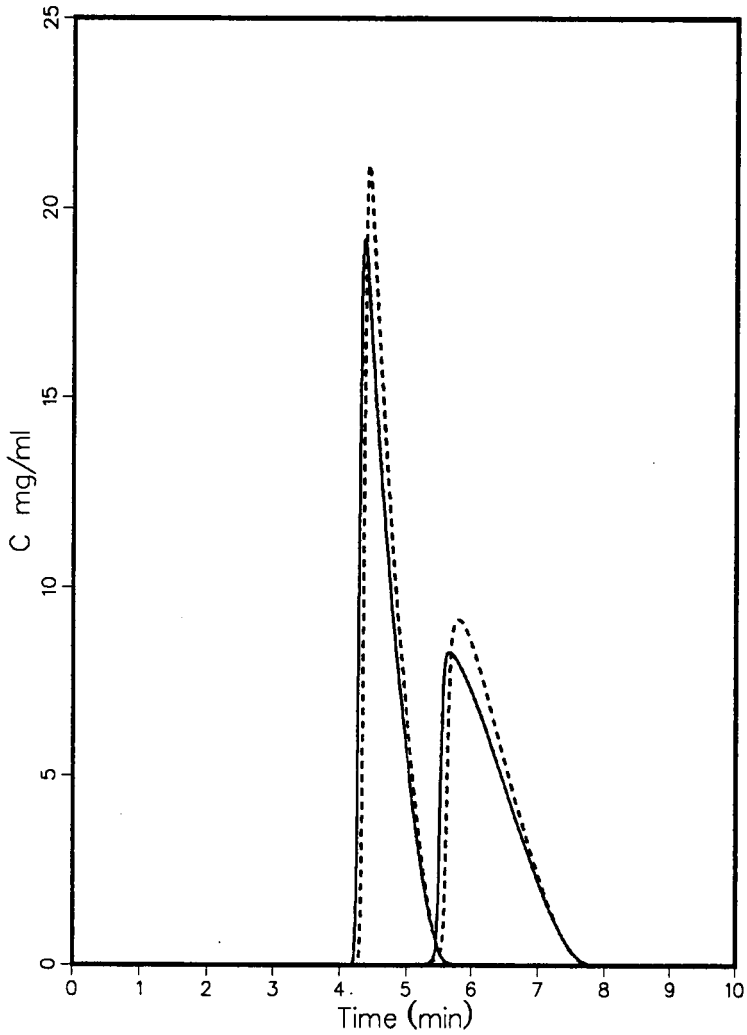
(c) 3/1 Mixture

Figure 4.51 (continued)



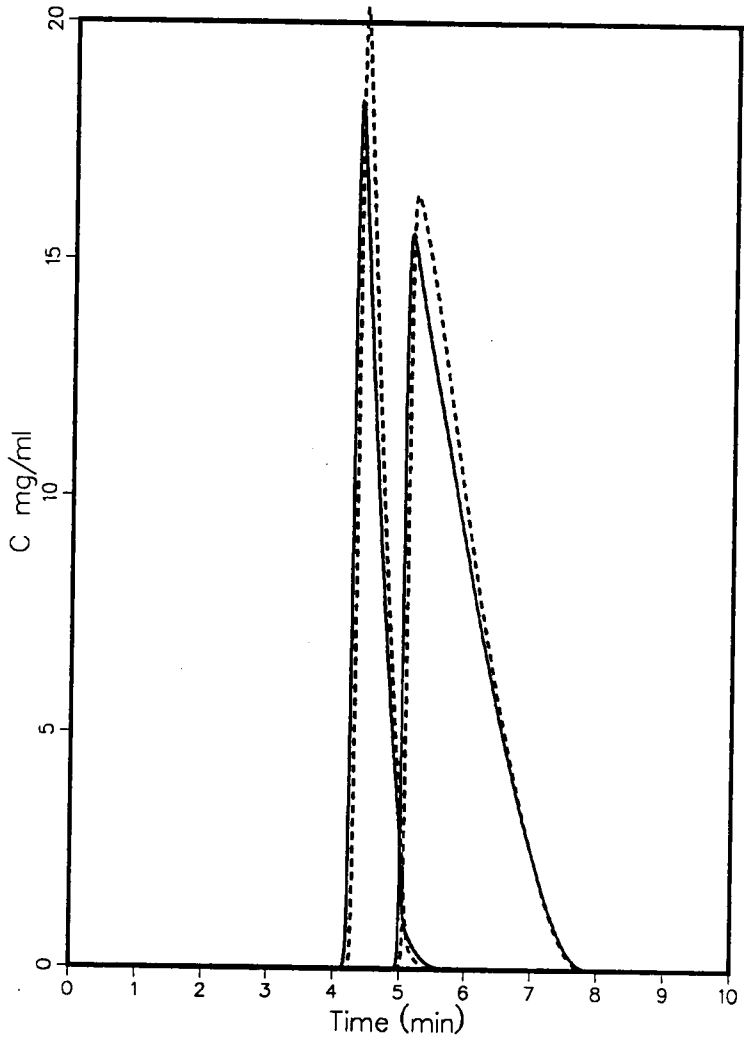
(d) 9/1 Mixture

Figure 4.51 (continued)



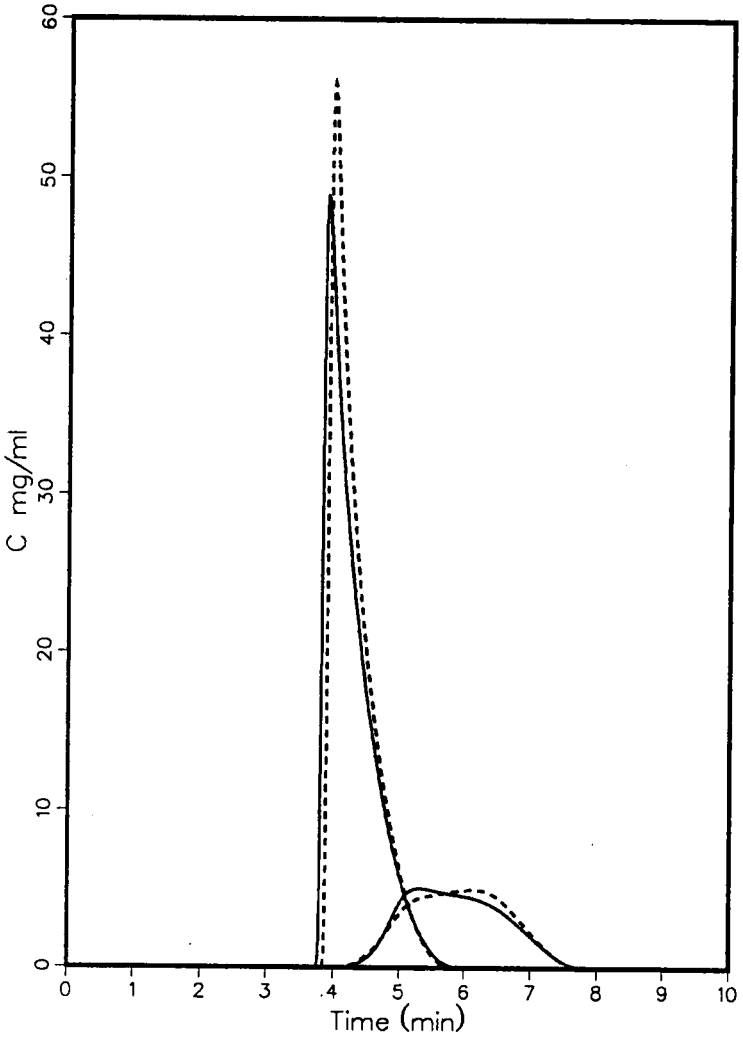
(a) 1/1 Mixture, - Rectangular, -- Half Gaussian

Figure 4.52 Comparison of Rectangular and Gaussian Injection Profiles



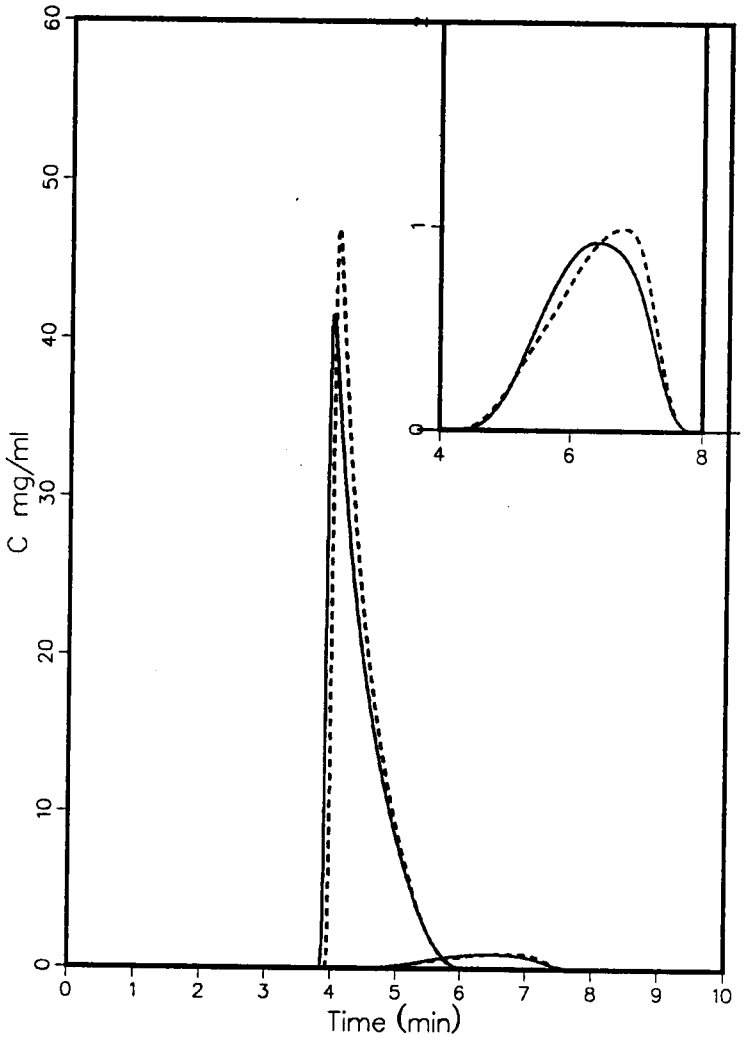
(b) 1/3 Mixture

Figure 4.52 (continued)



(c) 3/1 Mixture

Figure 4.52 (continued)



(d) 9/1 Mixture

Figure 4.52 (continued)

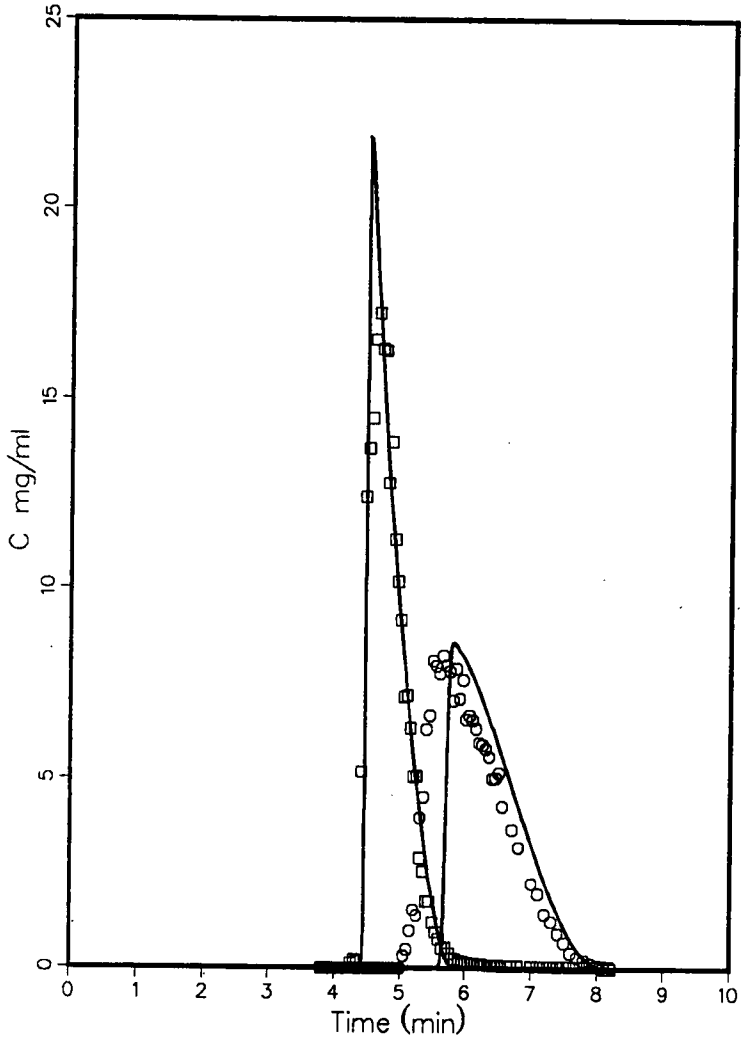
The Craig model was used to calculate the band profiles in overloaded elution chromatography. A comparison between predictions using the Craig model and experimental data is shown in Figure 4.53a-d. In general, the Craig model gives sharper bands. This is due to differences in the way the calculation is carried out and the resulting difference in the capacity factor dependence on HETP. The front and rear boundaries of the first and second components are predicted well, but the degree of interference is better predicted by the semi-ideal model.

Controlled Diffusion Model

Lastly, the controlled diffusion model was used to make predictions of the band profiles using the Half-gaussian injection profile. The control diffusion method gives results half way between the semi-ideal model and the Craig model, Figure 4.54a-d. Though very little difference can be seen between the Craig and control diffusion model, Figure 5.55a-d.

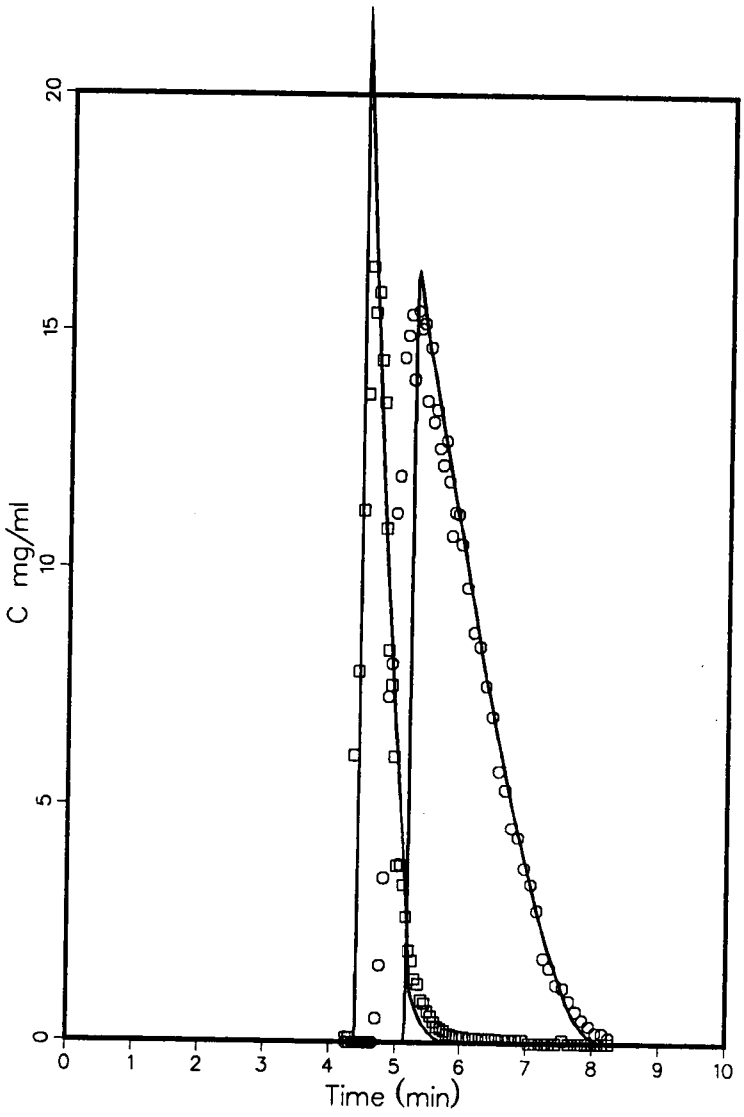
4.4 Quantitative Comparison of the Different Models for Predicting Overloaded Elution Profiles

The experimental and theoretical profiles of various models for a pulse injection can be summarized quantitatively by defining various characteristic parameters. These parameters are defined in Figure 4.56 which illustrates the ideal solution for a binary mixture. Table 4.3-4.6 summarizes the values of these parameters for the different overloaded elution conditions studied. In parenthesis is the



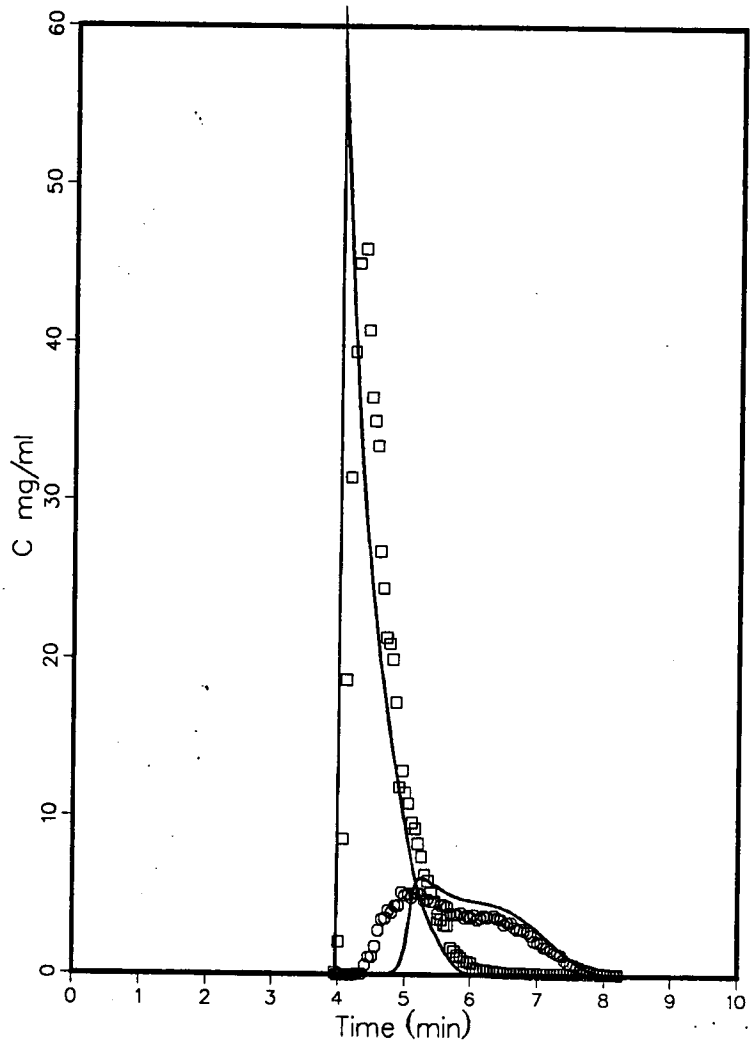
(a) 1/1 Mixture, - Theoretical, □ Phenyl-ethanol, o Phenyl-propanol

Figure 4.53 Comparison of Experimental and Predicted Profiles using Craig Model with Half-Gaussian Injection function



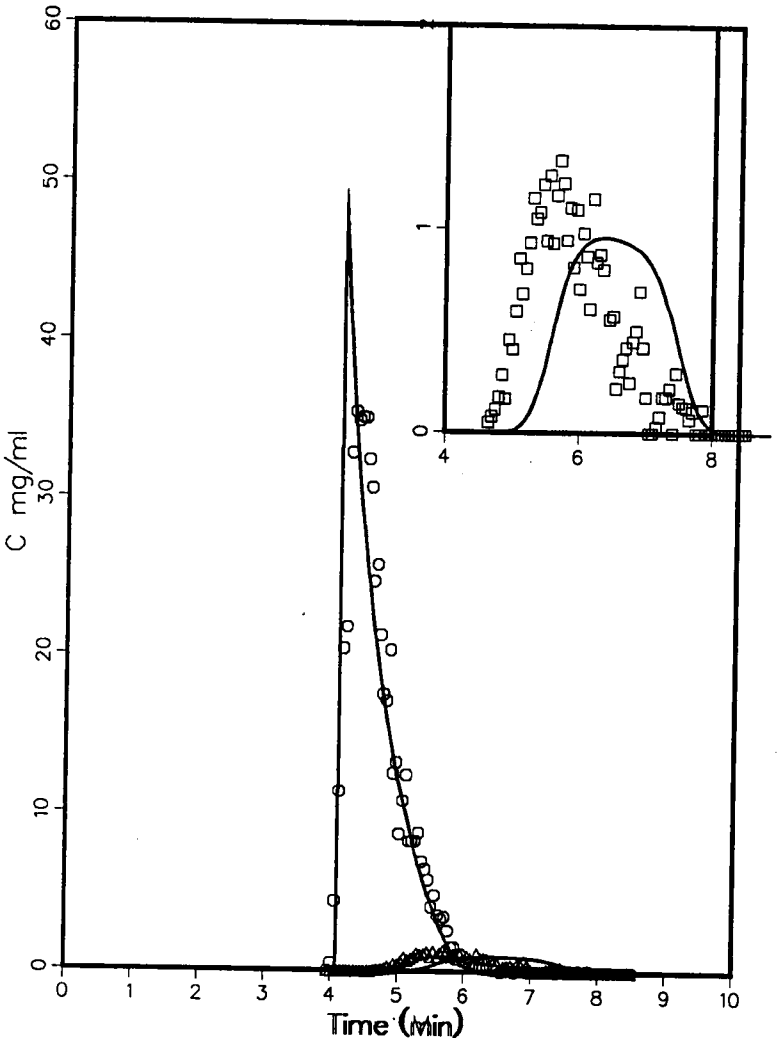
(b) 1/3 Mixture

Figure 4.53 (continued)



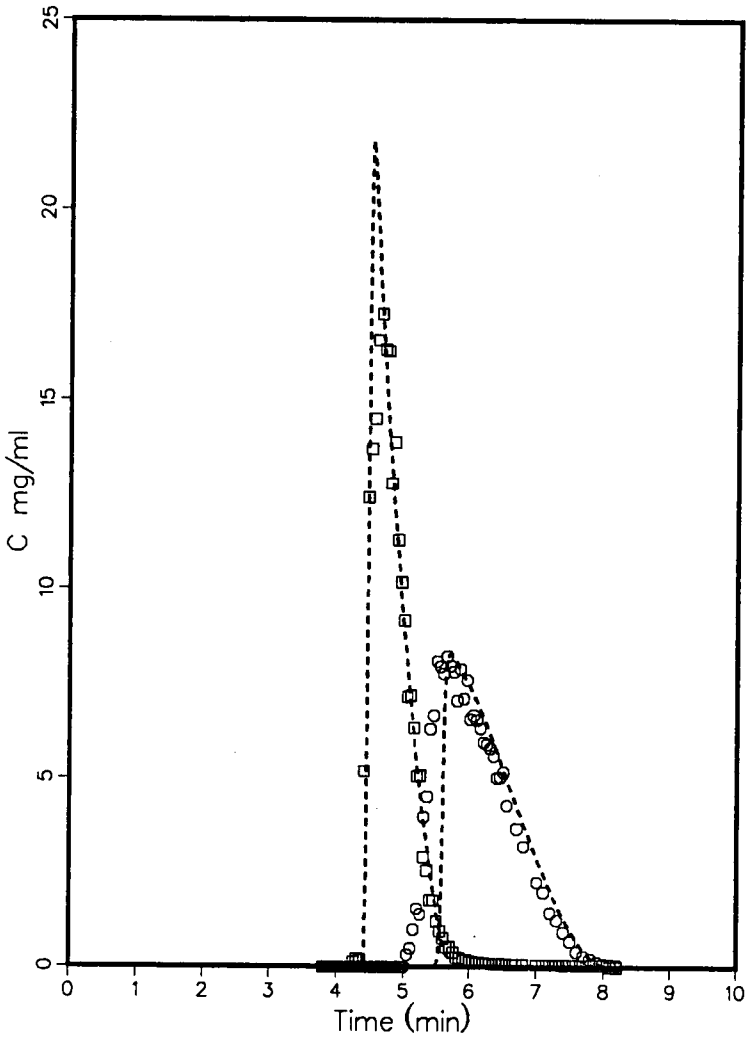
(c) 3/1 Mixture

Figure 4.53 (continued)



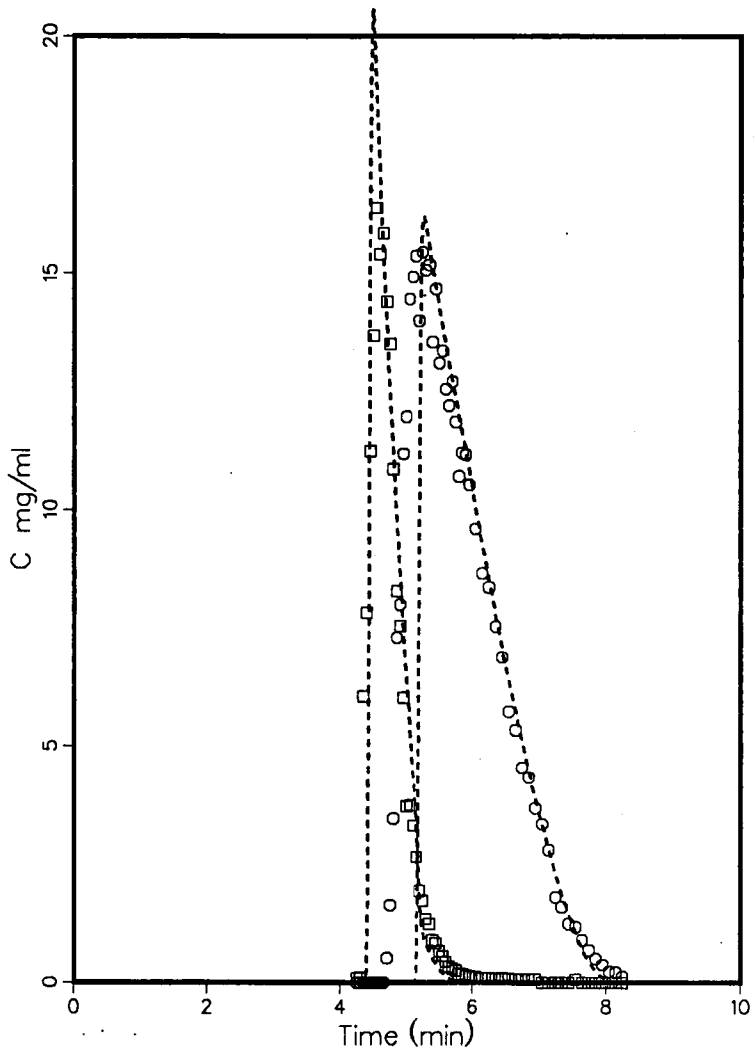
(d) 9/1 Mixture

Figure 4.53 (continued)



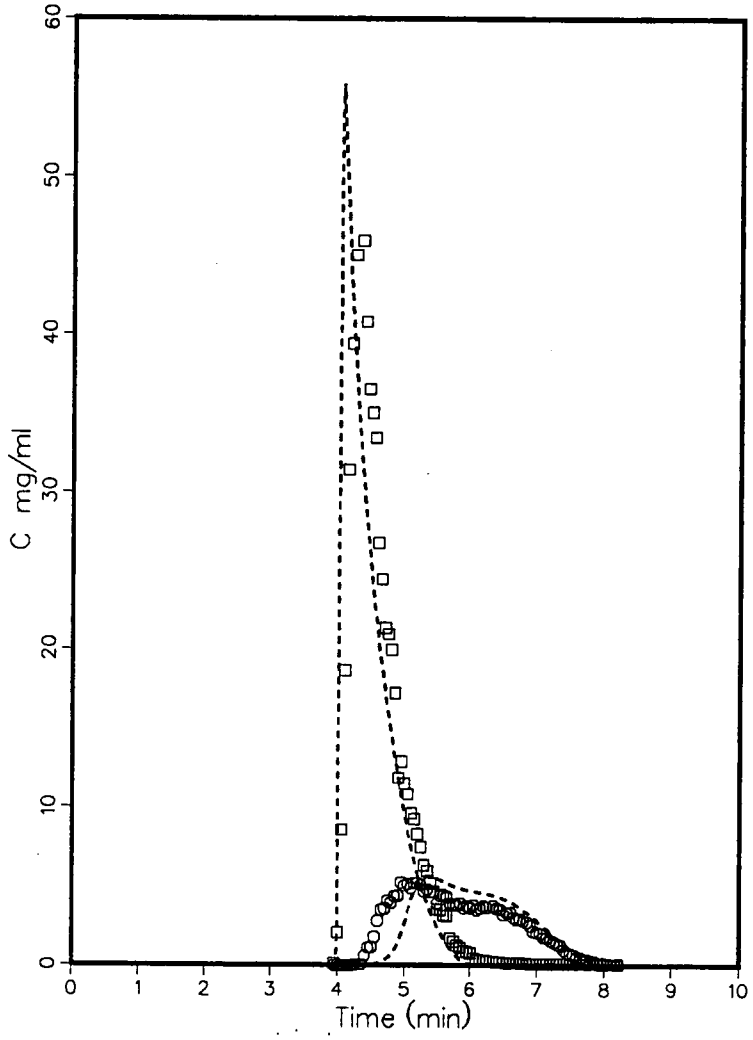
(a) 1/1 Mixture, -- Theoretical, □ Phenyl-ethanol
o Phenyl-propanol

Figure 4.54 Comparison of Experimental and Predicted Profiles using Controlled Diffusion Model with Half-Gaussian Injection function



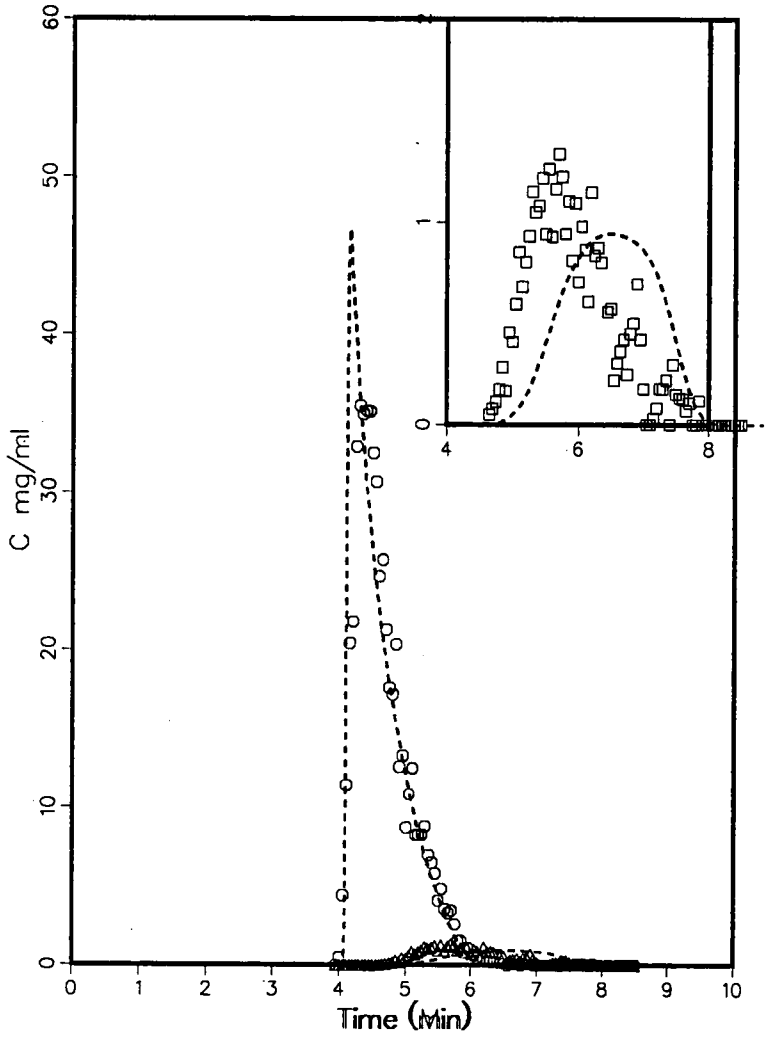
(b) 1/3 Mixture

Figure 4.54 (continued)



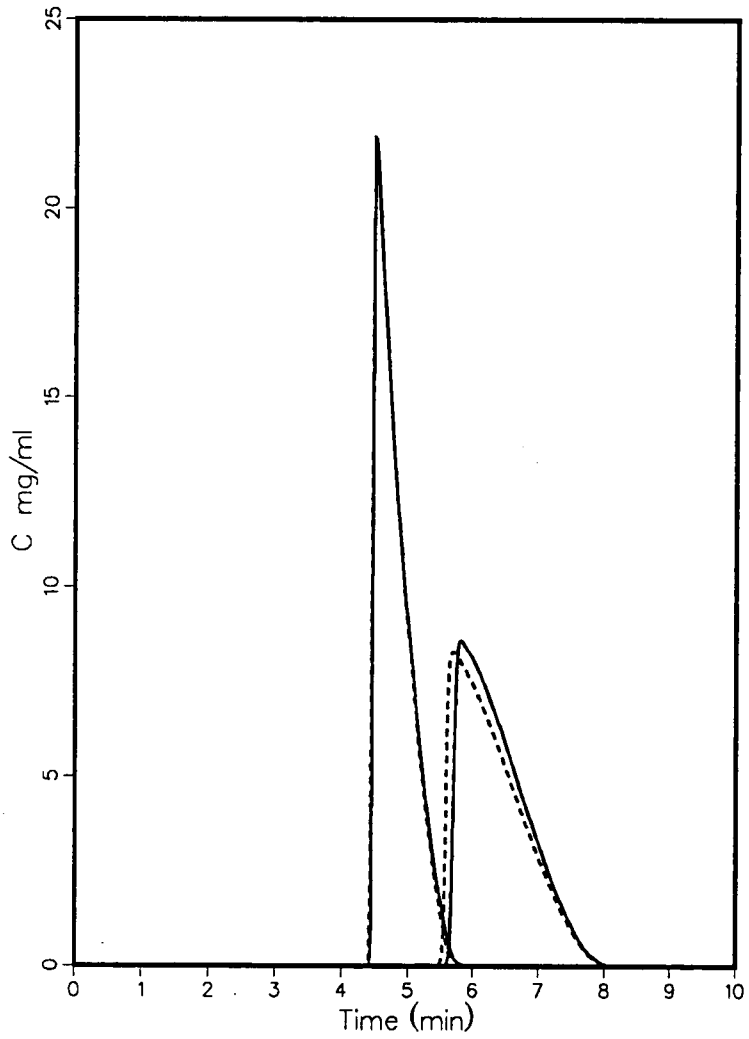
(c) 3/1 Mixture

Figure 4.54 (continued)



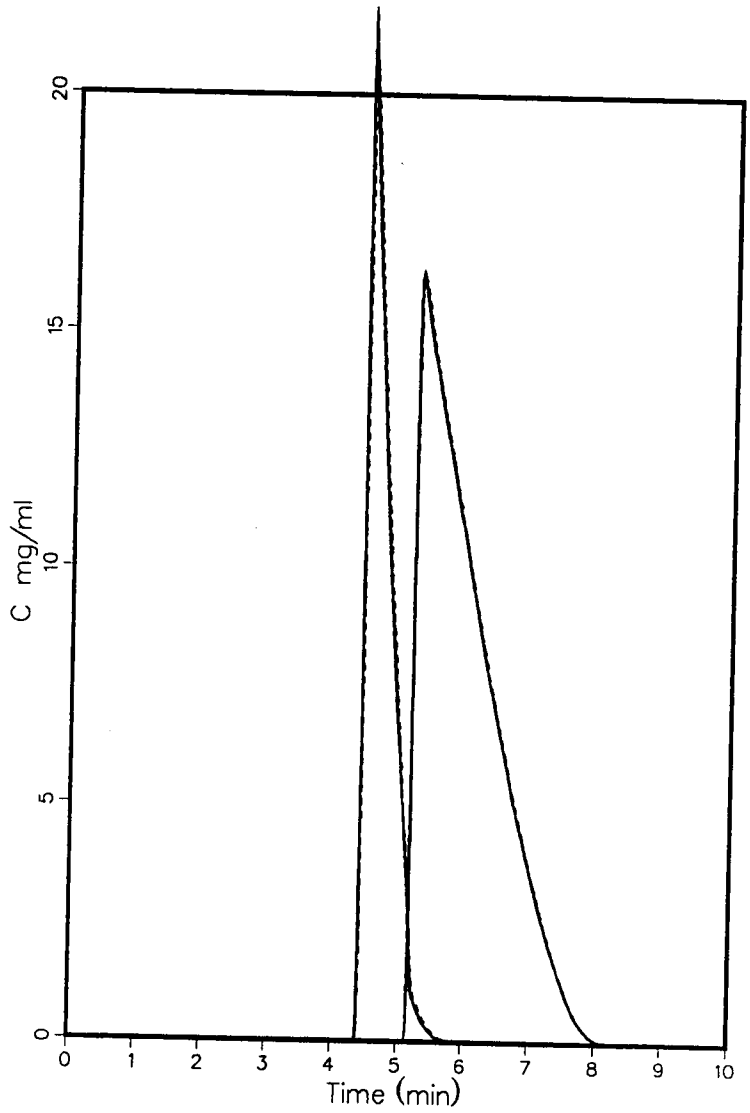
(d) 9/1 Mixture

Figure 4.54 (continued)



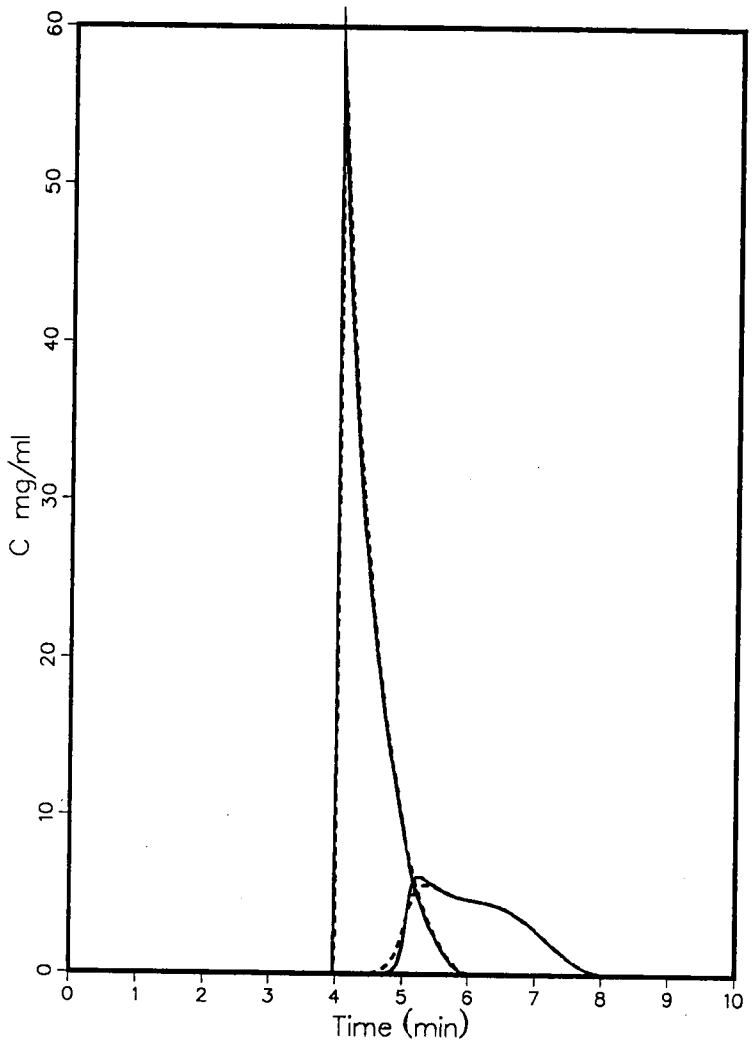
(a) 1/1 Mixture

Figure 4.55 Comparison of Craig (-) and Control Diffusion (--) Models



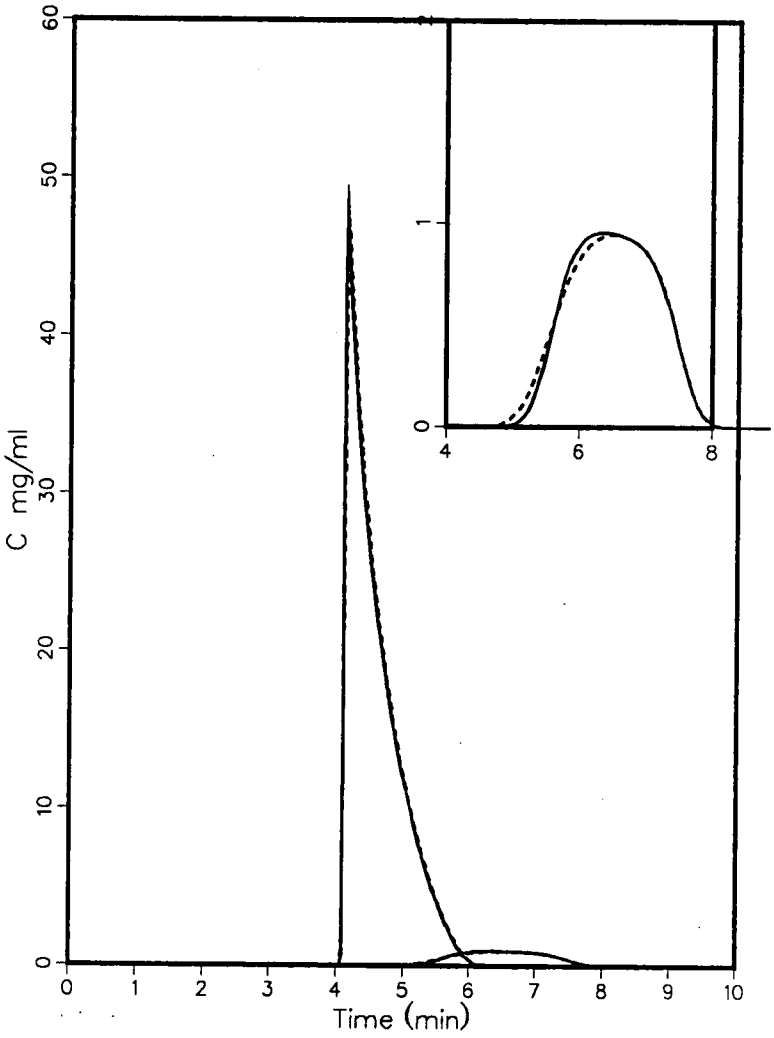
(b) 1/3 Mixture

Figure 4.55 (continued)



(c) 3/1 Mixture

Figure 4.55 (continued)



(d) 9/1 Mixture

Figure 4.55 (continued)

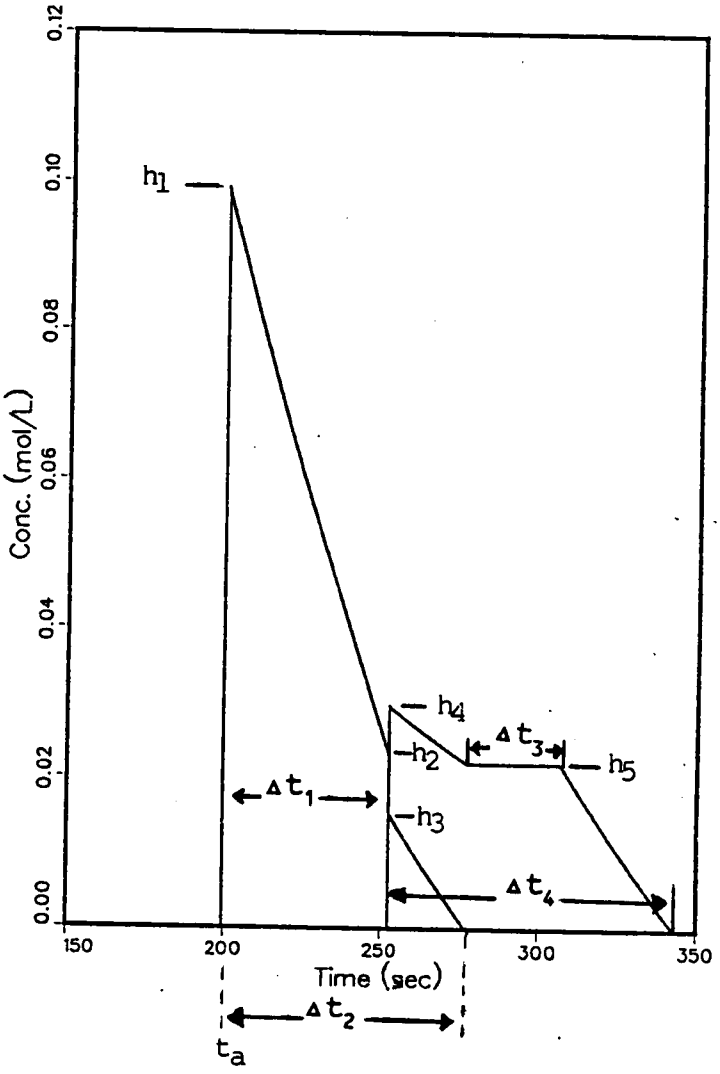


Figure 4.56 Ideal Model Representation of Binary Overloaded Elution Profiles Marking the Characteristic Parameters 201

Table 4.3 Quantitative Evaluation of the 1/1 Mixture in Overloaded Elution Chromatography

	Characteristic Parameter (error)				
	Exp.	Model 1	Model 2	Model 3	Model 4
ta	4.2	4.2 (0)	4.2 (0)	4.3 (.1)	4.2 (0)
dt1	-	-	-	-	-
dt2	1.8	1.75 (.05)	1.2 (.6)	1.4 (.4)	1.8 (0)
dt3	-	-	-	-	-
dt4	2.8	1.4 (1.4)	2.0 (.8)	2.1 (.7)	2.2 (.6)
sum of errors		1.45	1.4	1.2	.6
h1	17.4	21 (3.6)	21.2 (3.8)	19.3 (1.9)	21.6 (4.2)
h2	-	-	-	-	-
h3	-	-	-	-	-
h4	8.3	11 (2.7)	10.1 (1.8)	8.4 (.1)	8.4 (.1)
h5	-	-	-	-	-
sum of errors		6.3	5.6	2.0	4.3

Table 4.4 Quantitative Evaluation of the 1/3 Mixture in Overloaded Elution Chromatography

	Characteristic Parameter (error)			
Exp.	Model 1	Model 2	Model 3	Model 4
ta 4.2	4.3 (.1)	4.2 (0)	4.1 (.1)	4.2 (0)
dt1 0.54	0.88 (.34)	0.72 (.18)	0.7 (.16)	0.77 (.23)
dt2 1.8	0.7 (1.1)	1.1 (.7)	1.2 (.6)	1.2 (.6)
dt3 -	-	-	-	-
dt4 3.26	2.58 (.68)	2.4 (.86)	2.7 (.56)	2.7 (.56)
sum of errors	2.22	1.74	1.42	1.39
h1 16.5	21.5 (5)	21 (4.5)	17 (.1)	21.6 (5.1)
h2 9	3.7 (5.3)	3.0 (6)	3.3 (5.7)	3.3 (5.7)
h3 7	.95 (6.05)	1.1 (5.9)	2.2 (4.8)	2.2 (4.8)
h4 15.5	21.0 (5.5)	17.7 (2.2)	16.6 (1.1)	16.1 (.6)
h5 -	-	-	-	-
sum of errors	21.85	18.6	11.7	16.2

Table 4.5 Quantitative Evaluation of the 3/1 Mixture in Overloaded Elution Chromatography

		Characteristic Parameter (error)			
	Exp.	Model 1	Model 2	Model 3	Model 4
ta	4.05	4.1 (.05)	4.2 (.15)	3.8 (.25)	3.95 (.1)
dt1	-	-	-	-	-
dt2	1.95	1.6 (.35)	1.6 (.35)	1.9 (.05)	1.8 (.13)
dt3	2.1	0 (2.1)	0 (2.1)	0.55 (1.55)	0.55 (1.55)
dt4	3.3	2.6 (.7)	2.4 (.9)	2.8 (.5)	2.7 (.6)
sum of errors		3.2	3.5	2.35	2.38
h1	46.2	55.2 (9)	50 (3.8)	48.3 (2.1)	58 (11.8)
h2	-	-	-	-	-
h3	-	-	-	-	-
h4	5	17.1 (12.1)	7.5 (2.5)	4.95 (.05)	7.1 (2.1)
h5	3.3	0 (3.3)	0 (3.3)	8.8 (5.5)	4.7 (1.4)
sum of errors		24.4	9.6	7.65	15.3

Table 4.6 Quantitative Evaluation of the 9/1 Mixture in Overloaded Elution Chromatography

	Characteristic Parameter (error)			
Exp.	Model 1	Model 2	Model 3	Model 4
ta 4.05	4.1 (.05)	4.05 (0)	3.8 (.25)	4.03 (.02)
dt1 -	-	-	-	-
dt2 1.9	1.8 (9.1)	1.7 (.2)	2.0 (.1)	1.8 (.1)
dt3 -	-	-	-	-
dt4 3.03	3.07 (.05)	2.4 (.63)	2.9 (.13)	2.8 (.23)
sum of errors	9.2	.83	.45	.35
h1 35.7	46.6 (10.9)	42.3 (6.6)	42 (6.3)	48 (12.3)
h2 -	-	-	-	-
h3 -	-	-	-	-
h4 1.1	1.2 (.1)	1.3 (.2)	0.92 (.18)	0.92 (.18)
h5 -	-	-	-	-
sum of errors	11	6.8	6.48	12.48

difference between the experimental and theoretical characteristic parameter for each case.

Of the different theoretical representations presented in Chapter 4, four models where chosen to make a quantitative comparison with experimental data. Model 1: Employ the Rouchon-Golshan-Shirazi semi-ideal model with single component Langmuir isotherm parameters in a competitive Langmuir model and assume a rectangular injection profile. Model 2: Employ the semi-ideal model with single component Langmuir parameters in the competitive Langmuir isotherm and assume a half Gaussian injection profile. Model 3: Employ the semi-ideal model with the average hodograph parameter and assume a half Gaussian injection profile. Model 4: Employ the Craig Model with the average Hodograph parameter and assume a half Gaussian injection profile.

The results from these tables show that Model 3, use of the semi-ideal model with the average hodograph parameter in the competitive Langmuir model with a half-gaussian injection profile, consistently gives the least error in the retention time and in the height parameter for all the different mixture compositions. Model 4, use of the Craig model with the average hodograph parameter in the competitive Langmuir model with a half-gaussian injection profile, gives results which are similar with Model 3. For the 1/1 and 9/1 mixture, the sum of the errors for the time parameter are less than for Model 4; however, in all cases Model 3, Craig, gives much taller peaks than Model 4.

Thus, this quantitative comparison shows that the method of Hodograph transform provides a more accurate representation of the isotherm and thus gives improved prediction of overloaded elution data

than using single component parameters isotherm parameters in a competitive Langmuir model.

Chapter 5

Trace Enrichment of an Impurity

Trace analysis is usually carried out using elution chromatography by injecting the largest sample size compatible with nearly linear behavior of the chromatographic columns. Some degree of band compression may be achieved through gradient elution. In many practical cases, the detection limits are too high and dilution of the band in elution chromatography further prevents any quantitative analysis. Sensitivity can be improved only by resorting to the development of sophisticated enrichment methods and/or the use of advanced laser induced spectrofluorescence detection. Such methods are usually extremely specific to the analytical problem for which they have been developed and lack generality.

The first section of this chapter will discuss the enrichment of or extraction of small amounts of an early eluting component in the presence of large amount of a later eluting component. The second section proposes a general method for the enrichment of trace impurities regardless of the elution order of the impurity and the major component. Quantitative analysis of the trace can be made subsequent to this enrichment procedure. The enrichment procedure is based on utilizing the effect of sharp boundaries in displacement chromatography.

5.1 By Overloaded Elution Chromatography

When deoxyribonucleic acids in living cells is exposed to ultraviolet radiation, damaging structural alterations occur. Produced are various classes of pyrimidine cyclobutane dimers, pyrimidine hydrates, glycols, various addition products and some purine products. The pyrimidine cyclobutane dimers, including thymine-thymine, thymine-cytosine and cytosine-cytosine, are the most abundant, representing as much as 90 % of the UV damaged products. At physiologically significant exposures (< 10 J/m2 at 254 nm), the concentration of these compounds in extremely low, of the order 0.02% or less of the base concentration.

One problem is the accurate determination of trace constituents from components in large quantity is applied in this section to the problem of quantitating small amounts of thymine-thymine dimer from solutions of thymine. A complete analytical procedure involves the quantitative extraction of the dimers from a mixture of regular bases followed by derivatization of the dimers and their quantitative analysis by gas chromatography. This scheme makes possible the achievement of low detection limits in spite of the small sample sizes available, often not exceeding 500 ug.

To aid in the selection of optimum conditions for the isolation and determination of trace amounts of thymine dimer from solutions of thymine, HPLC under overloaded elution was examined.

Theoretical

The semi-ideal model of chromatography is employed to predict band profiles of the mixtures in this study. The mass balance equation is described in Chapter 2.

Consider a two component mixture where one component is in large quantity and the second is in small quantity. In general, the equilibrium isotherm for the major components is given by the competitive Langmuir isotherm:

$$q_i = \frac{a_i C_i}{(1+\Sigma b_i C_i)} \qquad (5.1)$$

For the component which is in small quantity, it is not necessary to determine the b_1 parameter since that component is in the linear region of its isotherm. However, its adsorption behavior is effected by the amount of the other components in solution. Therefore, the adsorption isotherm for the component(s) in small quantity is written:

$$q_1 = \frac{a_1 C_1}{(1+b_2 C_2)} \qquad (5.2)$$

For the component in large quantity, the impurity is in such small concentration that equation (5.1) reduces to:

$$q_2 = \frac{a_2 C_2}{(1+b_2 C_2)} \qquad (5.3)$$

Using these simplified isotherm models, the isotherm parameters a_1, a_2 and b_2 were determined experimentally. From the isotherm data, elution profiles of large samples were made.

The elution chromatogram of a synthetic mixture of thymine monomer and dimer is shown in Figure 5.1. The retention time of the dimer and monomer is 1011 and 1101 seconds; respectively. The dead time, determined from the retention time of uracil is 195 seconds. The relative retention of the two compounds is 1.11. The resolution is 1.43. The column efficiency is 5000 plates.

The equilibrium adsorption isotherm of thymine in the chromatographic system was determined by ECP. The data are reported in Figure 5.2 in squares and the curve represents the best fit langmuir isotherm. The curvature of the isotherm is not vary large in the concentration range investigated.

The values of the coefficients obtained by least square regression of equation 5.2 for thymine are a_2= 15.908 ml/ml and b_2= 0.11774 ml/mg. The coefficient a_1 determined from the retention time of pure dimer and the phase ratio is equal to 14.03 ml/ml.

Validity of Model

Knowing the adsorption isotherm, the porosity, the mobile phase velocity and the column dimensions, as shown in Chapter 3, it is possible to make accurate predictions of the band profiles. Figure 5.3a illustrates the concentration time chromatogram obtained for thymine injected at a concentration of 2 mg/ml for a 1 ml and a 1.25 ml injection. The theoretical predictions are shown in Figure 5.3b. This model also permits the prediction of band profiles of binary mixtures. Figure 5.4 shows a predicted elution chromatogram for thymine dimer to monomer in a ratio of 1:1405. The inset shows an

Figure 5.1 Linear Elution Chromatogram of Thymine Dimer and Monomer

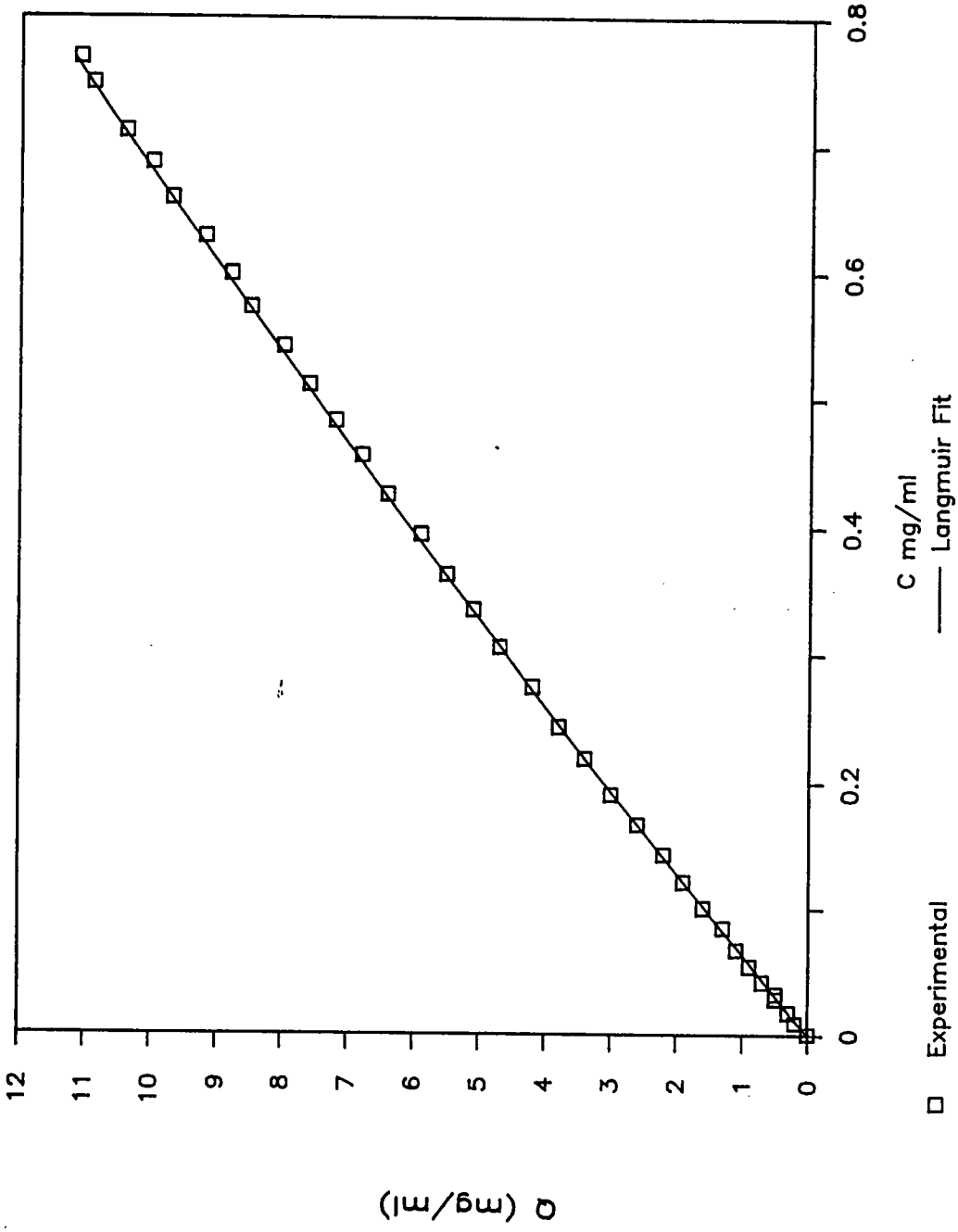
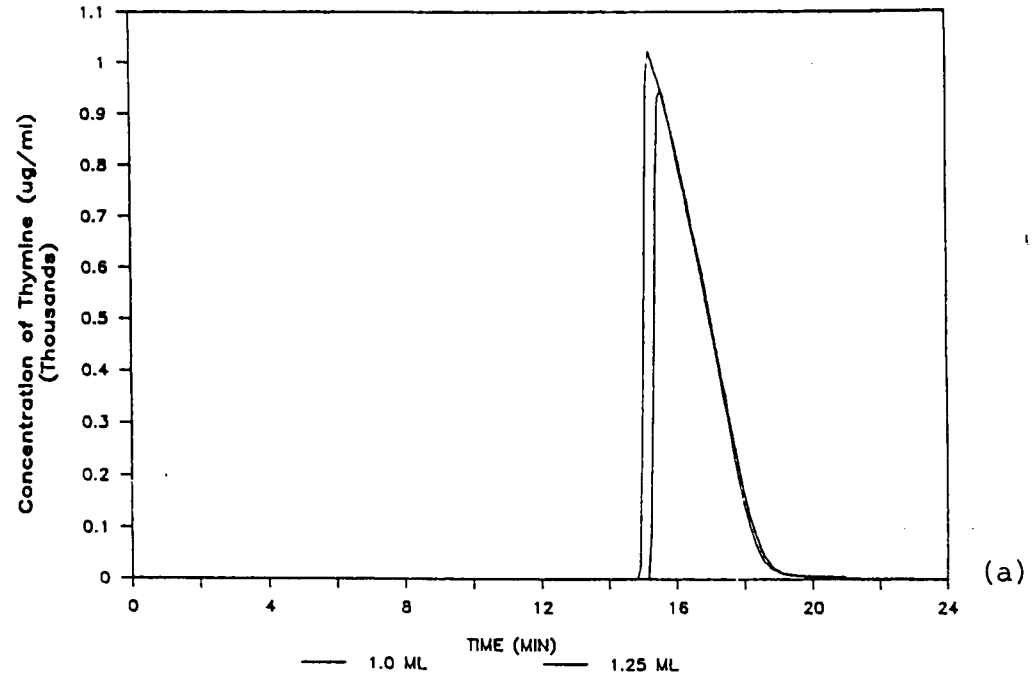
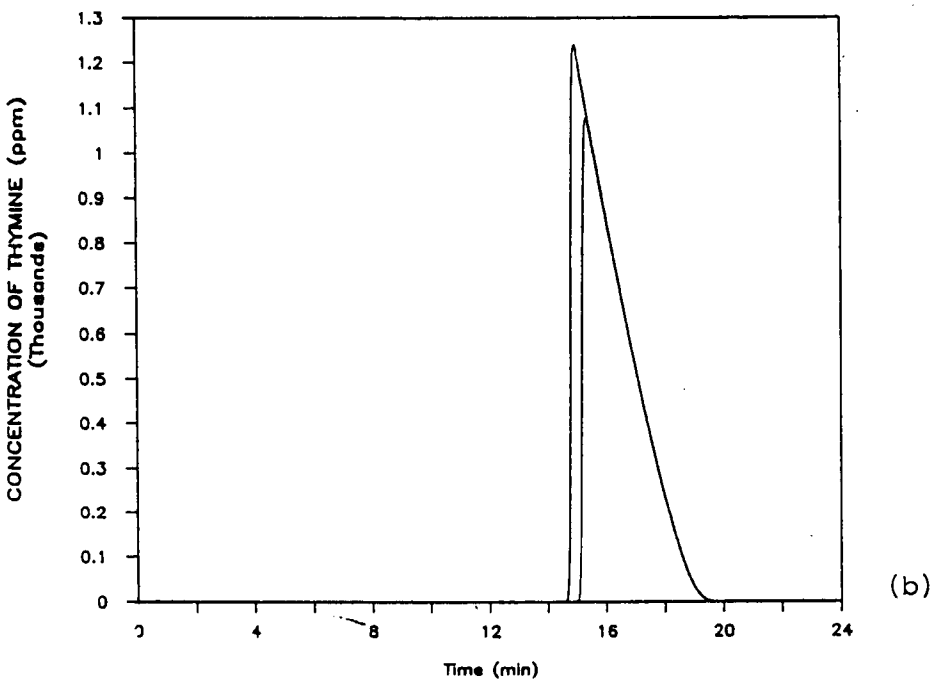


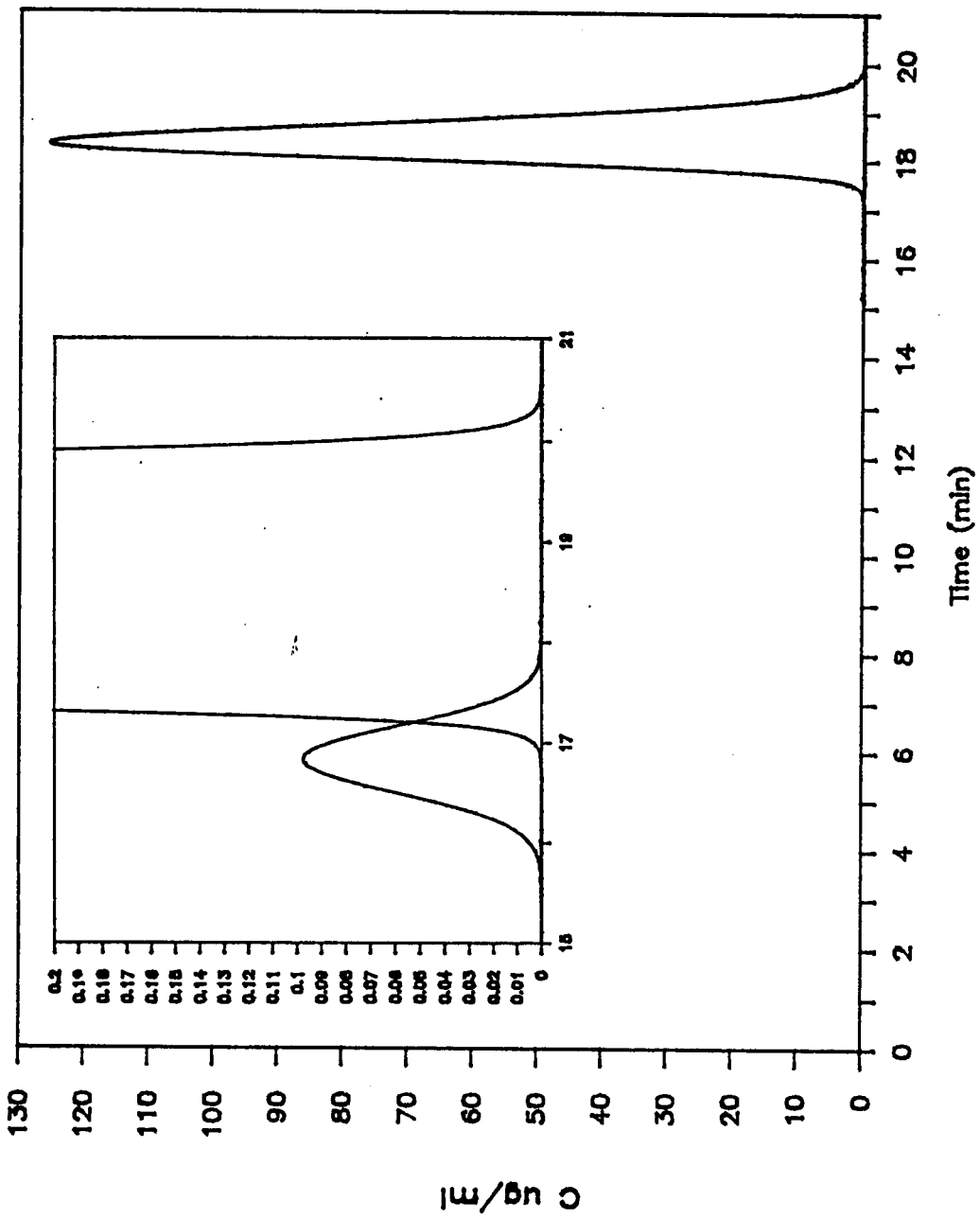
Figure 5.2 Equilibrium Adsorption Isotherm of Thymine by ECP





(a) Experimental Profile, 1.0 ml and 1.25 ml
(b) Predicted Band Profile

Figure 5.3 Experimental and Predicted Profiles of Thymine



insert: Expansion around base of thymine peak

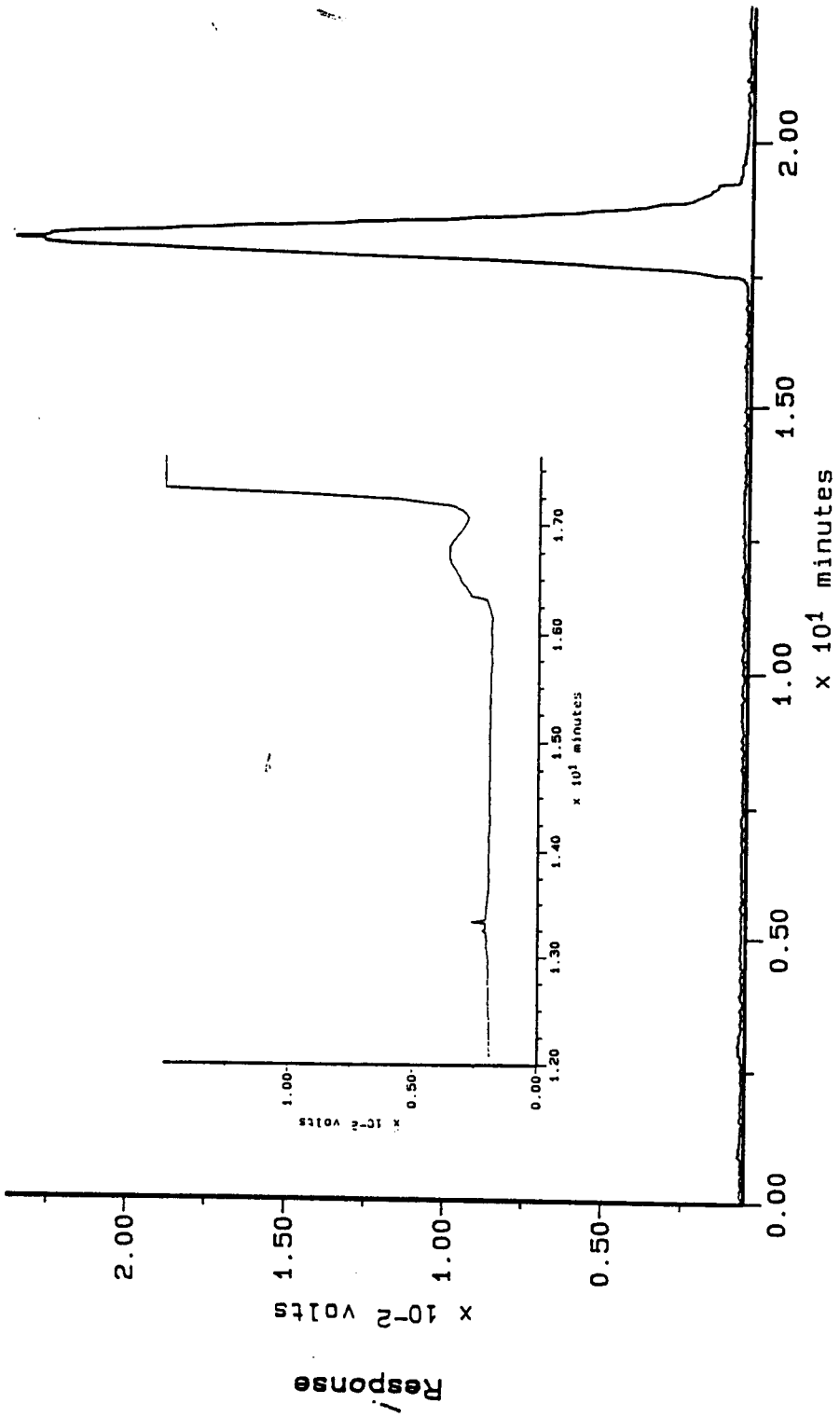
Figure 5.4 Theoretical Profile of Dimer and Monomer in 1:1405 Ratio

expansion around the base of the thymine peak. Figure 5.5 shows the detector response at 300 nm showing only the thymine peak and the inset shows the response at 210 showing the dimer. These experimental results support qualitatively the theoretical predictions. The resolution between the bands is comparable. Similar results were found for 1:112 mixtures.

Effect of Sample Size

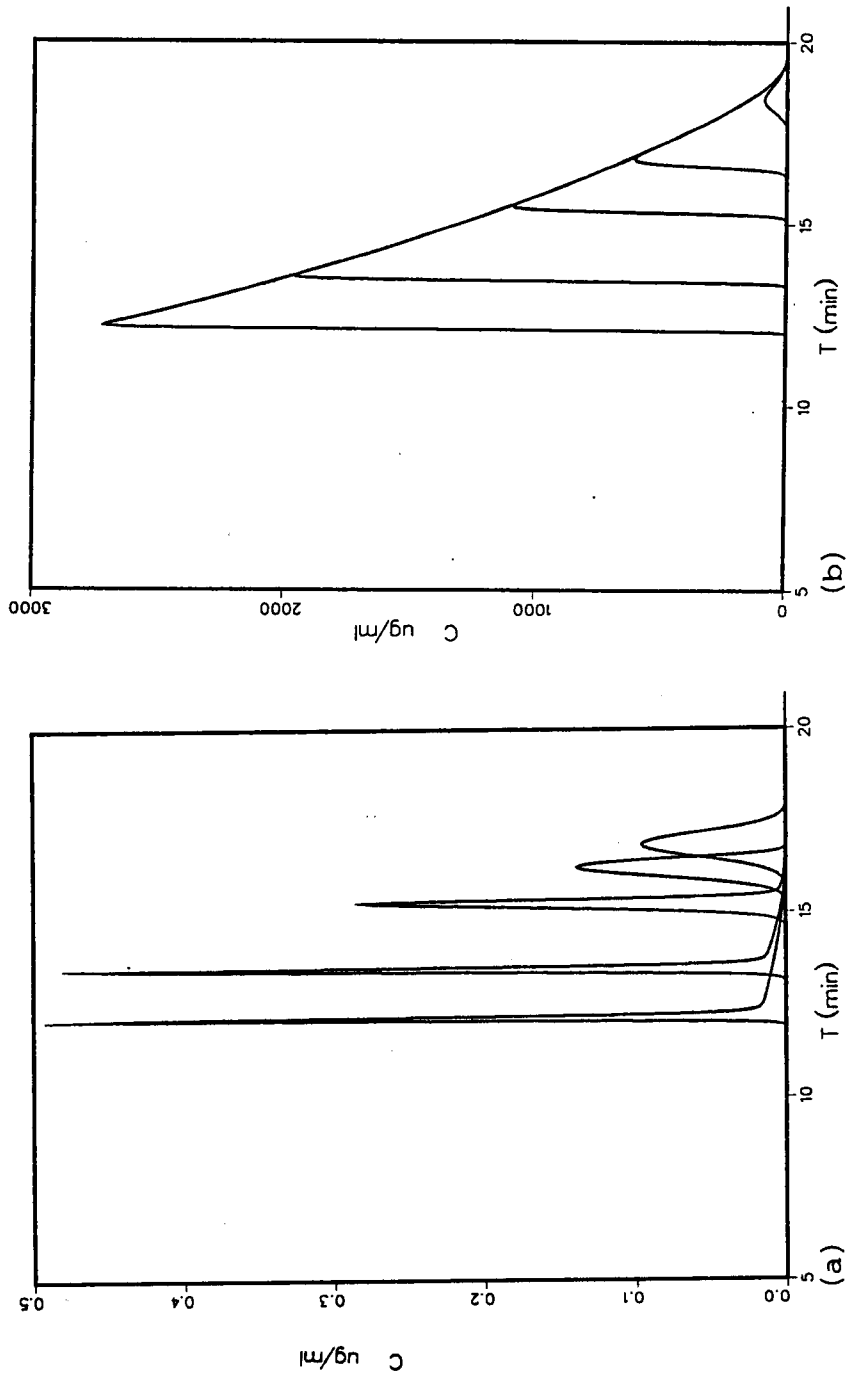
The study of the effect of sample size aids in the understanding the concentration effect. Figure 5.6a shows the theoretical profile of the dimer as if the detector were calibrated and specific only to the dimer. This figure represents the elution profile of 82 ng of dimer in samples containing increasing amount of thymine (0.082, 0.82, 2.0, 5.0 and 8.2 mg). The profile of Thymine was not drawn. Figure 5.6b shows the profile of increasing amount of thymine in the presence of dimer (which cannot be seen). By adding increasing amounts of the later eluting components, the concentration of the early eluting compound is increased. Because the retention time of the front of the band decreases with increasing concentration of thymine, the dimer is compressed and concentrated.

Exactly the same behavior is seen when 8.2 or 0.82 ng of dimer is injected. The band profiles have the same shape, only the maximum value of the ordinate is reduced from 0.05 to 0.005; respectively.



insert: Expansion around base of thymine peak

Figure 5.5 Experimental Profile of Dimer and Monomer in 1:1405 Ratio



(a) Profile of Dimer
(b) Profile of Monomer (1:0.082, 2:0.82, 3:2.0, 4:5.0 and 5:8.2 mg)

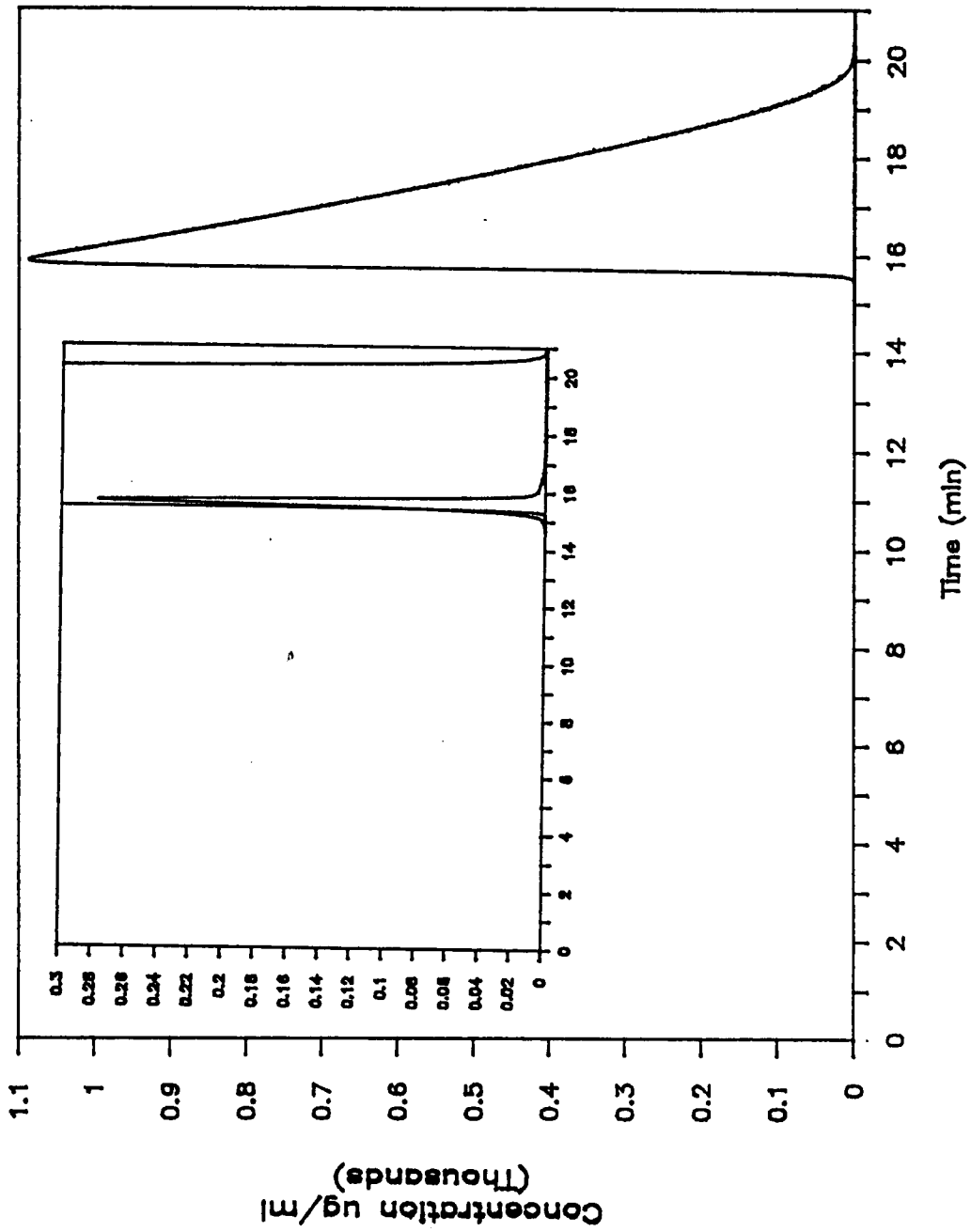
Figure 5.6 Profile of 82 ng of Dimer in the presence of Increasing Amount of Monomer

Enrichment by Recycling

The use of recycling techniques for the enrichment of traces was investigated using the numerical scheme. The extraction of 1/24000 and 1/5000 (w/w) binary mixtures dimer in aqueous solutions of monomer was studied. The sample size was 82 ng of dimer and 400 ng of dimer for the two respective cases.

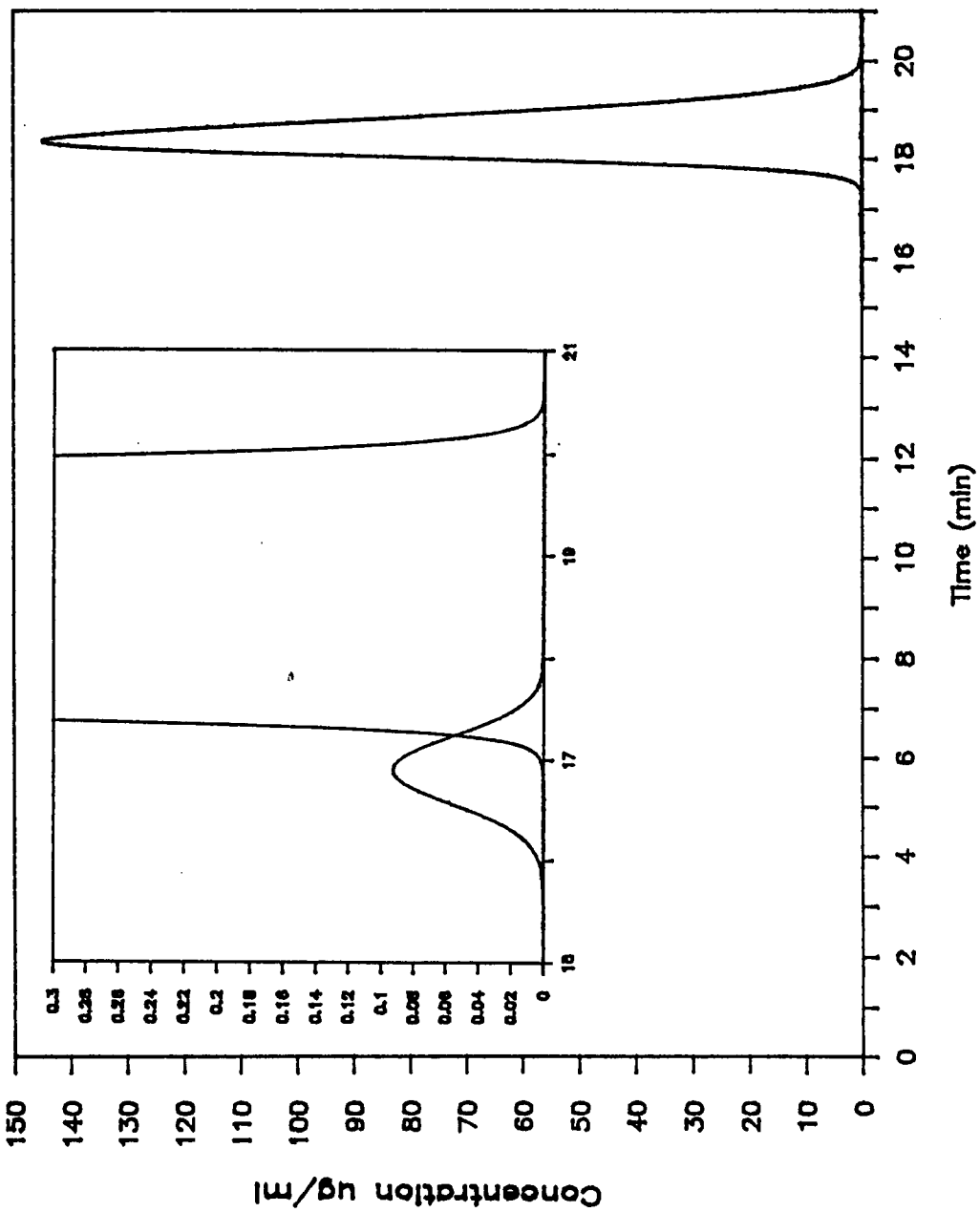
For the case of the 1/24000 (w/w) mixture, under conditions of strong band overloading such as in Figure 5.7, coelution of the band fronts take place. A fraction of the elution band was collected so as to recover 95 % of the early eluting component. This fraction contains 1:1700 (w/w) ratio of dimer to monomer and its volume is between 1 and 2.5 ml. It was assumed that this volume could be reduced to 100 ul and reinjected. Upon reinjection, the chromatogram shown in Figure 5.8 was predicted. From this chromatogram it was calculated that 95 % of the dimer could be collected where it has been enriched to a ratio of 1:1.6.

A similar study was made with a 1:5000 mixture. After the first cycle, it was found that 95 % of the early eluting compound could be recovered in a fraction with a 1:287 (w/w) mixture. If a 99 % yield was required a 3-fold enrichment occurs resulting in a 1:1894 mixture. Subsequent reinjection of the first fraction led to a considerably enriched second fraction containing a 10:1 mixture. By accepting a 95% yield instead of a 99 % yield, substantial enrichment is obtained by a slight decreasing in yield. These results are summarized in Table 5.1.



insert: Expansion around base of thymine peak

Figure 5.7 Theoretical Profile of a 1/24000 Mixture of Dimer/Monomer



insert: Expansion around base of thymine peak

Figure 5.8 Theoretical Prediction of First Recycle

Table 5.1 Enrichment by Recycling

	Initial	1st Cycle*	2nd Cycle*
First Case			
Amount D (ng)	82	78	74
Amount T (mg)	2	0.13	4.7E-5
Ratio (w/w)	1:24300	1:1700	1:1.6
Second Case			
Amount D (ng)	400	396	377.3
Amount T (mg)	2	0.109	3.45 E-5
Ratio (w/w)	1:5000	1:290	10:1

*All yields are 95 %

An experimental study was made to test the theoretical results. Figure 5.9 illustrates the elution chromatogram of 82 ng of dimer in the presence of 2 mg of thymine, monitored at 300 nm. The retention time of the band front are in nearly quantitative agreement with Figure 5.7. The slight difference in elution time is attributed to experimental error resulting from fact that the elution profiles were determined several weeks after the determination of the isotherm. On collecting the eluate from 15.6 to 16.5 min, concentrating the fraction to 230 ul and reinjecting it under the same elution conditions, the chromatogram in Figure 5.8 was recorded at 300 nm. The inset shows the chromatogram at 210 nm. The experimental chromatogram in Figure 5.10 is in excellent agreement with the predicted result in Figure 5.7. Good resolution is observed between the dimer and the thymine band. The retention time of both bands are slightly shorter than predicted.

The collection of fractions has to be made drop by drop and slight differences between the number of drops collected drastically changes the composition of the fraction collected. This more serious experimental problem prevents exact duplication of the conditions selected for the calculation runs.

This work shows that overloaded elution permits the collection of highly enriched fractions of an impurity for quantitative analysis accuracy and precision.

5.2 By Displacement Chromatography

Proposed is a method for the enrichment of impurities from a mixture by allowing the rectangular shaped bands in displacement

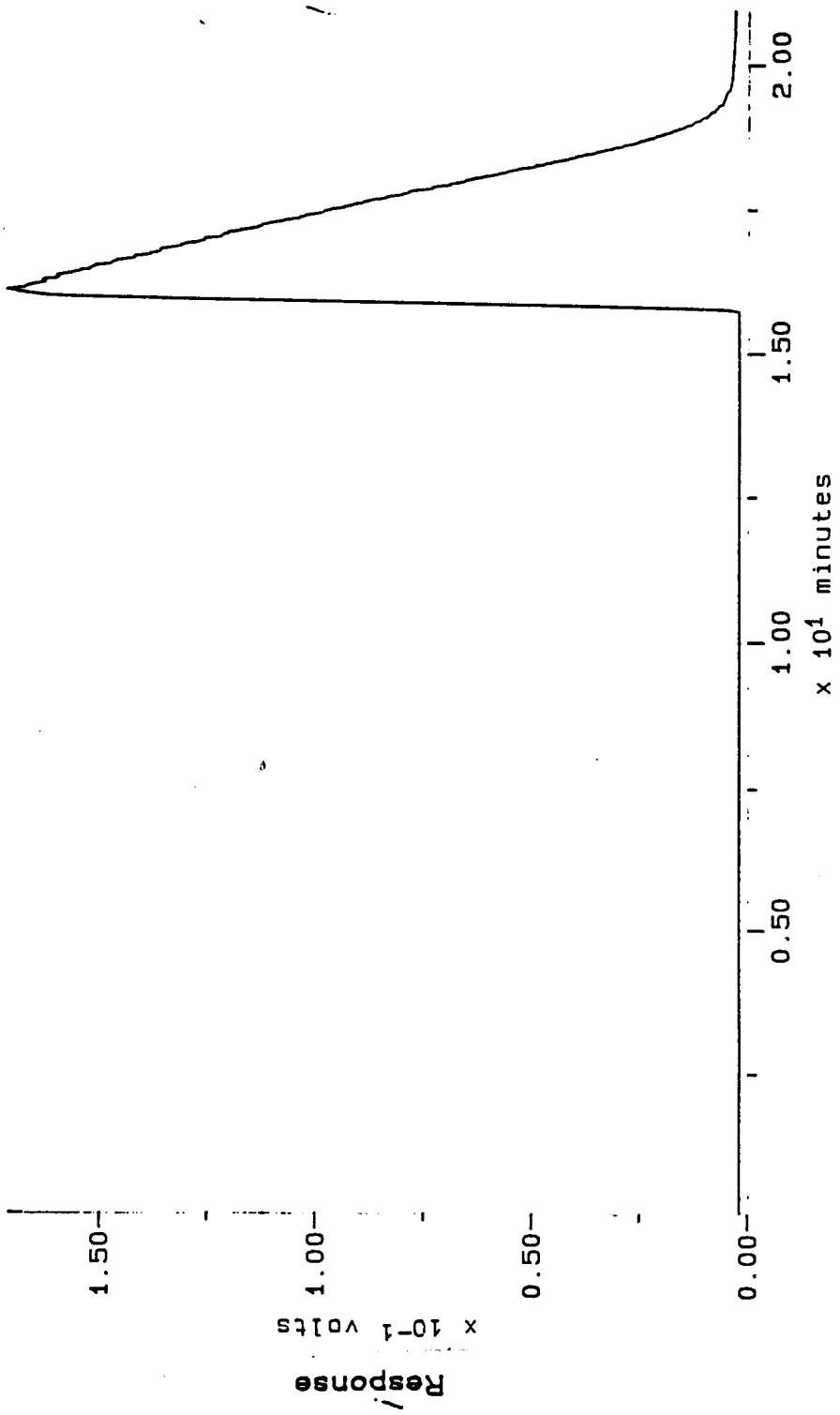
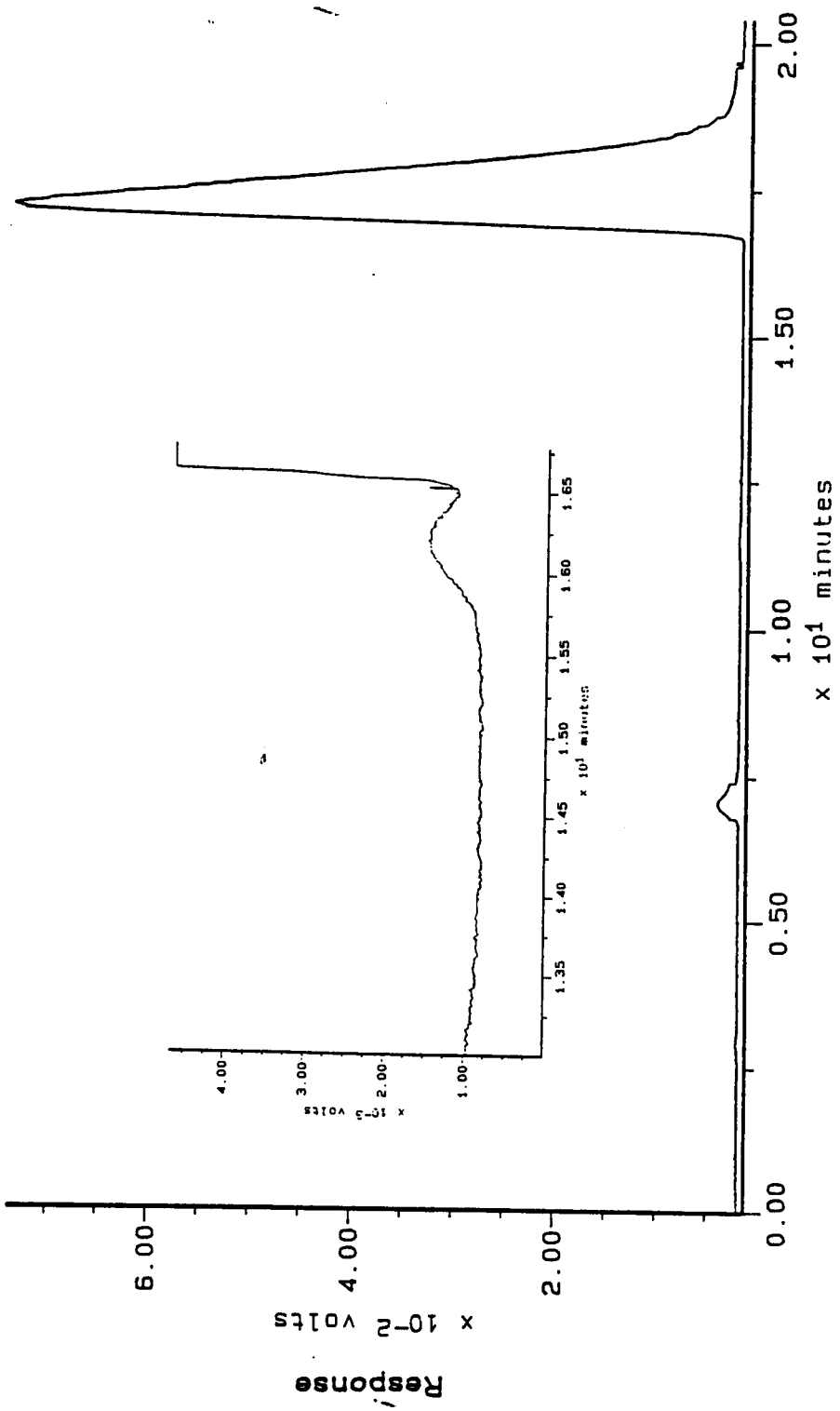


Figure 5.9 Experimental Profile of Monomer at 300 nm



insert: Expansion around base of thymine peak

Figure 5.10 Experimental Profile after First Recycle

chromatography make concentrated zones of impurities. Addressed in this chapter is where does the band trace appear and what is it's profile.

Calculation Parameters

The band profiles for a three component mixture were studied where the sample has two major components having equal concentration and a trace component whose isotherm is either below the first main component, in between the two main components or between the main component and the displacer. The single component isotherms are shown in Figure 5.11.

The isotherm are assumed to follow competitive Langmuirian behavior. The column capacity factor at infinite dilution are 7.5 and 11.25; respectively for the two main components and 16.5 for the displacer. The column saturation capacities are 4.8 g and 6.5 g for the two main components. Chromatograms for 25 cm and 50 cm columns are shown. The mobile phase velocity was 0.625 cm/sec and the column HETP is 30 um. The column capacity factor for the three different possible impurities are 6, 9 and 13.75; respectively. Calculations were made using 100 mg samples of each of the main components and impurities with a concentration of 5 ppm.

Results and Discussion

Figure 5.12a shows the individual band profiles for the displacement separation on a 50 cm column. The trace components are too small to be seen in this figure. As isotachic train is formed.

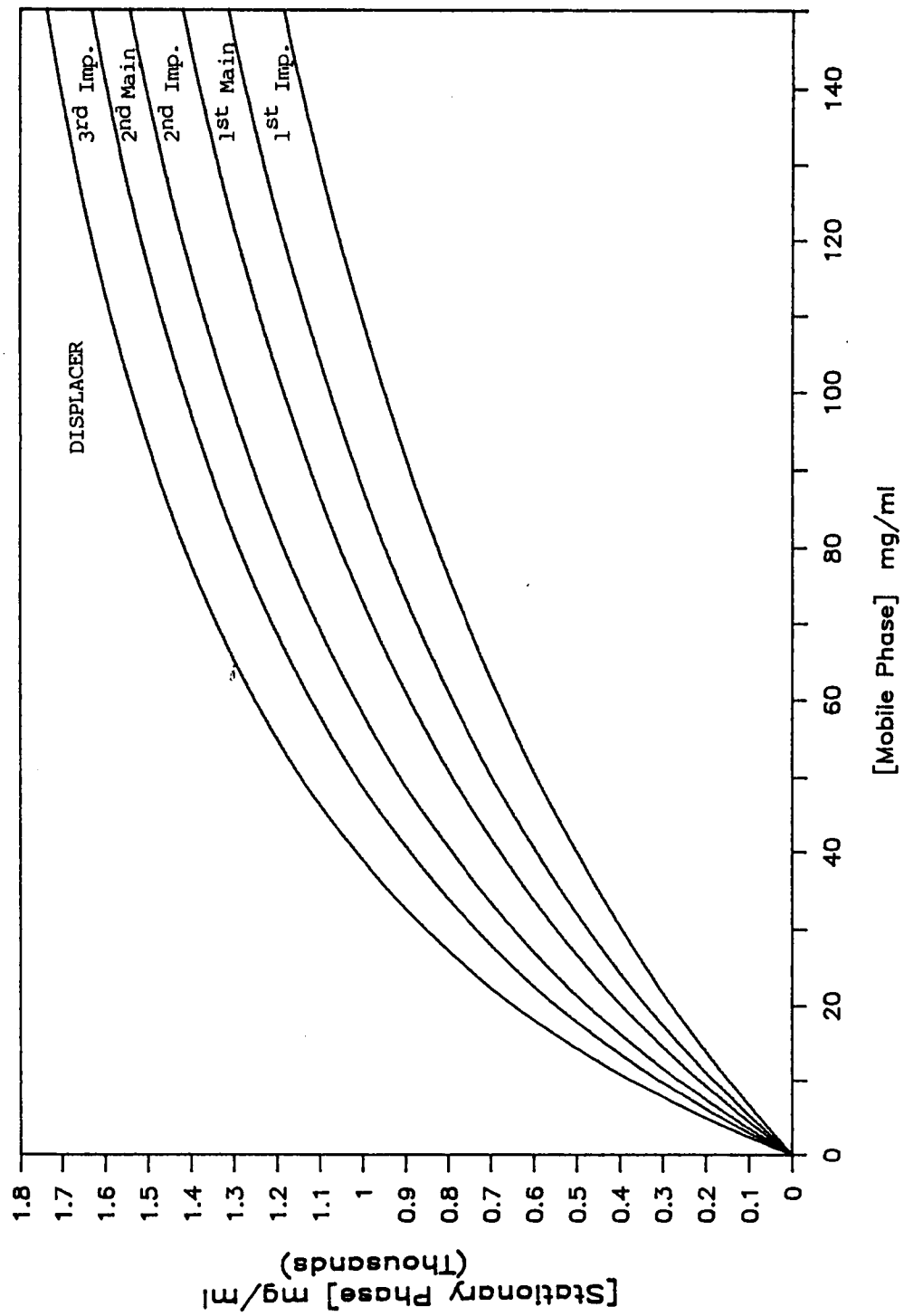
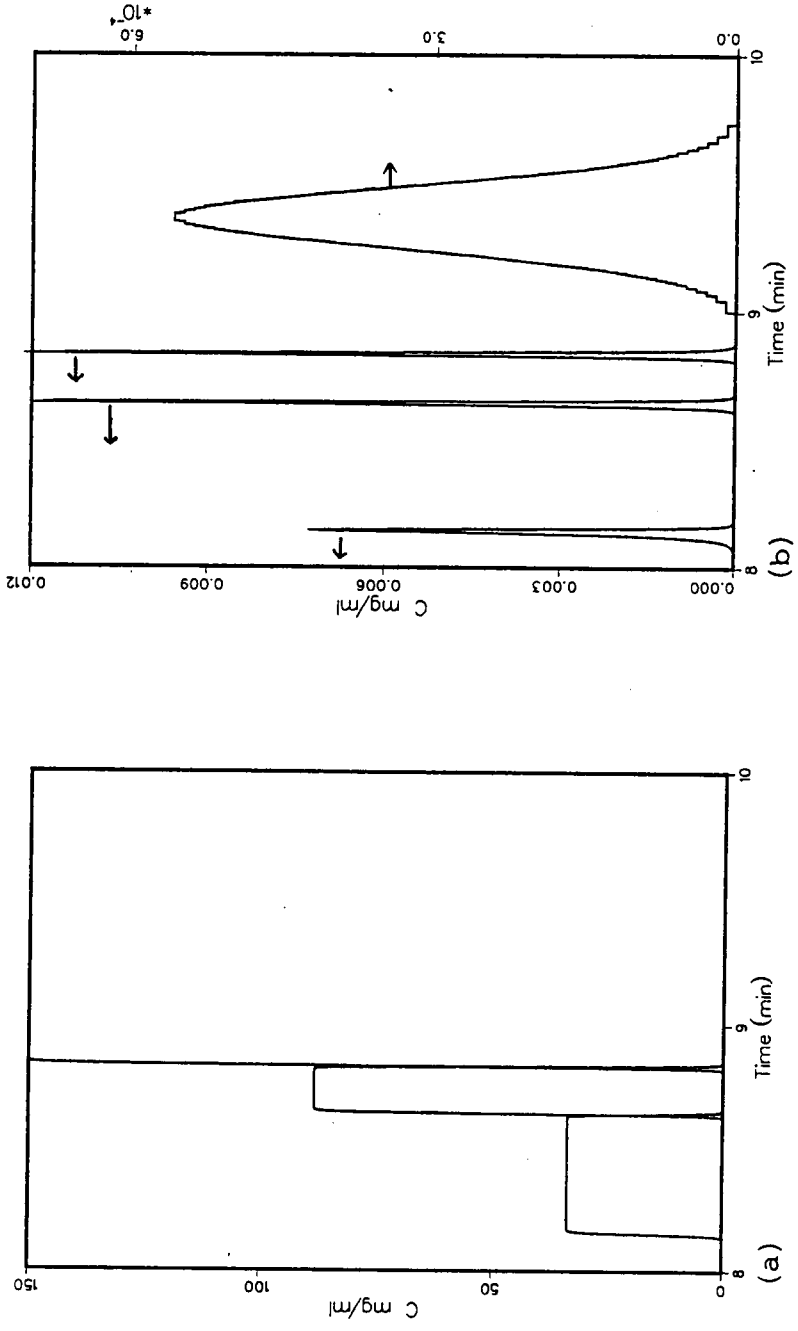


Figure 5.11 Equilibrium Adsorption Isotherms used in Displacement Calculations



(a) Displacement Train of 2 Major component and Displacer
(b) Profiles of the Impurity at Different Position and Linear

Figure 5.12 Displacement of 2 Major and 1 Minor Component on 50 cm Column

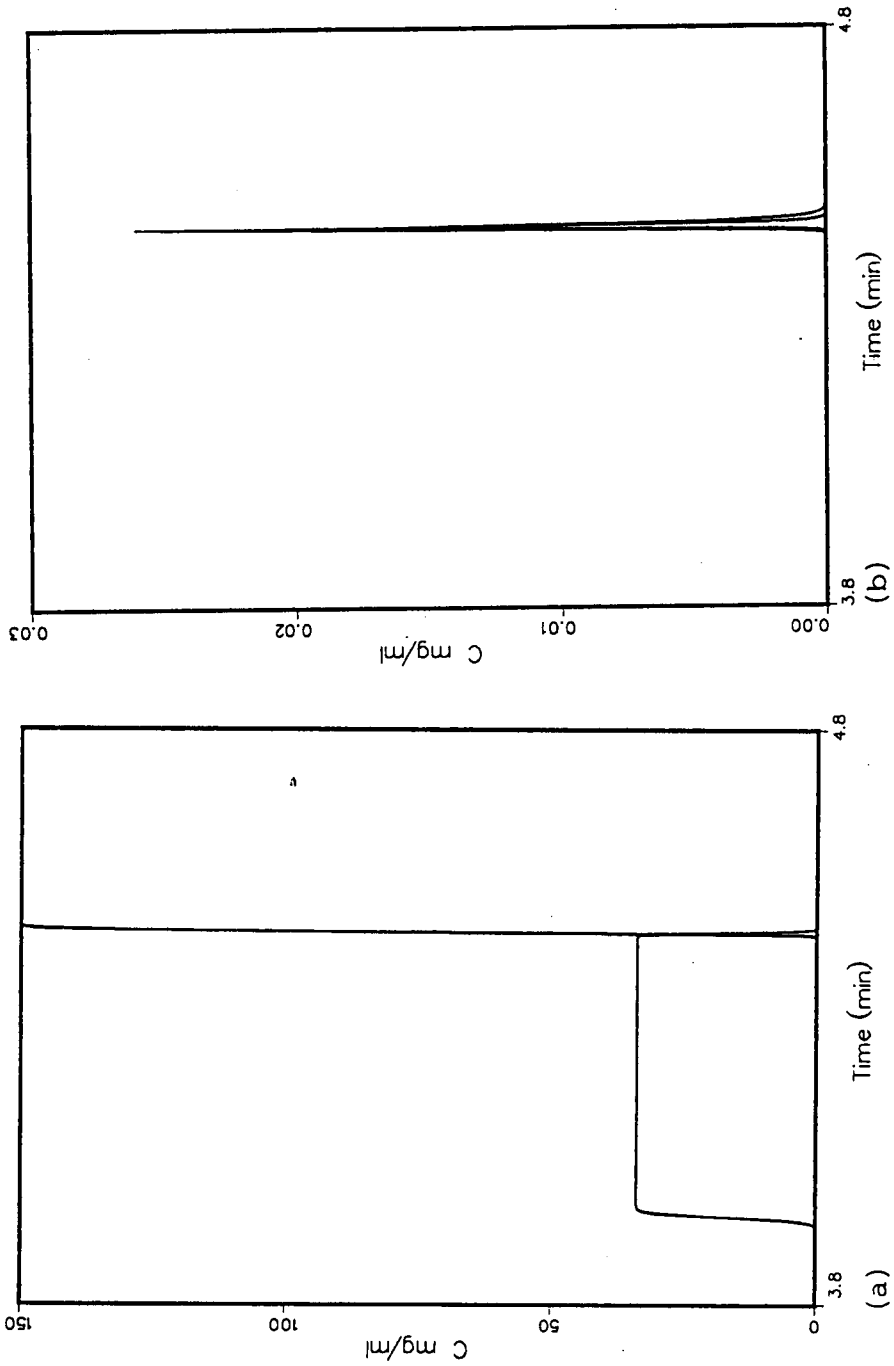
Figure 5.12b shows the profiles of the trace impurities eluting in the three positions studied. The impurity is more concentrated when it is compressed between two bands (b and c) than when it elutes first (a). The fourth profile (d) whose ordinate axis is on the right, corresponds to linear elution of the same amount of the impurity as if were injected alone. Note the 20 fold increase in the maximum concentration of the band and the eight fold difference in the base band width.

A system was considered with one major component and two impurities eluting between the major component and the displacer. The chromatograms are shown in Figure 5.13a and 5.13b. Figure 5.13a is the isotachic band profile and 5.13b is the profile of the two impurities. The impurities are compressed into a single zone with no separation.

Isotachic displacement bands were also obtained at 25 cm. Figures 5.14a and 5.14b show the displacement train the profile of the impurity as if it were eluted third. As expected, the band shapes are exactly the same for the 50 and 25 cm columns. The breakthrough front dramatically increase the production time especially in view of column regeneration.

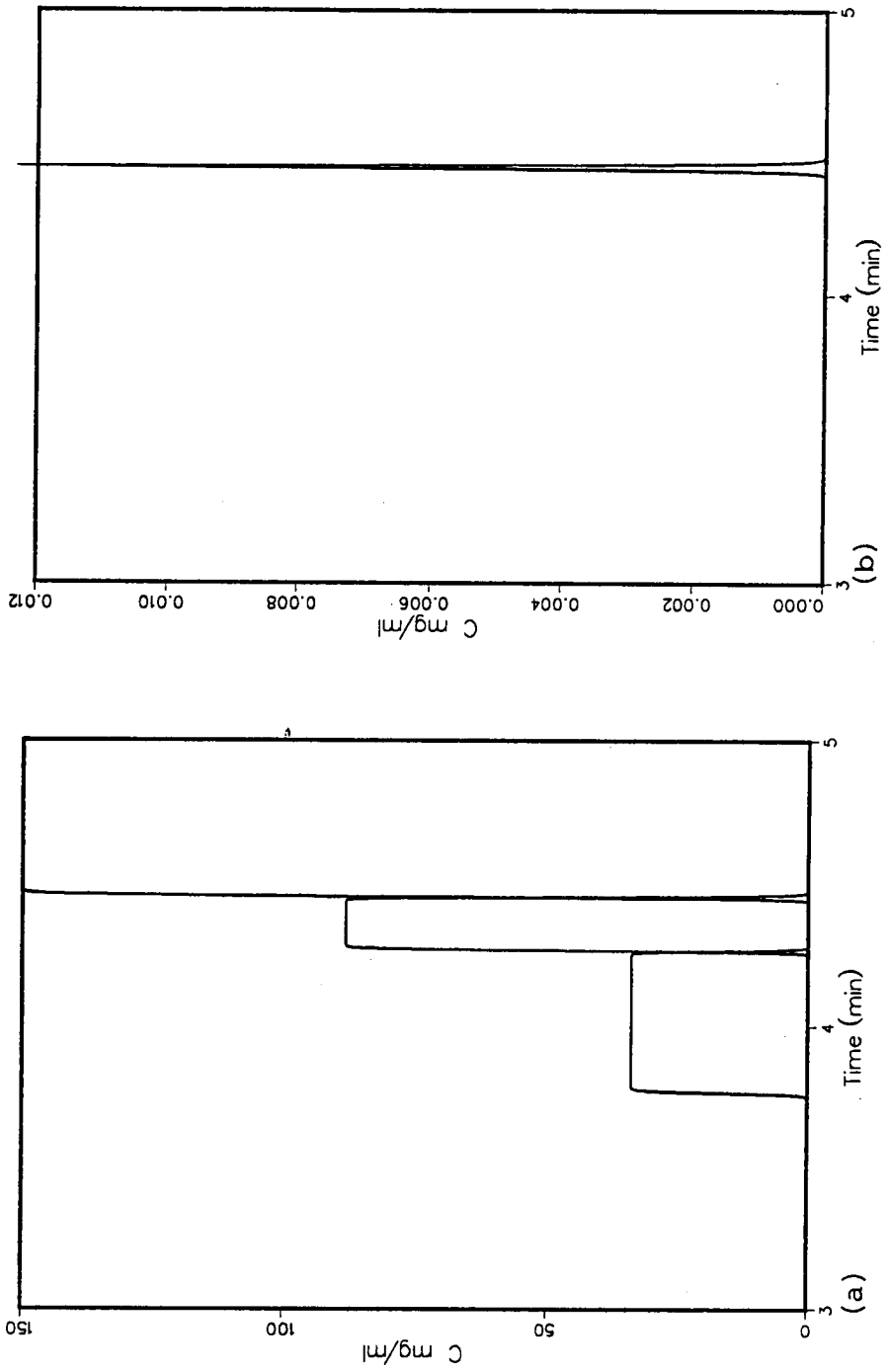
These results show that displacement chromatography can aid in the solution of two different problems. First is the removal of trace impurities from a major component when the major component is of interest. Second is the concentration and enrichment of impurities from concentrated solutions.

These results were compared with the overloaded elution mode chromatography. Using the same isotherms and injecting the same amount, Figure 15a shows the overloaded elution band containing 100 mg



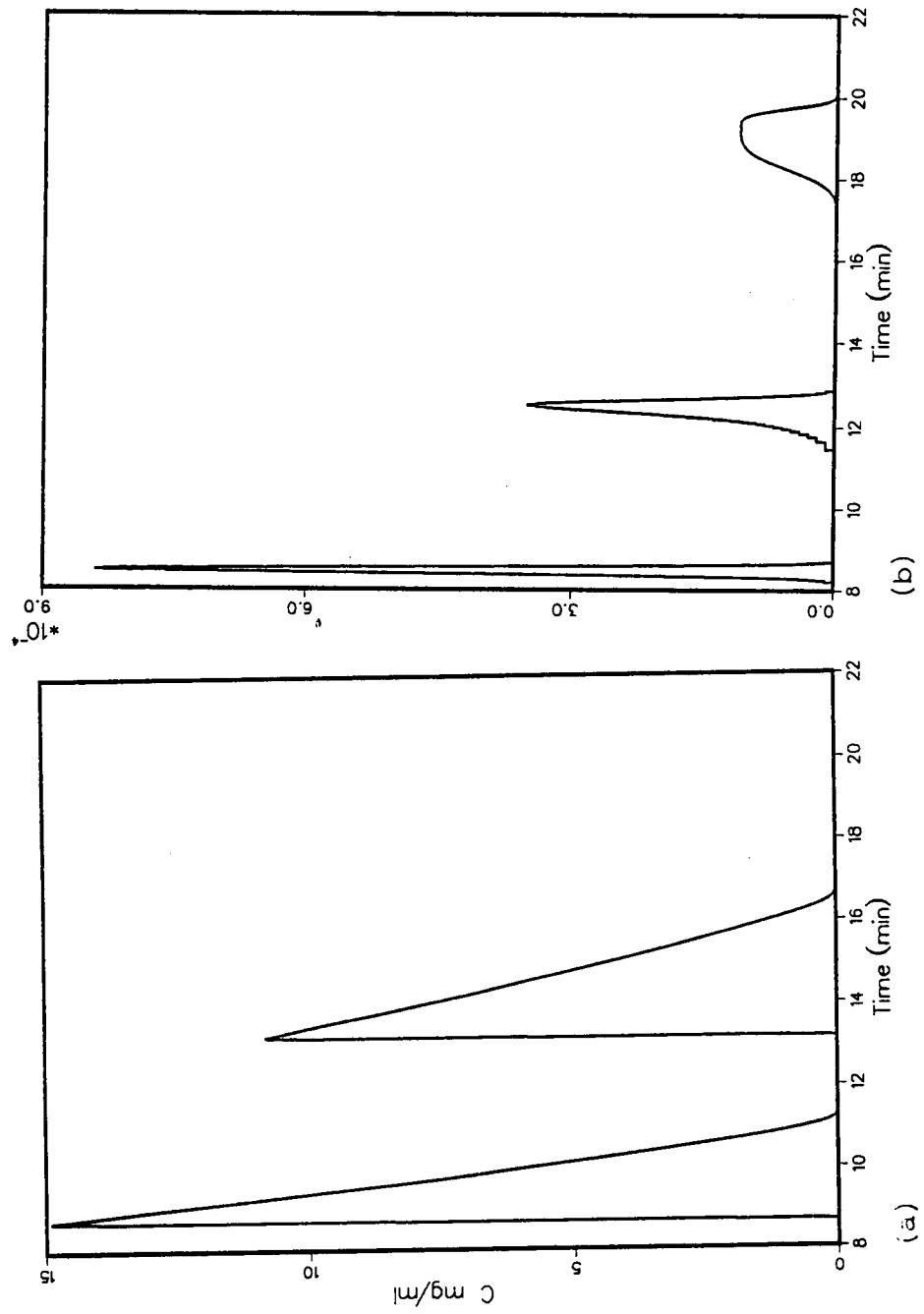
(a) Displacement Profile of Major Component and Displacer
(b) Profile of Coeluting Impurities

Figure 5.13 Displacement Train with 1 Major component and 2 Minor Components on 25 cm Column



(a) Displacement Profile of 2 Major Components and Displacer
(b) Profile of Impurity Eluting between 2nd Major Component and Displacer

Figure 5.14 Displacement Train with 2 Major Components and 1 Minor Component on 25 cm Column



(a) Overloaded Elution Profile of Major Components
(b) Elution Profile of Impurities at Different Positions

Figure 5.15 Overloaded Elution Chromatogram on 25 cm Column with Impurities at different Positions

of each of the major components on a 50 cm column. Figure 15b shows the profiles of the impurities eluting in their respective positions. Although the first elution impurity is compressed, its maximum concentration is 9 times less than the first eluting in displacement chromatography. However its maximum concentration is two-thirds higher than in linear elution chromatography and is 8 times narrower at the base of the band. The second and third elution components are more dilute than in linear elution chromatography are even broader at the base.

These results show that the advantage of fast cycle times of overloaded elution chromatography has a disadvantage of the hiding impurities during elution. The advantage of high concentration zones of displacement chromatography has the disadvantage of column regeneration.

Chapter 6

Optimization of Binary Overloaded Elution Separations

The semi-ideal model of chromatography is used to calculate the influence of the sample amount and the volume for several binary mixture on the production rate achieved in preparative liquid chromatography. Among the unsolved problems, one of the simplest, yet of highest practical importance, is to know whether large volume dilute samples or small volume concentrated samples, holding the amount injected constant, should be injected into preparative columns for maximum production rate of the desired component. Another question addressed is what is the optimum amount injected which yields the largest production rate. This chapter will be restricted to binary separations in overloaded elution chromatography.

6.1 Effect of Loading Factor and Sample Volume

This section assumes that the column length is constant, 25 cm, the production rate is proportional to the cross-sectional area and the HETP is 56 um (4450 theoretical plates). The column is operated at a high mobile phase velocity, 0.625 cm/sec. For the separations studied in this section, the dead time was 40 seconds, the retention time of the first component was 270 seconds and the elution time for the second component was adjusted according to the relative retention. The void fraction was 0.8 and the phase ratio 0.25. In all cases, the

production rate and yield were calculated assuming 99 % purity for all the fractions collected.

The Langmuir competitive isotherm parameters are a_1=23 ml/ml, a_2= 25 ml/ml, b_1 = 2.38 M^{-1} and b_2 - 2.56 M^{-1}.

The effect of the sample amount and the sample volume on the production rate (umole/cm2 s) of a binary mixture at 99 % purity was studied for six two-component mixtures. Three of the mixtures have the same relative amount injected (1/3), but the separation factors was varied (1.09, 1.25 and 1.7). At a separation factor of 1.7 mixtures having a relative composition of 1/9, 1/3, 3/1 and 9/1 were studied. Table 6.1 summarizes the conditions for the optimum production rate which are discussed in detail below.

Definitions

Throughput: Amount of sample injected per unit time per unit cross-sectional area.

Production Rate: The amount of sample recovered at the desired degree of purity per unit time per unit column area.

$$Pr_i = \frac{Y_i L_f \left(\frac{a}{b}\right) f_{i,comp} (1-\epsilon) L}{t_{cycle}} \qquad (6.1)$$

where Y_i is the yield of component i, L_f is the loading factor, (a/b) is the ratio of the Langmuir parameters (mmole/cm3 stationary phase), f_{icomp} is the fraction of component i in the mixture, L is the column length, e is the porosity and t_{cycle} is the cycle time. Thus, the definition of production rate is reported per unit cross-sectional area.

Table 6.1 Experimental Conditions for Optimum Production Rate

Total Comp. #	alpha	Mix Comp.	Individual Production Rates*	Yield	L_f (%)	Vol+ (s)	Prod. Rate!
1	1.09	1/3	1.494	0.383	4.25	1	3.298
2			2.30	0.983	0.9	1	3.196
1	1.25	1/3	6.99	0.503	29.2	1	15.515
2			12.17	0.983	5.9	1	16.244
1	1.7	1/3	16.581	0.590	95.2	3	46.463
2			35.059	0.993	34.0	1	46.477
1	1.7	3/1	49.005	0.546	104	5	57.208
2			92.82	0.959	29.1	1	38.134
1	1.7	1/9	65.27	0.649	82.5	1	53.652
2			52.717	0.992	43.1	1	58.073
1	1.7	9/1	64.831	0.517	122	5	67.919
2			34.64	0.812	33.2	1	41.383

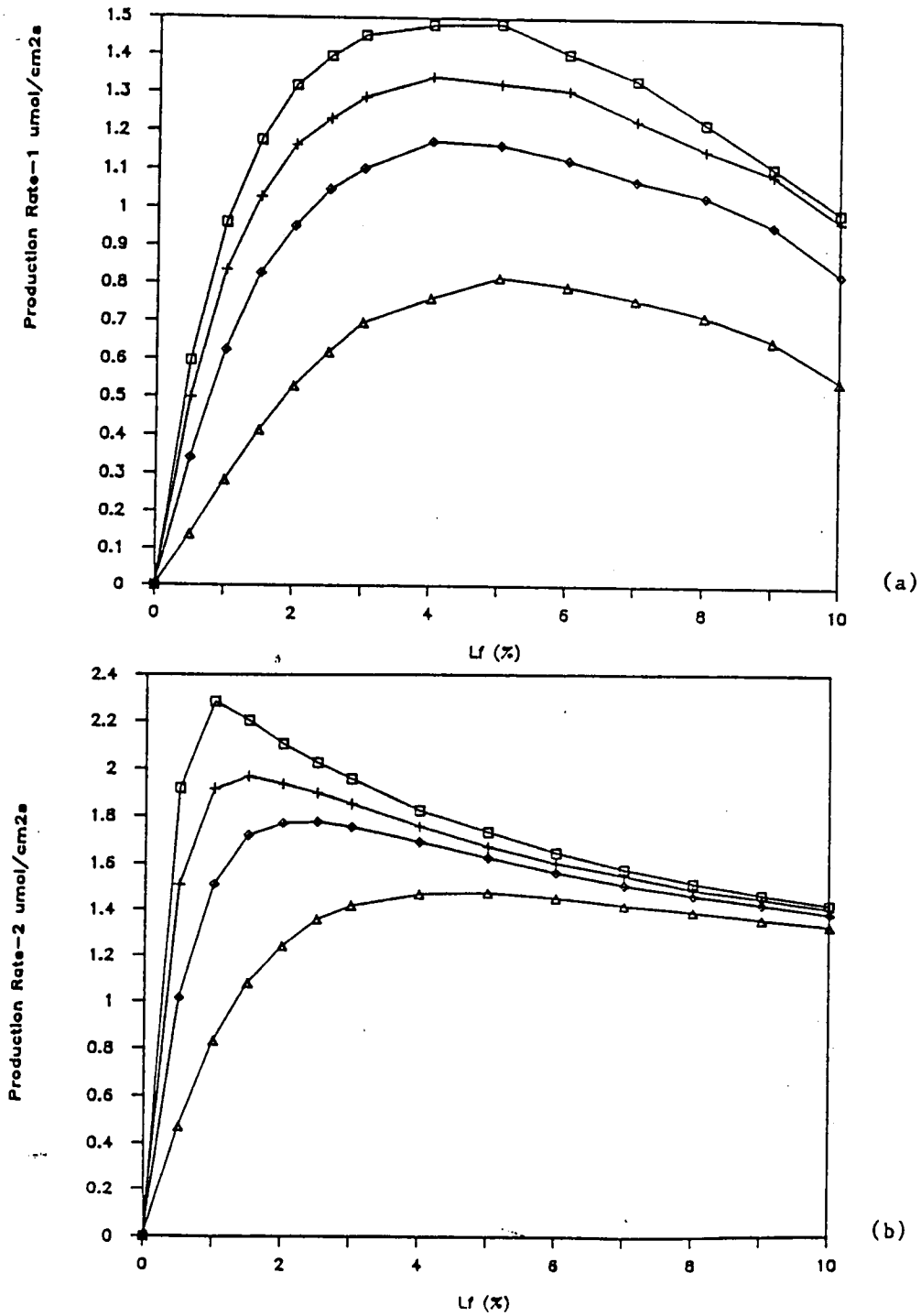
* umoles/cm²s
\+ the injection width in number sigma units
! production rate of component 1 and 2 at the specified conditions

Cycle Time: The cycle time in this study is considered the minimum cycle time required for consecutive repeated isocratic injections. The first component of the (n+1)th injection begins to elute just after the second component of the nth injection. The endpoints of the chromatogram are defined arbitrarily as the time when the concentration equals 10-15 moles (femtomole).

Loading Factor: The amount of sample reported as the fraction of the column saturation capacity, $L_f = 100\ n_i/n_{sat}$.

Influence of the Separation Factor

Figure 6.1 illustrates the effect of the loading factor and the sample volume on the production rate of components 1 and 2 for a sample having a separation factor of 1.09 and a relative composition of 1/3. Each curve corresponds to constant sample injection volume of 1, 3, 5 and 10 standard deviations of a Gaussian peak; respectively. This corresponds to a 500 ul, 1.5 ml, 2.4 ml and 5 ml injection on a standard analytical column. Figure 6.1a shows the production rate versus loading factor curves at different volumes injected for component 1 and Figure 6.1b for component 2. For both components, as the injection volume increases the production rate at a given loading factor decreases. In particular, the maximum production rate decreases with increasing volume. The maximum production rate for a dirac injection is slightly smaller than for the 1 sigma injection. However, in most cases it would be unrealistic to consider a dirac injection because of practical limitations in solubility. Knox and Pyper have already shown that little band broadening is achieved for a pure



□ 1, + 3, ♦ 5, ▽ 10 standard deviations

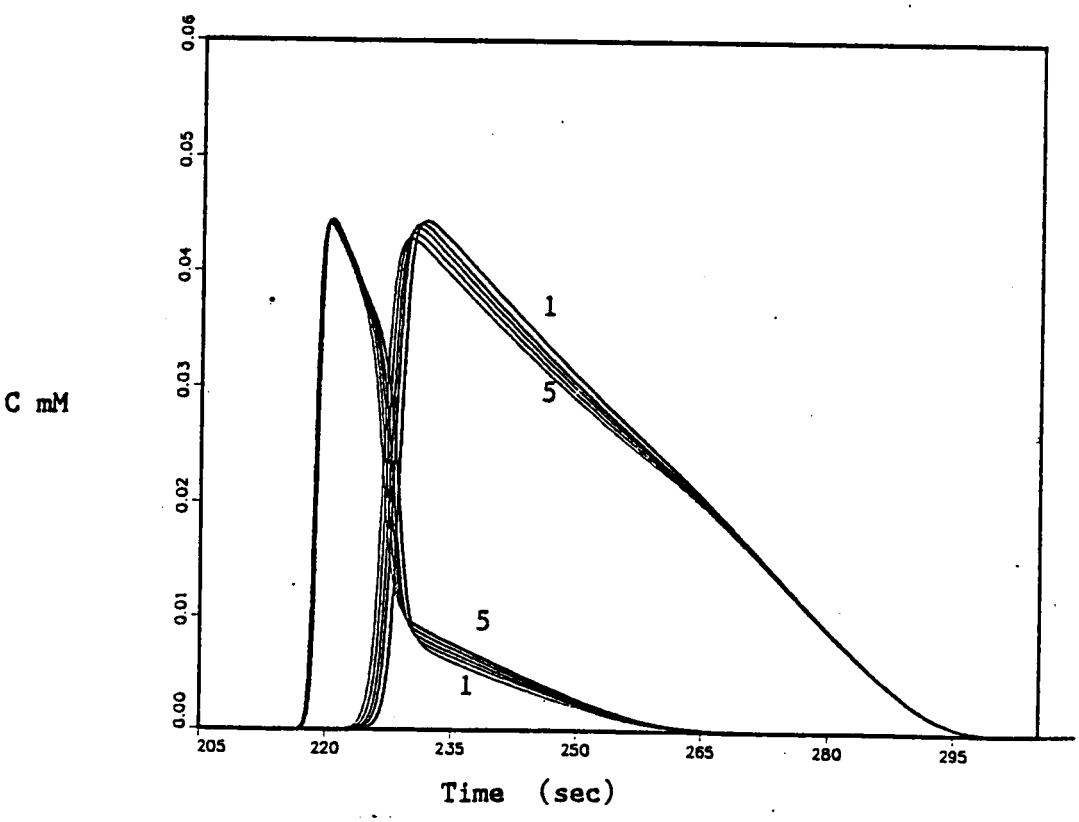
(a) Component 1 (b) Component 2

Figure 6.1 Production Rate versus Loading Factor (%), 1/3, α=1.09

component as long as the sample volume does not exceed half the volume of the peak (2 sigma).

The optimum loading factor for maximum production rate at constant column length, linear velocity and particle size is 4.5 % for component 1. The maximum production rate decreases form 1.5 to 0.75 um/(cm^2 s) when the sample volume is increased from 1 to 10 standard deviations while the corresponding loading factor increases from 4.3 % to 5 %. For the second component, the optimum loading factor at the maximum production rate increases from 0.8 % at 1 sigma to 5 % for a 10 sigma injection while the corresponding production rate decreasing with increasing volume from 2.3 to 1.5 umole/(cm^2 s). In contrast to the first component, at large loading factors an asymptotic value of the production rate for component 2 appears at approximately 1.2 umole/(cm^2 s).

Figure 6.2 illustrates the influence of the injection volume for a 1/3 mixture at a selectivity of 1.09 and a loading factor of 2 %. This loading factor is intermediate between the optimum value for component 2 (0.9 %) and 1 (4.3 %). The elution time for this set of chromatograms is adjusted by subtracting the injection time. Using the adjusted time, the band fronts and tails coincide. The peak height of component 1 is unaffected by the injection volume while that of component 2 decreases slightly as the injection concentration increases. The width of the first component decreases with increasing volume, while the width of the second component increases with increasing volume. The asymmetry factor (width at 10 % of the peak height) for the first component increases with increasing sample volume



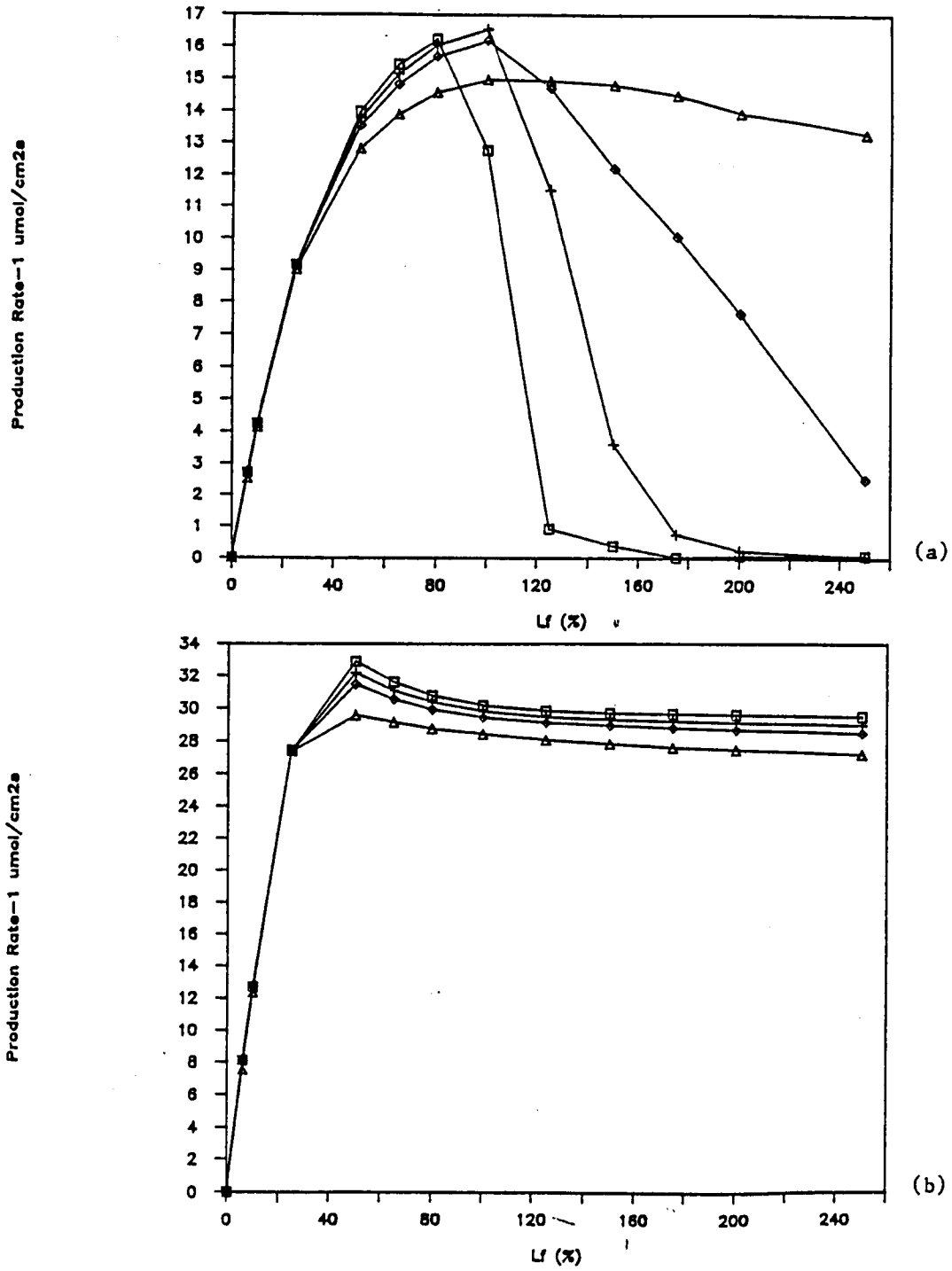
(1) Dirac, 2, 3, 4, 5 standard deviations (5)

Figure 6.2 Influence of the Sample Volume on the Band Profile, L_f 2 %

and it follows a similar pattern for the second component.

The selectivity was increased to 1.25 and to 1.7 for the same sample composition (1/3). The variation of the production rate for each component as a function of the loading factor are qualitatively very similar for these two selectivities. Accordingly, only the results obtained for a separation factor of 1.7 are reported in Figure 6.3. A plot of the production rate versus loading factor for component 1 and 2 are shown in Figures 6.3a and 6.3b; respectively. For this mixture where the selectivity is large, the sample volume has little effect on the production rate except at very large loading factors where a large drop in the production rate with increasing volume is seen. This is because the loading factor is so large that the nonlinear self-sharpening effects are stronger than the band broadening introduced by the injection. As the loading factor increases, the first component in compressed and concentrated. However near the maximum production rate, slight increases in the amount injected cause the fronts of the two components to become very close to each other thus giving a sharp drop in the production rate.

The curves in Figure 6.3a are very similar to those in Figure 6.1a except for the curve corresponding to the 10 sigma injection. It is believed that this curve is qualitatively different from the others due completely different band shapes caused by frontal effects. Figure 6.3b shows the production rate of component 2 as a function of the loading factor. Similar to Figure 1b, the curve goes through a maximum, but in contrast to the Figure 1b, separation factor 1.09, the maximum is less pronounced. An asymptote is seen at large loadings



□ 1, + 3, ♦ 5, △ 10

(a) Component 1 (b) Component 2

Figure 6.3 Plot of the Production Rate vs the Loading Factor, 1/3, α = 1.7

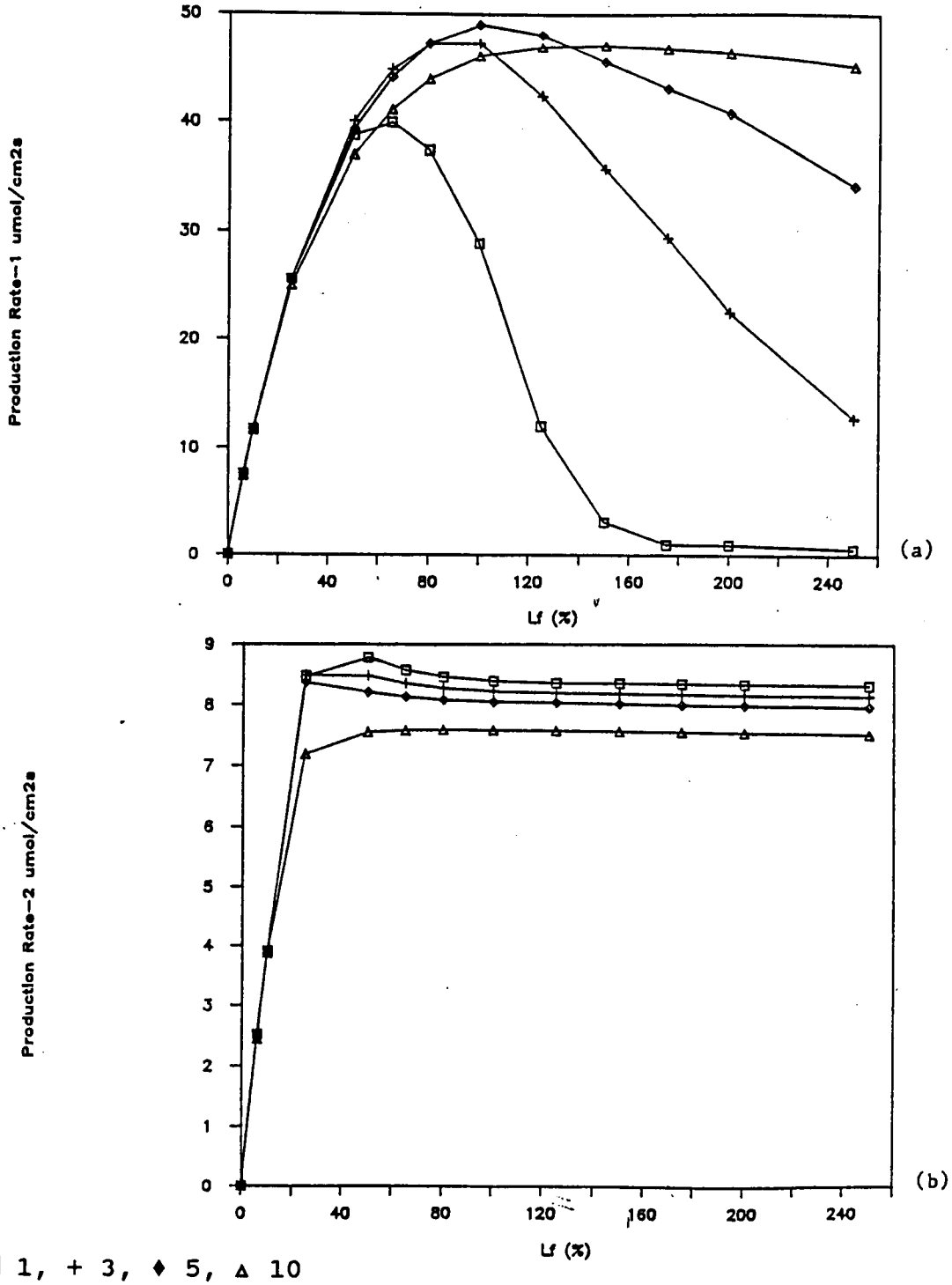
approaching 26 umole/(cm^2 s).

It appears for this mixture that the optimum loading factor is nearly the same for the different sample volumes. This is also true for the 1/3 mixture with a relative retention of 1.25 which is not shown. For components 1 and 2, separation factor of 1.7, the values of the optimum loading factor is approximately 90 % and 40 %; respectively. The production rates at these values of the loading factor are 16 and 33 umoles/(cm^2 s) for each component.

Influence of the Composition of the Binary Mixture

The production rate for a 3/1 mixture, separation factor 1.7 is shown in Figure 6.4. In contrast to the 1/3 mixture, the sample volume influences somewhat the values of the maximum production rate of component 1 and of the optimum loading factor (see Figure 6.4a). In this case there is an optimum sample volume, giving the highest production rate for the first component. This optimum volume is 5 standard deviations. The optimum loading factor is large, approximately 105% column saturation capacity and the maximum production rate, 49 umoles/cm^2s.

The same result is not true for component two (see Figure 6.4b). The production rate increases rapidly at first with increasing value of the loading factor, and then it tends asymptotically towards values of 8.3, 8.1, 8.0 and 7.4 umoles/cm^2s for 1, 3, 5, and 10 sigma injections; respectively. The optimum loading factor is approximately constant, at 30 % of column saturation capacity corresponding to a production rate of 9.3 umoles/cm^2s.



□ 1, + 3, ♦ 5, ▵ 10

(a) Component 1, (b) Component 2

Figure 6.4 Plot of the Production Rate vs the Loading Factor, 3/1, α = 1.7

Similar studies to the ones described above were carried out for a 1/9 and a 9/1 mixture. The qualitative trends observed for the influence of the loading factor and the sample volume on the production rate are similar to those already reported for the 1/3 and 3/1 mixtures.

Table 6.1 summarizes the conditions under which the maximum production rate is achieved for the first and the second components, for all the mixtures investigated. The first observation is that the values of the maximum production rate, the optimum sample volume and amount injected corresponding to this maximum production, are different for the two components of a binary mixture. The loading factor which gives the maximum production rate for component one is always much greater than that for component two. This is because, in order to optimize the production rate for component one, it is important to take advantage of the displacement effect which tend to concentrate this component. In contrast, in optimizing the production rate for component two, one should use displacement effects, but to a limited degree.

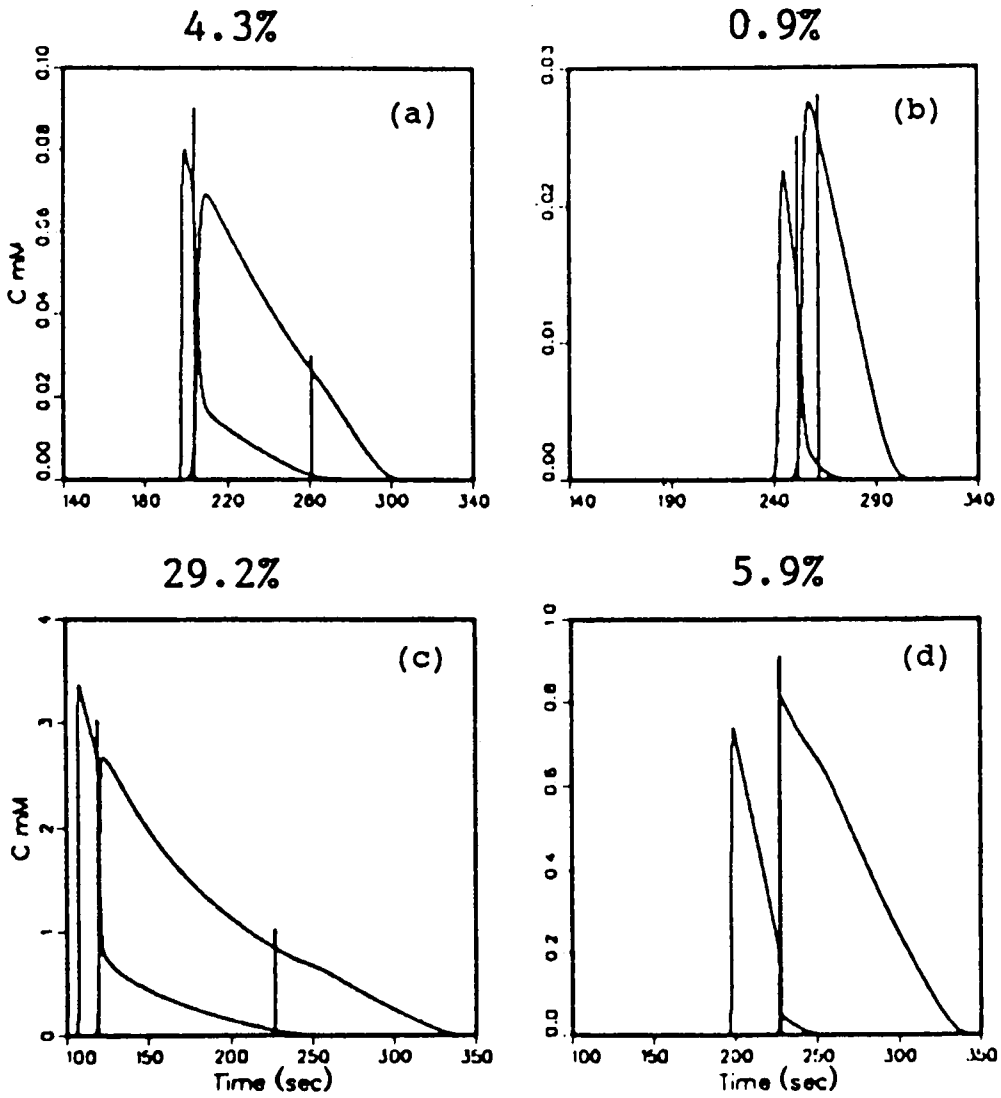
Clearly, the larger the separation factor the more the column has to be overloaded in order to achieve the maximimum production rate and throughput. The values of the total production rates corresponding to the maximum production of either component 1 or 2 are very close, except for mixtures containing more component 1 than 2. In this case the throughput corresponding to the maximum production rate of compound 1 is much larger (about 50%) than the throughput corresponding to maximum production of component 2. The difference between the two

throughput values is large when the lesser concentrated component elutes last because of the tag-along effect [Ghodbane (1988a)].

Elution Band Profiles under Optimum Conditions.

Elution band profiles of the two components of the mixture simulated under different sets of experimental conditions (different values of the selectivity and composition) are shown on Figures 6.5.to 6.7. In each case the values of the loading factor and the sample volume corresponding to the maximum production of either component 1 or 2 have been selected. On each chromatogram the cut points for 99 % purity are also shown. The area between the two vertical lines is the portion which requires recycling. It should be emphasized that the optimum experimental conditions, especially the optimum value of the loading factor, corresponding to the maximum production of one component are very different from those corresponding to the maximum production of the other. Accordingly, when both compounds have to be recovered pure, a compromise involving the operation cost and the value of the production has to be found.

Figure 6.5 shows the chromatograms corresponding to the optimum conditions for 1/3 mixtures having separation factors of 1.09 (Figs. 6.5a and 6.5b) and 1.25 (Figs. 6.5c and 6.5d); respectively. If component 1 is the product of interest (Figs. 6.5a and 6.5c), the second component which is in a higher concentration is employed to displace and concentrate the first component. The amount injected and processed is large, but the yields are moderate or low. For component 1, the yields vary between 40 and 60% (see Table 6.1), depending on



(a) Component 1, selectivity 1.09, Mixture Composition 1/3, Lf 4.25%, sample volume 1s
(b) Component 2, selectivity 1.09, Mixture Composition 1/3, Lf 0.90%, sample volume 1s
(c) Component 1, selectivity 1.25, Mixture Composition 1/3, Lf 29.2%, sample volume 1s
(d) Component 1, selectivity 1.25, Mixture Composition 1/3, Lf 5.90%, sample volume 1s

Figure 6.5 Calculated Chromatograms Corresponding to the Optimum Production Rate for each Component, 1/3, selectivity 1.0 and 1.25

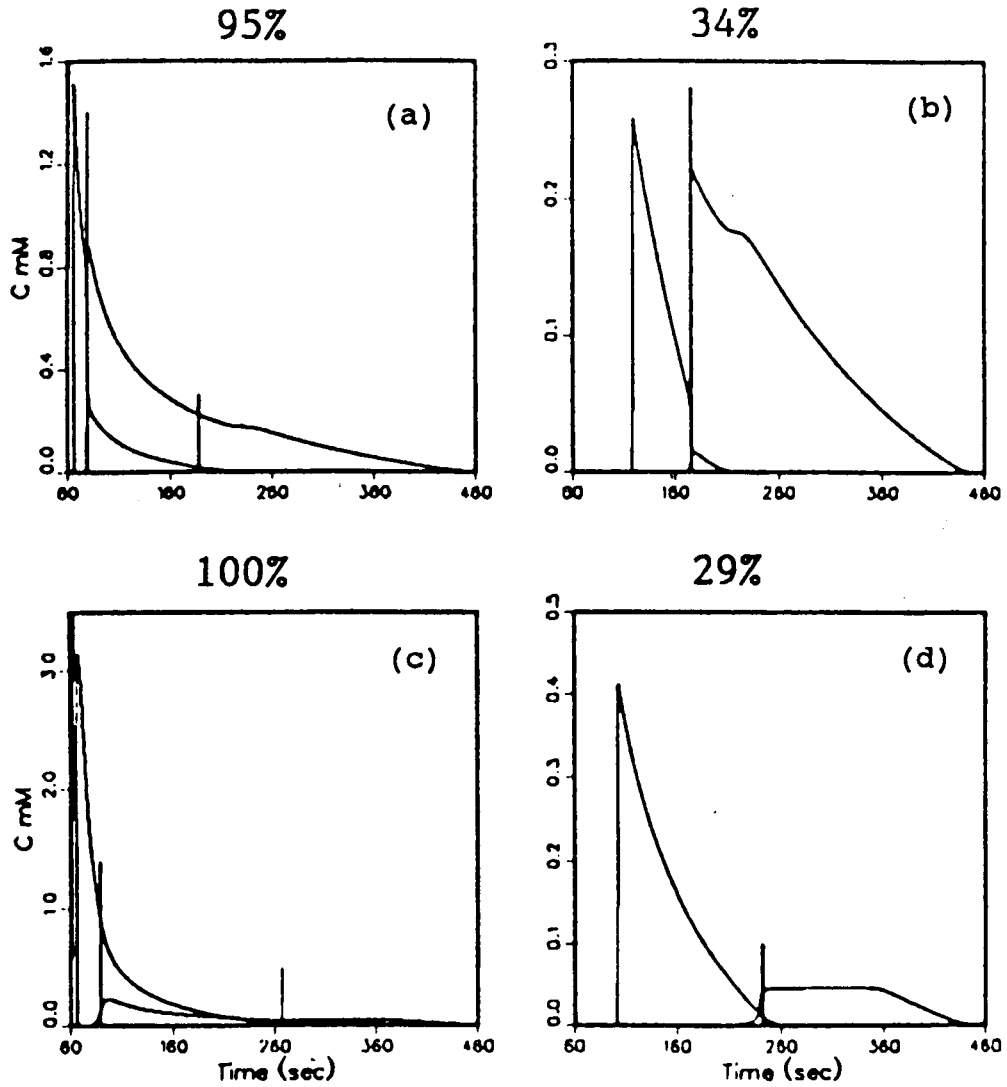
the characteristics of the mixture. The yield increases with increasing selectivity. If component 2 is the product of interest, on the contrary, more modest degrees of column overload permit a marked reduction of the relative importance of the intermediate zone of overlap in the chromatogram (see Figs. 6.5b and 6.5d). The yields achieved for the component of interest are much larger than in the previous case. Most yields exceed 95% (see Table 6.1).

It is interesting to compare Figures 6.5b and 6.5d, which illustrate the chromatograms corresponding to the optimum conditions for maximum production of component 2, for a = 1.09 (Fig. 6.5b) and for a = 1.25 (Fig. 6.5d). Since the separation factor is small in the former case, there is band overlap and at the cut point the displacement effect is still small, barely sufficient for the band of component two to begin pushing the tail of component one.

On the other hand, when the separation factor is increased to 1.25 for the same mixture composition, the chromatogram corresponding to the optimum conditions for the production of component 2 (Fig. 6.5d) exhibits nearly complete separation of the two bands. Although considerable interaction between the bands still takes place. The tail of the first component band is almost completely displaced and the little part which is eluted after the second shock of the band system is small enough that the fraction cut may be placed at the second shock. This allows achievement of 99% purity of component 2, 100% yield for the second component and 99% yield for the first component at a purity largely exceeding 99%.

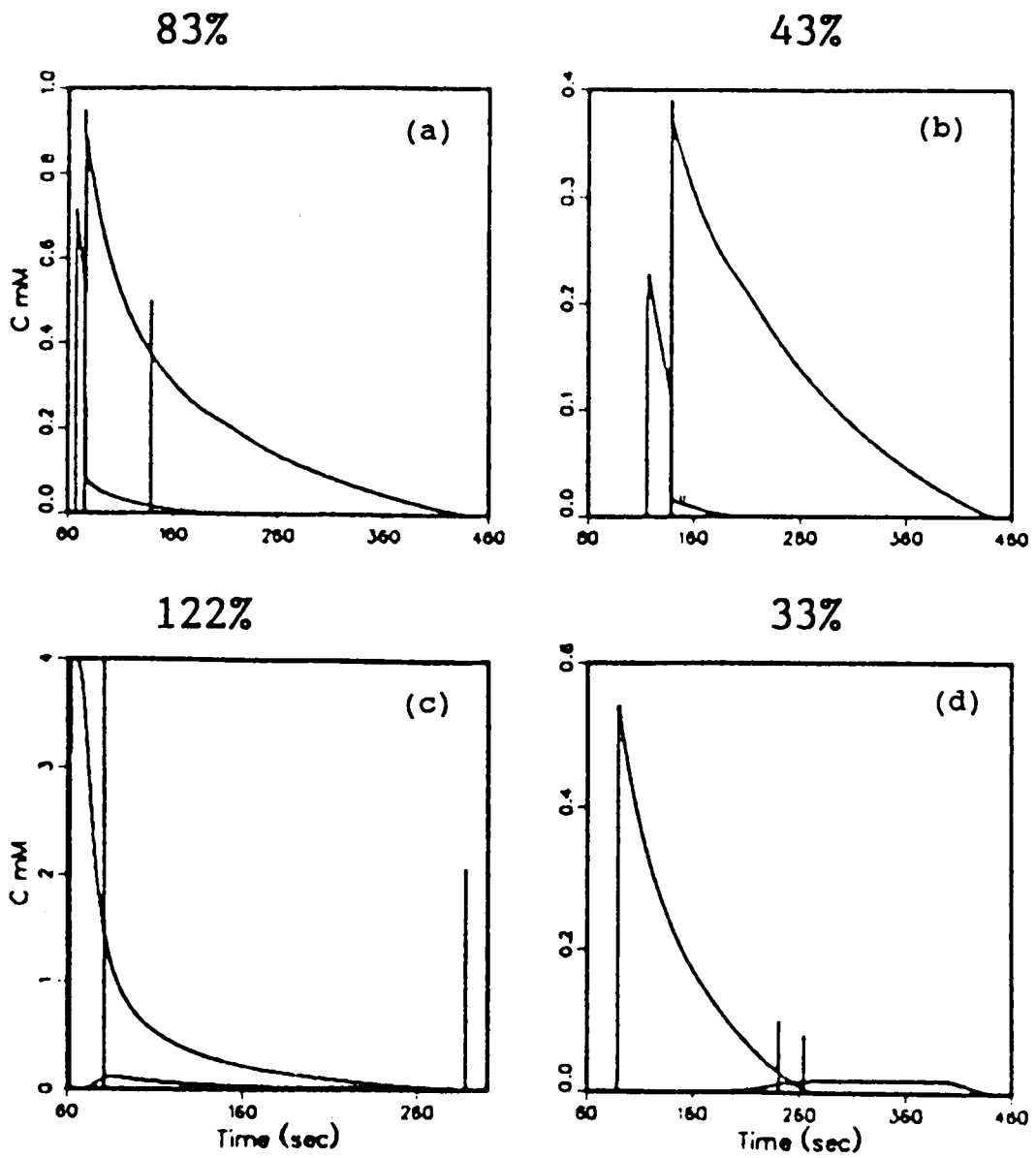
Figure 6.6 shows the chromatograms obtained for the 1/3 and the 3/1 mixtures at a separation factor of 1.7. With larger separation factors, much larger injected amounts are required to achieve equivalent displacement effects. This in turn means higher band velocities. Thus, concentration shocks of the first component are eluted nearly at the dead time: the elution time of the front of the first component (60 sec) is very near the dead time (40 sec), as seen in the case of the optimization of the production of the first component from both the 1/3 and the 3/1 mixture (see Figs. 6.6a and 6.6c). This is in contrast with the elution time of the first component front observed with a separation factor of 1.25, 100 seconds (Fig. 6.5c) and 200 seconds (Fig. 6.5d) for the optimization of the production of components 1 and 2, respectively. For the production of component two, on the contrary, displacement effects are used minimally to achieve the highest production rate with just enough band overlap to permit the achievement of the purity requirements (Figs. 6.6b and 6.6d).

Lastly, the chromatograms for the optimum production of either components 1 or 2, for a 9/1 and a 1/9 mixture is presented in Figure 6.7. In general, the displacement effects are used to squeeze and concentrate the band of component 1, which permits a large production if a moderate yield is acceptable. The experimental conditions become rapidly critical, however. If the amount injected is increased slightly beyond the optimum in the case of Figure 6.7a, the front of component two would soon catch up with that of component one and be eluted nearly at the same time, which would thus result in a severe



(a) Component 1, selectivity 1.7, Mixture Composition 1/3, Lf 95.2 %, sample volume 3s
(b) Component 2, selectivity 1.7, Mixture Composition 1/3, Lf 34.0 %, sample volume 1s
(c) Component 1, selectivity 1.7, Mixture Composition 3/1, Lf 104 %, sample volume 5s
(d) Component 2, selectivity 1.7, Mixture Composition 3/1, Lf 29.1 %, sample volume 1s

Figure 6.6 Calculated Chromatograms Corresponding to the Optimum Production Rate for each Component, 1/3, 3/1, selectivity 1.7



(a) Component 1, selectivity 1.7, Mixture Composition 1/9, Lf 82.5%, sample volume 1s
(b) Component 2, selectivity 1.7, Mixture Composition 1/9, Lf 43.1%, sample volume 1s
(c) Component 1, selectivity 1.7, Mixture Composition 9/1, Lf 122%, sample volume 5s
(d) Component 1, selectivity 1.7, Mixture Composition 9/1, Lf 33.2%, sample volume 1s

Figure 6.7 Calculated Chromatograms Corresponding to the Optimum Production Rate for each Component, 1/9, 9/1, selectivity 1.7

loss of production (see Figure 6.3a). In the case of component two, the column should be overloaded only up to the point where the front of the second component is eluted just before the end of the tail of the first one, allowing moderate overlap only. This permits in the same time the achievement of a high (98%) yield and of the purity specifications.

6.2 Comparison with Knox and Pyper

Knox and Pyper have presented a method for finding the optimum throughput which uses a very simple model. They consider that the adsorption behavior of the two components of a binary mixture follows the Langmuir isotherm, but neglect solute-solute interactions. Later Snyder [Eble et al. (1987c)] has attempted to improve over this model by going to the other extreme assumption. The "blockage effect" assumes that there is no competition, but that the molecules of the first eluted component do not "see" the stationary phase in the first part of the column which is "saturated" by the molecules of the second component. The profiles shown above on Figures 6.5 to 6.7 demonstrate that the actual behavior of the eluites is intermediate between those considered in these two models. Even for a selectivity of 1.7, there is some significant degree of competition between the molecules of the two components for adsorption.

The optimum throughput was calculated according to the equations in the reference 1 and are presented in Table 6.2. Since this model does not include solute-solute interactions there is no discrimination between mixtures of different composition (1/3, 3/1, 1/9, 9/1). Knox

Table 6.2 Comparison between Throughputs Calculated by Knox and This Work

alpha	Mixture Composition	Throughput* (umoles/cm^{2}s) ref. Knox	This work
1.09	1/3	0.32	15.5 (1) 4.5 (2)
1.25	1/3	5.69	55.3 (1) 16.6 (2)
1.7	1/9	51.5	100.5(1) 59.1 (2)
-	1/3	51.5	112.0(1) 47.1 (2)
-	3/1	51.5	119.9(1) 38.7 (2)
-	9/1	51.5	139.2(1) 42.7 (2)

*Amount injected per cycle time

and Pyper predict values of the optimum throughput which are much lower than predicted with the semi-ideal model for mixtures having a separation factor of 1.09 and 1.25. However, for the mixtures with a separation factor of 1.7, there is a good agreement for component 2 between their approximate value for the optimum throughput and than those obtained by the semi-ideal model. For component 1, values of the throughput are still double or triple those of Knox and Pyper. This is because the optimum loading factor for component two corresponds to a chromatography which gives a resolution of one, but for component 1 this is not true. The close agreement at high values of the selectivity may be due to the fact that competitive effects are less significant than at lower separation factors. This is in agreement with the fact that the "blockage effect" accounts reasonably well for results obtained at high values of the selectivity (i.e., above ca 1.7 to 2). Moreover, Knox and Pyper assume 100 % yield at 99 % purity will give the optimal production rate which is very near to the conditions for the optimum in this work for component 2.

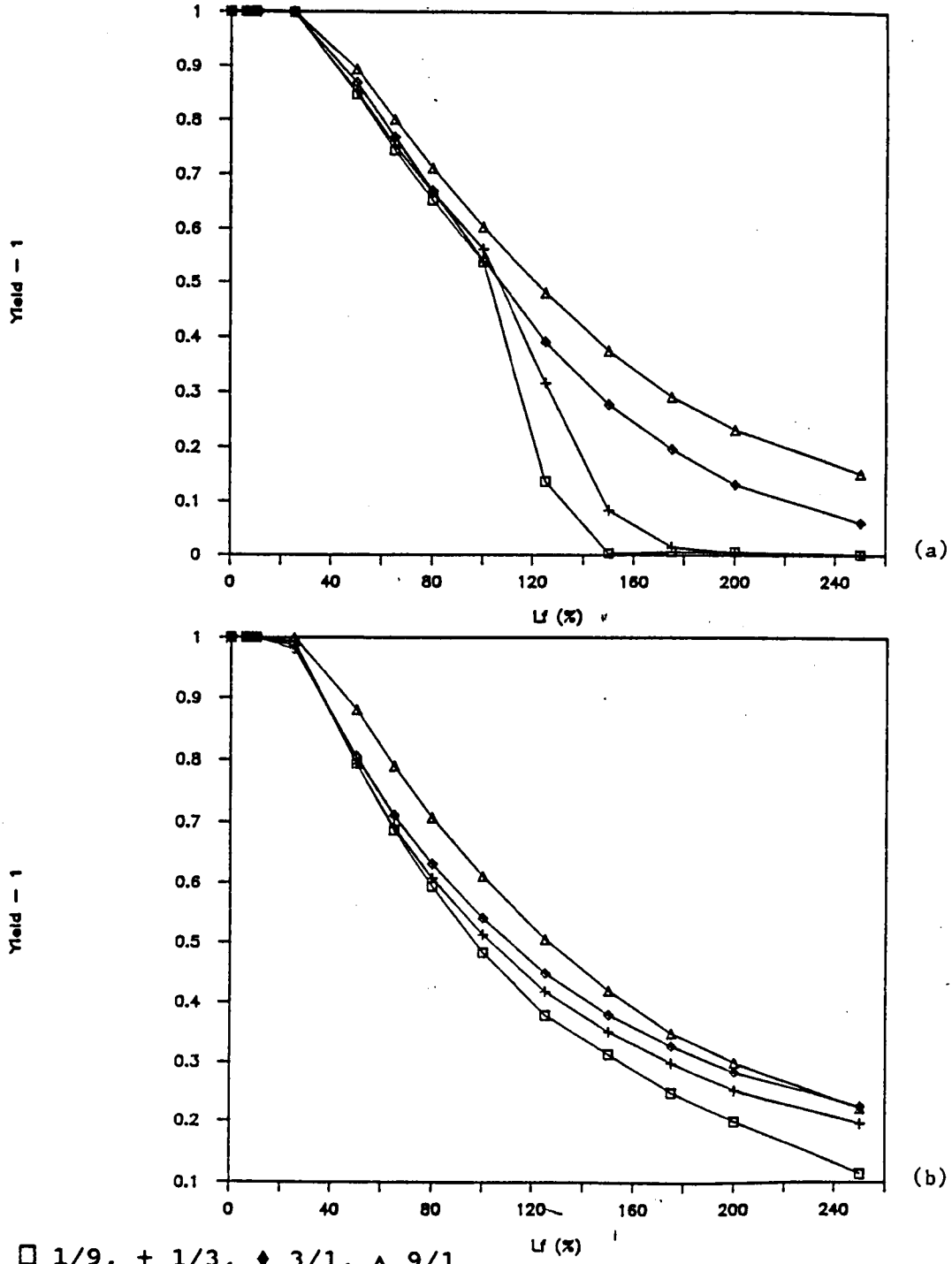
6.3 The Tradeoff between Yield and Production Rate

The yield was studied as a function of the loading factor (fraction of column saturation capacity) for various mixture compositions (1/9, 1/3, 3/1, 9/1) and at 4 different sample volumes (i.e. 1, 3, 5 and 10 standard deviations of the solute gaussian band at infinite dilution). In all cases we observed that all of the yield versus loading factor curves were monotonically decreasing and concave up. More specifically, a pattern can be seen for components 1 and 2

for all the different types of sample mixtures, Figure 6.8 (a=1.7). For component 1, a 1 sigma injection, the yield is practically unaffected by the mixture composition as long as the sample amount is lower than the saturation capacity of the column (see Fig. 6.8a). At values of the loading factor in excess of unity, the yield increases with increasing sample volume as one proceeds from a 1/9 mixture to a 9/1 mixture.

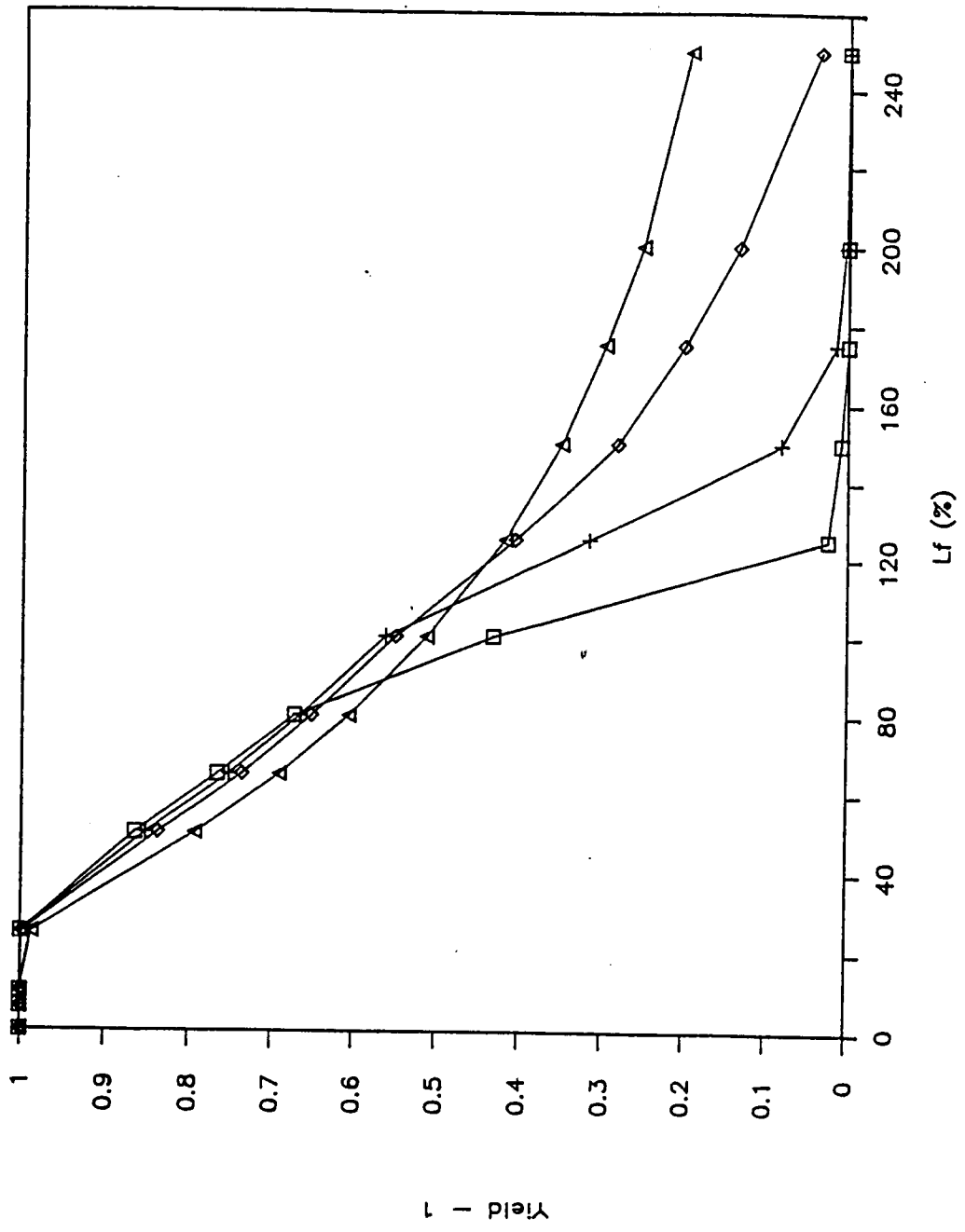
Figure 6.8b illustrates the relationship between yield and loading factor for component 2. As the relative concentration of component 1 increases, the yield decreases at all loading factors, over the entire range of loading factors.

We observed also (results not shown) that at any given sample composition, the sample volume does not affect the yield for component 2. This statement is valid for all sample compositions studied, for selectivities of 1.25 and 1.7. In contrast, the sample injection volume affects the yield for component 1; especially for large loading factors. Figure 6.9 shows a typical example of this effect for a 3/1 mixture. The yield remains nearly the same for all sample volumes up to a loading factor equal to unity. beyond, it falls down rapidly for small sample volumes, less so for moderate values of this volume. The curve for a 10 sigma sample volume injection is qualitatively different from those calculated for the other values of the injection band widths. This is because with a large sample volume frontal effects are taking place. Results similar to those shown on Figure 6.9 are obtained for the 1/3, 1/9 and 9/1 mixtures as well.



□ 1/9, + 1/3, ♦ 3/1, ▲ 9/1
(a) Component 1, (b) Component 2, injection volume 3s

Figure 6.8 Plot of the Yield as a Function of the Loading Factor for Binary Mixtures of Different Composition, selectivity 1.7

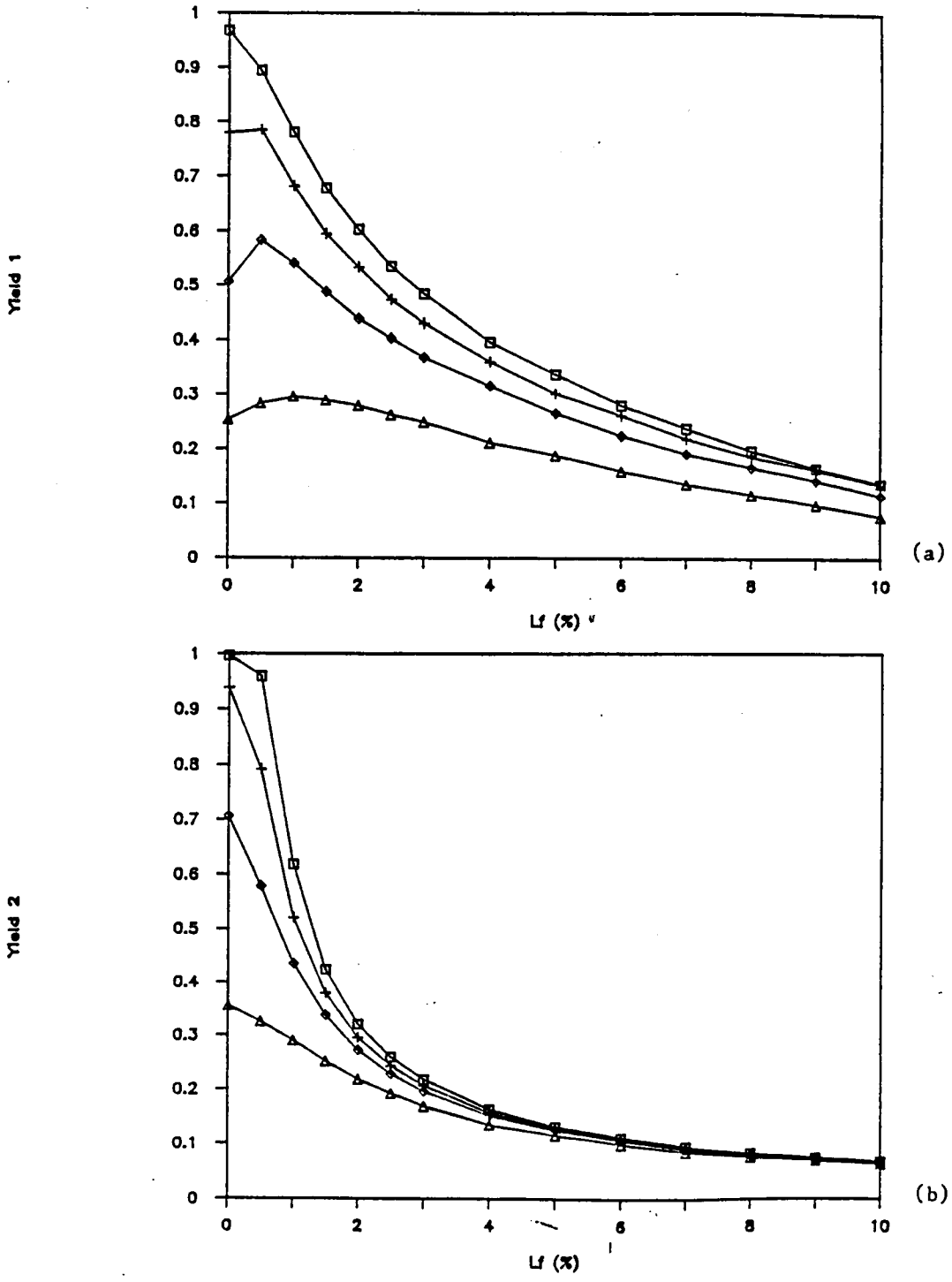


□ 1, + 3, ♦, ▵ 10

Figure 6.9 Plot of the Yield of Component 1 as a Function of the Loading Factor for Samples of Different Volume, 1/3, selectivity 1.7

When the selectivity becomes small, for example equal to 1.09, the yield is strongly affected by the sample volume over a much wider range of sample loadings, i.e., at values well below unity, as illustrated by Figure 6.10 which shows this effect for components 1 (Fig. 6.10a) and 2 (Fig. 6.10b). For both components the yield increases with decreasing sample volume. For component 2, the yield is unaffected by the sample volume at values of the loading factor in excess of 0.03 (3%); however, the recovery yields are very low at such high loadings, which are well above the optimum value for maximum production (see Fig. 6.1).

In preparative liquid chromatography at the process scale, a yield in excess of 80% is often considered desirable. Table 6.1 presents the yield obtained at the optimum production rate for the various mixtures studied. For component 1, the yield at maximum value of the production rate tends to lie between 30% and 70%, a value which is often to low, while for component two the yields are usually greater than 98% a value which is always satisfactory. Even in the difficult case of a 9/1 mixture, the yield is still higher than 80%. Thus, if one wants to meet the yield criteria, losses of component 2 are not much of a problem as long as one operates under the optimum experimental conditions or even under conditions somewhat less than optimum. However, if component 1 is the product of interest, meeting the yield criteria can result in a considerable loss of product or in high production costs, due to the large amount of material to be recycled. The reduction in sample amount injected during each cycle time can be calculated by comparing the data in Figures 6.1 and 6.10.



□ 1, + 3, ♦ 5, ▵ 10

Figure 6.10 Plot of the Yield as a Function of the Loading Factor for Samples of Different Volume, 1/3, selectivity 1.09

This shows that, for a 1/3 mixture with a selectivity of 1.09, a 40 % loss in the production rate is incurred to obtain a 80 % yield. When the selectivity is 1.7, the losses range between 10 and 20 % depending on the sample composition.

Chapter 7

Optimization of the Separation in Displacement Chromatography

In displacement chromatography, the column is first equilibrated with a carrier stream, a mobile phase which retains the solutes strongly. Then the feed, the solute dissolved in the mobile phase, is injected or pumped onto the column. Lastly, the displacer, a solution containing a solute which is more strongly adsorbed than any of the feed components is pumped continuously through the column until all the components of the feed have left the column. The final step is regeneration of the column and reequilibriation of the carrier stream. The regeneration process has not been modeled here.

The difference in modeling elution chromatography versus displacement chromatography is the need for an additional mass balance equation for the displacer and the competitive isotherm for the displacer and correct application of the initial and boundary conditions. The initial and boundary conditions for displacement chromatography are

$$t = 0 \qquad 0 < z < L, \qquad C_i = 0, \qquad i = 1,n \tag{7.1}$$

$$0 < t < R\delta t \qquad z = 0, \qquad C_i = C_i^{\circ}, \quad i = 1,n-1, \quad C_n = 0 \tag{7.2}$$

$$R\delta t < t < t_a \qquad z = 0, \qquad C_i = 0, \quad i = 1,n-1, \quad C_n = D_o \tag{7.3}$$

where C_i^o is the concentration of component i in the stream entering the column, D_o is the displacer concentration, t_a is the analysis time and Rdt is the time it takes for the sample to enter the column. In practice, the sample volume can be significant compared to the column volume since the components are strongly retained in the carrier and will be concentrated during displacement.

In displacement chromatography, the displacer plays an essential role in the separation process. It can be shown that provided the concentration of the displacer is large enough and the column is long enough, an isotachic train forms. Then, the profile of each zone is stable and its width depends on the amount of each solute in the sample. The plateaux concentration of each zone in an isotachic train depends on the concentration of the displacer and the individual component isotherms. The concentration of the individual solute species under isotachic conditions are given by the intersection of the solute isotherms and the operating line. The operating line is the cord extending from the origin to the point on the displacer isotherm corresponding to the displacer concentration, shown in Figure 7.1. The slope of the operating line is q_1/D_1, where q_1 is the equilibrium concentration of displacer in the stationary phase corresponding to a mobile phase concentration of D_1.

The isotherm parameters and column operating parameters used to study displacement are the same used in section 6.1-6.3 of the previous chapter with the addition of conditions for the displacer. The results presented here consider the separation of a binary mixture, the ratio of the amount injected is 1/3, with capacity factors for each component

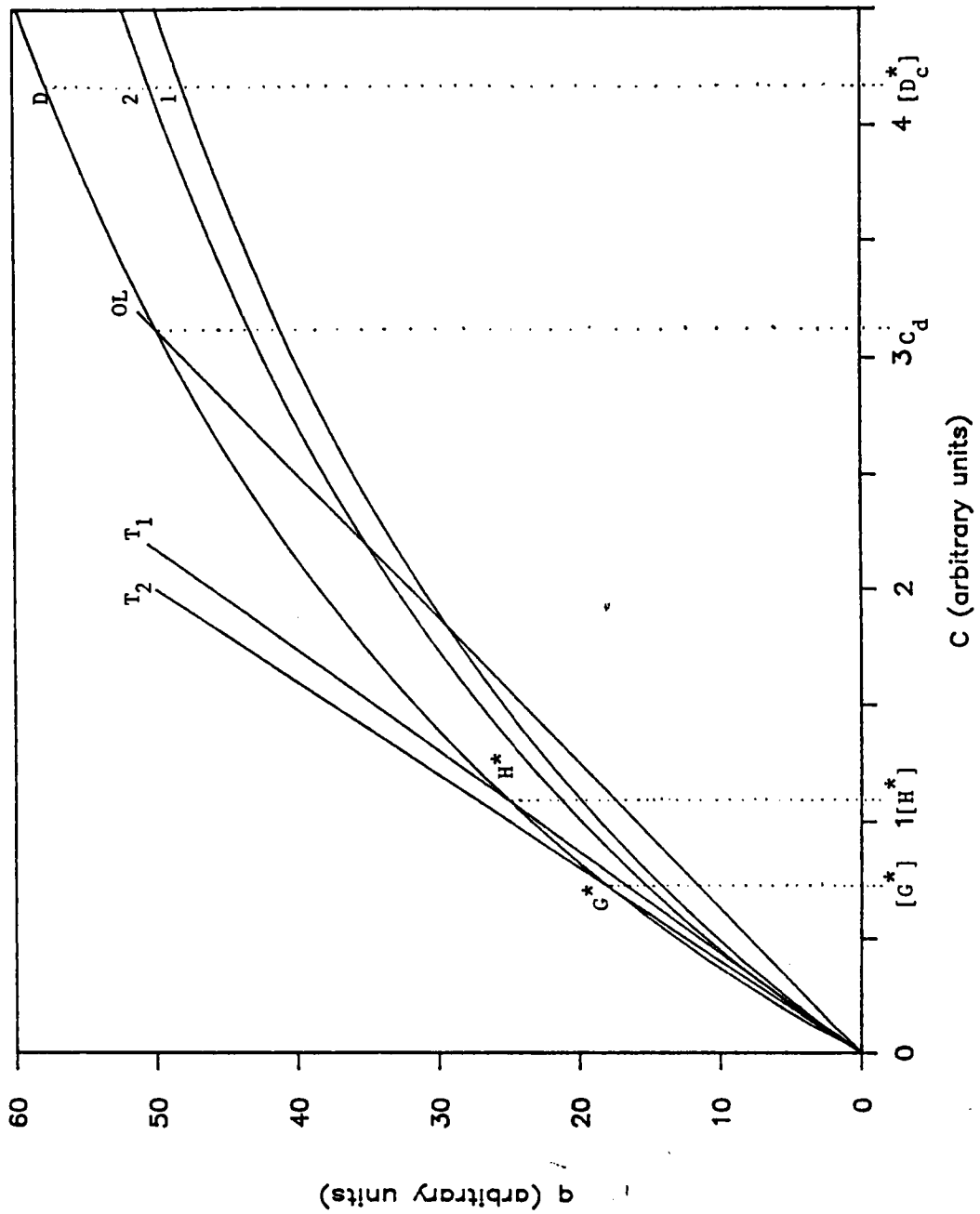


Figure 7.1 The Single Component Adsorption Isotherms for each Solute and the Displacer

and for the displacer 5.75, 6.25 and 7.5; respectively. The relative retention between the second component and the displacer is 1.2 and it need not be too large. The column void fraction is assumed to be 0.8. The parameters for the ternary isotherm, b_1, b_2 and b_3 are 2.38, 2.56 and 2.8 $mmol^{-1}$; respectively. The column HETP was 48 micron which corresponds to a well packed column with 15-20 micron particles.

7.1 Effect of Displacer Concentration

The effect of the displacer concentration on the shape of the band profiles on a 25 cm column with the parameters specified above is illustrated in Figures 7.2 and 7.3. Figure 7.2a shows that at low displacer concentrations the band shape corresponds to that obtained in overloaded elution chromatography. The velocity of the solute band is greater than the velocity of the displacer and no interference occurs between the zones of the displacer and the solute. As the displacer concentration is increased, the velocity of the displacer front increases; however, the retention time of the overload band remains unchanged until a critical displacer concentration is reached, G*, Figure 7.2b. This critical concentration corresponds to the intersection of the initial slope of the second component (n-1th component) isotherm with the displacer isotherm, illustrated in Figure 7.1. At this concentration the front of the displacer meets the tail of the second component just as it exits the column, thus the displacer has essentially does not interfere. Separation occurs in the column as in overloaded elution chromatography, Figure 7.2b. At concentrations below G*, components one and two propagate down the

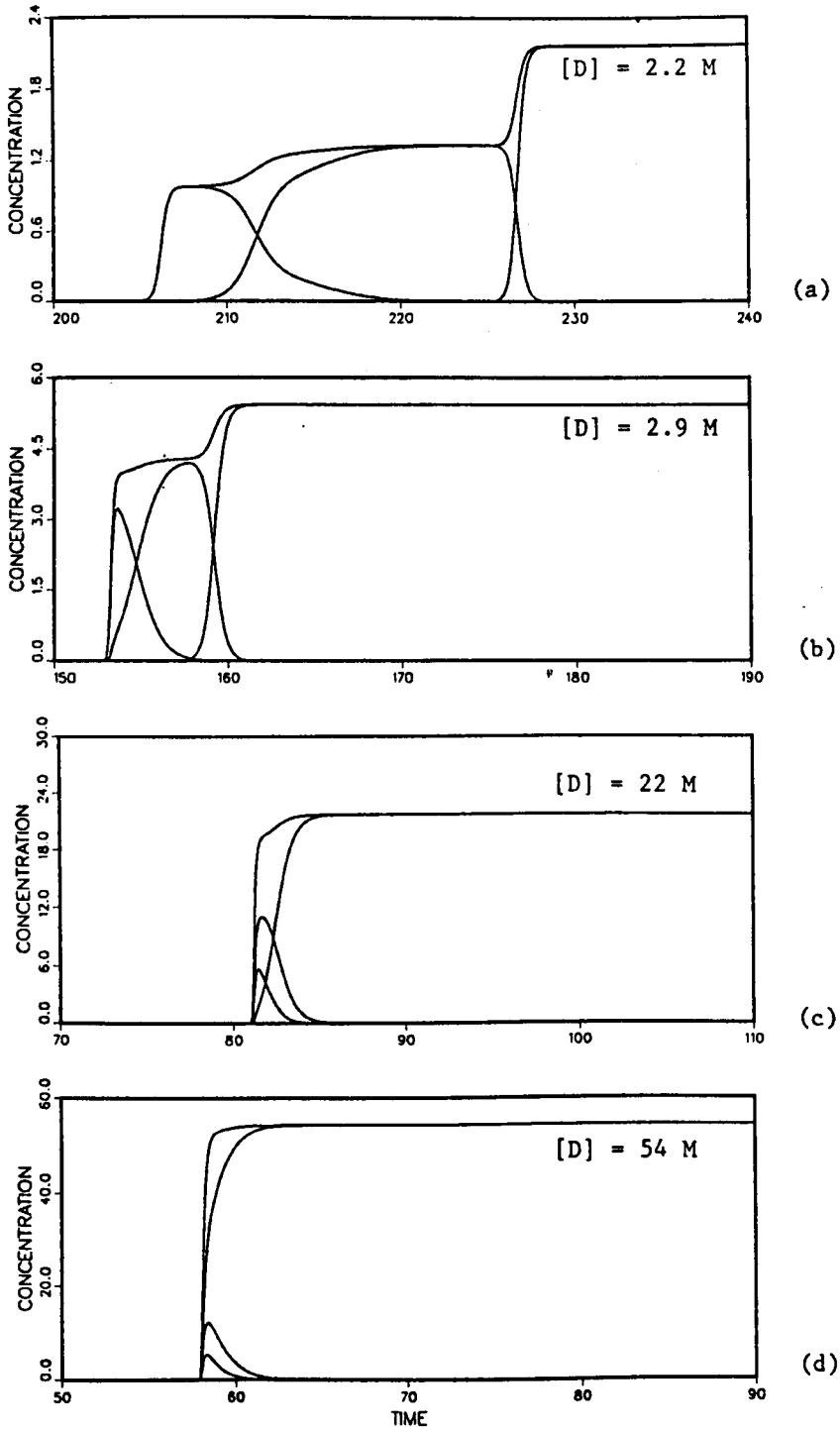


Figure 7.2 The Effect of the Displacer Concentration on the Displacement Profile at 25 cm (abscissa scales are the same for all figures)

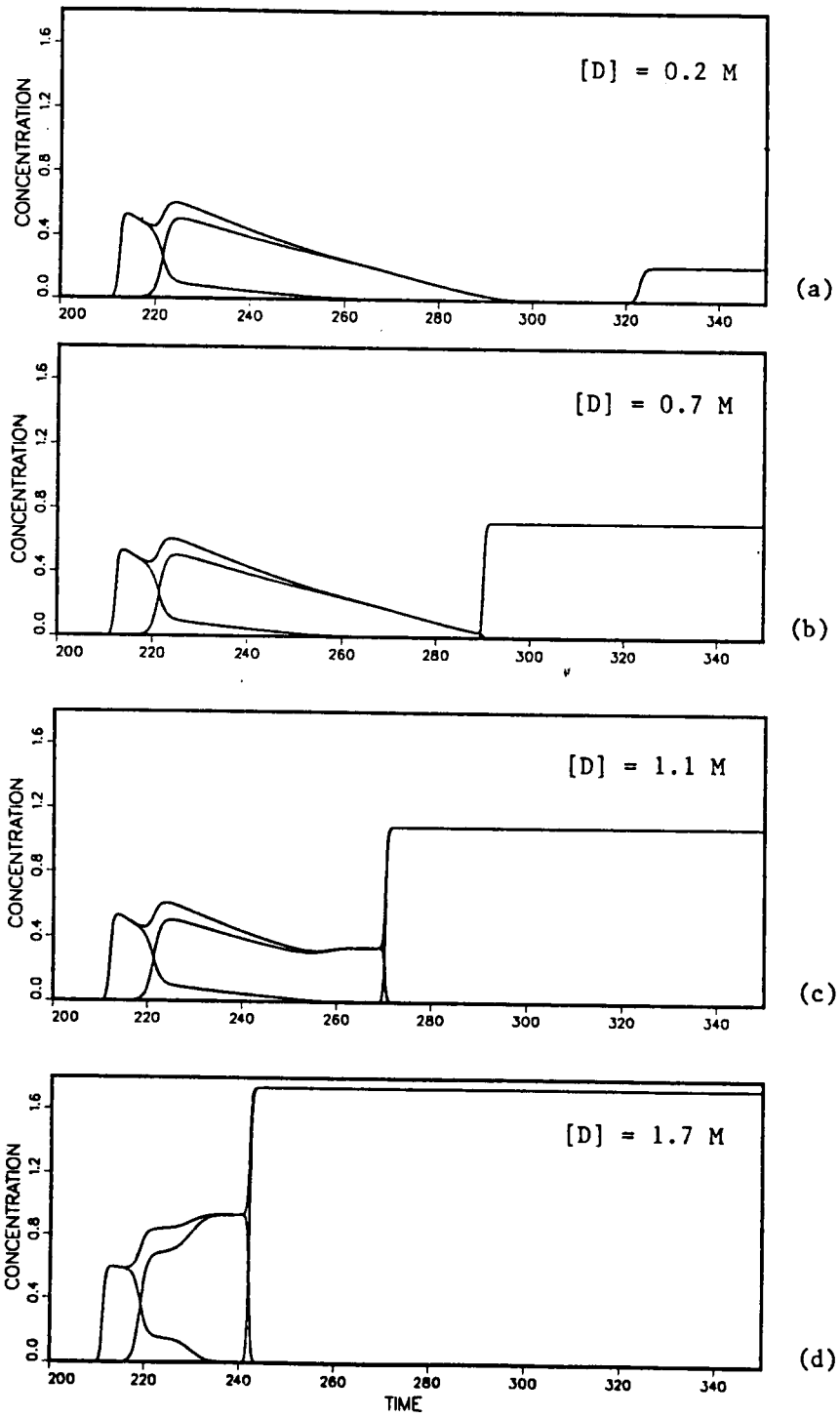


Figure 7.3 The Effect of the Displacer Concentration on the Displacement Profile at 25 cm (the width of the chromatogram is constant).

column as in overloaded elution chromatography.

As the displacer concentration is increased beyond G* interference occurs between the bands of the second component and the displacer, in addition to interference between the bands of the two solutes, Figure 7.2c. The displacer front begins to push and sharpen the rear of the second component, giving rise to the early stages of displacement development as seen by the formation of a secondary front, Figure 7.2c. When the operating line coincides with the tangent to the first component isotherm at zero concentration, the intersection is given by H^* and is illustrated in Figure 7.1. Under isotachic conditions, displacer concentrations corresponding to H^* result in the first component eluting as an overloaded band when its concentration is sufficiently large to be in the nonlinear region of the isotherm or an elution band if its concentration is in the linear region of the isotherm. Under nonisotachic conditions, however, Figure 7.2c shows that after 25 cm, the secondary front has reached the tail of the first component. For displacer concentrations larger than H^*, at 25 cm, the secondary front has distorted the tail of the first component giving rise to the displacement effect for the first component, Figure 7.2d. For displacer concentrations larger than H^*, but less than some critical value to be discussed later, isotachic displacement bands form with plateaux on both peaks on columns of sufficient length.

As the displacer concentration is increased further, beyond H^*, there is sharpening of the tails of the bands, their width decreases and their height increases, Figure 7.3a. Note that the time scales in Figure 7.2 are much larger than in Figure 7.3, moreover, in Figure 7.2

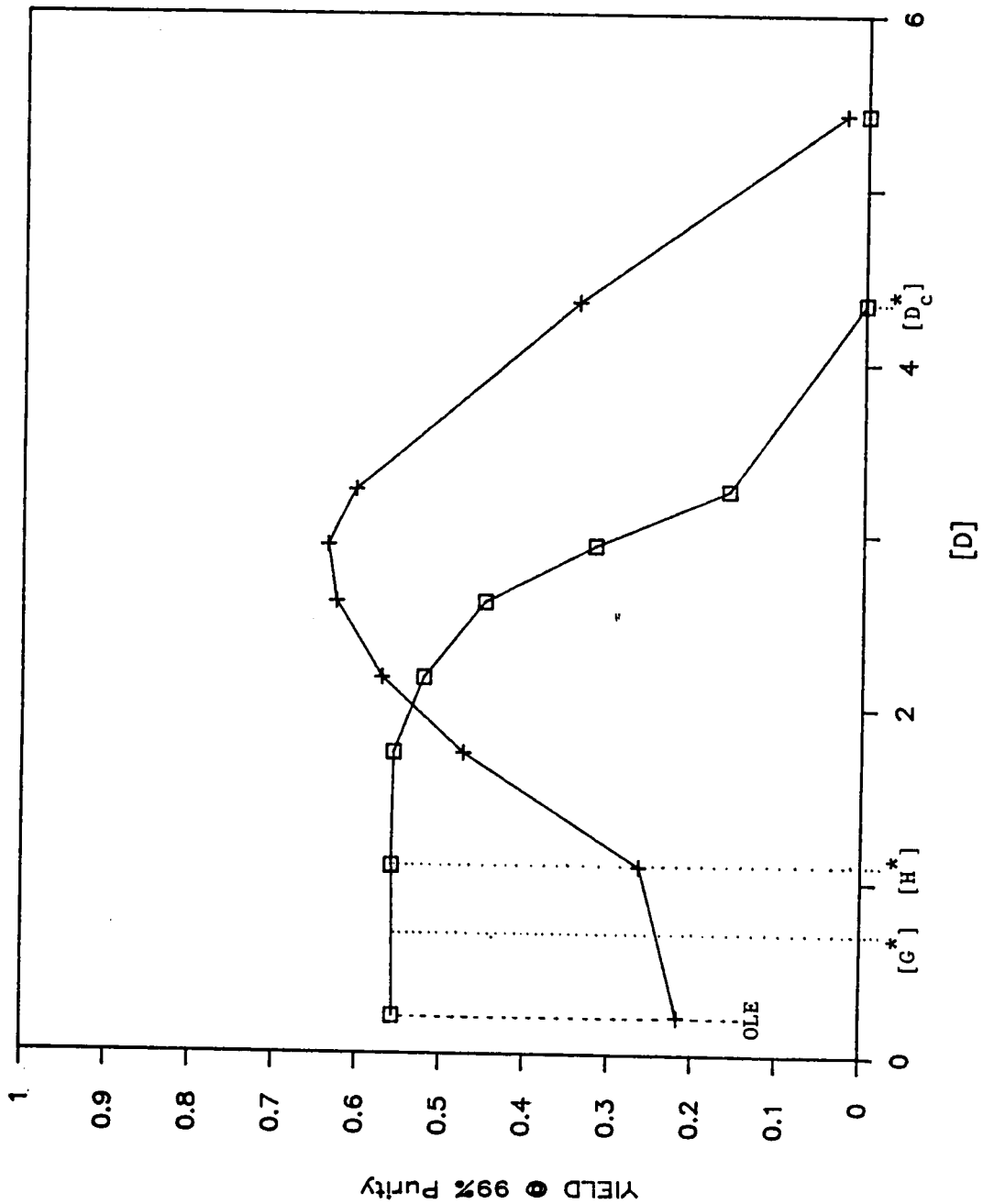
the absolute scale is the same on the graphs while in Figure 7.3 the absolute scale changes, but the relative scale is the same. However, since it is not physically possible to obtain a infinitely large concentration for an infinitely narrow band, nor would one expect to return to the initial injection conditions because band broadening has occurred, something must occur at large displacer concentrations. As the displacer concentration is increased further, the displacer begins to squeeze components one and two whose bands interfere more and more strongly. The amount of band overlap equals the band width, Figure 7.3b, and eventually neither product can be obtained with 99% purity. We call this critical displacer concentration D_c^* and define it as the displacer concentration for which the yield of 99% pure component 1 becomes zero. Under the conditions studied here, this concentration is about 4 M, Figure 7.3b. Increasing the displacer concentration still further results in very strong band interference and in the displacer overtaking the rear boundaries of the first component, such that the front of the second component coincides with the front of the first component, Figure 7.3c, and then to the displacer overtaking the peak maxima of the first and second components until all of the fronts coincide, Figure 7.3d.

At low displacer concentrations, the breakthrough time of the first component does not change, Figures 7.2a-d, however, at larger displacer concentrations, it can be seen that the breakthrough time decreases, since the velocity of the displacer front increases with increasing concentration for a Langmuir isotherm. At the same time the degree of interference between neighboring bands increases and the

yield decreases, Figures 7.2d, 7.3a, and 7.3b. There is an optimum concentration which lies between H^* and D_c^* which would lead to maximum production of the desired product(s). For the conditions under present investigation, the displacer concentration at G^*, H^* and D_c^* are 0.071 M, Figure 7.2b, 0.109 M, Figure 7.2c, and 0.4 M; respectively. Although the results presented here are for a specific set of conditions, similar peak profiles are seen at other values of the parameters. This specific problem is used to illustrate some of the basic stages in displacement development.

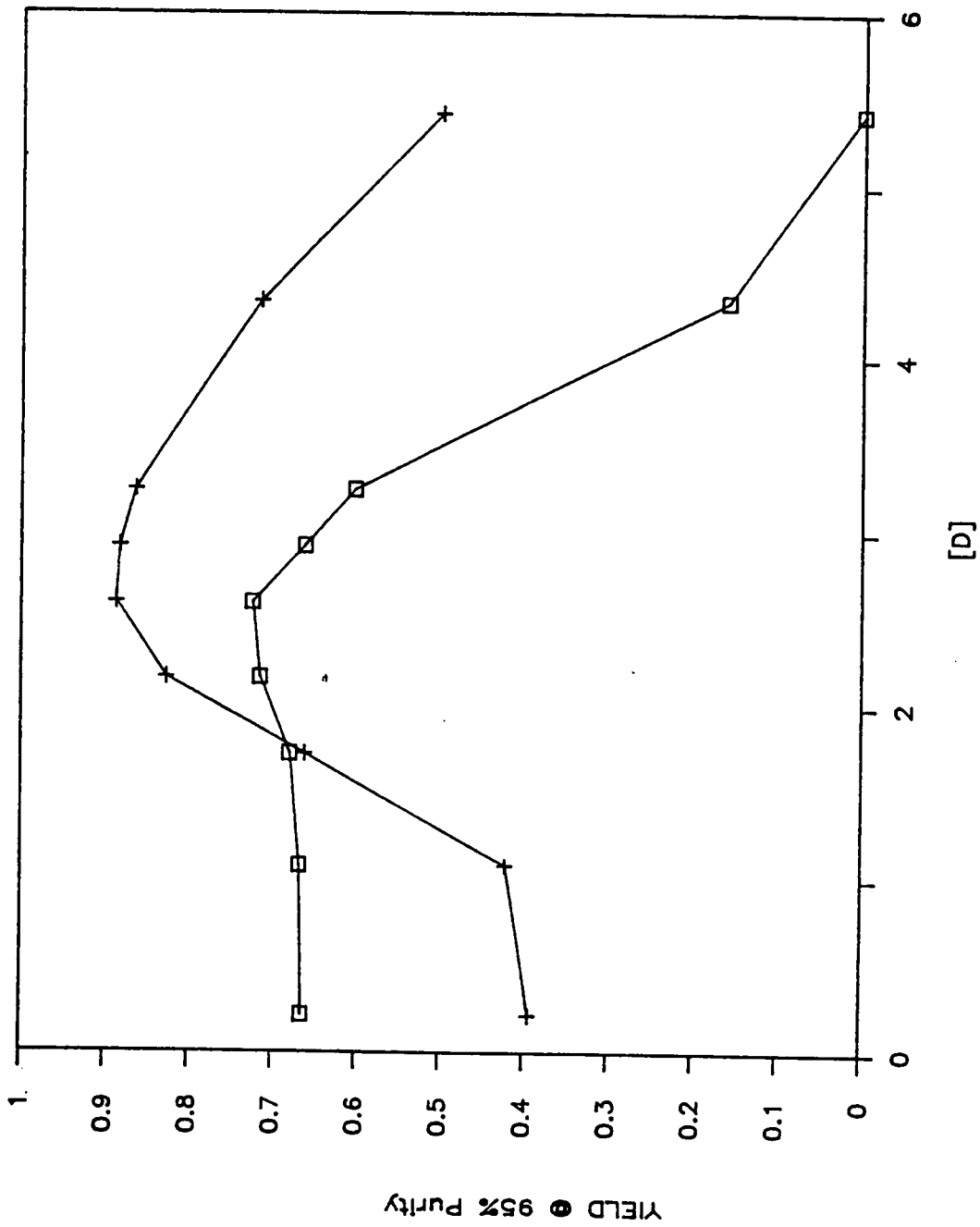
Investigation of the effect of the displacer concentration on the yields of the separation for components 1 and 2 at 99%, 98% and 95% purity shows that the yield of component two can be increased with the use of a displacer, Figures 7.4 and 7.5. This is not always true for component 1. The displacer concentrations for which the yield of component 2 is a maximum is slightly higher when the required purity is higher. At 99% purity, Figure 7.4, the yield of component one at first remains constant and equal to the yield achieved in overloaded elution and then decreases with increasing displacer concentration. At 98% and 95% purity the yield of component one goes through a weak maximum, Figure 7.5. The increase in yield at 98% purity is small but for 95% purity it is more pronounced. The result arises from the fact that component one has a tail and the amount to be recycled is reduced when the purity demanded is decreased.

The effect of the displacer concentration on the production was also investigated for 99%, 98% and 95% purity for both components one and two, Figure 7.6. In this work, production is defined as the



□ Component 1, x - Component 2, OLE- Overloaded Elution

Figure 7.4 The Effect of the Displacer Concentration on the Yield at 99 % Purity



□ Component 1, + Component 2

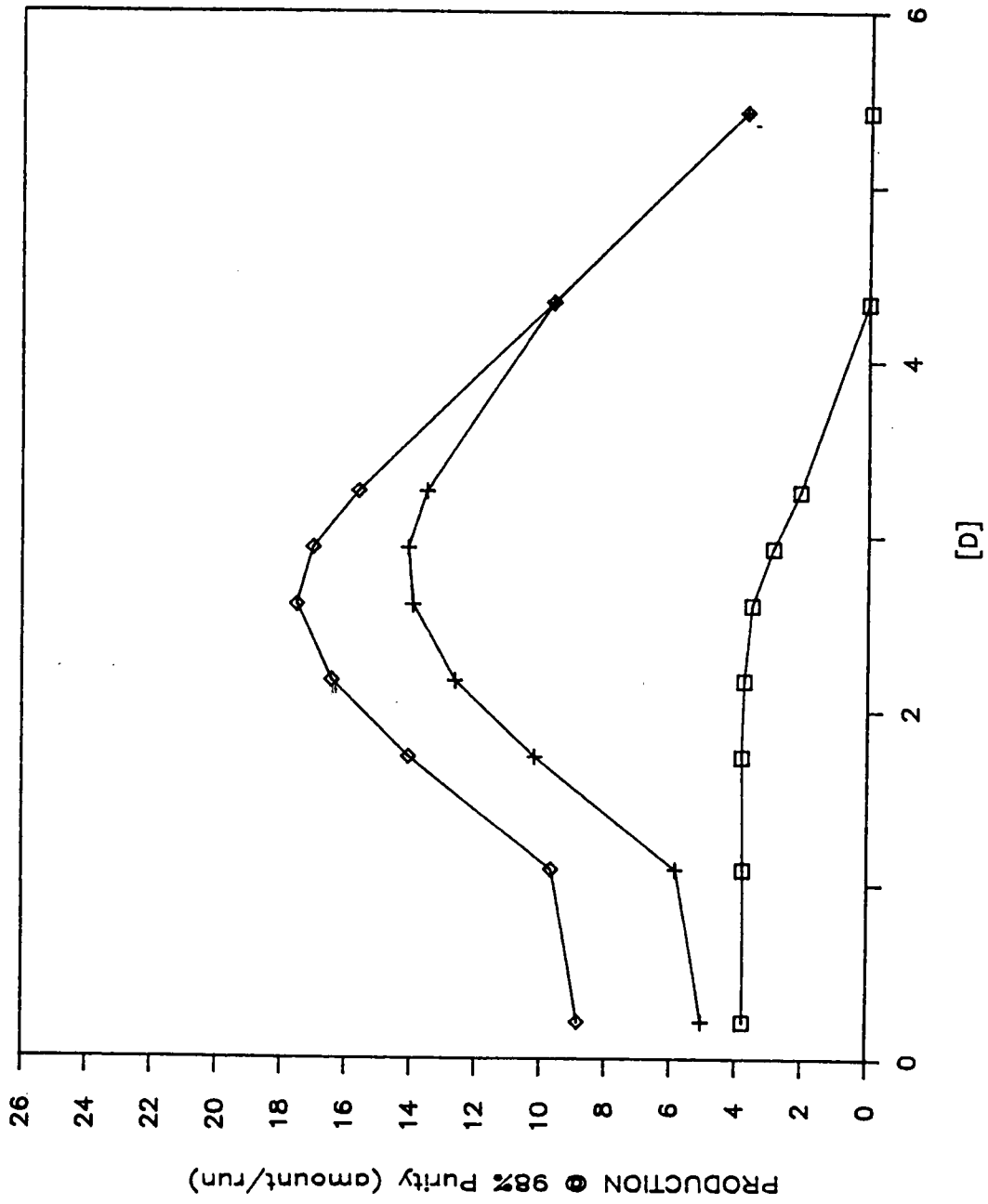
Figure 7.5 The Effect of the Displacer Concentration on the Yield at 95 % Purity, 25 cm Column

amount of product at a specified purity recovered per run. A more realistic production rate figure would require an estimate of the time needed to regenerate the column. Since the production is the product of the yield and the amount of feed, the trends are the same as for the yield. Figure 7.6 illustrates the effect of production for component one and two at 98% purity. The key point is that the production of component two increases considerably with displacer concentration, more than three fold.

The effect of the displacer concentrations on the isotachic length (i.e. the column length at which an isotachic train is formed) was studied semi-quantitatively by comparison of the peak profiles obtained at various column lengths. The results show that the length required to reach isotachic conditions decreases with increasing displacer concentration. For example, at displacer concentrations of 0.2 M, 0.3 M, and 0.5 M, isotachic lengths are approximately 45 cm, 35 cm, and 25 cm; respectively.

7.2 Effect of the Column Length

The effect of column length, holding all other parameters constant, was investigated at the displacer concentration corresponding to the maximum production of component two. Figure 7.7 illustrates the effect of the column length on the peak profiles at a displacer concentration of 0.3 M. In the first 5 cm, the rectangular injection plug collapses to a band having a height of about 2 and a width of about 15 sec, Figure 7.7a. This illustrates the early stages of the displacement effect indicated by the formation of the secondary front



□ Component 1, + Component 2, ♦ Total

Figure 7.6 Effect of the Displacer Concentration on the Production at 98 % Purity, 25 cm Column

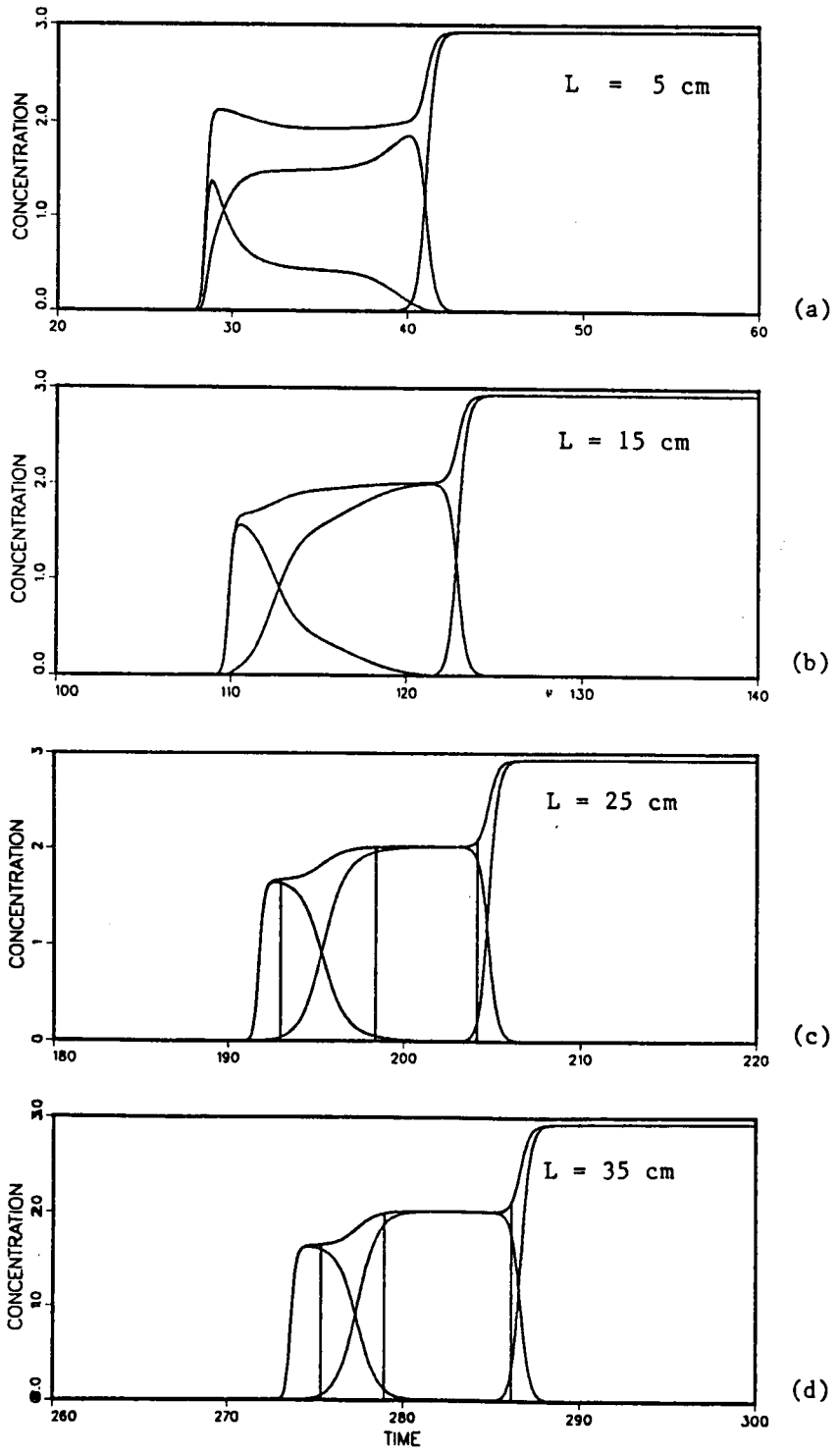
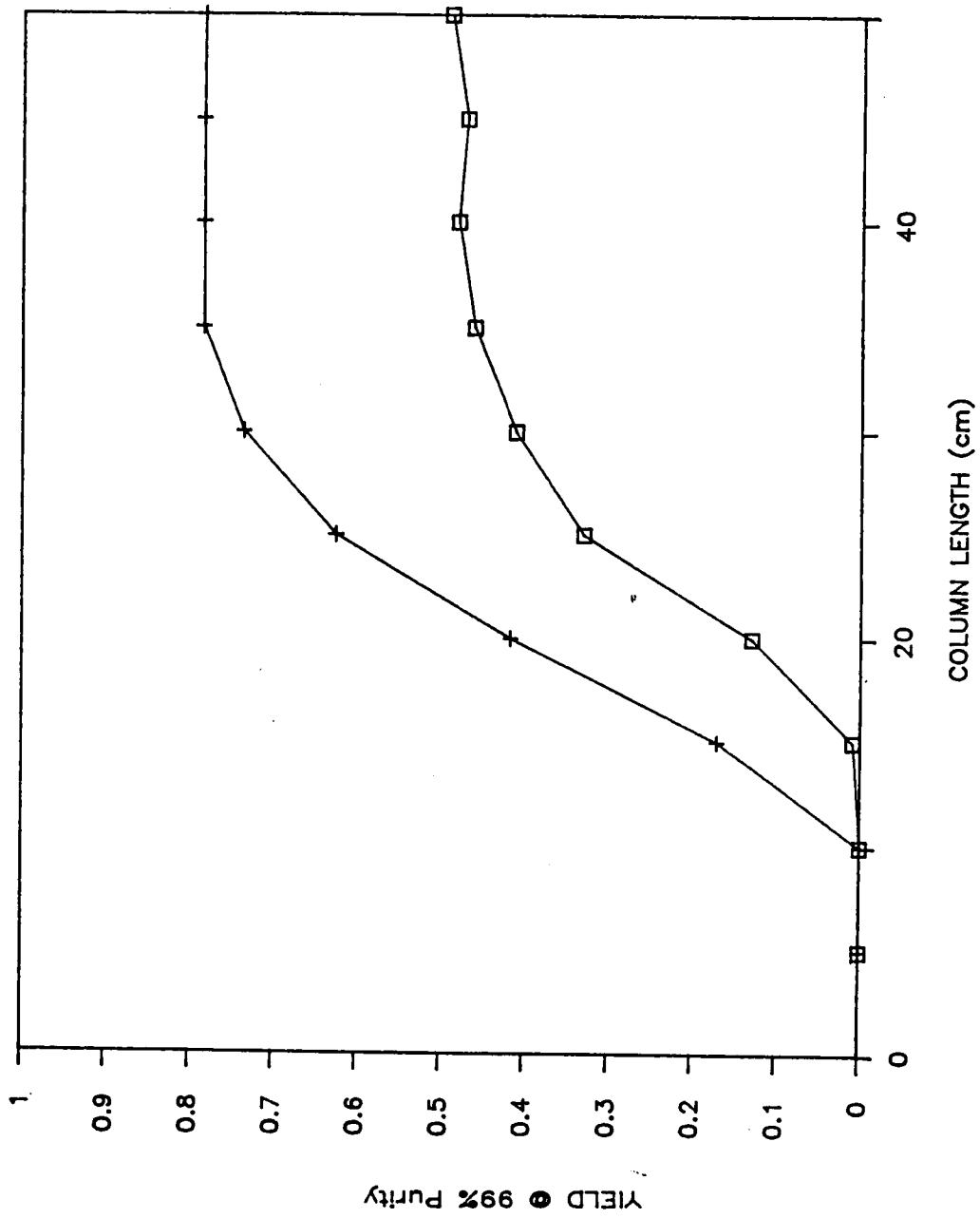


Figure 7.7 Displacement Profiles as a Function of Column Length at Displacer Concentration of 0.3M

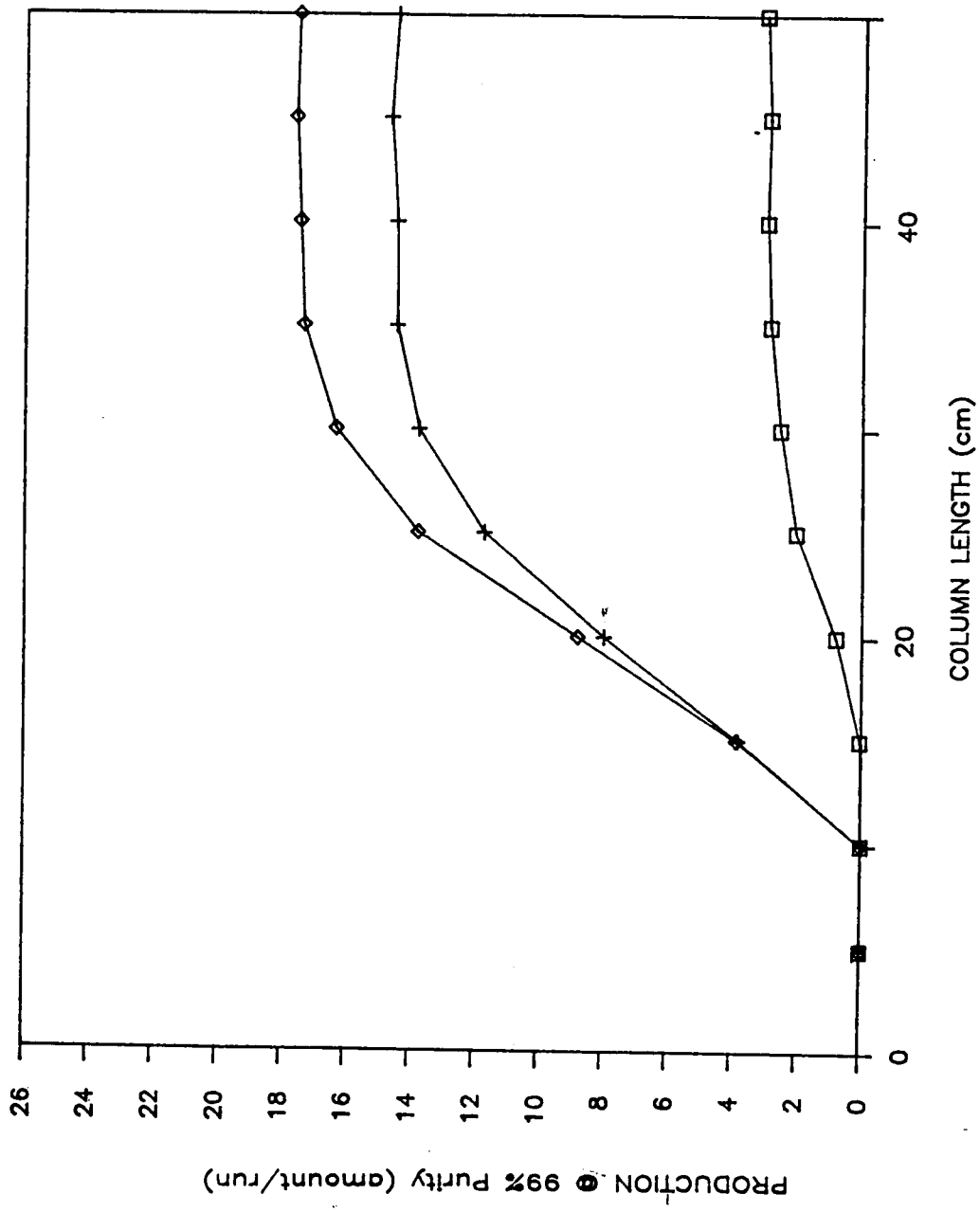
on component two which begins to push the tail of component one. At 15 cm, Figure 7.7b, the rear boundary has already sharpened considerably, the tail of component 1 is less important and the fronts of the two zones are better separated. At 25 cm, Figure 7.7c, the bands are resolving with increased sharpening of the rear boundary of the first component. At 35 cm, Figure 7.7d, isotachic conditions have been reached giving the maximum yield possible under the specified conditions. The band of component 2 exhibits a wide plateau, but not the band of component 1. The interference zone is reduced. The cut points corresponding to 99% purity are shown for the 25 cm and 35 cm columns, Figure 7.7c and 7.7d. The area between the first two vertical lines represents the amount to be recycled.

The effect of column length on the yield and the production at 99% purity for components one and two are shown in Figure 7.8 and 7.9. As the column length increases, the yield increases and a limit is reached for about 35 cm for 99 % purity, Figure 7.8. As expected, the same result is observed for the production, Figure 7.9. When isotachic conditions are reached, there is no further increase in the production or the yield. It is clear from the Figures 7.6 and 7.9, that there is an optimum column length and an optimum displacer concentration which will maximize the production at a specified purity. Obviously, these values depend on the sample size, velocity of the mobile phase, particle size and column efficiency.



□ Component 1, + Component 2

Figure 7.8 The Effect of Column Length on the Yield at Constant Displacer Concentration and 99 % Purity



□ Component 1, + Component 2, ♦ Total

Figure 7.9 The Effect of Column Length on Production at Constant Displacer Concentration and 99% Purity

7.3 Effect of Sample Volume

Figure 7.10 illustrates the progressive separation of a 5 ml rectangular injection through a column. After 5 cm the profile at the column outlet shows that the displacer has begun to concentrate a zone near the displacer front, 95 seconds, for both components. The second component has concentrated slightly the first component, as seen by the hump at 50 seconds. At 21 cm, the band has compressed considerably as the concentrated zones approach each other. At 22.7 cm, the two zones collide forming a peak amidst the plateaux at 240 seconds. At 25 cm the displacer pushes forward continuing to squeeze and concentrate the band giving an isotachic profile at 40 cm. This isotachic length is the same as for a pulse injection. In displacement chromatography, the sample volume has no effect on the final isotachic profile, although the path to the final profile is a function of the volume. These profiles are quite a contrast to the smooth development seen in Figure 7.9 for a pulse injection.

7.4 Comparison with Results from the Literature

Semi-quantitative agreement can be found between the intermediate profiles predicted by the numerical solution and data in the literature. Horvath et. al. (1981) have published ODS stationary phase intermediate profiles for the separation of 3,4-dihydroxyphenylacetic acid from 4-hydroxyphenyl acetic acid with phenol as the displacer along with the parameters of the single component isotherms of these 2 compounds. The single component isotherms for each component were employed in a competitive Langmuir model and an

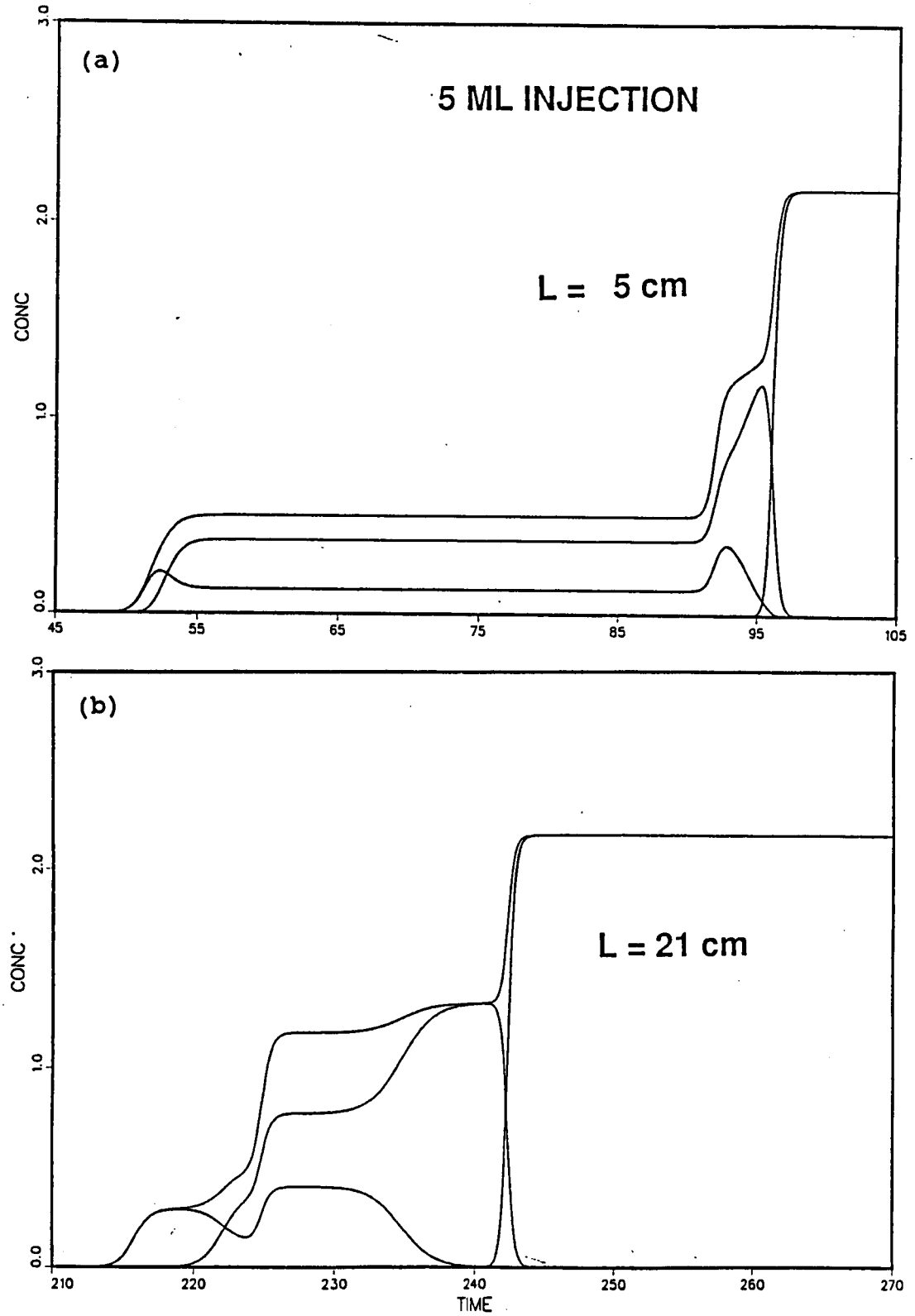


Figure 7.10 Displacement Profiles as a Function of Column Length for a 5 ml Injection Volume

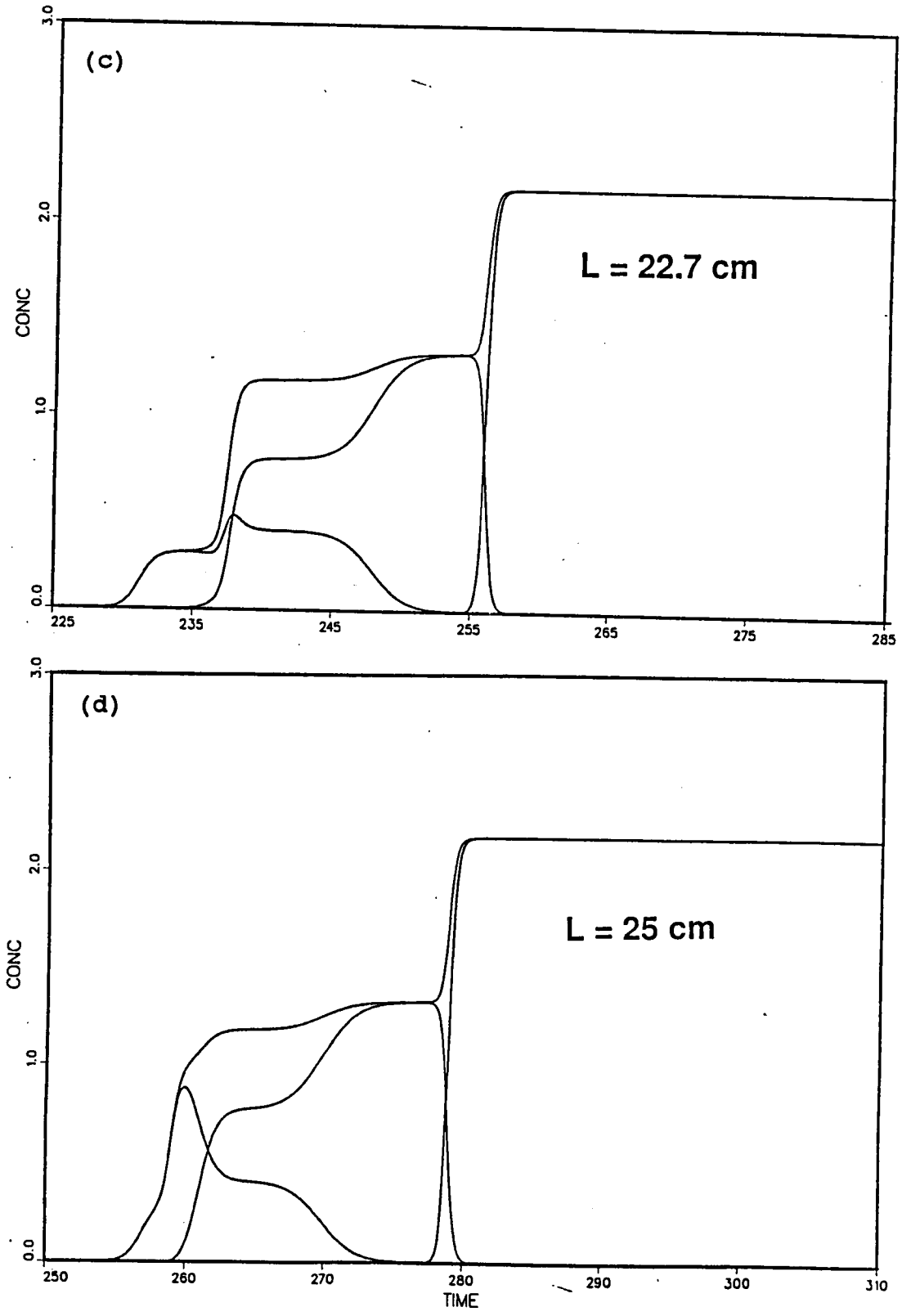


Figure 7.10 (continued)

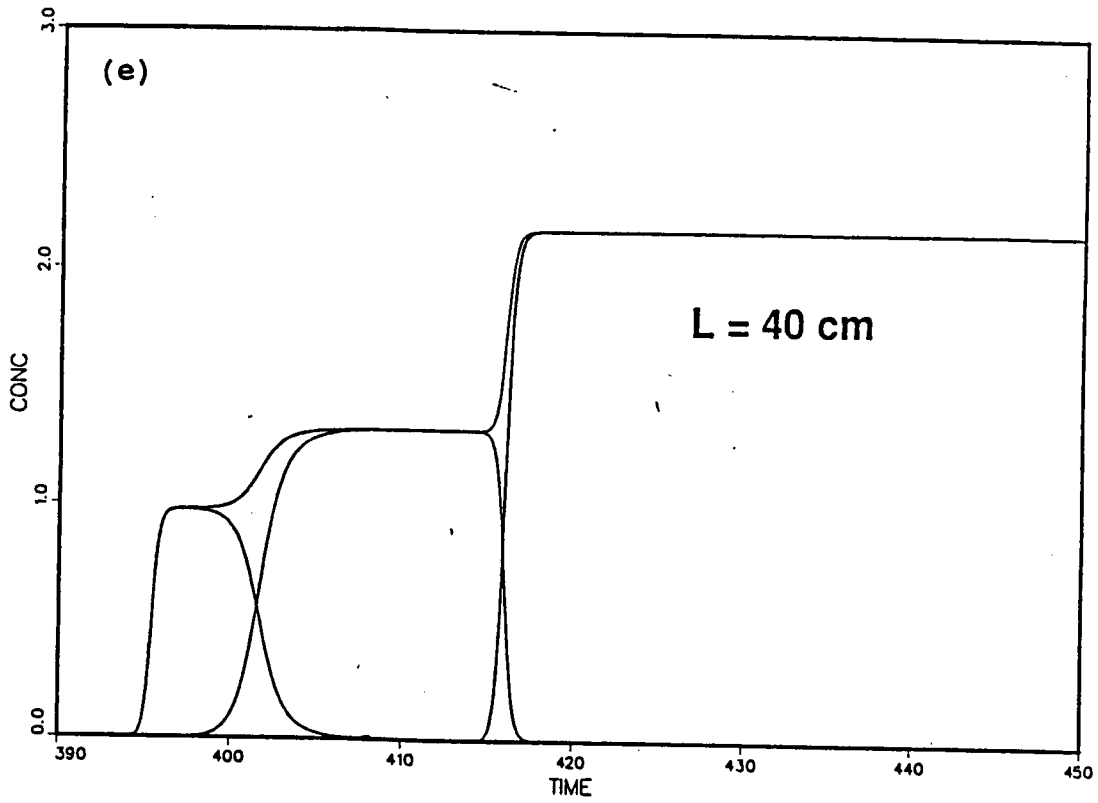
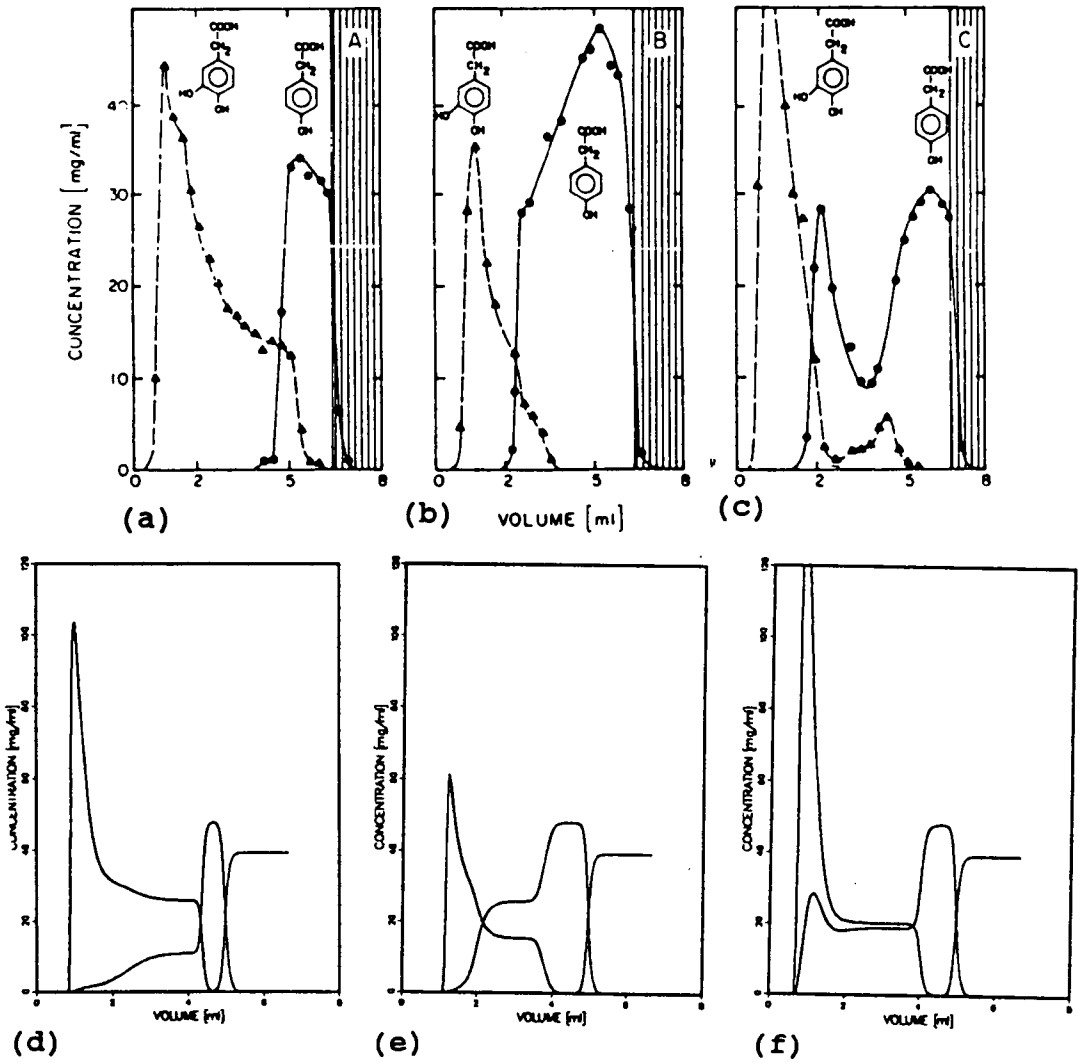


Figure 7.10 (continued)

isotherm was assumed for the displacer. The published experimental conditions for a 2:1, 1:2 and a 2:2 mixture were used in our model and the peak profiles predicted are shown in Figure 7.11a, 7.11b and 7.11c; respectively. Good agreement is seen between the chromatograms shown in Figure 7.11a, 7.11b and 7.11c and in Figure 7.12 of reference 7 replicated here, Figure 7.11d, 7.11e and 7.11f. The experimental and predicted profiles have similar breakthrough times, similar values for the peak maxima and similar waves appearing on the tail of the bands. Slight discrepancies which are seen, for example, in Figure 7.10c where the second component exhibits a plateau between the two humps, while in Horvath et al. it rather shows a deep minimum and no plateau. This can be explained by the fact that our assumption of competitive Langmuir isotherms modeled by combining single component isotherms is very crude.

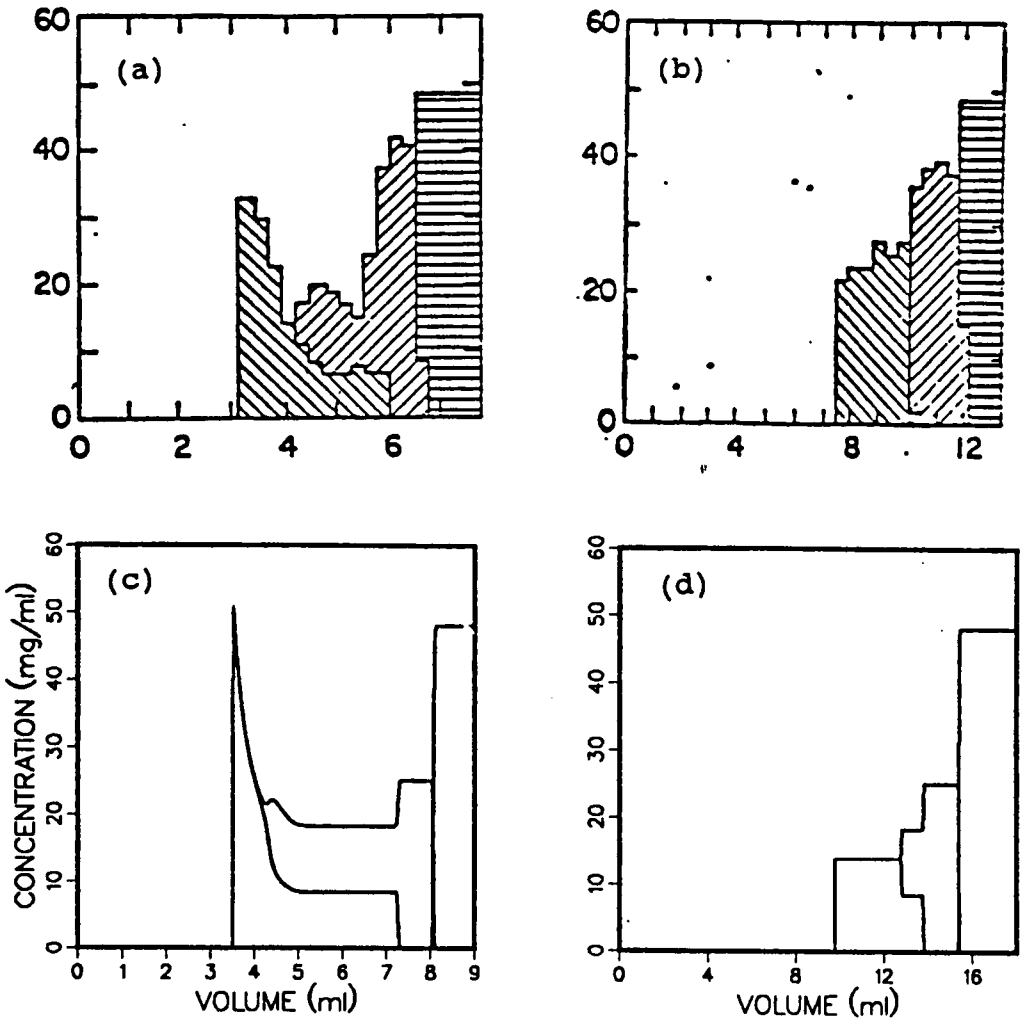
A second comparison in made in Figure 7.12 where experimental data was obtained from Frenz (1983) on the displacement of resorcinol and catechol with 48 mg/ml of n-propanol. Figure 7.12a and c are elution profiles after 25 cm while Figures 7.13b and d are after 50 cm. The flow rate was 0.2 ml/min of water and the feed was 50 mg of each solute dissolved in 1 ml water. A porosity of 0.8 was assumed, otherwise experimental conditions were used (i.e. HETP, mobile phase flow rate, column length). The breakthrough volume on the left two diagrams was at just over 3 ml while the predicted value was 3.4 ml. The plateau concentration of the tail of the first component was experimentally determined to be 10 mg/ml, the same as predicted. The peak maximum of the first component is predicted to be 50 mg/ml and



Profiles from the Literature: (a) 114:57 (b) 57:114
(c) 114:114 mg/mg

Predicted Profiles: (d-f)

Figure 7.11 The Effect of Sample Concentration on the Peak Shape, Comparison with Experimental Data in the Literature



(a) Experimental Profile from Literature, 25 cm Column
(b) Experimental Profile from Literature, 50 cm Column
(c) Predicted Profile, 25 cm Column
(d) Predicted Profile, 50 cm Column

Figure 7.12 The Effect of Column Length on the Peak Shape, Comparison with Experimental Data in the Literature

the maximum measured was 35 mg/ml. However, the double peaking observed experimentally was also predicted. At 50 cm a nearly isotachic train was observed and predicted. The heights of the bands are not exactly the same indicative of errors in the displacer isotherm.

Chapter 8

Summary and Conclusions

The major goal of this thesis was to demonstrate that the individual component profiles of a binary mixture can be predicted with accuracy. This thesis shows that this is possible if the competitive isotherm is represented accurately. Band widths, band heights and yields can be predicted with an absolute error of 5-20 %. It has also been shown that the isotherm surface of both components of a binary mixture of a representative small molecule system is accounted, to a first approximation, by a competitive Langmuir isotherm using single component isotherm parameters. Finally, we have reduced to practice and validated a new method of determining isotherms, the method of the Hodograph Transform , with high accuracy. Thus, an effective approach to the design of preparative separations in a fixed bed has been developed.

Additionally, the effect of sample size and sample volume on the production rate in overloaded elution chromatography at constant column length, particle size and linear velocity for several binary mixtures was determined. It was found that the sample size corresponding to the optimum production rate for component one was larger than component two. The optimum sample size for component one gives a yield between 40 and 70% assuming 99% purity. The optimum sample size for component two gives corresponds to 99% yield assuming a purity of 99%. Moreover,

the sample should be injected as a concentrated pulse subject to the solubility limitations in the mobile phase.

Lastly, as a consequence of this investigation along with theoretical considerations, a new method of trace analysis has been demonstrated using displacement and overloaded elution chromatography. Enrichment of trace impurities could decrease a thousand fold the detection limit.

8.1 Comparison of Overloaded Elution and Displacement Chromatography

Displacement chromatography and overloaded elution chromatography both have advantages and disadvantages. The choice of one mode or the other will depend largely on the nature of the sample to be purified. Thus, both techniques must be considered. Displacement chromatography has the advantage that high concentration products can be obtained from dilute solutions. Since the components in small amount elute between adjacent bands, high purity products can be obtained. A yield of 100 % is never obtained in practice. The yield depends on the column efficiency and the degree of overlap of the adjacent zones. Displacement chromatography has the disadvantage of requiring column regeneration which can reduce the life time of the stationary phase.

On the other hand, overloaded elution has the advantage of complete resolution, essentially 100 % yield is not uncommon. Although the displacement effect can minimize the extent of dilution, by definition, the pure sample is more dilute than the sample feed concentrations. The disadvantage is that it has the property that hidden impurities are overlooked because of dilution and because of the

tag-along effect. In order to increase the production rate, the column should be operated with short cycle times. By timing sequential injections so that the last eluting band of the first cycle elutes just before the first eluting band of the second cycle, the entire column can be used more effectively.

8.2 Recommendations

A complete and systematic multidimensional optimization study using the semi-ideal model needs to be performed. Depending on the application various parameters should be optimized in groups. The general optimization problem is to find the optimum sample size, mobile phase velocity, particle size, column length and in displacement chromatography the displacer concentration for systems having various separation factors and relative composition. However, often the column length is fixed or sometimes both the column length and the particle size are known and the purpose is to find the best values of the other parameters.

Second, a comparison of the method of the Hodograph transform and frontal analysis for determining competitive isotherms would be useful. Moreover, a comparison of the two methods to determine the isotherm for a nonLangmuir systems such as a nucleotide separation would be interesting.

Third, determination of mixed bands in overloaded elution for systems of larger molecules, peptides and proteins, is essential in finding the limitations of the equilibrium model. This would initiate the practical problem of determining kinetic parameters. Moreover, the

displacement mode should also be studied to determine experimentally kinetic effects.

Fourth, the work presented here applies when the mobile phase does not change (i.e. isocratic elution). However, for protein and peptide separations, gradient or step gradient techniques must be employed. However there is a need for methods to determine isotherms of components whose retention varies rapidly with solvent strength. In order to exactly predict the profiles and further optimize gradient separations.

Lastly, there is a need to develop simulation programs (like has been done for distillation, reactor design, and extraction) for use by a more general audience so that optimum conditions can be found for design of preparative separations in industrial applications.

LIST OF REFERENCES

LIST OF REFERENCES

Andrade, J.D., in Surface and Interfacial Aspects of Biomedical Polymers, J. D. Andrade Ed., Plenum Press, New York, NY 1985.

Antia F. and Horvath Cs., J. Chromatogr. 484 (1989) 1.

Aris R. and Amundson N. R. in Mathematical Methods in Chemical Engineering, Prentice-Hall, Englewood Cliffs, NY 1973.

Arve B.H. and Liapis, A.I., Biotech. and Bioeng., 30 (1987) 638.

Atwood J.G. and Golay M.J.E., J. Chromatogr., 218 (1981) 97.

Basmadjian D. and Coroyannakis P., Chem. Eng. Sci. 42 (1987) 1723.

Begovich J.M., Byers, C.H. and Sissin W.G., Sep. Sci. and Tech. 18 (1983) 1167.

Bristow P.A., Brittain P.N., Riley C.M., Williamson B.F., J. Chromatogr. 131, (1977) 57.

Broughton D.B., Sep. Sci. Technol. 19 (1984) 723.

Carta G., Chem. Eng. Sci. 43 (1988a) 2877.

Carta G., Saunders M.S., DeCarli J.P. and Vierow J.B., AICHE Symp. Ser., 84 (1988b) 54.

Carta. G., DeCarli J.P., Byers C.H. and Sisson W.G., Chem. Eng. Comm. 79 (1989) 207.

Claesson, S., Disc. Faraday Soc. 7 (1949) 34.

Coates J.I. and Glueckauf E., J. Am. Chem. Soc. (1947) 1309.

Colin H., Prochrom, Nancy, France, Private Communication, 1986.

Cooney D.O. and Lightfoot E.N., Ind. Eng. Fundam. 5 (1966) 212.

Coq B., Cretier G., Rocca J.L., J. Chromatogr. 186 (1979) 457.

Coq B., Cretier G., Rocca J.L., Kastner R., J. Chromatogr. 218 (1981) 97.

Cox G.B., Antle P.E. and L.R. Snyder, J. Chromatogr. 444 (1988a) 303.

Cox G.B., Antle P.E. and L.R. Snyder, J. Chromatogr. 444 (1988b) 325.

Cox G.B. and Snyder L.R., J. Chromatogr. 483 (1989a) 95.

Cox G.B., L.R. Snyder and Dolan J.W. J. Chromatogr. 484 (1989b) 409.

Craig L.C., J. Biol. Chem. 155 (1944) 519.

Cramer S.M., El Rassi Z. and Horvath Cs., J. Chromatogr. 394 (1987) 305.

Cramer S.M. and Horvath Cs., Prep. Chrom. 1(1) (1988) 29.

Cremer E. and Huber J.F.K., Agew. Chem. 73 (1961) 461.

Czok M. and G. Guiochon, Anal. Chem. 62 (1990) 189.

DeJong A.W.J., Poppe H. and Kraak J.C., J. Chromatogr. 148 (1978) 127.

DeCarli J.P., Carta G. and Byers C.H., Paper Prapered for AICHE Annual Meeting, Washington D.C., November 27-Dec 2 1988. paper 1d.

Decarli J.P., Carta G. and Byers C.H., AICHE J. (1990) in press.

DeCarli J.P., Univ. Virginia, PhD. Thesis (1989).

DeVault D.J., Am. Chem. Soc. 65 (1943) 532.

Do D.D. and Rice R.G., Chem. Eng. Sci. 42 (1987) 2269.

Dose E. and Guiochon G., Anal. Chem. 61 (1989) 2571.

Dose E. and Guiochon G., Anal. Chem. (1990) in preparation.

Eble J.E., Grob R.L., Antle P.E. and Snyder L.R., J. Chromatogr. 384 (1987a) 25.

Eble J.E., Grob R.L., Antle P.E. and Snyder L.R., J. Chromatogr. 384 (1987b) 45.

Eble J.E., Grob R.L., Antle P.E. and Snyder L.R., J. Chromatogr. 405 (1987c) 1.

Eble J.E., Grob R.L., Antle P.E. and Snyder L.R., J. Chromatogr. 405 (1987d) 51.

Eltekov Y.A., Kazakevich Y.V., Kiselev A.V. and Zhuchkov A.A., Chromatographia, 20 (1985) 525.

Eltekov Y.A. and Kazakevitch Y.V., J. Chromatogr. 365 (1986) 213.

El Rassi Z. and Horvath Cs., J. Chromatogr. 266 (1983) 319.

Fujii Y., Aida, M. Okamoto M. and Oi T. Sep. Si. Technol. 20 (1985) 377.

Fujine S., Sep. Sci. Technol. 17 (1982) 1049.

Fujine S., Saito K. and Shiba K. Sep. Sci. Technol. 18 (1983) 15.

Frenz J., Yale University, PhD Thesis (1983).

Frenz J, Van der Schrieck Ph. and Horvath, Cs., J. Chromatogr. 330 (1985) 1.

Frenz J. and Horvath Cs., "High-Performance Displacement Chromatography," in High-Performance Liquid Chromatography Advances and Perspectives, Vol. 5, Academic Press (1988)

Geldart R.W., Qiming Y., Wankat P.C. and Wang L. N.-H., Sep. Sci. and Tech. 21(9) (1986) 873.

Ghodbane S. and Guiochon G., J. Chromatogr. 440 (1988a) 9.

Ghodbane S. and Guiochon G., J. Chromatogr. 444 (1988b) 275.

Ghodbane S. and Guiochon G., J. Chromatogr. 450 (1988c) 27.

Ghodbane S. and Guiochon G., J. Chromatogr. 452 (1988d) 209.

Ghodbane S. and G. Guiochon, Chromatographia, 26 (1988e) 53.

Giddings J.C., Dynamics of Chromatography, Marcel Dekker, New York 1965.

Gluckauf E., Proc. Roy. Soc. A186 (1946) 35.

Glueckauf E., J. Chem. Soc. (1947a) 1302.

Glueckauf E. and Coates J.I., J. Chem. Soc. (1947b) 1315.

Glueckauf E., J. Chem. Soc. (1947c) 1321.

Glueckauf E., J. Chem. Soc. (1949a) 3280.

Glueckauf E., Disc. Faraday Soc. 7 (1949b) 12.

Godbille E. and Devaux P., J. Chromatogr. Sci. 12 (1974) 565.

Godbille E. and Devaux P., J. Chromatogr. 122 (1976) 317.

Goldstein S., Proc. Roy Soc. London, A219 (1953a) 151.

Goldstein S., Proc. Roy Soc. London, A219 (1953b) 171.

Golshan-Shirazi S. and Guiochon G., Anal. Chem. 60 (1988a) 2364.

Golshan-Shirazi S., Ghodbane S. and Guiochon G., Anal. Chem. 60 (1988b) 2630.

Golshan-Shirazi S. and Guiochon G., Anal. Chem. 60 (1988c) 2634.

Golshan-Shirazi S. and Guiochon G., Anal. Chem. 61 (1989a) 462.

Golshan-Shirazi S. and Guiochon G., Anal. Chem. 61 (1989b) 1276.

Golshan-Shirazi S. and Guiochon G., Anal. Chem. 61 (1989c) 1368.

Golshan-Shirazi S., Lin B.-C. and Guiochon G., Anal. Chem. 61 (1989d) 1960.

Golshan-Shirazi S., Lin B.-C. and Guiochon G., J. Phys. Chem. 93 (1989e) 6871.

Golshan-Shirazi S. and Guiochon G., J. Chromatogr. 461 (1989f) 1.

Golshan-Shirazi S. and Guiochon G., J. Chromatogr. 461 (1989g) 19.

Golshan-Shirazi S. and Guiochon G., J. Phys. Chem. 93 (1989h) 4143.

Golshan-Shirazi S. and Guiochon G., Anal. Chem. 61 (1989i) 2372.

Golshan-Shirazi S. and Guiochon G., Anal. Chem. 61 (1989j) 2380.

Golshan-Shirazi S. and Guiochon G., J. Chromatogr. 484 (1989k) 125.

Golshan-Shirazi S. and Guiochon G., J.Phys. Chem. 94 (1990a) 495.

Golshan-Shirazi S. and Guiochon G., J. Chromatogr. Special Issue Proceedings HPLC'89 Stockholm, Sweden (1990b) in press.

Golshan-Shirazi S. and Guiochon G., Anal. Chem. 62 (1990c) 217.

Guiochon G, Golshan-Shirazi, S. and Jaulmes A., Anal. Chem. 60 (1988a) 1856.

Guiochon G. and Ghodbane S., J. Phys. Chem. 92 (1988b) 3682.

Guiochon G and Ghodbane S, C.R. Acad. Sci. (Paris) 306(II) (1988c) 575.

Guiochon G, Ghodbane S., Goshan-Shirazi S., Juang J.-X., Katti, A., Lin B.-C and Ma, Z, Talanta, 36 (1989) 19.

Haarhoff P.C. and Van der Linde H.J., Anal. Chem. 38 (1966) 573.

Hiester N.K. and Vermeulen, T., Chem. Eng. Prog. 48(10) (1952) 509.

Helfferich, F and Klein, G. Multi-Component Chromatography. A Theory of Interference; Dekker: New York, NY 1970.

Horstmann B.J., 6th International Symposium on Preparative Liqiud Chromatography "Prep '89," Washington D.C., May 8-10, 1989.

Horvath Cs. and Lin H.-J., J. Chromatogr. 126 (1976) 401.

Horvath Cs. and Lin H.-J., J. Chromatogr. 149 (1978) 43.

Horvath Cs., Nahum A. and Frenz, J.H., J. Chromatogr. 218 (1981) 365.

Horvath Cs., Frenz J. and El Rassi, Z., J.Chromatogr. 255 (1983) 273.

Horvath Cs. in "The Science of Chromatography" Bruner F. Ed., J. Chromatography Library, Vol. 32, Elsevier, Amsterdam (1985) p. 179.

Houghton G., J. Phys. Chem. 67 (1963) 84.

Howard A.J., Carta, G. and Byers C.H., I.&EC Research, 27 (1988) 1873.

Huang J.-X. and Horvath Cs., J. Chromatogr. 406 (1987a) 275.

Huang J.-X. and Horvath Cs., J. Chromatogr. 406 (1987b) 285.

Huang J.-X. and Guiochon, J. Col. Int. Sci. 128 (1989) 577.

Huang J.-X., Schudel J.V.H. and Guiochon G., Preparative Chromatogr. (1990a).

Huang J.-X., Schudel J.V.H. and Guiochon G., J. Chromatogr. (1990b).

Huber J.F.K., Ber. Bunsen-Ges. Phys. Chem., 77 (1973) 179.

Jacobson J., Frenz, J. and Horvath Cs., J. Chromatogr. 316 (1984) 53.

Jacobson J.M., Frenz, J.H. and Horvath Cs., Ind. Eng. Chem. Res. 26(1) (1987) 43.

Jacobson S., Golshan-Shirazi S., Katti A.M., Czok M., Ma Z. and Guiochon G., J. Chromatogr. 484 (1989) 103.

Jacques R., Sep. Sci. Technol. 15 (1980) 533.

James D.H. and Phillips C.S.G., J. Chem. Soc. 1066 (1954).

Jennings P., 1987 Pittsburgh Conference., Anal. Chem. Paper 174.

Jonsson J.A. and Lovkvist P., J. Chromatogr. 408 (1987) 1.

Joraczko A., Jenota D., Wojt L., J. High Resolut. Chromatogr. Chrom. Commun. 9 (1986) 255.

Kalasz H. and Horvath Cs., J. Chromatogr. 215 (1981) 295.

Kalasz H. and Horvath Cs., J. Chromatogr. 239 (1982) 423.

Kaminiski M., Klawiter J. and Kowalszk J.S., J. Chromatogr. 243 (1982) 225.

Karol P.J., J. Chromatogr. 445 (1988) 207.

Karol P., Anal. Chem. 61 (1989) 1937.

Katti A.M. and Guiochon G., J. Chromatogr. 449 (1988) 25.

Katti A.M. and Guiochon G., Am. Lab., Oct (1989a) 17.

Katti A.M. Ramsey R. and Guiochon G., J. Chromatogr. 477 (1989b) 119.

Katti A.M. and Guiochon G., Anal. Chem. 61 (1989c) 982,

Katti A.M. and Guiochon G., C.R. Acad. Sci. Paris, Serie II, 309 (1989d) 1557.

Katti A.M. and Guiochon G., J. Chromatogr. 499 (1990) 15.

Keulemans A.I.M. in Gas Chromatography, C.G. Verver ed., Reinhold Publishing Corp, New York 1957, p. 107- 115.

Klinkenberg A. and Sjenitzer F., Chem. Engrg. Sci. 5 (1956) 258.

Knox J.H.and Laird G.R. and Raven P.A., J. Chromatogr. 122 (1976) 129.

Knox J.H. and Pyper H.M., J. Chromatogr. 363 (1986) 1.

Kuhn R. and Lederer E., Naturwissenschaften, 19 (1931a) 306.

Kuhn R., Winterstein A. and Lederer E., Z. Physiol. Chem. 197 (1931b) 141.

Lapidus L. and Amundson N.R., J. Phys Chem. 56 (1952) 984.

Lee A.L., Liao A.W. and Horvath Cs., J.Chromatogr. 443 (1988) 31.

Lee A.L., Velayudhan, A. and Horvath, C., in G. Durand, L. Bobichon and J. Florent (Ed.), 8th Int. Biotech. Symp., Societe Francaise de Microbiologie, Paris (1989) 593.

Lee C.K., Yu Q., Kim S.U. and Wang, N-H. L., J. Chromatogr. 484 (1989) 29.

Little J.W., Cotton R.L., Pendergast J.A., Mc Donald P.D., J. Chromatogr., 126 (1976) 439.

Lin B.-C., Golshan-Shirazi S., Ma Z. and Guiochon G., Anal. Chem. 60 (1988) 2647.

Lin B.-C., Golshan-Shirazi S. and Guiochon G., J. Phys. Chem. 93 (1989a) 3363.

Lin B.-C., Ma Z., Golshan-Shirazi, S. and Guiochon, G., J. Chromatogr. 475 (1989b) 1.

Lin B.-C. and Guiochon G., Sep. Sci. and Tech. 24(1) (1989c) 31.

Lin B.-C., Ma Z. and Guiochon G., Sep. Sci. and Tech. 24(11) (1989d) 809.

Lin B.-C., Ma Z. and Georges Guiochon, J. Chromatogr. 484 (1989e) 83.

Liao A.W., El Rassi Z., LeMaster D.M. and Horvath Cs., Chromatographia, 24 (1987) 881.

Lucy C.A., Wade J.L. and Carr P.W., J. Chromatogr. 484 (1989) 61.

Ma Z., Katti A.M. and Guiochon G., J. Phys. Chem. submitted.

Maa Y.-F. and Horvath Cs., J. Chromatogr. 445 (1988) 71.

Mair B.D., Gaboriault A.L. and Rossini F.D., Ind. Eng. Chem. 39 (1947) 1072.

Martin A.J.P and Synge R.L.M., Biochem J. 35 (1941) 1358

Martin A.J.P., Disc. Faraday Soc. 7 (1949) 332.

Newburger J. and Guiochon G., J. Chromatogr. 484 (1989) 153.

Peterson E.A., Anal. Biochem. 90 (1978) 767.

Phillips M.W., Subramanian G. and Cramer S.M., J. Chromatogr. 454 (1988) 1.

Poppe H. and Kraak J.C., J. Chromatogr. 255 (1983) 395.

Rhee H.-K., Aris R. and Amundson N.R., Proc. Roy. Soc. (London) A267 (1970) 419.

Rhee H.-K. and Amundsun, N.R., Chem. Eng. Sci. 29 (1974) 2049.

Rhee H.-K. and Amundson N. R., AICHE J. 28(3) (1982) 423.

Rixey W.G. and King C.J., AICHE J. 35 (1989) 69.

Rouchon, P., Valentin P., Schonauer, M. and Guiochon G., Sep. Sci. and Tech. 22 (1987) 1793.

Ruthven D.M. Principles of Adsorption and Adsorption Processes, John Wiley & Sons, New York 1984.

Saunders M.S., Mawengkang F. and Carta G., AICHE annual meeting, Washington D.C., November 27-December 2, 1988, paper 7a.

Saunders M.S., Vierow J.B., and G. Carta, AICHE J. 35 (1989a) 53.

Saunders M.S., University of Virgina, PhD Thesis (1989b).

Schay G. and Szekely G., Acta. Chim. Hung. 5 (1954) 167.

Scott C.D., Spence R.D. and Sisson W.G., J. Chromatogr. 126 (1976) 381.

Scott C.D., Sep. Sci. and Tech. 21 (1986) 905.

Snyder L.R., G.B. Cox and Antle P.E., Chromatographia, 24 (1987) 82.

Snyder L.R., Cox, G.B., Antle P.E., J. Chromatogr. 444 (1988) 303.

Snyder L.R. Dolan J.W. and Cox G.B., J. Chromatogr. 483 (1989a) 63.

Snyder L.R. and Cox G.B., J. Chromatogr. 483 (1989b) 85.

Snyder L.R., Dolan J.W. and Lommen D.C., J. Chromatogr. 484 (1989c) 425.

Snyder L.R. and Dolan J.W., J. Chromatogr. 484 (1989d) 437.

Spedding F.H., Fulmer E.I., Butler T.A. and Powell J.E., J. Am. Chem. Soc. 72 (1950) 2349.

Spedding F.H., Discuss. Farady Soc. 7 (1949) 38.

Subramanian G., Phillips M.W. and Cramer S. M., J. Chromatogr. 439 (1988) 341.

Subramanian G., Phillips M.W. Jayaraman G. and Cramer S. M., J. Chromatogr. 484 (1989) 225.

Taniguchi V.T., Doty A.W. and Byers C.H. in Rare Earths Extraction Preparation and Applications (Bautist R.G. and Wong M.M. Ed.) The minerals, Metals and Materials Society, Warrendale, PA (1988) p. 147.

Thomas H.C., J. Am. Chem. Soc. 66 (1944) 1664.

Tiselius A., Ark. Kemi. Mineral. Geol. 16a (1943) 1.

Tiselius A., Disc. Far. Soc. 7 (1949) 7.

Torres A.R. Edberg S.C. and Peterson E.A., J. Chromatogr. 389 (1987) 177.

Tswett M., Ber. Dtsch. Bot. Ges. 24 (1906) 316.

Valko K., Slegel P. and Bati J., J. Chromatogr. 386 (1987) 345.

Van Deemter J.J., Zuiderweg F.J. and Klinkenberg A., Chem. Eng. Sci. 5 (1956) 271.

Velayudhan A. and Horvath Cs., J. Chromatogr. 443 (1988) 13.

Verzele M. and Geeraert E., J. Chromatogr. 18 (1980) 559.

Vigh Gy., Varga-Puchony Z., Szepesi G. and M. Gazdag, J. Chromatogr. 386 (1987) 353.

Vigh G., Quintero G. and Farkas, Gy. J. Chromatogr. 484 (1989a) 237.

Vigh G., Farkas, Gy. and Quintero G. J. Chromatogr. 484 (1989b) 251.

Villermaux J. in Column Chromatography proc of the 5th International Symposium in Separation Methods E.sz. Kovats (eds.), Lausanne, Switzerland (1969), Sauerlander AG, Aarau Switzerland (1970)p. 66.

Villermaux J., Chem. Eng. Sci. 27 (1972) 1231.

Villermaux J., in PercolationProcesses, A.E. Rodrigues and D. Tondeur (eds.) Sijthoff and Noordhoff, Rockville, Md. 1981, p. 83.

Viscomi G., Lande S. and Horvath Cs., J. Chromatogr. 440 (1988) 157.

Viscomi G.C., Ziggiotti A. and Verdini A.S., J. Chromatogr. 482 (1989) 99.

Viscomi G.C., J. Chromatogr. 499 (1990) 35.

Wade J. L., Bergold A. F. and Carr P., Anal. Chem. 59 (1987) 1286.

Wankat P.C., "Large-Scale Adsorption and Chromatography," Vol 1 and 2, CRC Press, Boca Raton, Fl (1986).

Weiss J., J. Chem. Soc (London), (1943) 297.

Wilson J.N., J. Am. Chem. Soc. 62 (1940) 1583.

Wilson E.J. and Geankoplis J., Ind. Eng. Chem. Fundam. 5(1) (1966) 9.

Yamamoto S., Nomura M. and Sano Y., AICHE J. 33 (1987) 1426.

Yu Q and Wang N.-H. L., Computers Chem. Engng. 13(9) (1989) 915.

Yu Q, Yang, J. and Wang N.-H., Reactive Polymers, 6 (1987) 33.

Yu Q and Wang N.-H. L., Separation and Purification Methods, 15(2) (1986) 127.

APPENDICES

Appendix A

Programs for the Gilson 232-401

The Gilson 232-401 can function in many modes, fraction collection, vial dilution, autoinjection, backflusing, trace enrichment, sample preparation just to name a few. This is due to the hardware and software design of this equipment. The essential of the hardware is shown in Figure A.1 where two 6 port valves are plumbed accordingly to perform the desired task. The 3 tasks required in this work is fraction collection, vial dilution and autoinjection. Figure A.1 shows the plumbing required to carry out these tasks. In a nutshell, the injection valve is employed in the same capacity as a 6 port injection valve. The switching valve is used to change the flow path of the column effluent to waste or to the needle for fraction collection. With an external 0.5 ml low pressure syringe pump, it is possible to aspirate or dispense fluid from the needle to any location (i.e. another vial, the injection port, waste). The electronics has been designed so that through the keypad the needle can be instructed to move or and the pump to dispense or aspirate. Programs can be written and stored in memory or stored on a personal computer in ASCII format.

Following are listed the programs written to collect the data shown in Chapter 4. Each program is documented with a description of the variables.

A.1 Fraction Collection Program

```
$     Mon Dec 18 1989 14:03:31
$SampID=11
$Type=3
$Ver=1
$Arm=0
$Dilutor=0,500
  1:    Input    A2/6
  2:    Input    A3/83
  3:    Input    B2/8
  4:    Input    C10/86
  5:    Auxil.   1/2
  6:    Auxil.   7/2
  7:    Wait
  8:    For      A1=1/5
  9:    Rack     31/A1
 10:    Next     A1
 11:    LET      A4=6
 12:    LET      B4=18
 13:    LET      C4=5
 14:    LET      C5=0
 15:    Wait     C10
 16:    Inject   1/
 17:    For      C=1/C4/1
 18:    For      B=B2/B4/1
 19:    For      A=1/A4/1
 20:    LET      C5=C5+1
 21:    Print    C5
 22:    Wait
 23:    Tube     A/B/C
 24:    Height   23
 25:    Wait     A2
 26:    If       C5=A3
 27:    Goto     31
 28:    Next     A
 29:    Next     B
 30:    Next     C
 31:    Inject   0/
 32:    Auxil.   9/0
 33:    Rinse
 34:    Wait     3
 35:    Disp.    0/200/5
 36:    Home
```

Lines 1-4 are input parameters prior to starting the injection. 1: Enter the time between each vial (hundreths of a minute), 2: Enter the number of samples, 3: Enter the rack row number where the first vial is located, 4: Enter the delay time (time between start of run and collection of first fraction). Lines 5-6 start data acquision. Lines 8-10 initialize the rack code for each rack. Lines 11-14 initialize parameters. Line 16 rotates the switching valve so the column effluent goes through the needle and not to the waste. Lines 17-19 and 28-30 define a nested loop. Within this loop the following tasks are performed: 1) Displays the current vial number, 2) Moves the needle to the bottom of vial having coordinates A/B/C (row,column,rack), 3) waits A2 amount of time at that vial. When fractionation is complete, the needle is rinsed and goes to the home position.

A1 Rack Number
A2 Time at current Vial (hunderths of a minute)
A3 Number of Samples
A4 Number of Rows in Rack
B2 Rack Position
B4 Number of Columns in Rack
C4 Number of Racks
C5 Current Vial Number
C10 Delay time to start of fractionation

A.2 Consecutive Vial Dilution Program

```
$     Mon Dec 18 1989 14:57:47
$SampID=11
$Type=3
$Ver=1
$Arm=0
$Dilutor=0,500
  1:     Input    B1/24
  2:     Input    A3/83
  3:     Input    B2/8
  4:     Rinse
  5:     Disp.    0/300/6
  6:     Height   0
  7:     For      A1=1/4
  8:     Rack     30/A1
  9:     Next     A1
 10:     LET      A4=4
 11:     LET      B4=15
 12:     LET      C4=5
 13:     LET      C5=0
 14:     For      C=1/C4/1
 15:     For      B=B2/B4/1
 16:     For      A=1/A4/1
 17:     LET      C5=C5+1
 18:     Print    C5
 19:     Tube     A/B/C
 20:     Height   0
 21:     Disp.    0/B1/1
 22:     If       C5=A3
 23:     Goto     27
 24:     Next     A
 25:     Next     B
 26:     Next     C
 27:     Rinse
 28:     Disp.    0/200/5
 29:     Home
```

Lines 1-3 are input parameters before execution of the run. 1: Enter Dilution Volume (ul), 2: Enter number of samples, 3: Enter rack row where first vial is located. Lines 4-6 wash the needle. Lines 7-9 initialize the rack code for each of the 5 racks. Lines 10-13 initilize various parameters. Lines 14-16 and 24-26 mark the nested loop where the follow operations are performed on each vial from row to row and rack to rack: 1) the current vial number is displayed, 2) the needle goes to the vial having coordinates A/B/C (row,column,rack), 3) a volume of B1 is dispensed into the vial. When dilution has been performed on all the vials, the needle is rinsed and returned to the home position.

A3 Number of Samples
A4 Number of Vials in Row
B1 Dilution Volume (ul)
B2 Rack Row Number where first Vial is Located
B4 Number of Columns in Rack
C4 Number of Racks
C5 Current Vial Number

A.3 Sequential Injection Program

```
$     Mon Dec 18 1989 14:58:07
$SampID=11
$Type=3
$Ver=1
$Arm=0
$Dilutor=0,500
  1:     Input    A3/83
  2:     Input    B2/8
  3:     Input    A5/30/0/300
  4:     Input    A2/25
  5:     LET      A6=50
  6:     For      A1=1/5
  7:     Rack     31/A1
  8:     Next     A1
  9:     LET      A4=6
 10:     LET      B4=18
 11:     LET      C4=5
 12:     LET      C5=0
 13:     LET      C6=5
14:    For      C=1/C4/1
 15:     For      B=B2/B4/1
 16:     For      A=1/A4/1
 17:     Rinse
 18:     Disp.    0/800/8
 19:     Inject   0
 20:     Tube     0/0
 21:     Disp.    0/150/0/6
 22:     LET      C5=C5+1
 23:     Print    C5
 24:     Tube     A/B/C
 25:     Height
 26:     Aspir.   0/C6/1
 27:     Height   0
 28:     Aspir.   0/A5/1
 29:     Inject   0
 30:     Tube     0/0
 31:     Disp.    0/A5/0
 32:     Wait     2
 33:     Inject   1
 34:     Wait
 35:     Auxil.   1/2
 36:     Auxil.   7/2
 37:     Rinse
 38:     Disp.    0/150/7
 39:     Height
 40:     Wait     A2
 41:     If       C5=A3
 42:     Goto     46
 43:     Next     A
 44:     Next     B
 45:     Next     C
 46:     Rinse
 47:     Disp.    0/700/9
 48:     Tube     0/0
 49:     Disp.    0/150/0/7
 50:     Home
```

Lines 1-4 are input parameters prior to starting the run. 1: Enter the number of samples, 2: Enter the rack row number where the first vial is located, 3: Enter the injection load volume (ul), 4: Enter the elution time. Lines 6-8 initialize the rack code for each of the 5 racks. Lines 9-11 initializes the number of rows, columns and racks. Lines 14-16 and 43-45 are nested loops within which the system performes a series of tasks. These tasks are: 1) Rinse the needle at the rinsing station, 2) move the needle to the loopfiller port and dispense slowly 150 ul of solvent, 3) Move to the next vial having coordinates A/B/C aspirate C6 ul of air, 4) move the needle to the bottom of the vial and aspirate A5 volume of sample, 5) move to the injection port dispense A5 volume of sample and withdraw the needle, 6) actuate the injection valve, 7) send a signal to the data acquisition system to start acquiring data and 8) Rinse the needle and wait until the end of run. After all the samples are injected, the needle is rinsed and the arm returns to the home position.

A1 Rack Number
A2 Time Between Sequential Injections (hundreths of a minute)
A3 Number of Samples to be Injected
A4 Number of Rows in the Rack
A5 Injection Load Volume (ul)
A6 Rinse Volume (ul)
B2 Rack row number where fist vial is located
B4 Number of Columns in Rack
C4 Number of Racks
C5 Current Vial number
C6 Air Bubble Volume (ul)

A.4 Replicate Injections from One Vial

```
$     Mon Dec 18 1989 14:58:27
$SampID=11
$Type=3
$Ver=1
$Arm=0
$Dilutor=0,500
  1:    Input    A3/83              23:   Aspir.  0/C6/0
  2:    Input    A2/8               24:   Height  0
  3:    Input    B2/8               25:   Aspir.  0/A5/0
  4:    Input    C3/8               26:   Inject  0
  5:    Input    A7/6               27:   Tube    0/0
  6:    Input    A5/30              28:   Disp.   0/A5/0
  7:    Rack     31/C3              29:   Wait    2
  8:    LET      A6=50              30:   Inject  1
  9:    LET      A4=4               31:   Wait
 10:    LET      B4=18              32:   Auxil.  1/2
 11:    LET      C4=6               33:   Auxil.  7/2
 12:    LET      C5=0               34:   Rinse
 13:    LET      C6=5               35:   Disp.   0/A6/7
 14:    For      C=1/A3             36:   Height
 15:    Rinse                       37:   Tube    0/0
 16:    Disp.    0/800/8            38:   Disp.   0/A6/5
 17:    Inject   0                  39:   Rinse
 18:    Tube     0/0                40:   Wait    A7
 19:    Disp.    0/A6/7             41:   Next    C
 20:    Print    C                  42:    Rinse
 21:    Tube     A2/B2/C3           43:   Disp.   0/700/8
 22:    Height                      44:   Home
```

Lines 1-6 are input parameters before execution of the run. 1: Enter number of samples to be injected, 2: Enter the Row Number (coordinate) where the vial is located, 3: Enter the Column number the vial is located, 4: Enter the rack number where the vial is located, 5: Enter the time between consequtive injections, 6: Enter the Dilution Volume. Lines 8-13 initalize various parameters. Line 14 and 41 define a loop within which the system performs the following tasks: 1) wash the needle, 2) wash the sample loop, 3) aspirate A5 volume of sample from vial having coordinates A/B/C, 4) dispense A5 volume into sample loop, 5) actuate swiching of injection valve from load to inject, 6) send a signial to start data acquisition, 7) wash needle, 8) wash loop. After all the injections are made, the needle is rinsed and returned to the home position.

A2 Row number where sample vial is located
A5 Injection Volume
A7 Time between consequtive injections (hundreth of a minute)
B2 Column number where sample vial is located
C3 Rack number where sample vial is located
A3, A4, A6, B4, C4, C5, C6 have same definitions as Table A.4

A.5 Program to Begin Data Acquisition

```
$     Mon Dec 18 1989 15:21:26
$SampID=11
$Type=3
$Ver=1
$Arm=0
$Dilutor=0,500
  1:     Auxil.   1/2
```

Appendix B

Listing of Experimental Data

B.1 Overloaded Elution Data, 1/1 Mixture
Delay Time: 0.416 seconds included

Time min	C1 mg/ml	C2 mg/ml
3.8	0	0
3.85	0	0
3.9	0	0
3.95	0	0
4	0	0
4.05	0	0
4.1	0	0
4.15	0	0
4.2	0	0
4.25	0.134027	0
4.3	0.212499	0
4.35	0.178472	0
4.4	5.190277	0
4.45	12.42152	0
4.5	13.69166	0
4.55	14.49930	0
4.6	16.57152	0
4.65	17.26111	0
4.7	16.32291	0
4.75	16.28333	0
4.8	12.78402	0
4.85	13.86458	0
4.9	11.29791	0
4.95	10.17708	0
5	9.173611	0
5.05	7.158333	0.325694
5.1	7.196527	0.488194
5.15	6.342361	0.986111
5.2	5.059722	1.538888
5.25	5.084722	1.388888
5.3	2.913194	3.972916
5.35	2.560416	4.521527
5.4	1.765972	6.310416
5.45	1.763888	6.672916
5.5	1.203472	8.106944
5.55	0.951388	7.968749
5.6	0.761805	7.782638

5.65	0.528472	8.238888
5.7	0.538194	7.981249
5.75	0.392361	7.824999
5.8	0.257638	7.063194
5.85	0.236805	7.896527
5.9	0.184722	7.114583
5.95	0.190972	7.600694
6	0.144444	6.566666
6.05	0.129166	6.672916
6.1	0.122916	6.545138
6.15	0.114583	6.332638
6.2	0.099999	5.956944
6.25	0.097222	5.904861
6.3	0.091666	5.796527
6.35	0.085416	5.587499
6.4	0.079861	5.017361
6.45	0.078472	5.031249
6.5	0.077777	5.161805
6.55	0.069444	4.274999
6.7	0.065277	3.669444
6.8	0.061805	3.194444
7	0.056944	2.239583
7.1	0.05625	1.979861
7.2	0.054166	1.427083
7.3	0.054166	1.238194
7.4	0.052083	0.914583
7.5	0.053472	0.680555
7.6	0.051388	0.402777
7.7	0.052777	0.293055
7.8	0.052083	0.215972
7.9	0.051388	0.127083
8	0.051388	0.091666
8.1	0	0.063194
8.2	0	0.049305

B.2. Overloaded Elution Data, 1/3 Mixture
Delay Time: 0.416 seconds included

Time min	C1 mg/ml	C2 mg/ml
4.25	0.098	0
4.3	0.1098	0
4.35	6.0598	0
4.4	7.8298	0
4.45	11.2338	0
4.5	13.6727	0
4.55	16.3852	0
4.6	15.4044	0
4.65	15.8405	0
4.7	14.3948	0.511
4.75	13.4945	1.6288
4.8	10.8498	3.4636
4.85	8.2834	7.2964
4.9	7.5504	8.0005
4.95	6.0272	11.1711
5	3.7235	11.9573
5.05	3.7456	14.4528
5.1	3.3214	14.9241
5.15	2.6515	15.3703
5.2	1.9368	13.9871
5.25	1.7275	15.4453
5.3	1.342	15.0671
5.35	1.2373	15.1813
5.4	0.8929	13.5334
5.45	0.8376	14.6696
5.5	0.6623	13.0864
5.55	0.5626	13.3514
5.6	0.4407	12.5344
5.65	0.3415	12.1866
5.7	0.2979	12.6934
5.75	0.26	11.8431
5.8	0.1905	10.6955
5.85	0.1753	11.1891
5.9	0.1463	11.1508
5.95	0.1376	10.5196
6.05	0.1161	9.599
6.15	0.09795	8.66
6.25	0.0912	8.3644
6.35	0.0823	7.5312
6.45	0.0926	6.8821
6.55	0.0801	5.7323
6.65	0.0682	5.3346
6.75	0.0648	4.5343
6.85	0.0638	4.3297

6.95	0.0619	3.6863
7.05	0	3.347
7.15	0	2.7947
7.25	0	1.7958
7.35	0	1.5893
7.45	0	1.2389
7.55	0.0644	1.1745
7.65	0	0.9021
7.75	0	0.6837
7.85	0	0.4974
7.95	0	0.3719
8.05	0	0.228
8.15	0	0.2105
8.25	0	0.126

B.3 Overloaded Elution Data, 3/1 Mixture
Delay Time: 0.416 seconds included

Time min	C1 mg/ml	C2 mg/ml
3.95	0.1258	0
4	2.067	0
4.05	8.571	0
4.1	18.67	0
4.15	31.42	0
4.2	39.4	0
4.25	45.02	0.02957
4.35	45.94	0.05386
4.4	40.76	0.5925
4.45	36.5	1.112
4.5	35.01	1.135
4.55	33.43	1.787
4.6	26.78	2.821
4.65	24.46	3.523
4.7	21.38	3.609
4.75	20.98	4.093
4.8	19.97	3.968
4.85	17.23	4.367
4.9	11.85	4.42
4.95	12.9	5.246
5	11.49	5.045
5.05	10.82	5.153
5.1	9.628	4.904
5.15	9.248	5.177
5.2	8.316	5.195
5.25	7.483	5.095
5.3	6.35	4.697
5.35	5.954	4.801
5.4	5.201	4.642
5.45	4.669	4.634
5.5	3.544	3.904
5.55	3.509	4.417
5.6	3.161	4.439
5.65	3.147	4.341
5.7	1.729	3.899
5.75	1.492	3.887
5.8	1.272	3.788
5.85	1.12	3.943
5.9	0.8867	3.648
5.95	0.838	3.758
6	0.7548	3.644
6.05	0.4258	3.819
6.1	0.3525	3.527
6.15	0.3284	3.622
6.2	0.3032	3.746

6.25	0.2708	3.661
6.35	0.2359	3.772
6.4	0.2093	3.579
6.45	0.2004	3.53
6.5	0.1754	3.208
6.55	0.169	3.323
6.6	0.1624	3.357
6.65	0.15	3.041
6.7	0.1428	2.905
6.75	0.1415	2.943
6.8	0.1345	2.795
6.85	0.132	2.733
6.9	0.1229	2.515
6.95	0.1145	2.163
7	0.1156	2.084
7.05	0.1135	2.013
7.1	0.1105	1.774
7.15	0.1105	1.763
7.2	0.11	1.572
7.25	0.1091	1.447
7.3	0.1036	1.344
7.35	0.1065	1.274
7.4	0.1002	0.9673
7.45	0.1029	0.811
7.5	0.0973	0.7192
7.55	0.09735	0.6551
7.6	0.09176	0.5321
7.65	0.09243	0.4692
7.7	0.08948	0.3822
7.75	0.09189	0.3458
7.8	0.08949	0.2865
7.85	0.08782	0.2321
7.9	0.08884	0.1793
7.95	0.08598	0.158
8	0.08064	0.1282
8.05	0.08166	0.1056
8.1	0.07741	0.08224
8.15	0.07543	0.07235
8.2	0.07829	0.07092

B.4. Overloaded Elution Data, 9/1 Mixture
Delay Time: 0.416 seconds included

Time min	C1 mg/ml	C2 mg/ml
3.95	0	0
4	0.489	0
4.05	4.424	0
4.1	11.39	0
4.15	20.42	0
4.2	21.8	0
4.25	32.89	0
4.3	35.45	0
4.35	34.92	0
4.4	35.13	0
4.45	35.1	0
4.5	32.48	0
4.55	30.67	0
4.6	24.67	0
4.65	25.74	0.04876
4.7	21.28	0.07735
4.75	17.56	0.1143
4.8	17.16	0.173
4.85	20.34	0.2809
4.9	12.56	0.1658
4.95	13.26	0.4538
5	8.723	0.408
5.05	10.82	0.5941
5.1	12.47	0.8537
5.15	8.245	0.6794
5.2	8.268	0.8034
5.25	8.255	0.9316
5.3	8.792	1.152
5.35	6.972	1.049
5.4	6.498	1.082
5.45	5.814	1.218
5.5	4.087	0.9416
5.55	4.846	1.263
5.6	3.566	0.9281
5.65	3.312	1.164
5.7	3.457	1.336
5.75	2.595	1.224
5.8	1.538	0.943
5.85	1.533	1.104
5.9	1.011	0.8112
5.95	1.111	1.095
6	0.6043	0.7037
6.05	0.6557	0.979
6.1	0.4612	0.8651
6.15	0.2646	0.607

6.2	0.3602	1.149
6.25	0.2214	0.8368
6.3	0.1828	0.8753
6.35	0.1466	0.8005
6.45	0.09233	0.5551
6.5	0.08753	0.5712
6.55	0	0.2185
6.6	0.06561	0.3029
6.65	0.0683	0.3619
6.7	0.06786	0.4181
6.75	0	0.2479
6.8	0.06562	0.4476
6.85	0.06995	0.4999
6.9	0.0725	0.6943
6.95	0	0.4185
7	0	0.1757
7.05	0	0
7.1	0	0
7.15	0	0.03053
7.2	0	0.08107
7.25	0	0.1767
7.3	0	0.1768
7.35	0	0.2187
7.4	0	0
7.45	0.07097	0.2947
7.5	0	0.1495
7.55	0	0.1311
7.6	0.06495	0.1269
7.65	0	0.06856
7.7	0.06734	0.1068
7.75	0	0
7.8	0	0
7.85	0.08074	0.1183
7.9	0	0
7.95	0	0
8	0	0
8.05	0	0
8.1	0	0
8.15	0	0
8.2	0.008465	0
8.25	0	0
8.3	0.007973	0
8.35	0.00813	0
8.4	0	0
8.45	0	0
8.5	0	0

B.5 Large Volume Injection, 1/1 Rectangular

Time min	C1 mg/ml	C2 mg/ml
4.76	0.024586	0
4.81	0.185049	0
4.86	1.59384	0
4.91	2.38815	0
4.96	1.80177	0
5.01	7.4907	0
5.06	9.5613	0
5.11	10.3095	0
5.16	10.7706	0
5.21	10.8924	0
5.26	11.8842	0
5.31	12.1452	0
5.36	12.3975	0
5.41	12.2322	0
5.46	12.0843	0
5.51	12.5628	0
5.61	12.6672	0
5.66	12.8499	0
5.71	12.8847	0
5.76	12.6063	0.755794
5.81	12.1539	2.09264
5.86	11.3796	3.06762
5.91	11.5014	4.38864
5.96	10.9446	5.36198
6.01	11.0403	5.91384
6.06	10.4922	7.06594
6.11	10.2312	8.2082
6.16	10.8576	9.4382
6.21	10.179	8.8314
6.26	10.3878	9.2578
6.31	10.0398	9.1184
6.36	10.3791	9.758
6.41	10.266	9.553
6.46	10.3791	9.7334
6.51	10.2486	9.676
6.56	10.266	9.7826
6.61	10.1877	9.6596
6.66	10.3095	9.799
6.71	10.5009	10.004
6.76	10.092	9.635
6.81	10.3443	9.9712
6.86	10.2138	9.7826
6.91	10.5096	10.086
6.96	10.4835	10.0778
7.01	10.6401	10.25
7.06	10.6923	10.2992

7.11	10.527	10.1598
7.16	10.4835	10.1516
7.21	10.3095	9.9958
7.26	10.4835	10.1598
7.31	10.527	10.1844
7.36	10.5531	10.2172
7.41	10.5444	10.2008
7.46	10.527	10.168
7.51	10.9011	10.496
7.56	10.614	10.25
7.61	10.2573	9.9876
7.66	10.3443	10.1762
7.71	9.7962	9.8154
7.76	9.4656	9.7006
7.81	8.8044	9.2988
7.86	8.22063	9.02
7.91	7.76388	8.9134
7.96	7.08006	8.569
8.01	6.43017	8.2984
8.06	5.90991	8.1713
8.11	5.29482	7.96384
8.16	4.86939	8.00976
8.21	4.24299	7.7531
8.26	3.61398	7.44642
8.31	3.05631	7.18156
8.36	2.61609	7.08972
8.41	2.21154	7.06758
8.46	1.80699	6.95114
8.51	1.45116	6.8429
8.56	1.12491	6.6707
8.61	0.858777	6.43864
8.66	0.656589	6.37714
8.71	0.501033	6.3878
8.76	0.384975	6.457582
8.81	0.284142	6.38206
8.86	0.208452	6.355
8.91	0.156948	6.3304
8.96	0.115188	6.0311
9.01	0.0957	6.36156
9.06	0.074106	6.14836
9.11	0.058029	6.24676
9.16	0.042673	5.27588
9.21	0.037062	5.34558
9.26	0	5.24062
9.31	0	5.23816
9.36	0	5.02496
9.41	0	4.67974
9.46	0	4.79126
9.51	0	4.52394
9.56	0	4.33616
9.61	0	4.25088
9.66	0	4.24432

9.71	0	3.69164
9.76	0	3.50058
9.81	0	3.3087
9.86	0	3.09386
9.91	0	2.86754
9.96	0	2.65434
10.01	0	2.5379
10.06	0	2.27714
10.11	0	2.14184
10.16	0	1.95734
10.21	0	1.75562
10.26	0	1.72364
10.31	0	1.49322
10.36	0	1.31856
10.41	0	1.20458
10.46	0	1.06108
10.51	0	0.89462
10.56	0	0.779902
10.61	0	0.664446
10.66	0	0.56252
10.71	0	0.476256
10.76	0	0.387122
10.81	0	0.31898
10.86	0	0.26568
10.91	0	0.214922
10.96	0	0.168182
11.01	0	0.14063
11.06	0	0.108568
11.11	0	0.080843

B.6 Large Volume Data, 1/1 Non-Rectangular

Time min	C1 mg/ml	C2 mg/ml
4.2	0	0
4.25	0	0
4.3	0.015172	0
4.35	0	0
4.4	0	0
4.45	0.009910	0
4.5	0.033255	0
4.55	0.033200	0
4.6	2.083133	0
4.65	4.328064	0
4.7	7.139283	0
4.75	8.08984	0
4.8	8.716802	0
4.85	10.73926	0
4.9	10.19319	0
4.95	12.23588	0
5	12.84262	0
5.05	12.68082	0
5.1	12.66059	0
5.15	12.84262	0
5.2	12.98419	0
5.25	13.12576	0
5.3	12.94374	0
5.35	12.92351	0
5.4	9.788706	0.029776
5.45	13.26733	0.038867
5.5	12.78194	0.819587
5.55	12.90329	1.523174
5.6	12.31678	3.404305
5.65	12.07408	5.076242
5.7	11.87184	5.579838
5.75	11.12353	6.587029
5.8	11.06285	6.889186
5.85	11.02240	7.976952
5.9	10.69881	7.896377
5.95	10.61791	8.581267
6	10.61791	8.742417
6.05	10.61791	8.903568
6.1	10.39544	8.762561
6.15	11.00218	9.346732
6.2	10.77971	9.225869
6.25	10.59769	9.084862
6.3	10.82016	9.326588
6.35	10.29432	8.883424
6.4	10.33477	8.923712

6.45	10.57746	9.145294
6.5	10.51679	9.084862
6.55	10.40757	9.004287
6.6	10.45611	9.084862
6.65	10.75948	9.346732
6.7	10.47634	9.084862
6.75	10.17297	8.802849
6.8	10.07185	8.702130
6.85	10.07185	8.702130
6.9	10.17297	8.802849
6.95	10.01117	8.681986
7	10.1123	8.903568
7.05	9.910054	8.601411
7.1	10.31454	8.963999
7.15	10.59769	9.205725
7.2	10.21342	8.863280
7.25	10.23364	8.903568
7.3	10.19319	8.883424
7.35	10.07185	8.762561
7.4	10.07185	8.762561
7.45	9.829155	8.581267
7.5	10.23364	8.963999
7.55	9.768481	8.581267
7.65	9.687583	8.641698
7.7	9.181968	8.238822
7.75	9.262866	8.379829
7.8	9.080845	8.279110
7.85	8.979722	8.279110
7.9	8.797701	8.198534
8	8.757251	8.299253
8.05	8.312310	7.956808
8.1	8.453882	8.218678
8.15	7.887594	7.755370
8.2	8.130289	8.097815
8.25	8.069615	8.178390
8.3	7.725797	7.835945
8.35	7.746021	7.997096
8.4	7.462877	7.775514
8.45	7.462877	7.876233
8.55	7.159508	7.755370
8.6	6.856139	7.473357
8.65	6.734791	7.453213
8.7	6.451647	7.251775
8.75	6.289850	7.211487
8.8	6.107829	7.171199
8.85	5.905583	7.171199
8.9	5.460642	6.869042
8.95	5.096599	6.748179
9	4.773005	6.707892
9.05	4.348289	6.546741
9.15	3.417957	6.244584
9.2	2.993240	6.647460

9.25	2.548299	5.861851
9.3	2.103358	5.660413
9.35	1.690400	5.438831
9.45	1.074292	5.297824
9.5	0.827709	5.176961
9.6	0.479600	4.995667
9.65	0.369606	4.995667
9.75	0.207075	4.955379
9.8	0.160832	4.854660
9.85	0.121806	4.794229
9.9	0.097818	4.713653
9.95	0.095557	5.338112
10	0.071580	4.733797
10.05	0.058374	4.753941
10.1	0.048205	4.592790
10.15	0.043612	4.592790
10.2	0.039361	4.512215
10.25	0.035348	4.330921
10.3	0.033479	4.471928
10.35	0.026706	1.020012
10.4	0.030294	4.290633
10.45	0.028065	4.250346
10.5	0.027200	4.169770
10.55	0.026894	3.988476
10.6	0.025737	4.028764
10.65	0.025131	3.787038
10.7	0.023929	3.686319
10.75	0.023737	3.484880
10.8	0.023367	3.444593
10.85	0.023345	3.263298
10.9	0.022594	2.981285
10.95	0.021531	2.820134
11	0.022063	2.578408
11.05	0.021286	2.457546
11.1	0.021260	2.316539
11.15	0.025226	2.195676
11.2	0.023029	1.612216
11.25	0.022206	1.801997
11.3	0.020451	1.635176
11.35	0.020948	1.440909
11.4	0.021733	1.268242
11.45	0.021696	1.166496
11.5	0.019727	1.027399
11.55	0.019741	0.884335
11.6	0.021252	0.778389
11.65	0.021488	0.671323
11.7	0.020699	0.555467
11.75	0.020712	0.466132
11.8	0.018885	0.382253
11.85	0.020410	0.309088
11.9	0.019989	0.255071
11.95	0.019530	0.207735

12	0.019551	0.160743
12.05	0.019803	0.134540
12.1	0.018246	0.108746
12.15	0.018469	0.090526
12.2	0.017745	0.075190
12.25	0.017696	0.063847
12.3	0.016796	0.054388
12.35	0.017488	0.047793
12.4	0.016638	0.042463
12.45	0.016448	0.037747
12.5	0.016080	0.035777
12.55	0.033930	0.060640
12.6	0.014982	0.029013
12.65	0.016960	0.027165
12.7	0.014636	0.026734

B.7 Large Volume Injection, 1/3

Time min	C1 mg/ml	C2 mg/ml
4.6	0	0
4.65	0.1211	0
4.7	0.7284	0
4.75	1.778	0
4.8	2.916	0
4.85	4.003	0
4.9	4.938	0
4.95	5.57	0
5	6.387	0
5.05	7.021	0
5.1	8.506	0
5.15	7.559	0
5.2	7.66	0
5.25	7.663	0
5.3	8.255	0
5.35	7.821	1.066
5.4	7.331	2.83
5.45	6.922	4.91
5.5	6.676	6.928
5.55	6.362	9.084
5.6	6.214	10.82
5.65	5.622	11.47
5.7	4.088	9.246
5.75	6.502	16.16
5.8	5.311	14.03
5.85	4.999	13.66
5.9	5.082	14.26
5.95	5.169	14.8
6	5.05	14.54
6.05	5.001	14.58
6.1	5.229	15.09
6.15	5.219	15.26
6.2	5.186	15.03
6.25	5.087	14.87
6.3	4.871	14.28
6.35	5.066	14.81
6.4	5.184	15.25
6.45	5.002	14.52
6.5	4.927	14.45
6.55	5.247	15.28
6.6	5.097	14.93
6.65	5.133	15.13
6.7	5.03	14.75
6.75	5.346	15.79
6.8	5.058	14.74

6.85	5.265	15.55
6.9	4.869	14.22
6.95	5.239	15.39
7	5.12	15.13
7.05	5.083	14.94
7.1	5.067	14.98
7.15	5.255	15.32
7.2	5.148	15.17
7.25	5.061	14.82
7.3	5.267	15.48
7.35	5.156	15
7.4	5.198	15.03
7.45	5.099	14.82
7.5	5.266	15.09
7.55	5.277	15.37
7.6	5.268	15.17
7.65	5.117	14.85
7.7	5.086	14.93
7.75	4.85	14.31
7.8	4.858	14.67
7.85	4.874	15.01
7.9	4.35	14.15
7.95	3.999	13.78
8	3.628	13.64
8.05	3.123	13.18
8.1	2.735	13.1
8.15	2.298	12.79
8.2	1.816	12.03
8.25	1.442	11.8
8.3	1.087	11.3
8.35	0.8404	11.23
8.4	0.519	11.35
8.45	0.3188	11.03
8.5	0.2029	10.9
8.55	0.1112	10.61
8.6	0.06064	10.86
8.65	0.01616	10.66
8.7	0	10.5
8.75	0	10.44
8.8	0	10.24
8.85	0	9.95
8.9	0	9.726
8.95	0	9.424
9	0	9.046
9.05	0	8.516
9.1	0	8.799
9.15	0	8.189
9.2	0	6.654
9.25	0	7.545
9.3	0	7.226
9.35	0	6.811
9.4	0	6.459

9.45	0	6.086
9.5	0	5.92
9.55	0	5.447
9.6	0	5.12
9.65	0	4.863
9.7	0	4.493
9.75	0	4.037
9.8	0	3.865
9.85	0	3.533
9.9	0	3.236
9.95	0	2.974
10	0	2.632
10.05	0	2.45
10.1	0	2.163
10.15	0	1.92
10.2	0	1.684
10.25	0	1.384
10.3	0	1.195
10.35	0	1.014
10.4	0	0.8202
10.45	0	0.6856
10.5	0	0.5203
10.55	0	0.4117
10.6	0	0.31
10.65	0	0.2011
10.7	0	0.1461
10.75	0	0.09365
10.8	0	0.03462
10.85	0	0.02432
10.9	0	0

B.8 Large Volume Injection, 3/1

Time min	C1 mg/ml	C2 mg/ml
0.012375	0	4.7
1.767857	0	4.75
5.299285	0	4.8
8.508214	0	4.85
11.43214	0	4.95
12.35357	0	5
14.27142	0	5.05
15.19285	0	5.1
17.55000	0	5.15
16.32857	0	5.2
18.06428	0	5.25
16.86428	0	5.3
17.56071	0	5.35
17.18571	0	5.4
16.95000	0	5.45
16.30714	0	5.5
15.94285	0	5.55
17.87142	0	5.6
17.12142	0	5.7
17.89285	0.252857	5.75
19.36071	0.899035	5.8
19.44642	1.796785	5.85
15.98571	3.041785	5.9
16.05000	3.579642	5.95
17.97857	4.599642	6.05
14.98928	4.158214	6.1
15.57857	4.616785	6.15
15.90000	4.918928	6.2
15.05357	4.880357	6.3
14.30357	4.652142	6.35
15.32142	5.047500	6.4
15.72857	5.229642	6.45
16.32857	5.453571	6.5
14.94642	4.969285	6.55
15.82500	5.261785	6.6
15.69642	5.255357	6.65
15.08571	5.030357	6.7
14.23928	4.773214	6.75
14.19642	4.725000	6.8
14.66785	4.892142	6.95
15.55714	5.221071	7
16.10357	5.390357	7.05
15.00000	5.029285	7.1
15.75000	5.304642	7.15
15.67500	5.251071	7.2

16.21071	5.431071	7.25
16.01785	5.365714	7.3
14.93571	4.963928	7.35
16.06071	5.395714	7.4
15.60000	5.213571	7.6
15.92142	5.320714	7.65
14.98928	4.959642	7.7
14.48571	4.836428	7.75
14.41071	4.671428	7.8
14.21785	4.713214	7.85
14.35714	4.638214	7.9
14.20714	4.615714	7.95
14.42142	4.615714	8
14.12142	4.445357	8.05
14.98928	5.052857	8.1
14.71071	4.716428	8.15
15.66428	4.868571	8.2
14.01428	4.316785	8.25
14.68928	4.915714	8.3
15.62142	5.166428	8.35
15.40714	5.132142	8.4
14.06785	4.651071	8.45
15.60000	5.209285	8.5
14.71071	4.887857	8.55
15.47142	5.117142	8.6
14.65714	4.915714	8.65
13.96071	4.631785	8.7
14.73214	4.890000	8.75
15.41785	5.127857	8.8
15.19285	5.022857	8.85
14.37857	4.803214	8.9
14.71071	4.912500	8.95
14.45357	4.850357	9
13.17857	4.497857	9.05
14.06785	4.839642	9.1
12.75000	4.526785	9.15
12.38571	4.507500	9.2
11.76428	4.440000	9.25
11.33571	4.516071	9.3
9.177857	3.857142	9.35
9.270000	4.180714	9.4
7.553571	3.664285	9.45
6.866785	3.615000	9.5
8.411785	4.901785	9.55
5.030357	3.268928	9.6
4.755000	3.570000	9.65
3.793928	3.297857	9.7
3.122142	3.204642	9.75
2.482500	3.187500	9.8
1.990714	3.063214	9.85
1.477500	2.978571	9.9
1.108928	2.942142	9.95

0.830785	2.873571	10
0.608357	2.885357	10.05
0.446678	2.905714	10.1
0.441321	2.905714	10.15
0.424714	3.541071	10.2
0.226714	2.825357	10.25
0.153214	2.876785	10.3
0.100564	2.948571	10.35
0.057932	2.805000	10.4
0.037982	3.103928	10.45
0.003410	2.959285	10.5
0	2.958214	10.55
0	2.869285	10.6
0	2.920714	10.65
0	2.769642	10.7
0	2.656071	10.75
0	2.748214	10.8
0	2.762142	10.85
0	2.865000	10.9
0	2.868214	10.95
0	2.704285	11
0	2.570357	11.05
0	2.607857	11.1
0	2.482500	11.15
0	2.468571	11.2
0	2.297142	11.25
0	2.152500	11.3
0	2.005714	11.35
0	1.779642	11.4
0	1.587857	11.45
0	1.524642	11.5
0	1.162500	11.55
0	1.086428	11.6
0	0.897964	11.65
0	0.735535	11.7
0	0.606214	11.75
0	0.492642	11.8
0	0.396214	11.85
0	0.317571	11.9
0	0.235928	11.95
0	0.184392	12
0	0.144000	12.05
0	0.103221	12.1
0	0.079542	12.15
0	0.059464	12.2
0	0.041667	12.25
0	0.028789	12.3
0	0.017121	12.35
0	0.009835	12.4
0	0.003150	12.45
0	0	12.5
0	0	12.55

Appendix C

The Analogy Between HTU in Adsorption and HETP in Chromatography

The terms HETP or HTU are used to evaluate packed columns for use in adsorption towers, distillation columns or chromatography columns. Use of such reduced quantities instead of the mass transfer coefficient directly is preferable since it changes less over the length of the column. The term HTU is primarily used in design of adsorption and distillation columns and is defined as[1]:

$$HTU = Z/NTU \tag{1}$$

where NTU is the number of transfer units and Z is the height of the packed bed. Assuming overall mass transfer resistance in the gas phase for a adsorption column:

$$NTU = \int_{y_{A,a}}^{y_{A,b}} \frac{(1-y_A^*)_{lm} dy}{(1-y_A)(y_A-y_A^*)} \tag{2}$$

Analogously, the HETP for a chromatography column is given by:

$$HETP = Z/N \tag{3}$$

where N is the number of theoretical plates or sometimes called the column efficiency. For small sample sizes the efficiency can be calculated from the shape of the guassian peak:

$$N = (t_R/\sigma)^2 = 5.545\ (t_R/w_{1/2})^2 \tag{4}$$

A summary of the nomenclature for this appendix is given at the end. Since adsorption and distillation are continuous processes and chromatography is generally a batch process the NTU and N are analogous

quantities, representing the number of ideal equilibrium stages, but are calculated very differently.

In adsorption or distillation, the HTU is a function of the vapor or liquid flow rate and the mass transfer coefficient for the corresponding phase. The HTU represents resistance to mass transfer of the solute in the column assuming overall resistance in the gas phase:

$$HTUg = V/K_{og}'a \quad (5)$$

Similarly, in chromatography the HETP is a function of the Peclet Number (linear velocity, particle size and molecular diffusion coefficient), the mass transfer coefficient and the capacity factor of the solute. The HETP represents band broadening of the solute from various sources. Van Deemter[2] showed that the HETP varies according to:

$$HETP = \sigma^2/z \quad (6)$$

$$HETP/d_p = A + B/Pe + CPe \quad (7)$$

The first term is the contribution of eddy diffusion which results from curved flow streams and nonuniform flow through the channels of the packing. The second term is a result of molecular diffusion of the solute through the column which is significant at low flow rates. The last term is due to contributions because of a finite rate of mass transfer of the solute from the mobile phase to the particle. This can also be written as:

$$HETP = 2D_a/u_o + 2u_o\, k'_o/(1+k'_o)^2 k_f \quad (8)$$

Where the first term is an axial dispersion term and the second term is contributions to band broadening because of mass transfer

resistances. The mass transfer coefficient, k_f, is defined according to the linear driving force model

$$dq/dt = -k_f (q - q^*) \quad (9)$$

The number of plates required in a chromatographic separation is often much larger than in distillation. However in a distillation process, separation at a given time is occurring throughout the entire column, though a particular solute molecule traverses a fraction of the column. In chromatography at a given time only a small fraction of the column is utilized, although all the solutes have experienced the entire column upon elution.

In the design of adsorption or distillation towers the HTU is used in the calculation. However at one time the approach to designing a packed tower was from data for a tray tower and thus one had correlation to find the height of packing equivalent to a theoretical plate (HETP). The total height in the packed tower was determined by multiplying the number of equilibrium trays by the HETP. The HETP and the HTU are related:

$$HTU = HETP \ ((mV/L)-1)/\ln(mV/L) \quad (10)$$

For a straight equilibrium and operating line the HETP can be related the HTU and when (mV/L =1) the two quantities are equal.

When a tray tower is used, the adsorption or distillation process is continuous not batch and the column has been discritized in space by the tray, but is continuous (in the mathematical sense) in time. Chromatography on the other hand is a batch process and in its most common use as a packed column, it continuous in space as well as time. However, there are two ways of modeling chromatography. One is

to write the differential mass balance and solve it numerically which usually at some point involves discritization and minimizing the numerical errors which result. In the general case the space and time increments have no physical meaning, except in the case of the semi-ideal model. There are some implementations of the semi-ideal model, where dz is chosen to be equal to the HETP (Eqn.6) in order to have the specified amount of band broadening at infinite dilution. The second approach to modeling a chromatographic separation is to consider the process as a series of batch tanks, the Craig model. Then, the mobile phase is transferred from one tank to the next after equilibrium is reached. In this case the number of Craig stages (tanks) does not have physical meaning either. However, it can be shown that the number of ideal equilibrium stages is equal to the number of Craig stages for solutes with infinitely long retention times[3]

$$N = (N_c+1)\ (1 + k'_o)/k'_o \qquad (11)$$

where $k'_o/(1 + k'_o)$ represents the ratio of the amount of solute adsorbed in the stationary phase to the total amount of solute. The nature of the Craig model forces discritization in both time and space. It can be shown that the Craig model is equivalent to one form of finite difference discritization. In this case the ratio of the space and time increment is equal to the linear velocity which is consistent with the physical model of tanks in series. For columns of high efficiency the Craig model and the solution to the mass balance equation for a variety of implementations give the same result.

The term HETP or HTU is used to evaluate the performance of packed columns for various processes. Although these various processes are analogous in some ways, they are very different.

NOMENCLATURE

a	surface area of packing per unit volume of packing
D_a	Axial Dispersion Coefficient
d_p	Particle size
HETP	Height Equivalent to a Theoretical Plate
HTU	Height of a Transfer Unit
k'	capacity factor,
k'_o	capacity factor at infinite dilution
k_f	mass transfer coefficient in adsorption column
K_{og}'	Overall gas phase mass transfer coefficient
L	Liquid flow rate
m	slope of the equilibrium curve
N	Number of Theoretical Plates, Efficiency
N_c	Number of Craig stages
NTU	Number of Transfer Units
Pe	Peclet Number
q	instantaneous concentration of solute in stationary phase
q^*	equilibrium concentration of solute in stationary phase
σ	standard deviation
t	time
t_R	Retention time of solute
u_o	linear velocity of liquid through packed bed
V	Gas flow rate through packed column
$w_{1/2}$	Width at half height of a guassian peak
y_A	composition of solute A in the gas
y^*_A	concentration of solute A in the gas phase in equilibrium with the liquid
$y_{A,a}$	composition of solute A in gas stream entering the column
$y_{A,b}$	composition of solute A in gas stream leaving the column
z	length
Z	Adsorption or Distillation Column height

LIST OF REFERENCES

1. A.L. Hines and R.N. Maddox, Mass Transfer Fundamentals and Applications, Prentice Hall, Englewood Cliffs, NJ 1985.

2. J.J. Van Deemter, F.J. Zuiderweg and A. Klinkenberg, Chem. Eng. Sci. 5 (1956) 271.

3. B.L. Karger, L.R. Snyder and Cs. Horvath Introduction to Chromatography, John Wiley and Sons, New York (1973).

Vita

Ms. Anita M. Katti was born in Tallahassee, Florida on December 1, 1962. She attended Fairview Elementary school, West Junior High School and David H. Hickman High School in Columbia, MO. Upon graduating from high school in May 1979 she went to the University of Wisconsin-Madison in the summer to take additional courses and participate in undergraduate research. During the academic year she work toward her B.S. in Chemical Engineering which she completed from the University of Missouri-Columbia in May 1983. She completed a B.S. thesis entitled "The Prediction of Ethanol-Water Partition Coefficients" at the University of Missouri. Her undergraduate research at the University of Wisconsin was on the synthesis, purification and characterization of various polycyclosilanes.

In June of 1983 she accepted to participate in the University of Delaware Industrial Internship program with the Engineering Department of E.I. DuPont de Nemours located at the Experimental Station. In June of 1984 she completed the program with a Masters in Chemical Engineering and a thesis entitled: "The Performance of an Opposed-Jet Impingement Tee as a Rapid Mixer."

After completing this program she attended Yale University from August 1984-December 1987 gaining experience in High Performance Liquid Chromatography of proteins, where she also earned a Master of Science in Chemical Engineering. She then moved to Georgetown University in order to complete her degree and followed her advisor to the University of Tennessee, Knoxville where she graduated with a Ph.D. in Chemical Engineering in May 1990. Her dissertation was a result of

interdisciplinary research between the Department of Chemistry and the Department of Chemical Engineering.

The author is a member of ACS, AICHE, Sigma XI, Tau Beta Pi, Phi Kappa PHi and the East Tennessee Chromatography Discussion Group.